UNIVERSITEIT GENT

Faculty of Medicine and Health Sciences

Department Gastroenterology and Hepatology

Impact on angiogenesis and ER stress and its effect on chemoresistance through PlGF inhibition in a mouse model of hepatocellular carcinoma

Yves-Paul Vandewynckel

2015

Promotor: Prof. Dr. Hans Van Vlierberghe

Co-promotor: Prof. Dr. Anja Geerts

Thesis submitted in fulfillment of the requirements for the degree of

Doctor in Health Sciences

Funding:

This work was supported by the Research Foundation Flanders project 3G015612. YV is sponsored by a grant from the Special Research Fund (01D20012), Ghent University.

Artwork cover:

Painting of a tumour-bearing liver of Dr. A. Macphail (left) and a transmission electron microscopy image of a murine hepatocellular carcinoma cell showing the expanded endoplasmic reticulum (right).

What is a scientist after all? It is a curious man looking through a keyhole, the keyhole of nature, trying to know what's going on.

Jacques Yves Cousteau

Promotor: Prof. Dr. Hans Van Vlierberghe

Co-Promotor: Prof. Dr. Anja Geerts

Campus Ghent University Hospital

Department Gastroenterology and Hepatology

De Pintelaan 185, B-9000 Ghent, Belgium

Members of the doctoral exam committee:

Prof. Dr. Johan Van De Voorde (Ghent University, president)

Dr. sc. Michael Drennan (Ghent University)

Prof. Dr. Marleen Praet (Ghent University)

Prof. Dr. Roberto Troisi (Ghent University)

Dr. sc. Francesca Fornari (University of Bologna)

Prof. Dr. Hendrik Reynaert (University Brussels)

Dr. sc. Olivier Govaere (KU Leuven university)

Table of Content

List of acronyms

4-PBA	4-phenylbutyric acid
AASLD	American association for the study of liver diseases
AGREE	appraisal of guidelines research and evaluation
aPlGF	anti-PlGF antibody
ASK1	apoptosis signal-regulating kinase
ATF4	activating transcription factor 4
ATF6	activating transcription factor 6
BAX	BCL-2-associated X protein
BCL-2	B-cell CLL/lymphoma 2
BCLC	Barcelona-clinic liver cancer
BCL-XL	B-cell lymphoma-extra large
BH	BCL-2 homology
BI-1	BAX inhibitor 1
Bid	BH3 interacting domain death agonist
Bim	BCL-2 interacting mediator of cell death
BiP	binding immunoglobulin Protein
BrdU	bromodeoxyuridine
BWGE	Belgian week of gastroenterology
CALR	calreticulin
CaMKII	calcium/calmodulin-dependent kinase II
CANX	calnexin
CHOP	C/EBP homologous protein
CMA	chaperone-mediated autophagy
DCE	dynamic contrast-enhanced
DEB-TACE	drug-eluting beads transarterial chemoembolization

DEN	diethylnitrosamine
DESPARTH	dose-escalation study evaluating the safety and pharmacokinetics of oral artesunate in patients with advanced hepatocellular carcinoma
DHA	dihydroartemisinin
DUBs	deubiquitinases
EASL	European association for the study of the liver
EC	endothelial cells
ECCO	European cancer organization
EDEM1	degradation-enhancing α-mannosidase-like protein
eIF2α	α subunit of eukaryotic translation initiation factor 2
ER	endoplasmic reticulum
ERAD	ER-associated protein degradation
ERDJ4	endoplasmic reticulum DnaJ homolog 4
ERO1L	endoplasmic oxidoreductin-1-like protein
ERO1α	endoplasmic reticulum oxidase 1α
^{18}F-FDG	^{18}F-fluoro-deoxyglucose
FGF	fibroblast growth factor
FRG	Fah$^{-/-}$/Rag2$^{-/-}$/Il2rg$^{-/-}$
GADD34	growth arrest and DNA damage–inducible 34
GCLC	glutamate-cysteine ligase, catalytic subunit
GPX3	glutathione peroxidase 3
GRP78	glucose-regulated protein, 78 kDa
GRP94	glucose-regulated protein, 94 kDa
Gsta1	glutathione-S-transferase A1
Gsta2	glutathione-S-transferase A2
HBV	hepatitis B
HCC	hepatocellular carcinoma

HCV	hepatitis C
HERPUD1	homocysteine-responsive endoplasmic reticulum-resident ubiquitin-like domain member 1 protein
HIF	hypoxia inducible factor
IG	intragastric
IL-1β	interleukin-1β
IL-8	interleukin-8
IP	intraperitoneal
IP3R1	inositol-1,4,5-trisphosphate receptor 1
IRE1	inositol-requiring enzyme-1
ISRIB	integrated stress response inhibitor
JIK	c-Jun NH2-terminal inhibitory kinase
JNK	c-Jun N-terminal kinase
LDH	lactate dehydrogenase
MCL-1	myeloid cell leukaemia 1
MEF	mouse embryonic fibroblast
MRI	magnetic resonance imaging
MTD	maximum tolerated dose
mTOR	mammalian target of rapamycin
NAC	N-acetyl-L-cysteine
Nfe2l2	nuclear factor erythroid-derived 2, like 2
NFκB	nuclear factor kappa-B
NRF2	nuclear factor erythroid 2-related factor 2
OZ	oprozomib
PDGF	platelet-derived growth factor
PDIA4	protein disulfide-isomerase A4
PERK	PKR-like endoplasmic reticulum kinase

PERKi	PERK inhibitor
PET/CT	positron emission tomography/computed tomography
PI3K	phosphoinositide-3 kinase
PlGF	placental growth factor
PlGFKO	PlGF knockout
PP1C	protein phosphatase 1C
PTEN	phosphatase and tensin homolog
PUMA	p53 upregulated modulator of apoptosis
RIDD	regulated IRE1-dependent decay of mRNA
RIP	regulated intramembrane proteolysis
ROS	reactive oxygen species
S1P	serine protease site-1
S2P	site-2 protease
siRNA	small interfering RNA
SREBP-1	sterol regulatory element binding protein-1
TACE	transarterial chemoembolization
TRAF2	TNF receptor-associated factor 2
TUDCA	tauroursodeoxycholic acid
TKI	tyrosine kinase inhibitor
UEG	united European gastroenterology
UPR	unfolded protein response
UPS	ubiquitin-proteasome system
VEGF	vascular endothelial growth factor
W	week
XBP1	X-box-binding protein 1
XBP1s	spliced X-box-binding protein 1
XBP1u	unspliced X-box-binding protein 1

Summary

Hepatocellular carcinoma (HCC) is the second leading cause of cancer-related mortality worldwide. Because current treatment options for HCC are capable of providing good survival rates to only a small subset of patients, innovative therapeutic strategies are urgently required.
The endoplasmic reticulum (ER) is responsible for protein translocation, folding mediated by a machinery of molecular chaperones, and post-translational modifications that allow further transport of proteins to the Golgi apparatus. Protein folding and modification in the ER is highly sensitive to disturbances of homeostasis. Accumulation of unfolded proteins in the ER lumen, termed ER stress, activates intracellular signalling pathways to resolve the protein-folding defects. This unfolded protein response (UPR) increases the protein-folding capacity, reduces global protein synthesis and stimulates the ER-associated protein degradation. Three major ER stress transducers regulating the UPR have been identified: PKR-like endoplasmic reticulum kinase (PERK), inositol-requiring enzyme-1 (IRE1) and activating transcription factor 6 (ATF6). Paradoxically, if ER stress is too severe or persistent, numerous apoptotic signalling pathways are activated. The UPR has been implicated in a variety of diseases including metabolic diseases, neurodegenerative diseases, inflammatory diseases and cancer. Recently, UPR activation was shown in human HCC samples. Given the dichotomy in outcomes of UPR activation, it remains unclear whether a window exists in which manipulation of the UPR can be harnessed therapeutically. Thus, it is crucial to develop a precise understanding of the signal transduction in the UPR.
The present work focused on the exact role and therapeutic potential of ER stress and the UPR in hepatocarcinogenesis, which starts from the initial genotoxic insult, through the clonal expansion from a premalignant to a tumoural lesion (promotion) and finally to tumour progression.
First, we sequentially monitored the UPR over time in a commonly used orthotopic mouse model for HCC induced by 30 weeks of the carcinogen diethylnitrosamine and explored the effects of UPR modulation on cell viability and proliferation *in vitro* and in the mouse model. We observed that the expression of ER-resident chaperones peaked during tumour initiation and increased further during tumour progression, predominantly within the nodules. A peak in Ire1 signalling was observed early during tumour initiation. The Perk pathway was activated during tumour progression. The Atf6 pathway was modestly activated only after tumour initiation. Consistent with the UPR activation, electron microscopy demonstrated ER expansion and reorganization in isolated HCC cells *in vivo*.

Strikingly, under ER stress or hypoxia, the Perk inhibitor and not the Ire1 inhibitor reduced cell viability via escalating proteotoxic stress. Importantly, the Perk inhibitor significantly decreased tumour burden in the mouse model. Thus, we provided the first evaluation of the UPR dynamics in a long-term cancer model and identified a small molecule Perk inhibitor as a new strategy for HCC therapy. However, the antitumour effect of this inhibitor was modest and we found induction of hyperglycaemia in the mice treated with the Perk inhibitor, confirming the essential role of Perk in insulin biosynthesis.

Secondly, we assessed the impact of ER stress in tumour initiation and progression by applying tauroursodeoxycholic acid (TUDCA), a bile acid with chaperone properties reducing ER stress, in the diethylnitrosamine-induced HCC model in preventive and therapeutic settings. Administration of TUDCA in the preventive setting reduced carcinogen-induced elevation of liver enzyme levels, apoptosis of hepatocytes and tumour burden. TUDCA also suppressed carcinogen-induced pro-apoptotic UPR. Furthermore, TUDCA administration after tumour development did not alter orthotopic tumour or HepG2 xenograft growth. Thus, these results identified the UPR as a key pathway in hepatocarcinogenesis and showed that TUDCA attenuates hepatocarcinogenesis by suppressing carcinogen-induced ER stress-mediated cell death without stimulating tumour progression. Therefore, this chemical chaperone could represent a novel chemopreventive agent.

Thirdly, we assessed the effect of established or potential HCC treatments possibly modulating the UPR, including sorafenib, artesunate, PlGF inhibition and proteasome inhibition, on the tumour growth and UPR signature in HCC. Sorafenib, a multi-kinase inhibitor, is currently the only drug available for the treatment of advanced HCC, but effects are limited. Given the importance of the UPR and UPR-induced autophagy in HCC, we questioned whether the use of rationally designed combinations of sorafenib with clinically applicable modulators of the UPR and autophagy would be more effective than sorafenib monotherapy. We found that sorafenib activated the UPR and autophagy in HCC cells. Furthermore, sorafenib-mediated reduction in tumour cell proliferation was dependent on proteotoxicity and IRE1 RNase activity. Targeting of the UPR or autophagy separately did not enhance the antitumour efficacy of sorafenib. However, the combination with an ER stress inducer and an inhibitor of adaptive protein refolding or autophagy potentiated the efficacy. Thus, triple therapies of sorafenib with inducers of ER stress and inhibitors of autophagy seem to enhance the antitumour potential of sorafenib.

Artemisinins are antimalarial drugs that exert anticancer activity, possibly by inducing ER stress. We evaluated the effects of artesunate, a semisynthetic derivative of artemisinin, on tumour growth, angiogenesis and the UPR in HCC. We found that artesunate dose dependently reduced cell viability in different HCC cells. These effects were enhanced by hypoxia. In mice, artesunate decreased vessel density and tumour burden. These in-vivo effects were enhanced by combination with sorafenib. Furthermore, artesunate modulated the UPR *in vitro* and *in vivo*, increasing proapoptotic signalling. Thus, clinical trials with artesunate as monotherapy or in combination with current hypoxia-inducing approaches are necessary. Therefore, we initiated a phase I dose-escalation study evaluating the safety and pharmacokinetics of oral artesunate in patients with advanced HCC (DESPARTH trial).

We previously showed that the inhibition of placental growth factor (PlGF) exerts antitumour effects and induces vessel normalisation, possibly reducing hypoxia. However, the exact mechanism underlying these effects remains unclear. Because hypoxia and ER stress have been implicated in HCC progression, we assessed the interactions between PlGF and these microenvironmental stresses. Both the genetic and pharmacological inhibitions of PlGF reduced the chaperone levels and the activation of the PERK pathway in experimental HCC. We identified that tumour hypoxia was attenuated. Furthermore, hypoxic exposure activated the PERK pathway *in vitro*, suggesting PlGF inhibition may diminish PERK activation by improving oxygen delivery via vessel normalisation.

The first-in-class proteasome inhibitor bortezomib has been approved in clinical use against hematologic malignancies and has shown modest activity in a variety of solid tumours. However, a considerable proportion of subjects fail to respond to bortezomib and have adverse events. Recently, the next-generation orally bioavailable proteasome inhibitor oprozomib was developed. Oprozomib dose dependently reduced viability and proliferation of human HCC cells. The effect of oprozomib on the UPR pattern was dual: oprozomib inhibited the cytoprotective transcriptional program of ATF6 but increased the pro-apoptotic UPR-mediated protein levels by prolonging protein half-life. Oral oprozomib displayed antitumour effects in the HCC models. Importantly, combination of oprozomib with PERK activators stimulating CHOP induction improved the antitumour efficacy compared to oprozomib monotherapy without cumulative toxicity.

In conclusion, the UPR seems to be involved in the different steps of hepatocarcinogenesis and HCC survival under tumour microenvironmental stress. Consequently, chemopreventive and therapeutic targeting of the UPR holds significant potential in HCC.

Samenvatting

Hepatocellulair carcinoom (HCC) is wereldwijd de 2de belangrijkste oorzaak van kanker-gerelateerde mortaliteit. Aangezien de huidige behandelingsopties slechts voor een klein deel van de patiënten goede overlevingskansen bieden is er een dringende nood aan innovatieve behandelingen.

Het endoplasmatisch reticulum (ER) is verantwoordelijk voor eiwittranslocatie, opvouwing en post-translationele modificaties. Vervolgens worden de mature eiwitten na een kwaliteitscontrole verder getransporteerd naar het Golgi apparaat. Eiwitopvouwing is gevoelig aan stress in de cellulaire micro-omgeving en accumulatie van ongevouwen eiwitten in het ER lumen, een status die ER stress wordt genoemd, activeert intracellulaire signaalwegen die trachten de eiwithomeostase in het ER te herstellen. Deze "unfolded protein response" (UPR) verhoogt de eiwitopvouwingscapaciteit, vermindert de globale eiwitsynthese en stimuleert de ER-geassocieerde eiwitafbraak. Binnen de UPR zijn er drie voorname ER stress transducers geïdentificeerd: inositol-requiring enzyme-1 (IRE1), PKR-like endoplasmic reticulum kinase (PERK) en activating transcription factor 6 (ATF6). Echter, als de ER stress te ernstig of persistent is, wordt apoptose geïnitieerd. De UPR is betrokken bij diverse pathologieën, waaronder metabole, neurodegeneratieve en inflammatoire pathologieën, maar ook bij kanker. Zo werd recent UPR activatie in humane HCC stalen aangetoond. Aangezien de UPR kan leiden tot paradoxale effecten op celoverleving is het onduidelijk of er een therapeutisch venster bestaat waarbij UPR manipulatie kan worden aangewend in kankerbehandeling of -preventie. Hiervoor is een adequaat inzicht van de UPR signaaltransductie tijdens de verschillende stappen van de carcinogenese van essentieel belang.

Hepatocarcinogenese begint met de eerste genotoxische schade, gevolgd door klonale expansie van een premaligne naar een maligne laesie (tumorpromotie) en finaal tot tumorprogressie. Deze studie focust op de rol en het therapeutisch potentieel van ER stress en de UPR in de hepatocarcinogenese.

Vooreerst hebben we de UPR dynamiek gemonitord in de tijd in een orthotoop muismodel geïnduceerd door toediening van het carcinogeen diethylnitrosamine. Vervolgens hebben we de effecten van UPR-modulatie op de viabiliteit en proliferatie van HCC cellen *in vitro* en in het desbetreffende muismodel onderzocht. Hierbij stelden we vast dat de expressie van ER-residente chaperones piekte tijdens tumorinitiatie en verder toenam tijdens tumorprogressie. Tijdens tumorinitiatie werd eveneens een piek in het Ire1 signaal waargenomen.

De Perk pathway werd geactiveerd tijdens tumorprogressie. De Atf6 pathway werd mild geactiveerd na tumorinitiatie. Elektronenmicroscopie identificeerde ER expansie en reorganisatie, ultrastructurele kenmerken van ER stress, in HCC cellen *in vivo*. Verder werd er vastgesteld dat bij ER stress of hypoxie, de Perk inhibitor en niet de Ire1 inhibitor de celviabiliteit via escalerende proteotoxiciteit verminderde. Toediening van de Perk inhibitor reduceerde de tumorgroei. Kortom, deze studie leidde tot de eerste evaluatie van de UPR dynamiek in een kankermodel geïnduceerd door chronische carcinogeenexpositie en identificeerde de Perk inhibitor als een potentiële therapeutische strategie. Echter, het antitumoraal effect van deze inhibitor was beperkt en we detecteerden inductie van diabetes door de Perk inhibitor.

Ten tweede hebben we de impact van ER stress op tumorinitiatie en -progressie geanalyseerd door het toepassen van tauroursodeoxycholic acid of kortweg TUDCA, een galzuur met chaperone eigenschappen die ER stress antagoneert, in het HCC model in de preventieve en therapeutische setting. TUDCA toediening in de preventieve setting reduceerde de carcinogeen-geïnduceerde leverenzymen, incidentie van apoptotische hepatocyten, pro-apoptotische UPR signalisatie en tumorlast. TUDCA toediening na tumorontwikkeling daarentegen had geen effect op de tumorgroei. Deze resultaten identificeerden de UPR als een belangrijke as in hepatocarcinogenese en toonden aan dat TUDCA hepatocarcinogenese reduceert door onderdrukking van carcinogeen-geïnduceerd UPR-gemedieerde apoptose zonder stimulatie van tumorprogressie. Hierdoor kan dit chemisch chaperone als een nieuw chemopreventief agens worden beschouwd.

Ten derde onderzochten we het effect van erkende of potentiële HCC behandelingen die mogelijks de UPR moduleren. Hierbij includeerden we sorafenib, artesunaat, PlGF inhibitie en proteasoom inhibitie en onderzochten we het effect van deze op de tumorgroei en het UPR patroon in HCC. Sorafenib, een multi-kinase inhibitor, is momenteel het enige geneesmiddel beschikbaar voor gevorderd HCC. Echter is het overlevingsvoordeel door sorafenib beperkt tot enkele maanden. Gezien het belang van de UPR en autofagie, een katabool proces waarbij subcellulaire componenten via lysosomale enzymen worden afgebroken, vroegen we ons af of het gebruik van rationeel gedesignde combinaties van sorafenib met klinisch toepasbare modulators van de UPR en/of autofagie effectiever zou zijn dan sorafenib monotherapie. We stelden vast dat sorafenib de UPR en UPR-geïnduceerde autofagie activeert in HCC cellen en dat de sorafenib-gemedieerde reductie in cellulaire proliferatie afhankelijk is van proteotoxiciteit en IRE1. Inhibitie van de UPR of autofagie afzonderlijk verbeterde het anti-tumor effect van sorafenib echter niet.

Maar combinatie van een ER stress inductor samen met een remmer van adaptieve heropvouwing of autofagie versterkte het effect van sorafenib.

Artemisinines zijn antimalariamiddelen die een antitumoraal effect blijken te hebben in verschillende kankertypes, eventueel door inductie van ER stress. We evalueerden de effecten van artesunaat, een semi-synthetisch derivaat van artemisinine, op tumorgroei, angiogenese en de UPR in HCC. We vonden dat artesunaat dosisafhankelijk de viabiliteit van HCC cellen verminderde en dat deze effecten bovendien werden versterkt door hypoxie. Artesunaat verminderde tevens de bloedvatdensiteit en tumorlast *in vivo*. Hetgeen werd versterkt in combinatie met sorafenib. Verder moduleerde artesunaat de UPR waardoor pro-apoptotische UPR signalering optrad. Bijgevolg lijken klinische studies met artesunaat als monotherapie of in combinatie met huidige hypoxie-inducerende behandelingen aangewezen. Daarom zijn we gestart met een fase I dosisescalatie studie ter evaluatie van de veiligheid en farmacokinetiek van oraal artesunaat bij HCC patiënten (DESPARTH trial).

We toonden eerder aan dat inhibitie van de placentale groeifactor (PlGF) bloedvatnormalisatie en antitumorale effecten induceert. Het onderliggend mechanisme is echter onduidelijk. Omdat hypoxie en ER stress betrokken blijken bij HCC, onderzochten we de interacties tussen PlGF en deze stressoren. Zowel genetische als farmacologische PlGF inhibitie onderdrukte de chaperones en Perk pathway in HCC. We identificeerden dat PlGF inhibitie tumorhypoxie tempert en dat hypoxie de PERK pathway activeert, wat erop wijst dat PlGF inhibitie de Perk activatie reduceert door verbeterde zuurstofvoorziening via bloedvatnormalisatie.

De first-in-class proteasoominhibitor bortezomib is in klinisch gebruik bij hematologische maligniteiten en heeft een bescheiden activiteit aangetoond in verschillende solide tumoren. Echter, een aanzienlijk deel van patiënten reageren niet op bortezomib en hebben majeure bijwerkingen. Recent werd de next-generation proteasoominhibitor oprozomib ontwikkeld.

Oprozomib verminderde de proliferatie van HCC cellen op een dosisafhankelijke manier. Het effect van oprozomib op het UPR patroon was tweeledig: oprozomib remde het cytoprotectief transcriptioneel programma van ATF6, maar verhoogde de pro-apoptotische UPR-gemedieerde eiwitniveaus door verlengde halfwaardetijd. Oraal oprozomib reduceerde de tumorgroei *in vivo*. Combinatie van oprozomib met PERK activatoren verbeterde de werkzaamheid in vergelijking met oprozomib monotherapie zonder cumulatieve toxiciteit.

We besluiten dat de UPR betrokken is bij verschillende stappen van hepatocarcinogenese en de overleving van HCC cellen in de stressvolle tumor micro-omgeving. Bijgevolg heeft het chemopreventief en therapeutisch manipuleren van de UPR een belangrijk potentieel in HCC.

Chapter 1

General introduction

1. Hepatocellular carcinoma

1.1. Introduction

Tumours of the liver are classified as being either primary (originating from the liver) or metastatic (spread from another organ to the liver). Primary liver tumours may be further divided into those that are benign, which are not cancerous and remain in the liver, or malignant, which progress with local expansion, intrahepatic spread and distant metastases [1]. The most common primary malignant tumour of the liver is a **hepatocellular carcinoma** (HCC). HCC occurs predominantly in patients with underlying chronic liver disease and cirrhosis [1], [2].

Figure 1. Large hepatocellular carcinoma. Note the heterogeneity within the nodule. Image courtesy of Arief Suriawinata, Department of Pathology, Dartmouth Medical School, USA.

1.2. Pathophysiology of hepatocellular carcinoma

The ratio of cell growth and death is precisely balanced through developmental and homeostatic processes in multi-cellular organisms [3]. Sensu stricto, cancer is a **genetic** disease and the genetic alterations that lead to most cancers arise in the DNA of a somatic cell [4]. Because of these genetic changes, cancer cells proliferate irrepressibly, producing malignant cells that invade surrounding healthy tissue and tend to metastase, that is, to spawn cells that break away from the parent mass, enter the lymphatic or vascular circulation, and spread to distant sites in the body where they establish metastases that are no longer amenable to surgical resection [2].

The **hallmarks** of cancer comprise biological capabilities acquired during multistep carcinogenesis [3]. They include sustaining proliferative signalling, evading growth suppressors, resisting cell death, enabling replicative immortality, inducing angiogenesis, reprogramming of energy metabolism, evading immune destruction and activating invasion and metastasis. Underlying these hallmarks are genome instability, which generates the genetic diversity that expedites their acquisition, and inflammation, which fosters multiple hallmarks. In addition to cancer cells, tumours exhibit another dimension of complexity: they contain a repertoire of recruited, ostensibly normal cells that create the tumour microenvironment. Recent evidence suggests that pathophysiologic conditions unique to the tumour microenvironment initiate tumour cell stress signals that converge upon the endoplasmic reticulum (ER), resulting in a condition termed "ER stress" (see section 2.2) [5].

Also hepatocarcinogenesis is a **multistep** process: the presence of specific risk factors (see section 1.4) promotes genotoxicity leading to a cascade of molecular and cellular deregulations that ultimately result in malignant transformation of hepatocytes and generally develops within liver cirrhosis related to various aetiologies [1], [2]. In cirrhosis, precancerous dysplastic macronodules transform into early HCCs that evolve into small and progressed HCCs, and finally lead to advanced HCC [6], [7]. In rare cases, HCC develops in a normal liver, with some of these tumours potentially resulting from malignant transformation of hepatocellular adenomas [8].

High-resolution analyses have depicted the **molecular heterogeneity** of HCC [9]. A broad variety of **pathways** activated in HCC have been reported including the Wnt/β-catenin, Ras/MAPK, insulin-like growth factor, PI3K/Akt/mammalian target of rapamycin (mTOR), vascular endothelial growth factor (VEGF), hepatocyte growth factor/cMET signalling among many others [4]. Depending on the specific alterations, distinct molecular subclasses have been defined (see section 1.6) [10].

Furthermore, several **structural alterations** have been characterized. Recent studies identified an average of 30-40 mutations per tumour, among which 6–8 are considered oncogenic drivers [11]. Mutations in TERT (60%, telomere stability), TP53 (30%, genome integrity guardian), CTNNB1 (25%, Wnt signalling), NFE2L2 (6-10%, oxidative stress) and ARID1A (10-16%, chromatin remodelling) and high-level amplifications in 11q13 (7%) and 6p21 (5%, contains VEGF) are the most relevant ones [4], [10]. Another study identified 161 putative driver genes associated with 11 recurrently altered pathways [9]. Associations of mutations defined 3 groups of genes related to aetiology. However, no oncogenic addiction loop for any driver has been defined in HCC. Intriguingly, well-known genes commonly mutated in other solid tumours such as EGFR, PIK3CA or KRAS are rarely mutated in HCC [11].

Next to the structural alterations, several **prognostic mRNA-based molecular signatures** from tumour tissue have been reported [12], [13]. Signatures identifying progenitor cell-like and/or cholangiocyte profile (EPCAM signature3, CK19 signature) show worse prognosis [13]. Likewise, a 5-gene score signature (TAF9, RAN, RAMP3, KRT19, HN1) predicted overall survival in four independent cohorts [14]. However, there is significant **intratumour heterogeneity** (Figure 1) leading to an underestimation of the tumour genomics landscape portrayed from single tumour biopsy [15].

In conclusion, the interindividual and intratumour heterogeneity, biological redundancies and presence of several growth factors and cytokines potentially involved in HCC progression make it extremely difficult to select the best genetic target for therapy and stimulated us to target other hallmarks of cancer, such as angiogenesis or effect of peritumoural microenvironmental stress.

1.3. Epidemiology of hepatocellular carcinoma

HCC is the fifth most common cancer in men (554,000 cases, 7.5% of total cancer incidence) and the ninth in women (228,000 cases, 3.4%) [16]. HCC has a strong male preponderance with a male to female ratio estimated to be 2.4, which is partially explained by the protective role of oestrogens and HCC-promoting effects of androgens [17]. It is mainly a problem of the less developed regions where 83% of the estimated 782,000 new cases worldwide occurred in 2012. In men, high incidence regions are Eastern and South-Eastern Asia (age-standardised rates: 31.9 and 22.2 resp.). Intermediate rates occur in Southern Europe (9.5) and Northern America (9.3) and the lowest rates are in Northern Europe (4.6).

HCC is the **second leading cause of cancer-related mortality worldwide**, estimated to be responsible for nearly **746,000 deaths in 2012** (9.1% of total cancer-related mortality) [16]. The prognosis is very poor (overall ratio of mortality to incidence of 0.95). The incidence increases progressively with advancing age in all populations, reaching a peak at 70 years. Unfortunately, HCC is one of the cancers with a still increasing incidence rate [18], [19].

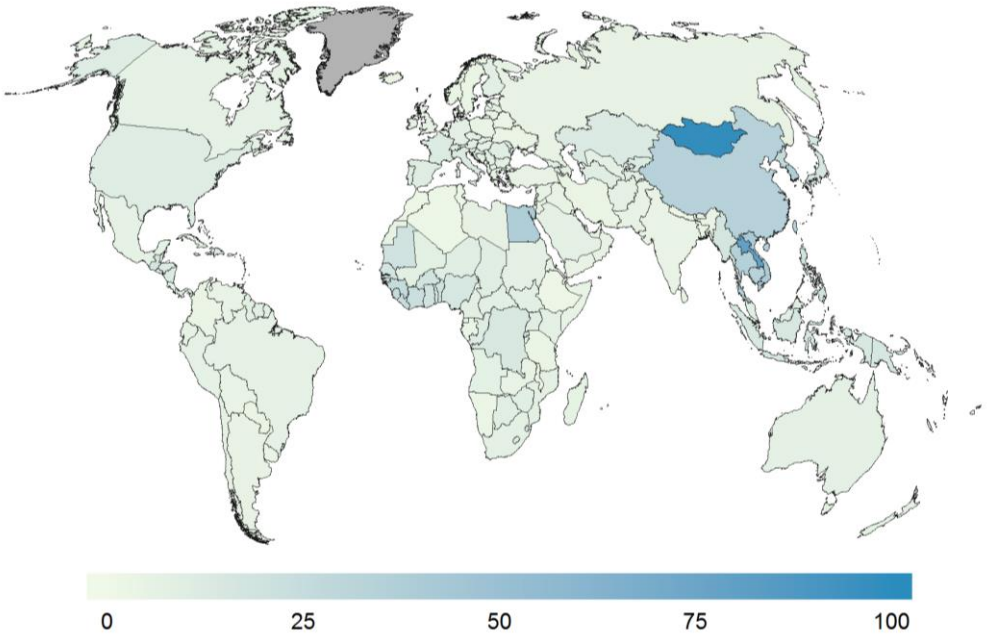

Figure 2. Estimated liver cancer incidence worldwide in 2012: men. Estimated age-standardised rates per 100,000 [16].

1.4. Aetiology of hepatocellular carcinoma

Hepatitis viral infection (hepatitis B (**HBV**) and C (**HCV**)), chronic **alcohol** abuse and non-alcoholic steatohepatitis (**NASH**) are the major risk factors of liver cirrhosis and cancer [1]. Other risk factors include fungal aflatoxin B1 exposure, hemochromatosis, α-1-antitrypsin deficiency and tyrosinaemia [2]. Worldwide, 54% of HCC cases can be attributed to HBV infection (which affects 400 million people globally), while 31% can be attributed to HCV infection (which affects 170 million people), leaving 15% to other aetiologies. In Africa and East Asia, the largest attributable fraction is due to HBV (60%) whereas in the Western world, only 20% of cases can be attributed to HBV, while chronic HCV and alcohol consumption appear to be the major risk factors (Table 1) [20]. Recently, great advances in HCV therapies were made. For more information, please see our review concerning 'New therapies for hepatitis C' (YP. Vandewynckel *et al.*, Tijdschr. voor Geneeskunde, 2014). Long-term follow-up studies have demonstrated that 1-8% of cirrhotic patients per year develop HCC [21]. Ultimately, one-third of cirrhotic patients will develop HCC during their lifetime [22]. In general, liver disease severity, age and male gender correlate with HCC development among cirrhotic patients [23]. Since risk factors are well known, prevention by risk factor reduction is an achievable objective. Control of HBV and HCV, as well as reduction in alcohol consumption is recommended [24]. While health plans are implemented to achieve this goal, the epidemic of overweight and metabolic syndrome leading to NASH-induced HCC has emerged as a significant risk factor [25]. Alternatively, development of chemopreventive agents could drastically reduce HCC mortality [26]. However, randomized controlled chemoprevention trials are logistically and ethically challenging.

Table 1. Geographical distribution of main risk factors for hepatocellular carcinoma worldwide.

Geographic area	AAIR	Risk factors		Alcohol	Others
	M/F	HCV (%)	HBV (%)	(%)	(%)
Europe	6.7/2.3	60-70	10-15	20	10
Southern	10.5/3.3				
Northern	4.1/1.8				
North America	6.8/2.3	50-60	20	20	10 (NASH)
Asia and Africa		20	70	10	10 (Aflatoxin)
Asia	21.6/8.2				
China	23/9.6				
Japan	20.5/7.8	70	10-20	10	10
Africa	1.6/5.3				
WORLD	16/6	31	54	15	

AAIR, age-adjusted incidence rate. Adapted from [1].

1.5. Diagnosis of hepatocellular carcinoma

Diagnosis of HCC is based on the diagnostic algorithm in Figure 4 [1]. In cirrhotic patients, nodules **less than 1 cm** in diameter detected by ultrasound should be followed every 4 months the first year and every 6 months thereafter. In cirrhotic patients, diagnosis of HCC for nodules of **1-2 cm** should be based on non-invasive criteria or biopsy-proven pathological confirmation. In cirrhotic patients, nodules **more than 2 cm** can be diagnosed for HCC based on typical features on one imaging technique. In case of uncertainty or atypical radiological findings, diagnosis should be confirmed by biopsy.

Pathological diagnosis is based on the recommendations of the International Consensus Panel [6]. Non-invasive criteria can only be applied to cirrhotic patients and are based on imaging techniques obtained by 4-phase multidetector CT or dynamic contrast-enhanced MRI [1]. Diagnosis is based on the typical hallmark of HCC, i.e. **hypervascular** in the arterial phase with **washout** in the portal venous or late phases (see section 4.1).

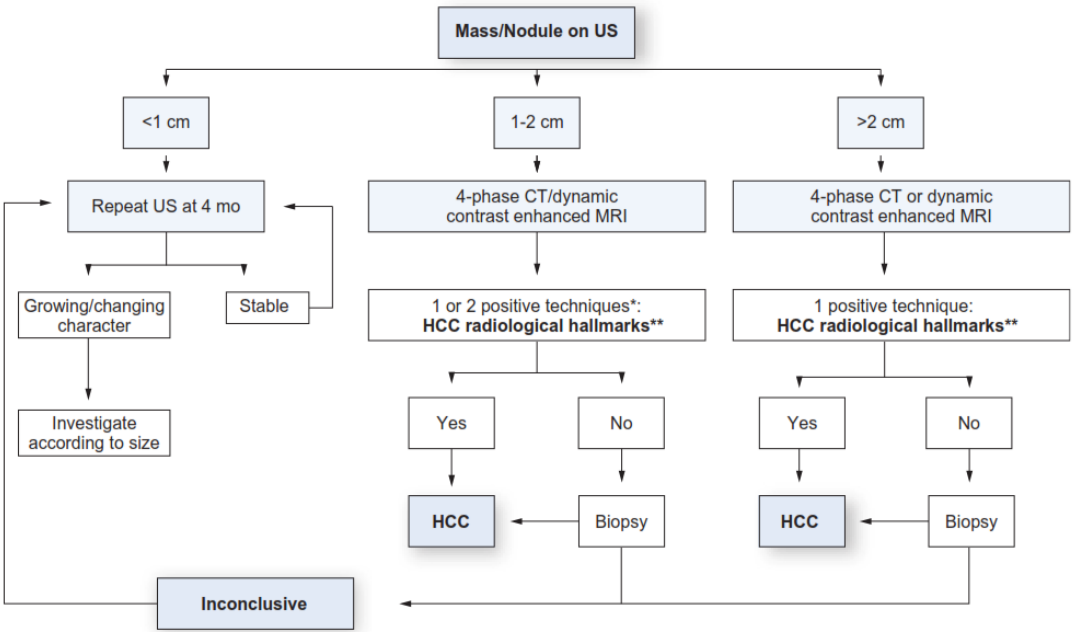

Figure 4. Diagnostic algorithm for hepatocellular carcinoma. **HCC radiological hallmark: arterial hypervascularity and venous/late phase wash-out. Adapted from [1].

1.6. Treatment of hepatocellular carcinoma

The **Barcelona-Clinic Liver Cancer (BCLC) staging** system is recommended for prognostic prediction and treatment allocation [1]. The BCLC classification divides HCC patients in 5 stages (0, A, B, C and D) according to pre-established prognostic variables and allocates therapies according to treatment-related status (Fig. 5). **Prognosis prediction** is defined by variables related to tumour status (size, number, vascular invasion, N1, M1), liver function (Child–Pugh's) and performance status of the patient (ECOG). **Treatment allocation** incorporates treatment dependant variables, which have been shown to influence therapeutic outcome, such as bilirubin, portal hypertension or presence of symptoms.

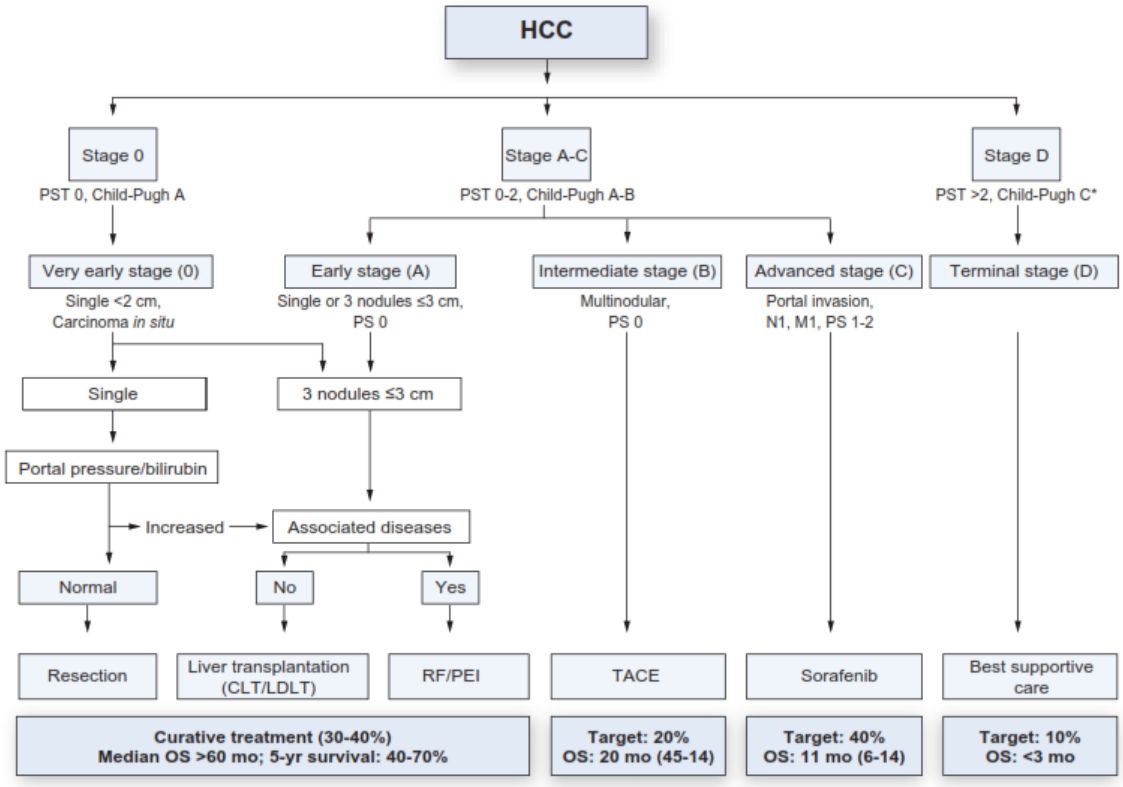

Figure 5. BCLC staging system and treatment strategy. Adapted from [1].

Resection is the treatment option for patients with solitary tumours and well-preserved liver function, as normal bilirubin with either hepatic venous pressure gradient ≤10 mmHg or platelet count ≥100,000. Large tumours are not well served by ablation because long lasting complete response in HCC >3 cm is less frequent and recurrence rate is high [27]. However, resection may be successful and this is why tumour size does not constitute a contraindication by itself [1]. Additional indications for patients with multifocal tumours meeting Milan criteria (≤3 nodules ≤3 cm) or with mild portal hypertension not suitable for liver transplantation require prospective comparisons with loco-regional treatments. Peri-operative mortality of resection in cirrhotic patients is expected to be 2-3%. **Tumour recurrence** represents the major complication of resection [28]. In case of recurrence, the patient will be re-assessed by BCLC staging and re-treated accordingly [1].

If patients present hepatic decompensation, the expected outcome offered by **liver transplantation**, if the Milan criteria are not exceeded, is superior to resection and ablation [18]. Peri-operative mortality and one-year mortality are expected to be approximately 3% and ≤10%, respectively [1]. Modest expansion of the Milan criteria applying the "up-to-seven" in patients without microvascular invasion achieves competitive outcomes.

Local ablation with radiofrequency or percutaneous ethanol injection is considered the standard of care for patients with BCLC 0-A tumours not suitable for surgery [1]. **Chemoembolization** is recommended for patients with BCLC B, multinodular asymptomatic tumours without vascular invasion or extra-hepatic spread. However, although severe events are infrequent, chemoembolization is associated with transient post-embolization syndrome in most cases and there is still no standardized protocol for chemoembolization in terms of treatment schedule, type and dosage of anti-cancer drug [18].

Multiple guidelines have been developed to assist clinicians in HCC management. Though, we reported that the methodological quality of guidelines on chemoembolization in HCC management is poor [29]. This results in important discrepancies between guideline recommendations, creating confusion in clinical practice. Incorporation of the Appraisal of Guidelines Research and Evaluation II (AGREE II) instrument in guideline development may improve quality of future guidelines by increasing focus on methodological aspects [30].

Conventional chemotherapy, either alone or in combination, administered intravenously or intra-arterially, never reached positive results [2]. Based on the positive phase III SHARP trial demonstrating a median overall survival of 10.7 months for sorafenib-treated vs. 7.9 months for placebo-treated HCC patients [31], **sorafenib** is the standard systemic therapy for advanced HCC. In terms of **toxicity**, there were more cases of diarrhoea, weight loss, hand-foot skin reaction and hypophosphatemia among the patients receiving sorafenib [31]. In addition, we reported (YP. Vandewynckel *et al. Cerebellar stroke in a low cardiovascular risk patient associated with sorafenib treatment for fibrolamellar hepatocellular carcinoma.* Clin Case Rep. 2014,2,4-6) a case of a 26-year-old man with fibrolamellar HCC, who had a cerebrovascular accident while being treated with sorafenib, illustrating a probable relationship between the use of sorafenib and vascular adverse effects in low cardiovascular risk patients.

Sorafenib acts by inhibiting the serine threonine kinases Raf-1 and B-Raf and the receptor tyrosine kinase activity of VEGF and platelet-derived growth factor (PDGF) receptors, among others [32] and is indicated for patients with well-preserved liver function (Child-Pugh A) and with advanced tumours (BCLC C) or those progressing upon loco-regional therapies [1]. To date, there are no biomarkers available to identify the best responders and no second-line treatment for patients with intolerance or failure to sorafenib.

Molecular classification should aid in understanding the biological subclasses and oncogenic drivers and optimize benefits from targeted therapies and enrich trial populations [1], [32]. Different molecular classes have been characterized including a Wnt class (25% of cases; enriched with CTNNB1 mutations and HCV aetiology), a proliferation/progenitor class (50% of cases; worse prognosis; with two subclasses: S1-TGF-β and S2-EpCAM positive) and an inflammation/interferon class [10], [12]. Nonetheless, no molecular subclass has been reported to respond to a specific targeted therapy.

Several therapies targeting signalling cascades involved in hepatocarcinogenesis have been explored in phase III trials [32]. However, none of the drugs tested have shown positive results in the first-line (tyrosine kinase inhibitors (TKI): brivanib, sunitinib, erlotinib and linifanib) or second-line (TKI: brivanib and mTOR inhibitor: everolimus) setting after sorafenib progression (Table 2). Regorafenib, lenvatinib, cabozantinib and tivantinib are currently being evaluated in phase III trials [18].

Reasons for **failure** are diverse and include lack of understanding of critical drivers of tumour progression, liver toxicity or marginal antitumour potency [32]. If targeted therapy is aimed to act on specific targets it would make sense to select patients according to the recognition of the pathway to be modulated. This enrichment policy is sound but the challenge is how to properly profile the biomarker status. As indicated earlier, HCCs present a marked heterogeneity within the same nodule (Figure 1) and across nodules making a single biopsy unlikely to provide an accurate profiling of the tumour.

Table 2. Randomized phase III clinical trials completed in HCC in first and second line (2007–2014). (Modified from [18])

Year	Randomized drugs	n	TTP (mo)	*p* value	OS (mo)	*p* value
2008	Sorafenib *vs.* placebo	299/303	5.5 *vs.* 2.8	<0.001	10.7 *vs.* 7.9	<0.001
2009		150/76	2.8 *vs.* 1.4	<0.001	6.5 *vs.* 4.2	0.01
2012	Sorafenib + erlotinib *vs.* sorafenib	362/358	3.2 *vs.* 4	n.s.	9.5 *vs.* 8.5	n.s.
2012	Linifanib *vs.* sorafenib	514/521	5.4 *vs.* 4	0.001	9.1 *vs.* 9.8	n.s.
2013	Sunitinib *vs.* sorafenib	530/544	3.6 *vs.* 3.6	n.s.	7.9 *vs.* 10.2	n.s.
2013	Brivanib *vs.* sorafenib	577/578	4.2 *vs.* 4.1	n.s.	9.5 *vs.* 9.9	n.s.
2013	FOLFOX-4 *vs.* doxorrubicin	184/187	2.9 *vs.* 1.8	n.s.	6.4 *vs.* 4.9	n.s.
2013	Brivanib *vs.* placebo	263/132	4.2 *vs.* 2.7	0.001	9.4 *vs.* 8.2	n.s.
2014	Everolimus *vs.* placebo	362/184	2.9 *vs.* 2.6	n.s.	7.6 *vs.* 7.3	n.s.
2014	Ramicirumab *vs.* placebo	283/282	3.5 *vs.* 2.6	<0.0001	9.2 *vs.* 7.6	n.s.

n.s., not significant; TTP, time to progression; OS, overall survival.

2. Endoplasmic reticulum stress and the unfolded protein response

2.1. The endoplasmic reticulum: a biosynthetic factory

The endoplasmic reticulum (ER; Figure 6) is the central organelle in the secretory pathway and provides a specialized environment for protein translocation, **protein folding** by a machinery of molecular chaperones and post-translational modifications that allow further transport of proteins to the Golgi and ultimately to vesicles for secretion or display on the membrane [33], [34]. The rates of protein synthesis, folding and trafficking are precisely coordinated by an efficient system termed **quality control** to ensure that only properly folded proteins exit the ER. Misfolded proteins are either retained within the ER or subject to degradation by the proteasome-dependent ER-associated protein degradation (ERAD) pathway or by autophagy (see section 3).

Furthermore, the ER is the major site for the synthesis of **sterols and phospholipids** that constitute the bulk of the lipid components of all membranes. The ER, therefore, plays an essential role in regulating the lipid composition of membranes, which, in turn, determines the biophysical properties and functions of cell membranes [35]. ER membrane expansion generally reflects the increased secretory capacity or the accumulation of unfolded proteins in the ER [35], [36].

Finally, the ER is the main site for storage of intracellular **Ca^{2+}**. The concentration of Ca^{2+} in the ER lumen can reach ~5 mM [37]. The majority of ER-luminal Ca^{2+} is bound to molecular chaperones and is essential for their function.

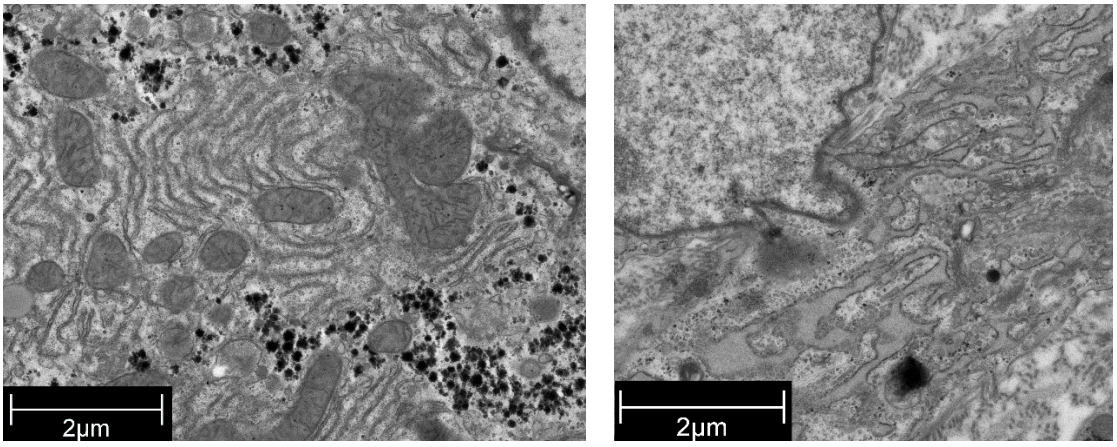

Figure 6. Transmission electron microscopy showing the normal morphology of the endoplasmic reticulum of a hepatocyte (left) versus the expanded morphology of a hepatocellular carcinoma cell (right).

2.2. Endoplasmic reticulum stress

The ER is a highly dynamic organelle and responds to perturbations in its function, a process named **ER stress**, through a series of signalling cascades known as the **unfolded protein response** (UPR) [38]. The UPR is a tightly orchestrated collection of intracellular signal transduction reactions designed to cope with misfolded proteins and restore ER proteostasis [33], [34]. However, chronic or irremediable ER stress results in cell apoptosis [39].

The UPR regulates the size, the shape and the components of the ER machinery to accommodate the fluctuating demands on protein folding, as well as other ER functions in coordination with different physiological and pathological conditions [40].

Recent studies on the integration of the UPR with metabolic stress, oxidative stress and inflammatory signalling highlight new insights into the diverse cellular processes regulated by the UPR [41], [42]. For example, UPR signalling was shown to intersect at many levels with the innate and adaptive immune responses [42].

Three canonical UPR branches have been identified: inositol-requiring protein-1α (IRE1), protein kinase RNA (PKR)-like ER kinase (PERK) and activating transcription factor 6 (ATF6). Next to the canonical UPR, the OASIS family represents a group of additional ER stress transducers and UPR regulators [43]. These ER membrane-bound sensors operate in parallel and use unique mechanisms of signal transduction. The IRE1 branch is the most conserved and sole branch of the UPR in lower eukaryotes [44]. Evolution later added the PERK and ATF6 branches to metazoan cells.

Under physiological conditions, the luminal domains of PERK and ATF6 are bound to the ER-resident chaperone Binding immunoglobulin Protein or glucose-regulated protein, 78 kDa (BiP or GRP78), which keeps them inactive [34]. When unfolded proteins accumulate in the ER, GRP78 binds with high affinity to the exposed hydrophobic regions of the unfolded proteins and is thereby released from these complexes to assist with the folding of accumulated proteins. Upon activation, PERK, IRE1 and ATF6 induce signal transduction that alleviate the accumulation of misfolded proteins by increasing expression of ER chaperones, inhibiting protein entry into the ER by arresting global mRNA translation and stimulating retrograde transport of misfolded proteins from the ER into the cytosol for ubiquitination and destruction by ERAD [45]. Under conditions when ER stress is chronically prolonged and the protein load on the ER greatly exceeds its folding capacity, cellular dysfunction and UPR-mediated apoptosis occur [33].

Among the UPR pathways **IRE1** is a key molecule that functions as a rheostat regulating cell fate upon ER stress [38]. The alternative outputs from IRE1-mediated downstream signalling dictate opposing cell fates (survival versus death) during ER stress, which are critically influenced by the intensity and longevity of ER stress [34]. IRE1 is a transmembrane protein that consists of an N-terminal luminal sensor domain, a transmembrane domain and a C-terminal cytosolic effector that is responsible for both protein kinase and endoribonuclease activities [38]. Accumulation of unfolded proteins in the ER triggers oligomerization and autophosphorylation. The RNase mediates splicing of an intron from the X-box-binding protein-1 (XBP1) mRNA to allow production of the spliced XBP1 (XBP1s) protein, which is a stronger transcription factor compared to unspliced XBP1 (XBP1u) protein. Notably, XBP1u is not the only mRNA targeted by the IRE1 RNase [46]. For example, IRE1 also controls its own expression by cleaving its own mRNA. The XBP1s protein binds to promoters of several genes involved in the UPR and ERAD to restore proteostasis [47]. In addition to its cytoprotective function, IRE1 also stimulates activation of the apoptotic-signalling kinase-1 (ASK1), which causes activation downstream of stress kinases Jun-N-terminal kinase (JNK) and p38 MAPK that promote apoptosis. Among the apoptosis-inducing substrates of JNK are Bcl-2 and Bim, which are inhibited and activated, respectively, by JNK [33]. Also, p38 MAPK phosphorylates and activates the transcription factor C/EBP homologous protein (CHOP), which leads to major changes in gene expression that favour cell apoptosis, including increasing expression of Bim and DR5, while decreasing expression of Bcl-2 [48]. Recently, regulated IRE1-dependent decay of mRNA (RIDD) was shown to reduce ER localized mRNAs [46]. RIDD selectively targets and degrades mRNAs encoding proteins involved in protein folding. Prolonged RIDD can promote cell death, but its exact role is currently not well understood.

ATF6 is a transcriptional factor that upon ER stress translocates to the Golgi where it is cleaved by the action of two proteases: the serine protease site-1 (S1P) cleaves ATF6 in the luminal domain, while the N-terminal portion is subsequently cleaved by the site-2 protease (S2P) [34]. The cleaved N-terminal cytosolic domain of ATF6 subsequently translocates into the nucleus where it binds to ATF/cAMP-response elements and ER stress-response elements to activate target genes, such as chaperones GRP78, PDIA4, GRP94 but also CHOP [49].

When activated upon sensing ER stress, **PERK** oligomerizes and phosphorylates itself and the α subunit of eukaryotic translation initiation factor 2 (eIF2α), inactivating eIF2α and inhibiting global mRNA translation. Phosphorylation of eIF2α inhibits the recycling of eIF2α to its active GTP-bound form, which is required for the initiation of polypeptide chain synthesis [33]. Thereby, PERK prevents influx of *de novo* synthesized proteins into the stressed ER providing a time frame to restore ER function [50]. However, some mRNAs containing short open reading frames in their 5'-untranslated regions are preferentially translated when eIF2α is limiting. One of these encodes the activating transcription factor 4 (ATF4), whose translation is thus induced upon eIF2α phosphorylation. Two important target genes driven by ATF4 are the proapoptotic CHOP and growth arrest and DNA damage–inducible 34 (GADD34) [51]. Thus, the PERK pathway is strongly protective at modest levels of signalling but, paradoxically, can contribute signals to apoptosis [33]. This dualism is likely played out at the level of eIF2α. GADD34 encodes a regulatory subunit of protein phosphatase 1C that dephosphorylates eIF2α. Selective inhibition of the GADD34-PP1c complex, either by salubrinal or GADD34 deletion, protects cells against ER stress by prolonging low-level eIF2α phosphorylation. Besides elF2α, PERK can phosphorylate nuclear erythroid 2-related factor 2 (NRF2), which contributes to dissociation of the NRF2-Keap1 complex and thereby promotes expression of genes containing antioxidant response elements, preventing oxidative stress [52].

2.3. Endoplasmic reticulum stress in disease

The UPR has been implicated in a variety of diseases including **metabolic** such as diabetes and atherosclerosis, **neurodegenerative** such as Alzheimer's and Parkinson's diseases, amyotrophic lateral sclerosis, as well as rare prion disorders, and **inflammatory** diseases, and **cancer** [53],[54]. Signalling components of the UPR are rapidly emerging as targets for treatment of human diseases [41]. Many extracellular stimuli and fluctuations in intracellular homeostasis disrupt protein folding. Consequently, the cell uses its ER protein-folding status as an exquisite sensor to monitor intracellular homeostasis. Pharmacological insults were used to elucidate how cells cope with immediate and severe challenges to the protein-folding quality control. It is now evident that intracellular signalling, such as insulin anabolic responses, as well as pathophysiological conditions including hypoxia, oxidative stress, high or low glucose levels, acidosis, hyperlipidaemia, hyperhomocysteinaemia and inflammatory cytokines all disrupt protein folding and activate the UPR [33]. In solid tumours, the UPR mediates adaptation to various micro-environmental stressors [55].

2.4. Endoplasmic reticulum stress in cancer

Y.-P. Vandewynckel, D. Laukens, A. Geerts, E. Bogaerts, A. Paridaens, X. Verhelst, S. Janssens, F. Heindryckx, H. Van Vlierberghe. *The paradox of the unfolded protein response in cancer*. Anticancer Res. 2013,33,4683-4694. (Times cited: 13)

Review: The Paradox of the Unfolded Protein Response in Cancer

ANTICANCER RESEARCH
International Journal of Cancer Research and Treatment

Yves-Paul Vandewynckel[1], Debby Laukens[1], Anja Geerts[1], Eliene Bogaerts[1], Annelies Paridaens[1], Xavier Verhelst[1], Sophie Janssens[2, 3], Femke Heindryckx[4], Hans Van Vlierberghe[1]

[1]*Department of Hepatology and Gastroenterology, Ghent University, Ghent, Belgium;*
[2]*GROUP-ID Consortium, Ghent University and University Hospital, Ghent, Belgium;*
[3]*Unit Immunoregulation and Mucosal Immunology, VIB Inflammation Research Centre, Ghent, Belgium*
[4]*Department of Medical Biochemistry and Microbiology, Uppsala University, Uppsala, Sweden*

2.4.1. **Abstract**

The endoplasmic reticulum (ER) is an elaborate organelle that is essential for cellular function and survival. Conditions that interfere with ER functioning can lead to the accumulation of unfolded proteins, which are detected by transmembrane sensors that then initiate the unfolded protein response (UPR) to restore ER proteostasis. If the adaptive response fails, apoptotic cell death ensues. Many studies have focused on how this failure initiates apoptosis, particularly because ER stress-induced apoptosis is implicated in the pathophysiology of several diseases, including cancer. Whether the UPR inhibits tumour growth or protects tumour cells by facilitating their adaptation to stressful conditions within the tumour microenvironment is unknown, and dissection of the UPR network will likely provide answers to this question. In this review, we aim to elucidate the paradoxical role of the UPR in apoptosis and cancer.

2.4.2. **Introduction**

The endoplasmic reticulum (ER) consists of a membranous network that extends throughout the cytosol; here, proteins are synthesized, post-translationally modified and folded into correct conformations. Unlike the cytosol, the ER luminal environment is sufficiently oxidised to permit for cysteine oxidation and subsequent formation of the disulfide bonds that are critical to the correct conformations of many mature proteins (1). The ER contains stringent quality control systems that selectively export correctly-folded proteins and extract terminally-misfolded proteins for ubiquitin-dependent proteolytic degradation, a process known as ER-associated protein degradation (2) (Figure 1). However, if degradation is insufficient, misfolded proteins can accumulate. This phenomenon is called ER stress, and it activates the unfolded protein response (UPR). The UPR is generally considered to be the transcriptional induction of molecular chaperones in response to ER stress (3). However, gene expression profiling has demonstrated that, parallel to the chaperones, the UPR regulates genes involved in protein entry into the ER, calcium and redox homeostasis, ER quality control, autophagy, lipid biogenesis and vesicular trafficking. Additionally, ER stress attenuates global protein synthesis, a process that subsequently reduces the protein load to help re-establish equilibrium and is associated with cell-cycle arrest and tumour dormancy. Three ER stress transducers have been identified: protein kinase RNA-like endoplasmic reticulum kinase (PERK), inositol-requiring enzyme-1 (IRE1) and activating transcription factor-6 (ATF6; Figure 2) (4, 5). Most targets are co-regulated by IRE1, PERK and ATF6 to ensure the redundancy and robustness of this adaptive response (6).

Following initiation of malignancy, rapid tumour growth and inadequate vascularization result in microenvironmental stress. This condition activates a range of stress response pathways, including the UPR, which meticulously coordinate adaptive and apoptotic responses to ER stress. During tumourigenesis, the UPR enhances the ER protein-folding capacity and maintains ER protein homeostasis (or proteostasis), thereby counteracting apoptosis. The UPR, when coupled with induced tumour dormancy, dually protects neoplastic cells from apoptosis and permits recurrence once favourable growth conditions have been restored (7, 8). However, if ER stress is prolonged and the UPR fails to restore ER proteostasis, tumour cell apoptosis ensues. This review addresses this paradoxical role in cancer.

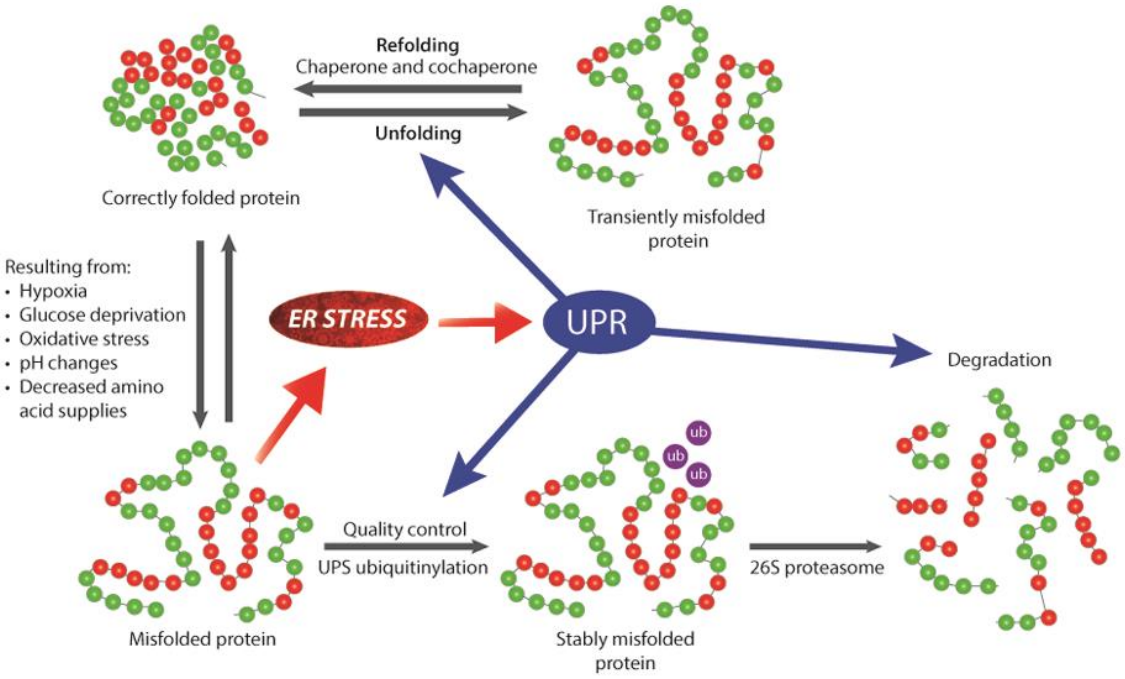

Figure 1. ***Cellular stress as the cause of protein misfolding.*** *Molecular chaperones stabilise and (un)fold newly-synthesised proteins into their proper conformations. During tumour formation, continuous endoplasmic reticulum (ER) stress eventually causes damage that the chaperones cannot correct. These proteins might then be recognised and degraded by the ubiquitin-proteasome system (UPS). However, if this process is insufficient to counter the accumulation of misfolded proteins, the unfolded protein response (UPR) is activated to induce chaperones, protein quality control and degradation.*

2.4.3. Extrinsic and Intrinsic Stressors that Activate the UPR During Tumourigenesis

Although tumours secrete angiogenic factors to promote angiogenesis, this is often insufficient to meet the elevated tumour metabolic requirements. Therefore, in addition to hypoxia (9), cells in developing tumours are subject to glucose deprivation, lactic acidosis, oxidative stress and decreased amino acid supplies (Figure 1). In addition to these extrinsic stressors, tumour-intrinsic stressors, such as errors in glycoprotein and lipid biosynthesis that result from an increased mutation rate, might also contribute to the induction of ER stress (10).

Hypoxia-mediated UPR activation is essential for tumour cell survival. The major UPR-inducing pathway in tumours is mediated by hypoxia. Human fibrosarcoma and lung carcinoma cells up-regulate 78-kDa glucose-regulated protein (GRP78) and X-box-binding protein 1 (XBP1) splicing under hypoxic conditions *in vitro*, whereas in human colon cancer cells, hypoxia induces the PERK-dependent phosphorylation of eukaryotic initiation factor-2α (eIF2α) and the translation of activating transcription factor-4 (ATF4; Figure 2) (8). A strong positive correlation was demonstrated between spliced XBP1 (XBP1s)-induced bioluminescence and tumour hypoxia in transgenic mice that developed spontaneous mammary carcinomas and exhibited luciferase reporter coupled XBP1 splicing (11). Additionally, the exposure of transformed mouse embryonic fibroblasts (MEFs) to hypoxia led to increased GRP78 and XBP1 expression, as well as increased ATF4 and C/EBP homologous protein transcription factor (CHOP) expression. A potential UPR trigger in hypoxic conditions is ER oxidase 1α (ERO1α), an oxidoreductase that catalyses disulfide bond formation in nascent proteins in an oxygen-dependent manner. Although hypoxia transcriptionally induces ERO1α, reduced oxygen tension impairs ERO1α activity and subsequent protein folding. Another UPR-inducing mechanism is the upregulation of glycogen synthase kinase 3B, which activates the PERK branch (12).

The UPR is required for tumour cell growth under hypoxic conditions (13). Cells are sensitised to hypoxia *in vitro* by antisense-mediated *GRP78* inhibition (14). PERK inactivation due to the generation of mutations in its kinase domain impairs cell survival under extreme hypoxia (15). PERK promotes cancer cell proliferation by limiting oxidative DNA damage through ATF4 (16).

Additionally, XBP1-deficient tumour cell survival was reduced during severe hypoxia *in vitro*, and these cells were unable to grow as tumours *in vivo*. Spliced XBP1 expression restored tumour growth, suggesting that the IRE1 branch is also required for tumour cell survival during hypoxia (17).

Thus, tumour formation with aberrant microcirculation leads to hypoxia, which induces the UPR. In turn, the UPR increases cellular survival and proliferation, which further enlarges the tumour and thereby increases hypoxia in the tumour core (Figure 3).

Activation of the UPR by glucose deprivation and subsequent acidosis. Tumour cells adapt to low glucose levels by switching to a high rate of aerobic glycolysis, which is known as the Warburg effect (18). The resulting lactic acid production reduces the pH, leading to aggravated local distress. Acidosis is a prominent feature of the tumour microenvironment that surprisingly promotes tumour survival and progression by regulating several B-cell leukaemia/lymphoma-2 (BCL-2) family members and CHOP (see below) (19). The glucose-regulated protein family, which includes the master UPR regulator GRP78, was originally discovered due to the up-regulation of its members in response to glucose deprivation (20). In the XBP1s reporter mouse model, which develops spontaneous mammary tumours, XBP1 splicing was found to increase upon exposure to a non-metabolizable glucose analog that simulates glucose deprivation (11). *CHOP* deletion in a mouse model of Kirsten rat sarcoma viral oncogene homolog-induced lung cancer increases tumour incidence and thus supports the notion that ER stress serves as a barrier to malignancy. UPR activation and the subsequent p58^{IPK} expression control the fates of malignant cells that face glucose deprivation. Overcoming this barrier requires for selective attenuation of the PERK-CHOP branch by p58^{IPK}. Furthermore, this p58^{IPK}-mediated fine-tuning enables cells to benefit from the protective features of chronic UPR (21).

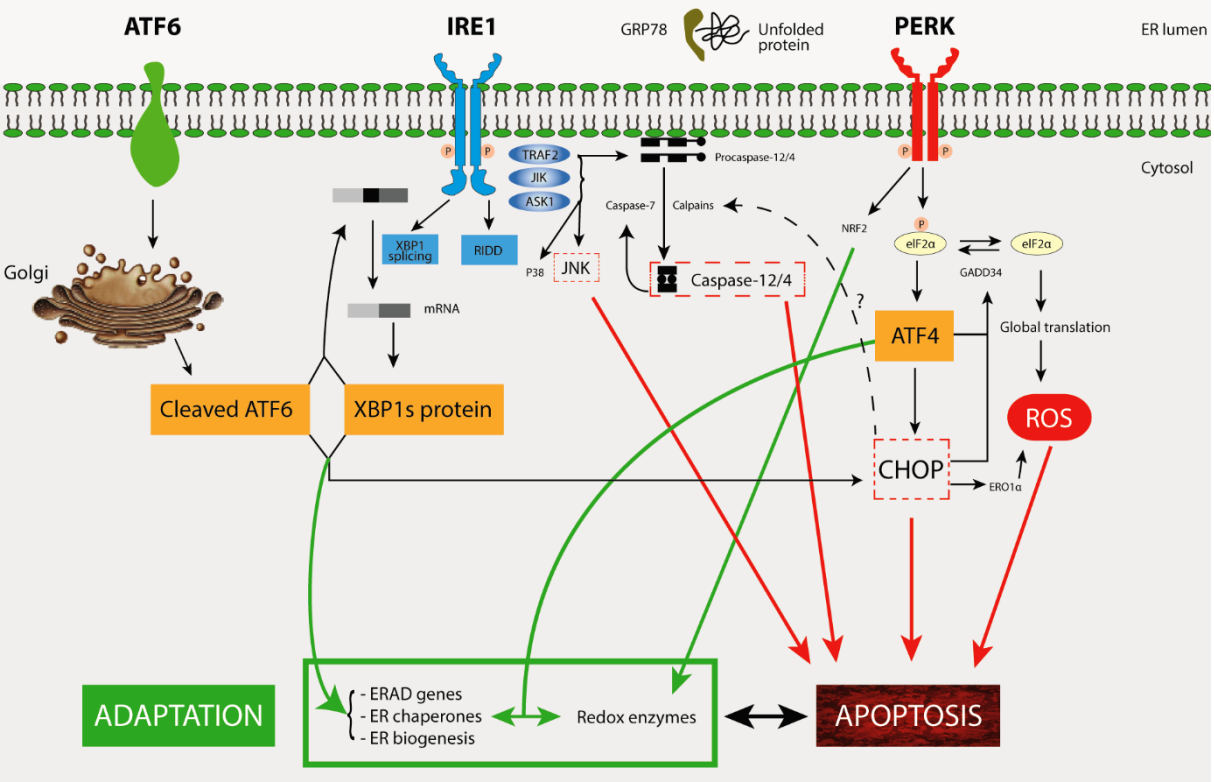

Figure 2. ***Endoplasmic reticulum (ER) stress induces the unfolded protein response (UPR) through a triple transcription factor system.*** *Misfolded proteins sequestrate 78-kDa glucose-regulated protein (GRP78), thus allowing the activation of three ER membrane-associated proteins. Activating transcription factor-6 (ATF6) translocates to the Golgi for cleavage, and the cleaved fragment subsequently regulates UPR gene expression. Inositol requiring enzyme 1 (IRE1) cleaves X-box-binding protein 1 (XBP1) mRNA to a spliced form (XBP1s) that is translated to a strong transcription factor. Along with selective XBP1 mRNA splicing, other mRNAs are degraded by the IRE1 RNase activity (RIDD). IRE1 promotes c-Jun N-terminal kinase (JNK) and p38 phosphorylation through direct interactions. Caspase-12 (murine) or -4 (human) activation is ER stress-dependent. Protein kinase RNA-like endoplasmic reticulum kinase (PERK) phosphorylates eukaryotic initiation factor 2α (eIF2α) to attenuate global translation. Phosphorylated eIF2α favours activating transcription factor 4 (ATF4) translation. The latter induces growth arrest and DNA damage-inducible protein (GADD34), which dephosphorylates eIF2α. PERK also phosphorylates nuclear factor erythroid 2-related factor 2 (NRF2), which induces an anti-oxidative response. ASK1: apoptosis signal-regulating kinase; CHOP: C/EBP homologous protein transcription factor; ERAD: ER-associated protein degradation; ERO1α: ER oxidase 1α; JIK: jun kinase-inhibitory kinase; ROS: reactive oxygen species; TRAF2: tumour necrosis factor receptor-associated factor-2.*

2.4.4. **Dual Role of GRP78 in and on Surface of Tumour and Endothelial Cells**

GRP78 is a key player in tumourigenesis and is involved in the three major hallmarks of cancer, namely the enhancement of cell proliferation, protection against apoptosis and promotion of tumour angiogenesis (22). The phosphoinositide-3 kinase (PI3K)/phosphatase and tensin homolog (PTEN)/protein kinase B (PKB) pathways play central roles in these hallmark processes. In mice, PKB activation in *PTEN*-null prostate epithelium was potently suppressed in a *GRP78*-knockout model, and a similar suppression of PKB activation was observed in human prostate cancer cells that had been transfected with small interfering RNA (siRNA) targeted against *GRP78* (23, 24). As *PTEN* mutations and PKB activation are major drivers of tumourigenesis, GRP78 inactivation might represent a novel approach to reducing tumourigenesis that results from loss of PTEN tumour suppression or oncogenic PKB activation (1). Apart from its abundant expression in the ER, GRP78 can localise at the cell surface, within the cytoplasm, in the mitochondria and in the nucleus, as well as in secretions from tumour and endothelial cells, and this protein is implicated in processes beyond protein folding.

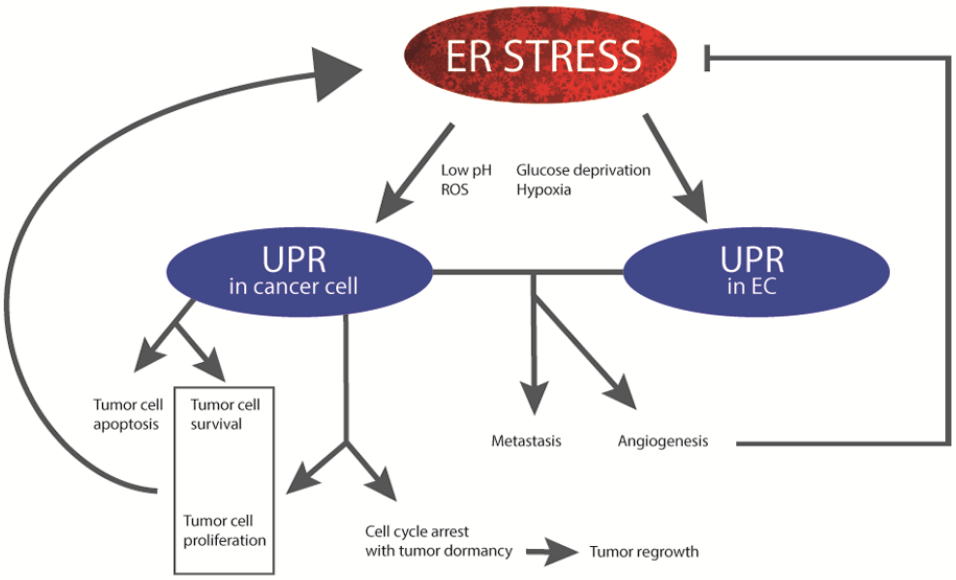

Figure 3. ***The paradoxical role of the unfolded protein response (UPR) in cancer.*** *During tumourigenesis, specific stressors activate the UPR in both cancer and endothelial cells (EC). In cancer cells, both apoptosis and survival can be induced by UPR components. Furthermore, cell-cycle progression or arrest (e.g. by reduced cyclin D1 translation) can occur in response to protein kinase RNA-like endoplasmic reticulum kinase (PERK) activation. This arrest can be temporary during stressful conditions such as chemotherapy. After the induced dormancy, tumour re-growth can occur upon the restoration of more favourable conditions. A positive feedback loop increases ER stress via cellular adaptation during tumour formation. Due to its effects on endothelial and cancer cell survival and function, the UPR also modulates metastasis and angiogenesis, which, if functional, reduces ER stress. ROS: Reactive oxygen species.*

GRP78 in tumour cells. The first causal correlation between GRP78 and *in vivo* carcinogenesis was reported in fibrosarcoma cells. *GRP78* silencing in these cells inhibited their ability to form tumours upon xenografting into mice (25). The essential role of GRP78 was confirmed in a transgenic mouse mammary tumour model. Mice that lacked one *GRP78* allele exhibited decreased breast adenocarcinoma growth and angiogenesis as well and showed survival compared to wild-type mice (26). Likewise, in glioma cells, high GRP78 levels were found to correlate with increased proliferation, and siRNA-mediated *GRP78* suppression reduced the cell proliferation rate (27).

GRP78 levels are known to be increased in various solid tumour types, including prostate, head and neck, melanoma, breast, lung, brain, gastric, colon, and hepatocellular carcinoma (HCC) (14, 28). Furthermore, elevated GRP78 levels correlate with gastric, breast, and liver cancer metastasis (7). In contrast, a recent report suggested that *GRP78* is downregulated in mouse prostate cancer models (29). Thus, although GRP78 and malignancy appear to be positively correlated, exceptions might occur. However, these unexpected results might be due to time-dependent alterations. Additionally, GRP78 plays a dual role in tumour cells. GRP78 controls early tumour development through tumour suppressive mechanisms such as the induction of dormancy (30). On the other hand, at more advanced stages of progression, during which tumours are exposed to more severe stress, GRP78 has been shown to promote tumour progression through its pro-survival (26) and pro-metastatic functions (7).

GRP78 on the tumour cell surface. Severe ER stress promotes GRP78 cell surface localization in various types of neoplastic and endothelial cells (14). The cell surface form of GRP78 affects cell membrane signalling pathways that regulate proliferation, apoptosis and tumour immunity (31). A growing number of cell surface GRP78-binding partners have been identified (1, 14). In prostate cancer cells, cell surface GRP78 binds the activated form of the proteinase inhibitor $\alpha_2$macroglobulin. This interaction promotes cell proliferation by activating p38 and PI3K (32). In addition to α_2-macroglobulin, cell surface GRP78 can interact with Cripto, a small tumour cell surface protein that regulates tumour progression by blocking the growth-inhibitory transforming growth factor β and activating c-SRC and PKB. Interestingly, antibody-mediated blockade of this interaction with cell surface GRP78 is sufficient to inhibit its oncogenic signalling (14, 33). Finally, neovascularization, together with the formation of cell surface GRP78/T-cadherin complexes, was accelerated by ER stress (34), whereas cell surface GRP78 might also serve as a receptor for the angiogenesis inhibitor Kringle 5; the binding of Kringle 5 to GRP78 is required to exert its anti-angiogenic and pro-apoptotic activities in stressed tumour and endothelial cells (14). Thus, the dual effects of cell surface GRP78 signalling depend on the availability of binding partners in the tumour microenvironment.

GRP78 in endothelial cells. The importance of GRP78 in tumour angiogenesis is reflected by its constitutively high expression within the glioblastoma vasculature, which is suggestive of the sustained stress experienced by tumour-associated endothelial cells (31). In a mammary tumour model, conditional heterozygous *GRP78* knockout in endothelial cells led to a dramatic reduction in tumour angiogenesis and metastatic growth, with minimal effects on normal tissue microvascular densities. *GRP78* knockdown in immortalised human endothelial cells revealed that *GRP78* regulated endothelial cell proliferation, survival and migration (7). Vascular endothelial growth factor (VEGF) is a major driver of endothelial proliferation, and all three UPR pathways directly regulate VEGF expression (35). However, the downstream target GRP78 also plays an active role in VEGF regulation. *GRP78*-knockdown suppresses VEGF receptor-2, as well as VEGF-induced endothelial cell proliferation (14).

2.4.5. **Three Proximal UPR Sensors in Cancer: An Integrated View**

After the sequestration of GRP78 by unfolded proteins, ATF6, IRE1, and PERK are activated to transduce the ER stress signal to the cytosol and nucleus (Figure 2).

ATF6: Fine-tuning of the UPR. Although the ATF6 branch in cancer is the least investigated, its potential as an effector of clinical outcomes should not be underestimated. Activated ATF6 translocates to the Golgi, where proteases cleave it and release a fragment into the cytosol. Indeed, enhanced nuclear translocation of the ATF6 fragment is observed in various types of cancer, including HCC (28) and Hodgkin's lymphoma (36), and its expression has been linked to metastasis and relapse (37). Additionally, whereas XBP1s is required for organismal development, the functional roles of ATF6 in ER proteostasis remodelling are adaptive and can adjust the ER capacity to match demand. Therefore, ATF6 modulation might sensitively tune proteostasis without globally influencing proteome folding, trafficking, or degradation (38).

In contrast to PERK and IRE1, ATF6 activation has no obvious paradoxical outcomes. The latter primarily induces cytoprotective responses, such as ER biogenesis, chaperone up-regulation and protein degradation (38, 39). Moreover, ATF6 induces transcription of *XBP1* mRNA, the major splicing target of the IRE1 endonuclease.

Recently, ATF6 was identified as a survival factor for quiescent, but not proliferative, squamous carcinoma cells and as essential for the adaptation of dormant tumour cells to chemotherapy, a process that is mediated by Ras homolog enriched in brain (RHEB) and mammalian target of rapamycin (mTOR) activation (37). ATF6 or RHEB down-regulation was able to reverse dormant cell resistance *in vivo*. Therefore, targeting survival signalling in dormant tumour cells after chemotherapy by abrogating the adaptive ATF6-RHEB-mTOR pathway might reduce the metastatic cancer relapse rate.

IRE1: The conserved core branch. After oligomerisation, IRE1 has at least three established outputs: *XBP1* mRNA splicing, regulation of IRE1-dependent decay (RIDD) of other mRNAs and direct interactions with downstream mediators (40) (Figure 2).

Increased XBP1 splicing has been demonstrated in numerous haematological and solid types of cancer and has been associated with more malignant phenotypes and poor survival (41-43). IRE1 has been shown to promote cell proliferation by regulating cyclin A1 expression through XBP1 splicing in prostate cancer cell lines (44). Notably, XBP1s enhances catalase expression, and the loss of XBP1s sensitizes cells to oxidative stress-induced apoptosis. Indeed, XBP1-deficient cells produce less catalase, which is associated with reactive oxygen species (ROS) generation and p38 activation (45). Moreover, XBP1 splicing itself might directly lead to tumourigenesis, as was evidenced by the observation that the maintenance of elevated XBP1s levels in B and plasma cells could drive multiple myeloma pathogenesis and promote hallmark myeloma characteristics, including bone lytic lesions and sub-endothelial immunoglobulin deposition (46). Moreover, a putative inhibitor of IRE1 RNase exhibited anti-myeloma activity in xenograft mice, suggesting that the IRE1-XBP1 pathway is an appealing target for anticancer therapies (47).

Xenograft glioma cells that expressed dominant-negative *IRE1* exhibited reduced proliferation. In this model, wildtype gliomas were characterised by an angiogenic/massive phenotype, whereas tumours that expressed dominant-negative *IRE1* exhibited an avascular/diffuse phenotype, suggesting that IRE1 is required for angiogenesis and functions as a switch between angiogenesis and invasion (48). The requirement for IRE1 in tumour angiogenesis during stress conditions *in vitro* could be attributed to its role in VEGF expression regulation (49). Additionally, the loss of XBP1 was shown to inhibit both tumour growth and blood vessel formation. However, these effects appeared to be VEGF-independent, indicating that the IRE1-XBP1s-VEGF axis only partially regulates the angiogenic functions of IRE1 (50). On the other hand, VEGF induces internalization of the VEGF receptor, which subsequently interacts with IRE1 to enhance XBP1 splicing (51).

The role of RIDD and the interactions of IRE1 with several downstream mediators during tumour growth and angiogenesis are not currently understood. Prolonged RIDD activation has been reported to increase apoptosis (40). Activated IRE1 recruits the adaptor protein tumour necrosis factor receptor associated factor-2 (TRAF2) to the ER membrane, which has been reported to further activate c-Jun *N*-terminal kinase (JNK) (see below), resulting in caspase-12 activation and apoptosis in a mouse model (52). The JNK pathway is a member of the mitogen-activated protein kinase superfamily, which also includes p38 (53), and this activated pathway is involved in ER stress-mediated apoptotic cascades.

XBP1s overexpression in breast cancer cells increased BCL-2 levels after antiestrogen stimulation, thereby suppressing apoptosis (54); however, JNK phosphorylates and paradoxically inhibits BCL-2. Thus, the effects of IRE1 on the BCL-2 family vary according to the output, which is anti-apoptotic when mediated by XBP1 splicing *versus* proapoptotic when mediated by JNK.

PERK and protein translation in cancer. PERK phosphorylates eIF2α, leading to a translation blockade and cap-independent ATF4 translation, as well as nuclear factor erythroid 2-related factor-2 (NRF2), leading to the upregulation of antioxidative enzymes (6) (Figure 2). PERK has been implicated in tumour progression and angiogenesis. PERK inactivation in mouse fibroblasts and human colon cancer cells, using targeted mutagenesis or a dominant-negative *PERK*, resulted in smaller tumours that demonstrated impaired angiogenic abilities upon grafting into immunodeficient mice (13, 55). *PERK* deletion in a mammary tumour mouse model was found to modestly increase tumour latency while profoundly inhibiting metastatic spread (16).

Similar observations were made in a colorectal carcinoma xenograft model that expressed a dominant-negative *PERK*. *PERK*-knockdown in human esophageal and breast carcinomas resulted in cell-cycle arrest at the G_2/M phase (16). This G_2/M arrest could likely be attributed to reduced NRF2 activity in these PERK-deficient cells, resulting in ROS accumulation that causes oxidative DNA damage and subsequently triggers cell-cycle arrest *via* the DNA double strand-break checkpoint (31). Similar to IRE1 deficiency, PERK-deficient tumours exhibited reduced viability and impaired angiogenic ability during hypoxia; these effects were attributed to the losses of phosphorylated eIF2α and ATF4. The requirement for PERK in tumour angiogenesis was further confirmed with a mouse $PERK^{-/-}$ insulinoma model in which $PERK^{-/-}$ tumours exhibited reduced vascularity (56). Thus, both downstream transcription factors of PERK, namely ATF4 and NRF2, contribute to cellular adaptation and tumour promotion.

In contrast to the previous results, p38-induced dormancy in squamous cell carcinoma cells was associated with increased PERK activation. Accordingly, pharmacologically activated PERK was found to induce growth arrest *in vitro* and to suppress tumour growth *in vivo*, indicating an additional role for PERK in tumour growth suppression (57). Indeed, eIF2α phosphorylation-induced translational arrest down-regulates cell-cycle regulators such as cyclin D1, resulting in cell-cycle arrest in the G_1 phase. Accordingly, a non-phosphorylatable eIF2α mutant was sufficient to drive the malignant transformation of human kidney cells or fibroblasts, and conditional *PERK* deletion was found to deregulate mammary acinar morphogenesis and to cause hyperplastic growth *in vivo* (58, 59).

Taken together, activation of the PERK axis induces tumour suppression (by G_1/S arrest) and dormancy, whereas inactivation appears to induce paradoxical effects on specific hallmarks of carcinogenesis (22), such as tumourigenesis, angiogenesis and metastasis.

Recently, a context-dependent impact of PERK on cell fate has been indicated. Downstream of PERK, CHOP directly transactivates the growth arrest and DNA damage inducible protein (GADD34). The latter promotes eIF2α dephosphorylation, thereby creating a negative feedback loop that leads to translational recovery (60). Additionally, both ATF4 and CHOP induce protein synthesis (61). This finding could explain the time-dependent balance in protein synthesis. After acute ER stress, protein synthesis is inhibited by eIF2α phosphorylation. However, downstream induction of *ATF4*, *CHOP*, and *GADD34* leads to protein synthesis recovery. If acute ER stress is addressed, survival is promoted by the restoration of translation. Conversely, if chronic ER stress continues or the acute ER stress was too severe to be addressed during a transient reduction of translation, protein synthesis leads to ROS formation and ultimately triggers apoptosis. Accordingly, salubrinal, an eIF2α dephosphorylation inhibitor, protects cells from ER stress-associated apoptosis (62).

2.4.6. **The UPR and Apoptosis: Adaptation or Suicide – A Double-edged Sword**

During ER stress, cells either survive by inducing adaptation mechanisms or commit suicide by apoptosis. The intrinsic apoptosis pathway is closely related to factors anchored on the mitochondria. The membrane insertion of pro-apoptotic proteins changes mitochondrial membrane permeability, resulting in cytochrome *c* release and caspase activation (53, 63).

CHOP: A key mediator of ER stress-induced apoptosis. Notably, *CHOP* induction strongly correlates with the onset of ER stress-associated apoptosis, and CHOP silencing protects cells (53). However, mouse embryonic fibroblasts (MEFs) derived from *CHOP*-knockout mice exhibit only partial resistance to ER stress-driven apoptosis, indicating that CHOP is not the only death pathway in this context (64). Precisely how CHOP mediates ER stress-induced apoptosis remains controversial because CHOP regulates numerous genes, the majority of which are involved in hallmarks of cancer, such as cell migration, proliferation, and survival (22, 65).

The down-regulation of anti-apoptotic *BCL-2* and the induction of the proapoptotic BCL-2 interacting mediator of cell death (BIM), p53 up-regulated modulator of apoptosis (*PUMA*) and BCL-2-associated X protein (*BAX*) are believed to contribute to CHOP-mediated apoptosis (63). *In vivo* data from breast carcinoma-derived cells corroborate these findings (66).

CHOP transcriptionally induces ERO1α (see above), which promotes disulfide bond formation but also generates hydrogen peroxide leakage into the cytoplasm (60). *In vivo*, partial *ERO1α* silencing was shown to protect against ER stress-induced death, and CHOP deficiency suppressed pancreatic β-cell apoptosis, which was associated with decreased ERO1α expression and oxidative stress markers. ERO1α activates the ER calcium channel inositol-1,4,5trisphosphate receptor 1 (IP3R1) (67). Upon release from the ER, calcium triggers apoptosis by activating calcium/calmodulin-dependent kinase II (CaMKII), which subsequently induces four apoptotic pathways. Firstly, CaMKII triggers JNK-mediated Fas antigen induction. Secondly, CaMKII promotes mitochondrial calcium uptake, thereby activating intrinsic apoptosis. Thirdly, CaMKII activates signal transducer and activator of transcription-1 (STAT1), a pro-apoptotic signal transducer (68). Finally, the CHOP-ERO1α-IP3R1-CaMKII axis induces NADPH oxidase subunit 2 and generates ROS to possibly amplify CaMKII activation as part of a positive feedback loop because ROS induces CHOP expression. Surprisingly, NADPH oxidase-induced ROS are also part of a second positive feedback loop that activates dsRNA-dependent protein kinase to subsequently phosphorylate eIF2α, thereby amplifying *CHOP* expression. For example, CHOP-induced hepatocyte death in a mouse protein-misfolding model was associated with oxidative stress and was relieved by an antioxidant. Because CHOP-induced apoptosis can be blocked by buffering cytosolic calcium, the ERO1α-IP3R1 pathway appears to comprise its main signalling axis (69).

Furthermore, CHOP activity is increased in response to phosphorylation by p38. p38 is a substrate of apoptosis signal-regulating kinase (ASK1, see below), which is recruited to the IRE1-TRAF2 complex upon ER stress. Thus, during prolonged stress, the PERK and IRE1 pathways might converge on CHOP, with IRE1-mediated ASK1 activation potentiating CHOP activity (4).

The JNK pathway in ER stress-mediated apoptosis. Several studies indicate a pivotal role for JNK in the mediation of ER stress-induced apoptosis (70). JNK recruitment by IRE1 is regulated by c-Jun NH_2-terminal inhibitory kinase (JIK), which has been reported to interact with both IRE1 and TRAF2. The IRE1-TRAF2 complex then recruits ASK1, causing ASK1 activation and regulating the JNK pathway that leads to cell death. In a mouse HCC model, ASK1 deficiency promoted HCC, whereas the reintroduction of ASK1 suppressed tumour development (71). Furthermore, cells from *ASK1*-knockout mice were found to be resistant to ER stress-associated apoptosis and exhibited reduced JNK and p38 activity (72). JIK overexpression was shown to promote the interaction between IRE1 and TRAF2 and JNK activation in response to ER stress, whereas the overexpression of an inactive JIK mutant inhibited JNK activation (52). Thus, the IRE1-TRAF2-JIK-ASK1-JNK pathway exerts an opposite effect on cell survival than that of the cytoprotective IRE1-XBP1s pathway. The regulation of these paradoxical IRE1 outputs requires further investigation. As described previously, JNK is a downstream effector of the CHOP-CaMKII pathway. Therefore, in conditions where both proapoptotic IRE1 activation and CHOP expression are prolonged, additive JNK activation might play a crucial role in apoptosis regulation.

Downstream apoptosis-related targets of JNK include antiapoptotic BCL-2, B-cell lymphoma-extra-large (BCLXL) and myeloid cell leukaemia sequence 1 (MCL-1), all of which are inhibited by JNK, and proapoptotic BID and BIM, which are activated by JNK-mediated phosphorylation (63, 73). During non-stress conditions, BIM is sequestered by dynein motor complexes. ER stress increases BIM levels by reducing BIM degradation and by CHOP-mediated gene induction. Phosphorylation by JNK releases BIM from its inhibitory association with the motor complexes, thus permitting its translocation to the mitochondrial outer membrane where it promotes cytochrome *c* release and caspase activation. Interestingly, a positive feedback loop exists between BIM and caspase-3. Phosphorylated BIM is a caspase-3 target and, once cleaved, becomes a more potent inducer of cytochrome c release (74, 75).

The mitochondria and the BCL-2 family. The proapoptotic BCL-2 family members trigger mitochondrial dysfunction and are sub-divided into the multi-BCL-2 homology (BH) domain proteins, such as BAX and BAK, and the BH3-only proteins, such as BAD. Of the 11 BH3-only protein subfamily members, PUMA, NOXA, BID, HARAKIRI and BIM have been reported to mediate ER stress-induced apoptosis (74, 75).

Additionally, the BCL-2 family also regulates ER stress through physical interactions with certain UPR components. For example, BAX and BAK directly interact with the IRE1 cytosolic domain upon ER stress; this interaction is essential for IRE1 activation (76). In cells that exclusively express ER-localised BAK, BIM and PUMA selectively activate the TRAF2-JNK arm of IRE1 in the absence of XBP1 splicing (77). In *BAX/BAK* double-knockout mice, ER stress failed to induce XBP1s, IRE1 or JNK. Moreover, *BAX/BAK* double-knockout MEFs are resistant to apoptosis mediated by various ER stressors, and the reconstitution of BAK expression in these MEFs restored JNK phosphorylation, suggesting a direct connection between the UPR and the apoptotic machinery (76). Thus, BAX and BAK are required for IRE1 signalling, although both are also involved in ER stress-induced apoptosis. This response could represent a switch toward pro-apoptotic signalling by IRE1. The association of IRE1 with BAX and BAK is influenced by BAX inhibitor-1 (BI-1), an ER transmembrane protein. BI-1 directly interacts with the IRE1 cytosolic domain to inhibit its endoribonuclease activity. BI-1-deficient cells were found to exhibit enhanced IRE1 activity and sustained XBP1 splicing, whereas BI-1 overexpression disrupted the interaction between IRE1 and BAX or BAK (78). Similar to ER-localised BAX/BAK oligomers (see below), BI-1 also modulates ER calcium homeostasis by forming a calcium-permeable channel pore (79).

BCL-2, BAX and BAK associate with both mitochondrial and ER membranes. During ER stress, ER-targeted BAX and BAK undergo conformational changes and oligomerisation, which leads to calcium release from the ER to the cytosol to activate m-calpain and, subsequently, procaspase-12 (see below) (81, 82). In contrast, mitochondria-targeted BAK enhances caspase-7 cleavage to create parallel pathways of caspase activation by BAX and BAK (80).

Each branch acts on different levels to tightly modulate the BCL-2 family. During hypoxia, ATF4 induces the BH3only proteins HARAKIRI, PUMA and NOXA following PERK activation (75). Additionally, CHOP transactivates BIM and down-regulates *BCL-2* and *MCL-1*. The less studied ATF6 has been linked to ER stress-induced apoptosis in a myoblast cell line through the indirect inhibition of MCL-1 expression (83). The IRE1 branch can affect BH3only proteins such as PUMA or BID. Functional integration likely occurs because BAX/BAK acts through mitochondrial permeabilisation, a key pro-apoptotic effect of the CHOPERO1α-CaMKII pathway.

Caspases. The processing of caspases-2 to -9 and caspase-12 has been observed in various models of ER stress-induced apoptosis (84, 85). In mouse models, caspase-12 was proposed as a key mediator of ER stress-induced apoptosis. Caspase-12knockout MEFs exhibited partial resistance, specifically against ER stressors. However, another study that used different caspase-12-knockout MEFs did not show any resistance to apoptosis (86). Procaspase-12 is localised on the cytosolic ER surface and is activated by ER stress *via* IRE1-TRAF2dependent mechanisms. TRAF2 promotes procaspase-12 clustering at the ER membrane (52). The interaction between TRAF2 and procaspase-12 is inhibited by ER stress, and IRE1 overexpression. Therefore, caspase-12 activation might require for the dissociation of procaspase-12 from TRAF2, which is subsequently recruited to IRE1. Calpains, a family of calcium-dependent proteases, also play a role in caspase-12 activation, and calpain-deficient MEFs exhibit reduced ER stress-mediated caspase-12 activation and apoptosis (85). Therefore, it is plausible that a CHOP-ERO1α-IP3R-calcium-calpain pathway contributes to caspase-12 activation. Surprisingly, human caspase-12 has no similar function because its gene has been disrupted by a frame shift. Instead, human caspase-4 is specifically cleaved under ER stress, suggesting that it might be a functional mouse caspase-12 ortholog. Transmembrane protein 214 (TMEM214) mediates stress-induced apoptosis by acting as an anchor for the ER recruitment and subsequent activation of procaspase-4 (87).

Caspase-7, which also translocates from the cytosol to the cytosolic ER surface in response to ER stress, cleaves procaspase-12. A dominant-negative catalytic caspase-7 mutant was shown to inhibit caspase-12 activation. Caspase-7 is also a downstream executioner of caspase-12, a fact that suggests an amplification loop in the ER stress-induced apoptotic cascade (53).

2.4.7. **Future Perspectives and Remaining Conundrums**

Recently, ER stress research has received unprecedented attention. A basic PubMed search revealed that more than 830 ER stress investigational studies have so far been published in 2013. However, to integrate these links with hypoxia-inducible factor 1(HIF1)-VEGF or inflammatory pathways in a comprehensive network, the focus should be placed on elucidating the downstream mediators and crosstalk for all three UPR pathways. The observed paradox of the UPR in cancer (Figure 3) is likely due to functional redundancy and time-dependent outcomes of the UPR, although there are also some methodological issues.

ER stress-induced apoptosis is not completely suppressed when a single UPR effector is experimentally silenced. The fact that *CHOP* is a transcriptional target of both PERK and IRE, and even ATF6 provides an obvious link among all three branches. One caveat is that the IRE1 and ATF6 branches have weaker activities, compared to the PERK-CHOP branch, during prolonged ER stress (63). Most targets can be regulated separately by each pathway; moreover, each pathway possesses its own transcriptional activity for a certain target that determines its effect on cell fate. Some targets even require the concomitant activation of two pathways, for example, $p58^{IPK}$ requires ATF6/IRE1 cooperation (38). Additionally, a single downstream effector can exhibit different mechanisms of action. For example, the anti-apoptotic mechanisms of GRP78 include the prevention of UPR sensor activation, and the preservation of ER calcium homeostasis and its chaperone activity by limiting misfolded protein aggregation (1, 26).

The majority of studies measured the expression of only two or three ER stress markers such as GRP78 or CHOP; only a minority included target genes from each branch. Future therapeutic targeting of the UPR will likely affect one branch. The pleiotropic effects and acute toxicities of global

UPR inducers, including the most commonly used thapsigargin (an ER calcium pump inhibitor) and tunicamycin (an N-linked glycosylation inhibitor), complicate studies that focus on an understanding of how the UPR remodels ER proteostasis in the absence of acute ER stress or how partitioning between ER client protein folding and trafficking *versus* degradation can be influenced by arm-selective UPR modulation. Moreover, UPR research that includes a variety of acute ER stress inducers introduces difficulties when comparing data from different studies. The recent development of targeted inhibition [*e.g.* PERK inhibitors (88)] or activation [*e.g.* PERK activators (89)] approaches, as opposed to the concomitant activation of all three branches, will lead to a new era in UPR research.

The duration and severity of ER stress determine the survival/apoptosis switch. The three branches provide opposing signals, and the timing of their induction shifts the balance between cytoprotection and apoptosis in response to unmitigated ER stress. For example, IRE1 signalling is an early event that is attenuated upon prolonged ER stress (90), and likewise, PERK induces its own de-activation *via* the upregulation of GADD34 (Figure 2). Both pathways thus contain intrinsic 'timers' that likely contribute to cellular lifeor-death decisions. Because *CHOP* mRNA and protein half-lives were found to be short, compared to those of prosurvival UPR outputs such as GRP78, sustained PERK activity (which is primarily responsible for *CHOP* upregulation) might therefore be necessary to accumulate CHOP levels sufficiently to stimulate the pro-apoptotic BCL-2 family proteins. Additionally, despite ATF4, CHOP, and GADD34 being able to restore protein synthesis, sustained PERK activity results in a protracted translational block that is incompatible with cell survival (38, 61). Similarly, sustained IRE1-mediated mRNA degradation might deplete ER cargo and protein-folding activities (40). Currently, it is unclear how tumour cells adapt to chronic ER stress *in vivo*. Although the UPR components are clearly activated in several types of tumours, the long-term evolution of this activity is unknown. Therefore, the use of experimental models with which to monitor temporal dynamics is required. For example, under hypoxia, there is a bi-phasic response to eIF2α phosphorylation. Phosphorylation is increased after 8 h but reduced after 24 h (possibly by PERK-ATF4-CHOPGADD34) and is again enhanced after 48 h. Thus, following the initial attenuation in protein translation, there might be a transient period in which additional protein synthesis is permitted before a more permanent reduction occurs (15). Consequently, the effects of future drug interventions might be time-dependent, and whether cancer incidence might be reduced through the enhancement of protein-folding capacities during carcinogen exposure remains unknown. For example, the development of molecules that protect the liver by reducing alcohol-induced ER stress might dramatically reduce the incidence of HCC because chronic alcohol use increases HCC risk (91).

Deciphering this paradox could permit for the development of novel therapeutic modalities. In cancer, the UPR could be targeted to promote apoptosis by inhibiting UPR components and thus abrogating cellular adaptation (*e.g.* the use of versipelostatin, a repressor of GRP78 expression) or overloading the UPR (*e.g.* the use of proteasomal inhibitors). Overall, an ideal approach would integrate both targets without any toxicity.

In principle, UPR inhibitors should specifically target the tumour tissue. However, certain normal cell types place high demands on ER function, such as antibody-producing B-cells or insulin-secreting β-cells, and the potential toxicities against these cell types would require close monitoring during future drug discovery efforts (92). Notably, tissue-specific UPR patterns might help to differentiate target tissues. However, current molecular insights into the adaptation/apoptosis switch during ER stress are insufficient, and UPR drugs might block ER stress-mediated apoptosis and might unintentionally promote tumour progression. In general, protein kinases such as PERK represent favourable targets for the development of small-molecule inhibitors. However, as described above, PERK exhibits both pro- and anti-tumour properties. PERK-targeted therapies might facilitate the proliferation of dormant tumour cells or might drive cancer cells into dormancy, thereby protecting them from chemotherapy. Additionally, the inhibition of one branch might result in altered signalling through the other branches. Indeed, HEK293 cells that overexpressed a kinase-dead PERK mutant were found to exhibit increased XBP1 splicing and ATF6 activation in response to ER stress. Despite delayed dynamics, these cells still induced CHOP expression, which partially accounts for the increased susceptibility of these cells to ER stress-induced apoptosis (93).

In conclusion, the ability of the UPR to regulate cell fate has been highlighted as a primary pathophysiology research focus and represents a potential cancer therapeutic axis. However, its paradoxical effects on survival and proliferation of neoplastic and endothelial cells complicate the clinical applications of UPR modulators. This paradox is primarily due to our incomplete understanding of redundancy, the opposing effects of the separate outputs of each pathway, the interplay between the UPR and other pathways and the temporal UPR dynamics in cancer, as well as other confounding factors, including the absence of a standardized definition of ER stress, and a lack of branch-specific research.

2.4.8. **References**

1 Wang M, Wey S, Zhang Y, Ye R and Lee AS: Role of the unfolded protein response regulator GRP78/BiP in development, cancer, and neurological disorders. Antioxid Redox Signal *11*: 2307-2316, 2009.

2 Stolz A and Wolf DH: Endoplasmic reticulum associated protein degradation: A chaperone assisted journey to hell. Biochim Biophys Acta *1803*: 694-705, 2010.

3 Kozutsumi Y, Segal M, Normington K, Gething MJ and Sambrook J: The presence of malfolded proteins in the endoplasmic reticulum signals the induction of glucose-regulated proteins. Nature *332*: 462-464, 1988.

4 Walter P and Ron D: The unfolded protein response: From stress pathway to homeostatic regulation. Science *334*: 1081-1086, 2011.

5 Hetz C, Martinon F, Rodriguez D and Glimcher LH: The unfolded protein response: Integrating stress signals through the stress sensor IRE1α. Physiol Rev *91*: 1219-1243, 2011.

6 Chakrabarti A, Chen AW and Varner JC: A review of the mammalian unfolded protein response. Biotechnol Bioeng *108*: 2777-2793, 2011.

7 Dong D, Stapleton C, Luo B, Xiong S, Ye W, Zhang Y, Jhaveri N, Zhu G, Ye R, Liu Z, Bruhn KW, Craft N, Groshen S, Hofman FM and Lee AS: A critical role for GRP78/BiP in the tumour microenvironment for neovascularization during tumour growth and metastasis. Cancer Res *71*: 2848-2857, 2011.

8 Mahadevan NR and Zanetti M: Tumour stress inside out: Cellextrinsic effects of the unfolded protein response in tumour cells modulate the immunological landscape of the tumour microenvironment. J Immunol *187*: 4403-4409, 2011.

9 Tagliavacca L, Caretti A, Bianciardi P and Samaja M: *In vivo* up-regulation of the unfolded protein response after hypoxia. Biochim Biophys Acta *1820*: 900-906, 2012.

10 Queitsch C, Sangster TA and Lindquist S: Hsp90 as a capacitor of phenotypic variation. Nature *417*: 618-624, 2002.

11 Spiotto MT, Banh A, Papandreou I, Cao H, Galvez MG, Gurtner GC, Denko NC, Le QT and Koong AC: Imaging the unfolded protein response in primary tumours reveals microenvironments with metabolic variations that predict tumour growth. Cancer Res *70*: 78-88, 2010.

12 Appenzeller-Herzog C and Hall MN: Bidirectional crosstalk between endoplasmic reticulum stress and mTOR signalling. Trends Cell Biol *22*: 274-282, 2012.

13 Bi M, Naczki C, Koritzinsky M, Fels D, Blais J, Hu N, Harding H, Novoa I, Varia M, Raleigh J, Scheuner D, Kaufman RJ, Bell J, Ron D, Wouters BG and Koumenis C: ER stress-regulated translation increases tolerance to extreme hypoxia and promotes tumour growth. EMBO J *24*: 3470-3481, 2005.

14 Li Z and Li Z: Glucose regulated protein 78: A critical link between tumour microenvironment and cancer hallmarks. Biochim Biophys Acta *1826*: 13-22, 2012.

15 Fels DR and Koumenis C: The PERK/eIF2α/ATF4 module of the UPR in hypoxia resistance and tumour growth. Cancer Biol Ther *5*: 723-728, 2006.

16 Bobrovnikova-Marjon E, Grigoriadou C, Pytel D, Zhang F, Ye J, Koumenis C, Cavener D and Diehl JA: PERK promotes cancer cell proliferation and tumour growth by limiting oxidative DNA damage. Oncogene *29*: 3881-3895, 2010.

17 Romero-Ramirez L, Cao H, Nelson D, Hammond E, Lee AH, Yoshida H, Mori K, Glimcher LH, Denko NC, Giaccia AJ, Le QT and Koong AC: XBP1 is essential for survival under hypoxic conditions and is required for tumour growth. Cancer Res *64*: 5943-5947, 2004.

18 Amann T and Hellerbrand C: GLUT1 as a therapeutic target in hepatocellular carcinoma. Expert Opin Ther Targets *13*: 14111427, 2009.

19 Ryder CB, McColl K and Distelhorst CW: Acidosis blocks CCAAT/enhancer-binding protein homologous protein (CHOP)and c-Jun-mediated induction of p53-up-regulated mediator of apoptosis (PUMA) during amino acid starvation. Biochem Biophys Res Commun *430*: 1283-1288, 2013.

20 Shiu RP, Pouyssegur J and Pastan I: Glucose depletion accounts for the induction of two transformation-sensitive membrane proteinsin Rous sarcoma virus-transformed chick embryo fibroblasts. Proc Natl Acad Sci USA *74*: 3840-3844, 1977.

21 Huber AL, Lebeau J, Guillaumot P, Pétrilli V, Malek M, Chilloux J, Fauvet F, Payen L, Kfoury A, Renno T, Chevet E and Manié SN: p58(IPK)-Mediated attenuation of the proapoptotic PERKCHOP pathway allows malignant progression upon low glucose. Mol Cell *49*: 1049-1059, 2013.

22 Hanahan D and Weinberg RA: Hallmarks of cancer: The next generation. Cell *144*: 646-674, 2011.

23 Fu Y, Wey S, Wang M, Ye R, Liao CP, Roy-Burman P and Lee AS: Pten null prostate tumourigenesis and PKB activation are blocked by targeted knockout of ER chaperone GRP78/BiP in prostate epithelium. Proc Natl Acad Sci USA *105*: 19444-19449, 2008.

24 Steelman LS, Chappell WH, Abrams SL, Kempf RC, Long J, Laidler P, Mijatovic S, Maksimovic-Ivanic D, Stivala F, Mazzarino MC, Donia M, Fagone P, Malaponte G, Nicoletti F, Libra M, Milella M, Tafuri A, Bonati A, Bäsecke J, Cocco L, Evangelisti C, Martelli AM, Montalto G, Cervello M and McCubrey JA: Roles of the RAF/MEK/ERK and PI3K/PTEN/ AKT/mTOR pathways in controlling growth and sensitivity to therapy-implications for cancer and aging. Aging *3*: 192-222, 2011.

25 Jamora C, Dennert G and Lee AS: Inhibition of tumour progression by suppression of stress protein GRP78/BiP induction in fibrosarcoma B/C10ME. Proc Natl Acad Sci USA *93*: 7690-7694, 1996.

26 Dong D, Ni M, Li J, Xiong S, Ye W, Virrey JJ, Mao C, Ye R, Wang M, Pen L, Dubeau L, Groshen S, Hofman FM and Lee AS: Critical role of the stress chaperone GRP78/BiP in tumour proliferation, survival, and tumour angiogenesis in transgene-induced mammary tumour development. Cancer Res *68*: 498-505, 2008.

27 Pyrko P, Schönthal AH, Hofman FM, Chen TC and Lee AS: The unfolded protein response regulator GRP78/BiP as a novel target for increasing chemosensitivity in malignant gliomas. Cancer Res *67*: 9809-9816, 2007.

28 Shuda M: Activation of the *ATF6, XBP1* and *GRP78* genes in human hepatocellular carcinoma: A possible involvement of the ER stress pathway in hepatocarcinogenesis. J Hepatol *38*: 605-614, 2003.

29 So AYL, de la Fuente E, Walter P, Shuman M and Bernales S: The unfolded protein response during prostate cancer development. Cancer Metastasis Rev *28*: 219-223, 2009.

30 Denoyelle C, Abou-Rjaily G, Bezrookove V, Verhaegen M, Johnson TM, Fullen CR, Pointer JN, Gruber SB, Su LD, Nikiforov MA, Kaufman RJ, Bastian BC and Soengas MS: Antioncogenic role of the endoplasmic reticulum differentially activated by mutations in the MAPK pathway. Nat Cell Biol *8*: 1053-1063, 2006.

31 Luo B and Lee AS: The critical roles of endoplasmic reticulum chaperones and unfolded protein response in tumourigenesis and anticancer therapies. Oncogene *32*: 805-818, 2012.

32 Kern J, Untergasser G, Zenzmaier C, Sarg B, Gastl G, Gunsilius E and Steurer M: GRP-78 secreted by tumour cells blocks the antiangiogenic activity of bortezomib. Blood *114*: 3960-3967, 2009.

33 Nagaoka T, Karasawa H, Castro NP, Rangel MC, Salomon DS and Bianco C: An evolving web of signalling networks regulated by Cripto-1. Growth Factors *30*: 13-21, 2012.

34 Nakamura S, Takizawa H, Shimazawa M, Hashimoto Y, Sugitani S, Tsuruma K and Hara H: Mild endoplasmic reticulum stress promotes retinal neovascularization *via* induction of *BiP/GRP78*. PloS One *8*: e60517, 2013.

35 Ghosh R, Lipson KL, Sargent KE, Mercurio AM, Hunt JS, Ron D and Urano F: Transcriptional regulation of VEGF-A by the unfolded protein response pathway. PloS One *5*: e9575, 2010.

36 Chang KC, Chen PCH, Chen YP, Chang Y and Su IJ: Dominant expression of survival signals of endoplasmic reticulum stress response in Hodgkin lymphoma. Cancer Sci 102: 275-281, 2011.

37 Schewe DM and Aguirre-Ghiso JA: ATF6α-RHEB-mTOR signalling promotes survival of dormant tumour cells *in vivo*. Proc Natl Acad Sci USA *105*: 10519-10524, 2008.

38 Shoulders MD, Ryno LM, Genereux JC, Moresco JJ, Tu PG, Wu C, Yates JR, Su AI, Kelly JW and Wiseman RL: Stressindependent activation of XBP1s and/or ATF6 reveals three functionally diverse ER proteostasis environments. Cell Rep *3*: 1279-1292, 2013.

39 Adachi Y, Yamamoto K, Okada T, Yoshida H, Harada A and Mori K: ATF6 is a transcription factor specializing in the regulation of quality control proteins in the endoplasmic reticulum. Cell Struct Funct *33*: 75-89, 2008.

40 Han D, Lerner AG, Vande Walle L, Upton JP, Xu W, Hagen A, Backes BJ, Oakes SA and Papa FR: IRE1alpha kinase activation modes control alternate endoribonuclease outputs to determine divergent cell fates. Cell *138*: 562-575, 2009.

41 Maestre L, Tooze R, Cañamero M, Montes-Moreno S, Ramos R, Doody G, Boll M, Barrans S, Baena S, Piris MA and Roncador G: Expression pattern of XBP1(S) in human B-cell lymphomas. Haematologica *94*: 419-422, 2009.

42 Fujimoto T, Yoshimatsu K, Watanabe K, Yokomizo H, Otani T, Matsumoto A, Osawa G, Onda M and Ogawa K: Overexpression of human X-box binding protein 1 (XBP-1) in colorectal adenomas and adenocarcinomas. Anticancer Res *27*: 127-131, 2007.

43 Davies MPA, Barraclough DL, Stewart C, Joyce KA, Eccles RM, Barraclough R, Rudland PS and Sibson DR: Expression and splicing of the unfolded protein response gene XBP-1 are significantly associated with clinical outcome of endocrine-treated breast cancer. Int J Cancer *123*: 85-88, 2008.

44 Thorpe JA and Schwarze SR: IRE1alpha controls cyclin A1 expression and promotes cell proliferation through XBP-1. Cell Stress Chaperones *15*: 497-508, 2010.

45 Zhong Y, Li J, Wang JJ, Chen CC, Tran JTA, Saadi A, Yu Q, Le YZ, Mandal MNA, Anderson RE and Zhang SX: X-box binding protein 1 is essential for the anti-oxidant defense and cell survival in the retinal pigment epithelium. PloS One *7*: e38616, 2012.

46 Carrasco DR, Sukhdeo K, Protopopova M, Sinha R, Enos M, Carrasco DE, Zheng M, Mani M, Henderson J, Pinkus GS, Munshi N, Horner J, Ivanova EV, Protopopov A, Anderson KC, Tonon G and DePinho RA: The differentiation and stress response factor XBP-1 drives multiple myeloma pathogenesis. Cancer Cell *11*: 349-360, 2007.

47 Papandreou I, Denko NC, Olson M, Van Melckebeke H, Lust S, Tam A, Solow-Cordero DE, Bouley DM, Offner F, Niwa M and Koong AC: Identification of an IRE1α endonuclease specific inhibitor with cytotoxic activity against human multiple myeloma. Blood *117*: 1311-1314, 2011.

48 Auf G, Jabouille A, Guérit S, Pineau R, Delugin M, Bouchecareilh M, Magnin N, Favereaux A, Maitre M, Gaiser T, von Deimling A, Czabanka M, Vajkoczy P, Chevet E, Bikfalvi A and Moenner M: Inositol-requiring enzyme 1α is a key regulator of angiogenesis and invasion in malignant glioma. Proc Natl Acad Sci USA *107*: 15553-15558, 2010.

49 Drogat B, Auguste P, Nguyen DT, Bouchecareilh M, Pineau R, Nalbantoglu J, Kaufman RJ, Chevet E, Bikfalvi A and Moenner M: IRE1 signalling is essential for ischemia-induced vascular endothelial growth factor-A expression and contributes to angiogenesis and tumour growth *in vivo*. Cancer Res *67*: 67006707, 2007.

50 Romero-Ramirez L, Cao H, Regalado MP, Kambham N, Siemann D, Kim JJ, Le QT and Koong AC: X-Box-binding protein 1 regulates angiogenesis in human pancreatic adenocarcinomas. Transl Oncol *2*: 31-38, 2009.

51 Zeng L, Xiao Q, Chen M, Margariti A, Martin D, Ivetic A, Xu H, Mason J, Wang W, Cockerill G, Mori K, Li JY, Chien S, Hu Y and Xu Q: Vascular endothelial cell growth-activated XBP1 splicing in endothelial cells is crucial for angiogenesis. Circulation *127*: 1712-1722, 2013.

52 Yoneda T, Imaizumi K, Oono K, Yui D, Gomi F, Katayama T and Tohyama M: Activation of caspase-12, an endoplastic reticulum (ER) resident caspase, through tumour necrosis factor receptor-associated factor 2-dependent mechanism in response to the ER stress. J Biol Chem *276*: 13935-13940, 2001.

53 Jing G, Wang JJ and Zhang SX: ER stress and apoptosis: A new mechanism for retinal cell death. Exp Diabetes Res *2012*: 589589, 2012.

54 Gomez BP, Riggins RB, Shajahan AN, Klimach U, Wang A, Crawford AC, Zhu Y, Zwart A, Wang M and Clarke R: Human X-box binding protein-1 confers both estrogen independence and antiestrogen resistance in breast cancer cell lines. FASEB J *21*: 4013-4027, 2007.

55 Healy SJM, Gorman AM, Mousavi-Shafaei P, Gupta S and Samali A: Targeting the endoplasmic reticulum-stress response as an anticancer strategy. Eur J Pharmacol *625*: 234-246, 2009.

56 Gupta S, McGrath B and Cavener DR: PERK regulates the proliferation and development of insulin-secreting beta-cell tumours in the endocrine pancreas of mice. PloS One *4*: e8008, 2009.

57 Ranganathan AC, Ojha S, Kourtidis A, Conklin DS and AguirreGhiso JA: Dual function of pancreatic endoplasmic reticulum kinase in tumour cell growth arrest and survival. Cancer Res *68*: 3260-3268, 2008.

58 Sequeira SJ, Ranganathan AC, Adam AP, Iglesias BV, Farias EF and Aguirre-Ghiso JA: Inhibition of proliferation by PERK regulates mammary acinar morphogenesis and tumour formation. PloS One *2*: e615, 2007.

59 Perkins DJ and Barber GN: Defects in translational regulation mediated by the alpha subunit of eukaryotic initiation factor 2 inhibit antiviral activity and facilitate the malignant transformation of human fibroblasts. Mol Cell Biol *24*: 20252040, 2004.

60 Marciniak SJ, Yun CY, Oyadomari S, Novoa I, Zhang Y, Jungreis R, Nagata K, Harding HP and Ron D: CHOP induces death by promoting protein synthesis and oxidation in the stressed endoplasmic reticulum. Genes Dev *18*: 3066-3077, 2004.

61 Han J, Back SH, Hur J, Lin YH, Gildersleeve R, Shan J, Yuan CL, Krokowski D, Wang S, Hatzoglou M, Kilberg MS, Sartor MA and Kaufman RJ: ER-stress-induced transcriptional regulation increases protein synthesis leading to cell death. Nature Cell Biol *15*: 481-490, 2013.

62 Boyce M, Bryant KF, Jousse C, Long K, Harding HP, Scheuner D, Kaufman RJ, Ma D, Coen DM, Ron D and Yuan J: A selective inhibitor of eIF2alpha dephosphorylation protects cells from ER stress. Science *307*: 935-939, 2005.

63 Gorman AM, Healy SJM, Jäger R and Samali A: Stress management at the ER: Regulators of ER stress-induced apoptosis. Pharmacol Ther *134*: 306-316, 2012.

64 Zinszner H, Kuroda M, Wang X, Batchvarova N, Lightfoot RT, Remotti H, Stevens JL and Ron D: CHOP is implicated in programmed cell death in response to impaired function of the endoplasmic reticulum. Genes Dev *12*: 982-995, 1998.

65 Jauhiainen A, Thomsen C, Strömbom L, Grundevik P, Andersson C, Danielsson A, Andersson MK, Nerman O, Rörkvist L, Ståhlberg A and Aman P: Distinct cytoplasmic and nuclear functions of the stress induced protein DDIT3/CHOP/ GADD153. PloS One *7*: e33208, 2012.

66 Weston RT and Puthalakath H: Endoplasmic reticulum stress and BCL-2 family members. Adv Exp Med Biol *687*: 65-77, 2010.

67 Li G, Mongillo M, Chin KT, Harding H, Ron D, Marks AR and Tabas I: Role of ERO1-α-mediated stimulation of inositol 1,4,5triphosphate receptor activity in endoplasmic reticulum stressinduced apoptosis. J Cell Biol *186*: 783-792, 2009.

68 Timmins JM, Ozcan L, Seimon TA, Li G, Malagelada C, Backs J, Backs T, Bassel-Duby R, Olson EN, Anderson ME and Tabas I: Calcium/calmodulin-dependent protein kinase II links ER stress with FAS and mitochondrial apoptosis pathways. J Clin Invest *119*: 2925-2941, 2009.

69 Nishitoh H: CHOP is a multifunctional transcription factor in the ER stress response. J Biochem *151*: 217-219, 2012.

70 Verma G and Datta M: The critical role of JNK in the ERmitochondrial crosstalk during apoptotic cell death. J Cell Physiol *227*: 1791-1795, 2012.

71 Nakagawa H, Hirata Y, Takeda K, Hayakawa Y, Sato T, Kinoshita H, Sakamoto K, Nakata W, Hikiba Y, Omata M, Yoshida H, Koike K, Ichijo H and Maeda S: Apoptosis signal-regulating kinase 1 inhibits hepatocarcinogenesis by controlling the tumour-suppressing function of stress-activated mitogen-activated protein kinase. Hepatology *54*: 185-195, 2011.

72 Kim I, Shu CW, Xu W, Shiau CW, Grant D, Vasile S, Cosford NDP and Reed JC: Chemical biology investigation of cell death pathways activated by endoplasmic reticulum stress reveals cytoprotective modulators of ASK1. J Biol Chem *284*: 15931603, 2009.

73 Weston CR and Davis RJ: The JNK signal transduction pathway. Curr Opin Cell Biol *19*: 142-149, 2007.

74 Puthalakath H, O'Reilly LA, Gunn P, Lee L, Kelly PN, Huntington ND, Hughes PD, Michalak EM, McKimm-Breschkin J, Motoyama N, Gotoh T, Akira S, Bouillet P and Strasser A: ER stress triggers apoptosis by activating BH3-only protein Bim. Cell *129*: 1337-1349, 2007.

75 Pike LRG, Phadwal K, Simon AK and Harris AL: ATF4 orchestrates a program of BH3-only protein expression in severe hypoxia. Mol Biol Rep *39*: 10811-10822, 2012.

76 Hetz C, Bernasconi P, Fisher J, Lee AH, Bassik MC, Antonsson B, Brandt GS, Iwakoshi NN, Schinzel A, Glimcher LH and Korsmeyer SJ: Proapoptotic BAX and BAK modulate the unfolded protein response by a direct interaction with IRE1α. Science *312*: 572-576, 2006.

77 Klee M, Pallauf K, Alcalá S, Fleischer A and Pimentel-Muiños FX: Mitochondrial apoptosis induced by BH3-only molecules in the exclusive presence of endoplasmic reticular Bak. EMBO J *28*: 1757-1768, 2009.

78 Lisbona F, Rojas-Rivera D, Thielen P, Zamorano S, Todd D, Martinon F, Glavic A, Kress C, Lin JH, Walter P, Reed JC, Glimcher LH and Hetz C: BAX inhibitor-1 is a negative regulator of the ER stress sensor IRE1α. Mol Cell *33*: 679-691, 2009.

79 Bultynck G, Kiviluoto S, Henke N, Ivanova H, Schneider L, Rybalchenko V, Luyten T, Nuyts K, De Borggraeve W, Bezprozvanny I, Parys JB, De Smedt H, Missiaen L and Methner A: The C terminus of Bax inhibitor-1 forms a Ca^{2+}permeable channel pore. J Biol Chem *287*: 2544-2557, 2012.

80 Zong WX, Li C, Hatzivassiliou G, Lindsten T, Yu QC, Yuan J and Thompson CB: Bax and Bak can localize to the endoplasmic reticulum to initiate apoptosis. J Cell Biol *162*: 59-69, 2003.

81 Lee AS: GRP78 induction in cancer: therapeutic and prognostic implications. Cancer Res *67*: 3496-3499, 2007.

82 Scorrano L, Oakes SA, Opferman JT, Cheng EH, Sorcinelli MD, Pozzan T and Korsmeyer SJ: BAX and BAK regulation of endoplasmic reticulum Ca^{2+}: A control point for apoptosis. Science *300*: 135-139, 2003.

83 Morishima N, Nakanishi K and Nakano A: Activating transcription factor-6 (ATF6) mediates apoptosis with reduction of myeloid cell leukaemia sequence 1 (Mcl-1) protein *via* induction of WW domain binding protein 1. J Biol Chem *286*: 35227-35235, 2011.

84 Hitomi J, Katayama T, Eguchi Y, Kudo T, Taniguchi M, Koyama Y, Manabe T, Yamagishi S, Bando Y, Imaizumi K, Tsujimoto Y and Tohyama M: Involvement of caspase-4 in endoplasmic reticulum stress-induced apoptosis and amyloid-β-induced cell death. J Cell Biol *165*: 347-356, 2004.

85 Tan Y, Dourdin N, Wu C, De Veyra T, Elce JS and Greer PA: Ubiquitous calpains promote caspase-12 and JNK activation during endoplasmic reticulum stress-induced apoptosis. J Biol Chem *281*: 16016-16024, 2006.

86 Saleh M, Mathison JC, Wolinski MK, Bensinger SJ, Fitzgerald P, Droin N, Ulevitch RJ, Green DR and Nicholson DW: Enhanced bacterial clearance and sepsis resistance in caspase12-deficient mice. Nature *440*: 1064-1068, 2006.

87 Li C, Wei J, Li Y, He X, Zhou Q, Yan J, Zhang J, Liu Y, Liu Y and Shu HB: Transmembrane protein 214 (TMEM214) mediates endoplasmic reticulum stress-induced caspase-4 activation and apoptosis. J Biol Chem *288*: 17908-17917, 2013.

88 Axten JM, Medina JR, Feng Y, Shu A, Romeril SP, Grant SW, Li WHH, Heerding DA, Minthorn E, Mencken T, Atkins C, Liu Q, Rabindran S, Kumar R, Hong X, Goetz A, Stanley T, Taylor JD, Sigethy SD, Tomberlin GH, Hassell AM, Kahler KM, Shewchuk LM and Gampe RT: Discovery of 7-methyl-5-(1-{(3-(trifluoromethyl)phenyl)acetyl}-2,3-dihydro-1H-indol-5-yl)-7Hpyrrolo(2,3-d)pyrimidin-4-amine (GSK2606414), a potent and selective first-in-class inhibitor of protein kinase R (PKR)-like endoplasmic reticulum kinase (PERK). J Med Chem *55*: 71937207, 2012.

89 Flaherty DP, Golden JE, Liu C, Hedrick M, Gosalia P, Li Y, Milewski M, *et al.* Selective Small Molecule Activator of the Apoptotic Arm of the UPR. National Center for Biotechnology Information (US), Probe Reports, 1 April 2012.

90 Lin JH, Li H, Yasumura D, Cohen HR, Zhang C, Panning B, Shokat KM, Lavail MM and Walter P: IRE1 signalling affects cell fate during the unfolded protein response. Science *318*: 944949, 2007.

91 Ji C: Mechanisms of alcohol-induced endoplasmic reticulum stress and organ injuries. Biochem Res Int *2012*: 216450, 2012.

92 Teodoro T, Odisho T, Sidorova E and Volchuk A: Pancreatic βcells depend on basal expression of active ATF6α-p50 for cell survival even under non-stress conditions. Am J Physiol Cell Physiol *302*: C992-C1003, 2012.

93 Yamaguchi Y, Larkin D, Lara-Lemus R, Ramos-Castañeda J, Liu M and Arvan P: Endoplasmic reticulum (ER) chaperone regulation and survival of cells compensating for deficiency in the ER stress response kinase, PERK. J Biol Chem *283*: 17020-17029, 2008.

2.5. Endoplasmic reticulum stress in hepatocellular carcinoma

Rapid tumour growth creates hypoxia, glucose deprivation and oxidative stress, activating the UPR in various solid tumour types [33]. In human HCC, Shuda et al. (2003) showed that elevated expression of GRP78 and ATF6 and splicing of XBP1 mRNA occurred in HCC tissues with increased histological grading [56]. Higher accumulation of the GRP78 product in the cytoplasm, concomitantly with marked nuclear localization of the activated ATF6 fragment, was observed in moderately to poorly differentiated HCC tissues. In addition, Al-Rawashdeh et al. (2010) showed that 100% of the 86 investigated human HCC samples exhibited increased expression of ER stress marker GRP78 [57]. Proteomic profiling of 146 HCC samples revealed that in response to the stressful microenvironment, tumour cells strived to increase the expression of chaperone proteins including GRP78 for cytoprotective function [58]. Moreover, upregulation of GRP78 was significantly associated with tumour venous infiltration. Also CHOP expression was shown to be upregulated in human HCC [59]. In contrast, unaffected liver tissue from HCC patients showed significantly less CHOP staining and control liver samples showed less still. In summary, the UPR was shown to be activated in human HCC [56]–[58]. However, the dynamics and the role of these pathways in hepatocarcinogenesis is currently unknown.

3. **Autophagy**

3.1. Autophagy: a lysosomal degradation pathway

Autophagy or "self-eating" digests proteins and organelles to reuse. Autophagy is an evolutionary highly conserved mechanism involved in cellular homeostasis under basal conditions and is upregulated during cellular stress [60]. During autophagy, cytoplasmic content is delivered to lysosomes for degradation to macronutrients and energy. As shown in Figure 7 , there are three isoforms: 1) micro-autophagy, i.e. direct engulfment of cytoplasmic content by a lysosome, 2) chaperone-mediated autophagy (CMA), i.e. delivery of cytoplasmic proteins by specific chaperones to the lysosome and 3) macro-autophagy, i.e. isolation of cytoplasmic material in a double membrane structure, which will subsequently fuse with the lysosome [61], [62]. **Macro-autophagy** is thought to play the most significant role under pathophysiological conditions and we refer to this isoform through this thesis [62]. Autophagy is a context-dependent tumour-suppressing mechanism that can also promote tumour cell survival upon stress and treatment resistance [63]. Because of this ambiguity, autophagy is considered as a double-edged sword, making therapeutic approaches highly challenging.

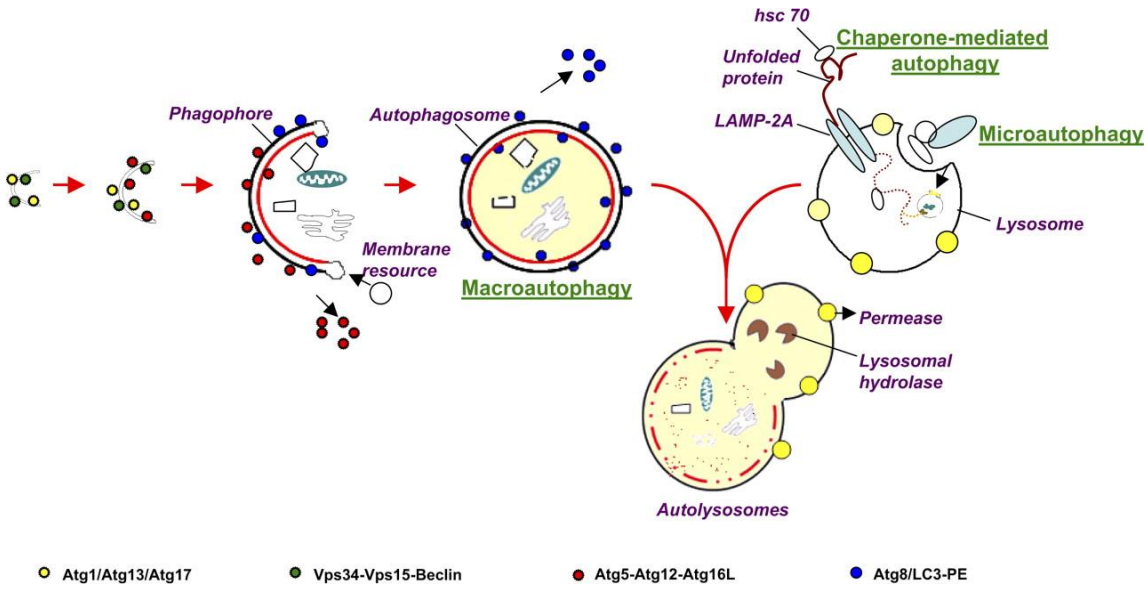

Figure 7. The three forms of autophagy: macroautophagy, microautophagy and chaperone-mediated autophagy. Macroautophagy starts with the *de novo* formation of a cup-shaped double membrane that engulfs a portion of cytoplasm. Microautophagy involves the engulfment of cytoplasm instantly at the lysosomal membrane by invagination, protrusion and separation. Chaperone-mediated autophagy is a process of direct transport of unfolded proteins via the lysosomal chaperonin hsc70 and LAMP-2A. All forms of autophagy subsequently lead to the degradation of intra-autophagosomal components by lysosomal hydrolases. PE, phosphatidylethanolamine. [64]

3.2. Autophagy and endoplasmic reticulum stress: integration of two double-edged swords

ER stress induces autophagy directly through upregulation of **GRP78** and through mechanisms downstream of the three UPR signal transducers [65]. A critical role for GRP78 in autophagy was demonstrated with GRP78 knockdown in normal and cancer cells, which prevented autophagosome formation in response to starvation or in response to tunicamycin, an inhibitor of N-linked glycosylation required for proper protein folding. The massively dilated and disrupted ER and deficient autophagosome formation induced by GRP78 knockdown were both alleviated by simultaneous knockdown of the IRE1-regulated XBP1 [66], suggesting that intact ER is maintained by and required for autophagy.

The link between the **IRE1** branch and autophagy is mediated by IRE1-activated JNK. A study conducted in neuroblastoma cells using siRNA knockdown of IRE1, PERK or ATF6 or using a JNK inhibitor, demonstrated that ER stress upregulated autophagy through a mechanism dependent on IRE1, but independently of PERK and ATF6 [67]. ER stress was induced with ER stress inducers tunicamycin or thapsigargin, an agent that blocks ER Ca^{2+} uptake by inhibiting ER Ca^{2+}-ATPase. In this model, autophagy protected against cell death as demonstrated by the increased cell death when autophagy was inhibited by chemical (3-methyladenine) or genetic manipulation (ATG7 siRNA) and suppressed cell death when autophagy was induced by chemical stimulation by the mTOR inhibitor rapamycin. The mechanism of autophagy induction downstream of JNK is a result of JNK phosphorylation of Bcl-2, which releases Bcl-2 repression of the autophagy factor Beclin1 [68].

The link between the **PERK** arm and autophagy is mediated by ATF4-driven upregulation of the ATG genes [69]. Treatment of embryonic carcinoma cells with misfolded polyglutamine repeats caused accumulation of polyubiquitinated protein aggregates and induced LC3 conversion through a PERK-dependent mechanism and resulting in autophagic elimination of the aggregates [70]. When proteasomal inhibitor bortezomib was used in pancreatic cancer cells, phospho-eIF2α led to ATF4-driven transcription of ATG5 and ATG7 [71].

All three of the UPR arms were involved in the induction of autophagy in breast cancer cells caused by accumulation of sphingosine-1-phosphate [72]. The resulting autophagy was prevented by silencing of PERK, IRE1 or ATF6. In conclusion, multiple levels of **integration between autophagy and the UPR** can maintain cellular homeostasis or default into apoptosis. Upon stress, the ultimate consequence of cell survival or apoptosis depends on the balance of events linked at multiple network connections between the UPR and autophagy.

4. Angiogenesis and endoplasmic reticulum stress

4.1. Angiogenesis

Angiogenesis refers to the sprouting, migration and remodelling of existing blood vessels and plays a crucial role in several physiological processes as well as in a number of diseases including liver diseases and cancer [73], [74]. Endothelial cells exhibit the ability to divide rapidly in response to physiological stimuli, such as hypoxia, inflammation and shear stress. However, when these stimuli become too pronounced, angiogenesis becomes a key pathophysiological process, for example, in tumour growth. HCC cells exhibit rapid growth and consequently require high oxygen and nutrient supply [75]. Hence, these tumour cells induce the formation of new blood vessels to counteract hypoxia. As mentioned previously, HCC lesions are characterised by arterial hypervascularity to provide the tumour with oxygenated blood [1]. However, these neo-vessels are marked by a disorganised vasculature, consisting of leaky and tortuous vessels, resulting in a chaotic and dysfunctional blood flow [75].

Angiogenesis is tightly regulated by pro- and anti-angiogenic factors that are produced in steady-state. Pro-angiogenic factors such as **VEGF**, fibroblast growth factor (FGF), PDGF and interleukin-8 (IL-8), bind to their receptors on endothelial cells causing proliferation, release of matrix metalloproteinases and migration towards the angiogenic stimuli, and finally inducing the formation of new blood vessels [76]. The best characterized pathway regulating VEGF is the hypoxia inducible factor (HIF) pathway activated by hypoxia [77]. HIF1 and HIF2 are heterodimeric transcription factors composed of an α and β subunit. The β subunit is constitutively expressed but the α subunit is labile in an oxygen rich setting. When hypoxia occurs the α subunit is stabilized, thereby activating the HIF-complex, which induces transcription of pro-angiogenic factors such as VEGF and leads to angiogenesis restoring the oxygen levels [77], [78].

4.2. Angiogenesis and endoplasmic reticulum stress

It is well established that hypoxia and glucose deprivation induce angiogenesis in tumours, triggering the growth of new capillaries from pre-existing vessels [79]. Importantly, ER stress was shown to stimulate angiogenesis in tumour cells, where the UPR shifts the balance from anti-angiogenic to pro-angiogenic events through modulating the expression of different factors including VEGF, FGF, interleukin (IL)-1β, IL-6 and IL-8 [79], [80]. In fact, hypoxia causes upregulation of VEGF through the HIF pathway as well as via the UPR [73].

Glucose or amino acid deprivation, as well as chemical ER stress inducers thapsigargin and tunicamycin also induce VEGF upregulation, but only via the UPR [81]. The PERK target ATF4 directly binds to the VEGF promoter [73]. The IRE1/XBP1 axis also increases angiogenesis in cancer models, including VEGF and IL-6 expression [73]. Moreover, GRP78 expression accelerates cancer progression also through induction of tumour angiogenesis [82]. Recently, Karali et al. (2014) revealed that VEGF signalling engages UPR sensors in an unconventional manner independently of ER stress, mediated by mTOR signalling, to promote endothelial cell survival and angiogenesis [81]. This finding extends the role of the UPR sensors beyond adaptation to ER stress.

4.3. The placental growth factor

Another member of the VEGF family which contributes to pathological angiogenesis is the placental growth factor (PlGF) [83], [84]. The PlGF gene is highly expressed in the placenta at all stages of human gestation. Unlike VEGF, the role of PlGF during embryogenesis and physiological angiogenesis is redundant. PlGF-deficient mice are viable and fertile and do not have any visible abnormalities [85]. Recently, HIF-1α and chromatin remodelling were shown to be involved in the hypoxia-mediated upregulation of PlGF [86]. Studies in transgenic mice revealed that the angiogenic activity of PlGF is **restricted to pathological conditions**. Loss of PlGF impairs angiogenesis in wounded skin, ischemic retina, limb or heart and in cancer, whereas administration of recombinant PlGF promotes collateral vessel growth in models of limb and myocardial ischemia [85], [87].

The effect of PlGF is mediated by binding to VEGFR-1 and neuropilin-1 [88]. VEGFR1 is minimally expressed in adult quiescent vessels but membranous localization is upregulated during pathological conditions, stimulating PlGF-dependent angiogenesis. Different direct and indirect effects after PlGF-receptor interaction can lead to increased angiogenesis [89]. PlGF has been proposed to stimulate angiogenesis by displacing VEGF from VEGFR-1, thereby increasing the fraction of VEGF available to activate its main receptor, VEGFR-2. Activation of VEGFR-1 can also induce a crosstalk with VEGFR-2 resulting in transphosphorylation of VEGFR-2, which becomes more active in signalling VEGF-driven angiogenesis. Alternatively, PlGF might stimulate angiogenesis by direct signalling via VEGFR-1 or by forming heterodimers with VEGF [89].

As the role of PlGF is mainly restricted to pathological conditions, blocking PlGF signalling may be an attractive target to avoid potential side-effects related to VEGF inhibition such as thrombosis, hypertension and proteinuria [90]. In contrast to VEGF inhibitors, a monoclonal anti-PlGF antibody (aPlGF) has been shown to reduce pathological angiogenesis in various spontaneous cancer and other disease models without affecting healthy blood vessels, resulting in no major side effects [91]–[93]. We previously showed that PlGF inhibition exerts **antitumour effects** and induces **vessel normalization** in experimental HCC (Fig. 8) [91], [93]. However, the exact role of PlGF in tumoural UPR activation remains elusive.

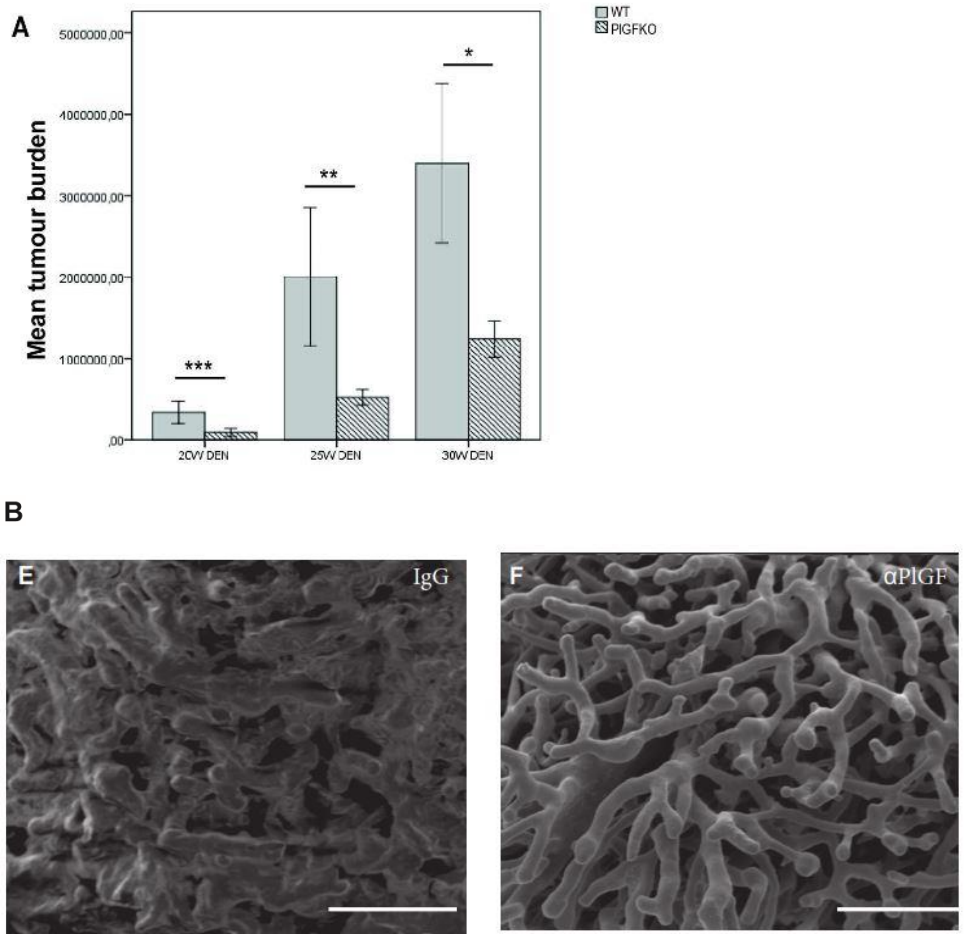

Figure 8. PlGF inhibition induces vessel normalization and antitumour effects in experimental HCC. (A) Mean tumour burden is reduced in placental growth factor knockout (PlGFKO) compared to wild type mice following 20, 25 and 30 weeks of diethylnitrosamine (DEN). *p<0.05, **p<0.01, ***p<0.001. (B) Scanning electron microscope images showing the microvasculature of IgG (chaotic) and anti-PlGF (αPlGF) (normalised) treated peritumoural vessels. Adapted from [91].

5. Artemisinins, cancer and endoplasmic reticulum stress

5.1. Artemisinins

Artemisinins are a family of sesquiterpene trioxane lactone anti-malarial agents originally derived from sweet wormwood Artemisia annua L. [94]. With its established safety record in millions of malarial patients, Artemisinins are also being investigated in cancer [95]. The active moiety is dihydroartemisinin (DHA), which is the reduced form of Artemisinin. Since DHA has unfavourable thermal stability, it is more convenient for pharmaceutical applications to use DHA prodrugs, including the stable succinate-ester derivative, **Artesunate** [96]. The latter confers substantial water-solubility and high oral bioavailability, resulting in a more favourable pharmacological profile. Artesunate is recommended by the World Health Organization in preference to quinidine for the treatment of malaria and has been used worldwide for many years. In 2007, the Food and Drug Administration made intravenous Artesunate available for treatment of malaria in the United States.

5.2. Artesunate and cancer: old drug, new tricks?

Artesunate has demonstrated remarkable cytotoxicity against a wide range of human tumour cell lines and showed anticancer activity in different animal models, including HCC [97], [98]. The multi-faceted mechanism of action of Artesunate involves the formation of free radicals via cleavage of the endoperoxide bond in its structure, protein alkylation, induction of apoptosis, angiogenesis inhibition, cell cycle regulation and abrogating cancer invasion and metastasis [99]. Importantly, the anti-cancer activity of DHA is also associated with induction of iron-dependent **ER stress** [100]. These preclinical results led to the development of clinical trials with Artesunate in cervical [101] and lung [102] cancer, which showed promising results.

6. Experimental mouse models for hepatocellular carcinoma

6.1. Carcinogen-induced mouse model

When selecting a model for HCC research, one must first understand the limitations and advantages that the specific model possesses. The advantage of chemically-induced models is the similarity with the injury-fibrosis-malignancy cycle observed in humans [103]. **Diethylnitrosamine** (DEN) is often used as a carcinogen and the target organ in which DEN induces tumours is species-dependent. Mice mostly develop liver tumours [104]. The carcinogenic capacity of DEN is situated in its capability of **alkylating DNA-structures**. In the first step DEN is hydroxylated to hydroxylnitrosamine. This bioactivation step is oxygen- and NADPH-dependent and mediated by cytochrome P450, an enzyme that has its highest activity in the centrilobular hepatocytes [105]. After cleavage of acetaldehyde, an electrophilic ethyldiazonium ion is formed and causes DNA-damage by reacting with nucleophiles such as DNA-bases. Furthermore, oxidative stress caused by DEN can contribute to the hepatocarcinogenesis [106]. **Reactive oxygen species** (ROS) generated by cytochrome P450 induce oxidative stress due to the formation of hydrogen peroxide and superoxide anions [106]. Production of ROS is known to cause DNA, protein and lipid damage; consequently oxidative stress has been known to play a significant role in DEN-elicited carcinogenesis.

Chronic DEN exposure for 25 weeks, in contrast to single DEN injection, induces small cell dysplasia, ductular hyperplasia and readily distinguishable HCC nodules occurring in a background of liver inflammation and mild fibrosis [104]. Additionally, we reported (YP. Vandewynckel, R. De Rycke, E. Bogaerts, H. Van Vlierberghe. *Intestinal metaplasia in an orthotopic mouse model for hepatocellular carcinoma*. Dig Liver Dis. 2014;46,e17) the rare occurrence of intestinal metaplastic cells in the liver parenchyma of DEN-treated mice. Intestinal metaplasia is the transformation of epithelium, usually of the stomach or the oesophagus but here of the hepatocytes, to an intestinal type. The existence of this phenotype is evidence of the multipotency of hepatic stem/progenitor cells involved in the hepatic healing response to DEN.

Limitations of this model include the high variability in tumour burden and high mortality (i.e. mean survival of 70% in our hands). In conclusion, DEN has been shown to induce tumours which are histologically similar to human HCC with poor prognosis.

6.2. Xenograft mouse model

In xenograft models, injecting human cancer cells from a cell culture in immune-deficient mice creates the tumours. Athymic (nude) or severe combined immune deficient mice are often used as hosts [103]. In the ectopic xenograft model, human tumour cells are subcutaneously injected in these mice and tumour volume is followed over time. The advantages of xenograft mouse models is the short time span needed for tumour development, low mortality and the low variability in tumour burden. However, the histological resemblance between xenograft and human tumours is rather poor [107].

7. **Reference list**

[1] "EASL-EORTC clinical practice guidelines: management of hepatocellular carcinoma.," *J. Hepatol.*, vol. 56, no. 4, pp. 908–43, Apr. 2012.

[2] A. Forner, J. M. Llovet, and J. Bruix, "Hepatocellular carcinoma.," *Lancet*, vol. 379, no. 9822, pp. 1245–55, Mar. 2012.

[3] D. Hanahan and R. a Weinberg, "Hallmarks of cancer: the next generation.," *Cell*, vol. 144, no. 5, pp. 646–74, Mar. 2011.

[4] A. Villanueva, P. Newell, D. Y. Chiang, S. L. Friedman, and J. M. Llovet, "Genomics and signaling pathways in hepatocellular carcinoma.," *Semin. Liver Dis.*, vol. 27, no. 1, pp. 55–76, Feb. 2007.

[5] Z. Li and Z. Li, "Glucose regulated protein 78: A critical link between tumor microenvironment and cancer hallmarks.," *Biochim. Biophys. Acta*, Mar. 2012.

[6] "Pathologic diagnosis of early hepatocellular carcinoma: a report of the international consensus group for hepatocellular neoplasia.," *Hepatology*, vol. 49, no. 2, pp. 658–64, Feb. 2009.

[7] M. Roncalli, L. Terracciano, L. Di Tommaso, E. David, and M. Colombo, "Liver precancerous lesions and hepatocellular carcinoma: the histology report.," *Dig. Liver Dis.*, vol. 43 Suppl 4, pp. S361–72, Mar. 2011.

[8] C. Pilati, E. Letouzé, J.-C. Nault, S. Imbeaud, A. Boulai, J. Calderaro, K. Poussin, A. Franconi, G. Couchy, G. Morcrette, M. Mallet, S. Taouji, C. Balabaud, B. Terris, F. Canal, V. Paradis, J.-Y. Scoazec, A. de Muret, C. Guettier, P. Bioulac-Sage, E. Chevet, F. Calvo, and J. Zucman-Rossi, "Genomic profiling of hepatocellular adenomas reveals recurrent FRK-activating mutations and the mechanisms of malignant transformation.," *Cancer Cell*, vol. 25, no. 4, pp. 428–41, Apr. 2014.

[9] K. Schulze, S. Imbeaud, E. Letouzé, L. B. Alexandrov, J. Calderaro, S. Rebouissou, G. Couchy, C. Meiller, J. Shinde, F. Soysouvanh, A.-L. Calatayud, R. Pinyol, L. Pelletier, C. Balabaud, A. Laurent, J.-F. Blanc, V. Mazzaferro, F. Calvo, A. Villanueva, J.-C. Nault, P. Bioulac-Sage, M. R. Stratton, J. M. Llovet, and J. Zucman-Rossi, "Exome sequencing of hepatocellular carcinomas identifies new mutational signatures and potential therapeutic targets.," *Nat. Genet.*, vol. 47, no. 5, pp. 505–11, Mar. 2015.

[10] D. Y. Chiang, A. Villanueva, Y. Hoshida, J. Peix, P. Newell, B. Minguez, A. C. LeBlanc, D. J. Donovan, S. N. Thung, M. Solé, V. Tovar, C. Alsinet, A. H. Ramos, J. Barretina, S. Roayaie, M. Schwartz, S. Waxman, J. Bruix, V. Mazzaferro, A. H. Ligon, V. Najfeld, S. L. Friedman, W. R. Sellers, M. Meyerson, and J. M. Llovet, "Focal gains of VEGFA and molecular classification of hepatocellular carcinoma.," *Cancer Res.*, vol. 68, no. 16, pp. 6779–88, Aug. 2008.

[11] A. Villanueva and J. M. Llovet, "Liver cancer in 2013: Mutational landscape of HCC--the end of the beginning.," *Nat. Rev. Clin. Oncol.*, vol. 11, no. 2, pp. 73–4, Feb. 2014.

[12] Y. Hoshida, S. Toffanin, A. Lachenmayer, A. Villanueva, B. Minguez, and J. M. Llovet, "Molecular classification and novel targets in hepatocellular carcinoma: recent advancements.," *Semin. Liver Dis.*, vol. 30, no. 1, pp. 35–51, Feb. 2010.

[13] A. Villanueva, Y. Hoshida, C. Battiston, V. Tovar, D. Sia, C. Alsinet, H. Cornella, A. Liberzon, M. Kobayashi, H. Kumada, S. N. Thung, J. Bruix, P. Newell, C. April, J.-B. Fan, S. Roayaie, V. Mazzaferro, M. E. Schwartz, and J. M. Llovet, "Combining clinical, pathology, and gene expression data to predict recurrence of hepatocellular carcinoma.," *Gastroenterology*, vol. 140, no. 5, pp. 1501–12.e2, May 2011.

[14] J.-C. Nault, A. De Reyniès, A. Villanueva, J. Calderaro, S. Rebouissou, G. Couchy, T. Decaens, D. Franco, S. Imbeaud, F. Rousseau, D. Azoulay, J. Saric, J.-F. Blanc, C.

Balabaud, P. Bioulac-Sage, A. Laurent, P. Laurent-Puig, J. M. Llovet, and J. Zucman-Rossi, "A hepatocellular carcinoma 5-gene score associated with survival of patients after liver resection.," *Gastroenterology*, vol. 145, no. 1, pp. 176–87, Jul. 2013.

[15] A. Villanueva and J. M. Llovet, "Impact of intra-individual molecular heterogeneity in personalized treatment of hepatocellular carcinoma.," *Hepatology*, vol. 56, no. 6, pp. 2416–9, Dec. 2012.

[16] International Agency for Research on Cancer, "GLOBOCAN 2012," *Estimated Incidence, Mortality and Prevalence Worldwide in 2012*, 2012. [Online]. Available: http://globocan.iarc.fr/Pages/fact_sheets_cancer.aspx.

[17] W.-C. Liu and Q.-Y. Liu, "Molecular mechanisms of gender disparity in hepatitis B virus-associated hepatocellular carcinoma.," *World J. Gastroenterol.*, vol. 20, no. 20, pp. 6252–61, May 2014.

[18] J. Bruix, K.-H. Han, G. Gores, J. M. Llovet, and V. Mazzaferro, "Liver cancer: Approaching a personalized care.," *J. Hepatol.*, vol. 62, no. 1S, pp. S144–S156, Apr. 2015.

[19] H. B. El-Serag and A. C. Mason, "Rising incidence of hepatocellular carcinoma in the United States.," *N. Engl. J. Med.*, vol. 340, no. 10, pp. 745–50, Mar. 1999.

[20] D. M. Parkin, F. Bray, J. Ferlay, and P. Pisani, "Global cancer statistics, 2002.," *CA. Cancer J. Clin.*, vol. 55, no. 2, pp. 74–108, Jan. .

[21] G. N. Ioannou, M. F. Splan, N. S. Weiss, G. B. McDonald, L. Beretta, and S. P. Lee, "Incidence and predictors of hepatocellular carcinoma in patients with cirrhosis.," *Clin. Gastroenterol. Hepatol.*, vol. 5, no. 8, pp. 938–45, 945.e1–4, Aug. 2007.

[22] A. Sangiovanni, E. Del Ninno, P. Fasani, C. De Fazio, G. Ronchi, R. Romeo, A. Morabito, R. De Franchis, and M. Colombo, "Increased survival of cirrhotic patients with a hepatocellular carcinoma detected during surveillance.," *Gastroenterology*, vol. 126, no. 4, pp. 1005–14, Apr. 2004.

[23] M. S. Ascha, I. A. Hanouneh, R. Lopez, T. A.-R. Tamimi, A. F. Feldstein, and N. N. Zein, "The incidence and risk factors of hepatocellular carcinoma in patients with nonalcoholic steatohepatitis.," *Hepatology*, vol. 51, no. 6, pp. 1972–8, Jun. 2010.

[24] S. C. Lu, "Where are we in the chemoprevention of hepatocellular carcinoma?," *Hepatology*, vol. 51, no. 3, pp. 734–6, Mar. 2010.

[25] E. E. Calle, C. Rodriguez, K. Walker-Thurmond, and M. J. Thun, "Overweight, obesity, and mortality from cancer in a prospectively studied cohort of U.S. adults.," *N. Engl. J. Med.*, vol. 348, no. 17, pp. 1625–38, Apr. 2003.

[26] S. Singh, P. P. Singh, L. R. Roberts, and W. Sanchez, "Chemopreventive strategies in hepatocellular carcinoma.," *Nat. Rev. Gastroenterol. Hepatol.*, vol. 11, no. 1, pp. 45–54, Jan. 2014.

[27] A. Cucchetti, F. Piscaglia, M. Cescon, A. Colecchia, G. Ercolani, L. Bolondi, and A. D. Pinna, "Cost-effectiveness of hepatic resection versus percutaneous radiofrequency ablation for early hepatocellular carcinoma.," *J. Hepatol.*, vol. 59, no. 2, pp. 300–7, Aug. 2013.

[28] J. Yamamoto, T. Kosuge, T. Takayama, K. Shimada, S. Yamasaki, H. Ozaki, N. Yamaguchi, and M. Makuuchi, "Recurrence of hepatocellular carcinoma after surgery.," *Br. J. Surg.*, vol. 83, no. 9, pp. 1219–22, Sep. 1996.

[29] T. Holvoet, S. Raevens, Y.-P. Vandewynckel, W. Van Biesen, K. Geboes, and H. Van Vlierberghe, "Systematic Review of Guidelines for Management of Intermediate Hepatocellular Carcinoma using the Appraisal of Guidelines Research and Evaluation II instrument," *Dig. Liver Dis.*, vol. accepted p, 2015.

[30] M. C. Brouwers, M. E. Kho, G. P. Browman, J. S. Burgers, F. Cluzeau, G. Feder, B. Fervers, I. D. Graham, J. Grimshaw, S. E. Hanna, P. Littlejohns, J. Makarski, and L.

Zitzelsberger, “AGREE II: advancing guideline development, reporting, and evaluation in health care.,” *Prev. Med. (Baltim).*, vol. 51, no. 5, pp. 421–4, Nov. 2010.

[31] J. M. Llovet, S. Ricci, V. Mazzaferro, P. Hilgard, E. Gane, J.-F. Blanc, A. C. de Oliveira, A. Santoro, J.-L. Raoul, A. Forner, M. Schwartz, C. Porta, S. Zeuzem, L. Bolondi, T. F. Greten, P. R. Galle, J.-F. Seitz, I. Borbath, D. Häussinger, T. Giannaris, M. Shan, M. Moscovici, D. Voliotis, and J. Bruix, “Sorafenib in advanced hepatocellular carcinoma.,” *N. Engl. J. Med.*, vol. 359, no. 4, pp. 378–90, Jul. 2008.

[32] J. M. Llovet and V. Hernandez-Gea, “Hepatocellular carcinoma: reasons for phase III failure and novel perspectives on trial design.,” *Clin. Cancer Res.*, vol. 20, no. 8, pp. 2072–9, Apr. 2014.

[33] Y.-P. Vandewynckel, D. Laukens, A. Geerts, E. Bogaerts, A. Paridaens, X. Verhelst, S. Janssens, F. Heindryckx, and H. Van Vlierberghe, “The paradox of the unfolded protein response in cancer.,” *Anticancer Res.*, vol. 33, no. 11, pp. 4683–94, Nov. 2013.

[34] P. Walter and D. Ron, “The unfolded protein response: from stress pathway to homeostatic regulation.,” *Science*, vol. 334, no. 6059, pp. 1081–6, Nov. 2011.

[35] P. Fagone and S. Jackowski, “Membrane phospholipid synthesis and endoplasmic reticulum function.,” *J. Lipid Res.*, vol. 50 Suppl, pp. S311–6, Apr. 2009.

[36] H. Bommiasamy, S. H. Back, P. Fagone, K. Lee, S. Meshinchi, E. Vink, R. Sriburi, M. Frank, S. Jackowski, R. J. Kaufman, and J. W. Brewer, “ATF6alpha induces XBP1-independent expansion of the endoplasmic reticulum.,” *J. Cell Sci.*, vol. 122, no. Pt 10, pp. 1626–36, May 2009.

[37] G. E. Stutzmann and M. P. Mattson, “Endoplasmic reticulum Ca(2+) handling in excitable cells in health and disease.,” *Pharmacol. Rev.*, vol. 63, no. 3, pp. 700–27, Sep. 2011.

[38] C. Hetz, “The unfolded protein response: controlling cell fate decisions under ER stress and beyond.,” *Nat. Rev. Mol. Cell Biol.*, vol. 13, no. 2, pp. 89–102, Feb. 2012.

[39] R. V Rao, A. Peel, A. Logvinova, G. del Rio, E. Hermel, T. Yokota, P. C. Goldsmith, L. M. Ellerby, H. M. Ellerby, and D. E. Bredesen, “Coupling endoplasmic reticulum stress to the cell death program: role of the ER chaperone GRP78.,” *FEBS Lett.*, vol. 514, no. 2–3, pp. 122–8, Mar. 2002.

[40] S. Schuck, W. A. Prinz, K. S. Thorn, C. Voss, and P. Walter, “Membrane expansion alleviates endoplasmic reticulum stress independently of the unfolded protein response.,” *J. Cell Biol.*, vol. 187, no. 4, pp. 525–36, Nov. 2009.

[41] C. Hetz, E. Chevet, and H. P. Harding, “Targeting the unfolded protein response in disease.,” *Nat. Rev. Drug Discov.*, vol. 12, no. 9, pp. 703–19, Sep. 2013.

[42] S. Janssens, B. Pulendran, and B. N. Lambrecht, “Emerging functions of the unfolded protein response in immunity,” *Nat. Immunol.*, vol. 15, no. 10, pp. 910–919, Sep. 2014.

[43] S. Kondo, A. Saito, R. Asada, S. Kanemoto, and K. Imaizumi, “Physiological unfolded protein response regulated by OASIS family members, transmembrane bZIP transcription factors.,” *IUBMB Life*, vol. 63, no. 4, pp. 233–9, Apr. 2011.

[44] K. Mori, “Signalling pathways in the unfolded protein response: development from yeast to mammals.,” *J. Biochem.*, vol. 146, no. 6, pp. 743–50, Dec. 2009.

[45] J. H. Lin, H. Li, D. Yasumura, H. R. Cohen, C. Zhang, B. Panning, K. M. Shokat, M. M. Lavail, and P. Walter, “IRE1 signaling affects cell fate during the unfolded protein response.,” *Science*, vol. 318, no. 5852, pp. 944–9, Nov. 2007.

[46] M. Maurel, E. Chevet, J. Tavernier, and S. Gerlo, “Getting RIDD of RNA: IRE1 in cell fate regulation.,” *Trends Biochem. Sci.*, Mar. 2014.

[47] D. Ron and P. Walter, “Signal integration in the endoplasmic reticulum unfolded protein response.,” *Nat. Rev. Mol. Cell Biol.*, vol. 8, no. 7, pp. 519–29, Jul. 2007.

[48] M. Lu, D. A. Lawrence, S. Marsters, D. Acosta-Alvear, P. Kimmig, A. S. Mendez, A. W. Paton, J. C. Paton, P. Walter, and A. Ashkenazi, "Cell death. Opposing unfolded-protein-response signals converge on death receptor 5 to control apoptosis.," *Science*, vol. 345, no. 6192, pp. 98–101, Jul. 2014.

[49] M. D. Shoulders, L. M. Ryno, J. C. Genereux, J. J. Moresco, P. G. Tu, C. Wu, J. R. Yates, A. I. Su, J. W. Kelly, and R. L. Wiseman, "Stress-Independent Activation of XBP1s and/or ATF6 Reveals Three Functionally Diverse ER Proteostasis Environments.," *Cell Rep.*, vol. 3, no. 4, pp. 1279–92, Apr. 2013.

[50] H. P. Harding, Y. Zhang, A. Bertolotti, H. Zeng, and D. Ron, "Perk is essential for translational regulation and cell survival during the unfolded protein response.," *Mol. Cell*, vol. 5, no. 5, pp. 897–904, May 2000.

[51] H. Zinszner, M. Kuroda, X. Wang, N. Batchvarova, R. T. Lightfoot, H. Remotti, J. L. Stevens, and D. Ron, "CHOP is implicated in programmed cell death in response to impaired function of the endoplasmic reticulum.," *Genes Dev.*, vol. 12, no. 7, pp. 982–95, Apr. 1998.

[52] S. B. Cullinan, D. Zhang, M. Hannink, E. Arvisais, R. J. Kaufman, and J. A. Diehl, "Nrf2 is a direct PERK substrate and effector of PERK-dependent cell survival.," *Mol. Cell. Biol.*, vol. 23, no. 20, pp. 7198–209, Oct. 2003.

[53] S. Wang and R. J. Kaufman, "The impact of the unfolded protein response on human disease.," *J. Cell Biol.*, vol. 197, no. 7, pp. 857–67, Jun. 2012.

[54] R. C. Austin, "The unfolded protein response in health and disease.," *Antioxid. Redox Signal.*, vol. 11, no. 9, pp. 2279–87, Sep. 2009.

[55] R. J. Kaufman, "Orchestrating the unfolded protein response in health and disease.," *J. Clin. Invest.*, vol. 110, no. 10, pp. 1389–98, Nov. 2002.

[56] M. Shuda, "Activation of the ATF6, XBP1 and grp78 genes in human hepatocellular carcinoma: a possible involvement of the ER stress pathway in hepatocarcinogenesis," *J. Hepatol.*, vol. 38, no. 5, pp. 605–614, May 2003.

[57] F. Y. Al-Rawashdeh, P. Scriven, I. C. Cameron, P. V Vergani, and L. Wyld, "Unfolded protein response activation contributes to chemoresistance in hepatocellular carcinoma.," *Eur. J. Gastroenterol. Hepatol.*, vol. 22, no. 9, pp. 1099–105, Sep. 2010.

[58] J. M. Luk, C.-T. Lam, A. F. M. Siu, B. Y. Lam, I. O. L. Ng, M.-Y. Hu, C.-M. Che, and S.-T. Fan, "Proteomic profiling of hepatocellular carcinoma in Chinese cohort reveals heat-shock proteins (Hsp27, Hsp70, GRP78) up-regulation and their associated prognostic values.," *Proteomics*, vol. 6, no. 3, pp. 1049–57, Feb. 2006.

[59] D. Dezwaan-McCabe, J. D. Riordan, A. M. Arensdorf, M. S. Icardi, A. J. Dupuy, and D. T. Rutkowski, "The Stress-Regulated Transcription Factor CHOP Promotes Hepatic Inflammatory Gene Expression, Fibrosis, and Oncogenesis.," *PLoS Genet.*, vol. 9, no. 12, p. e1003937, Dec. 2013.

[60] J. Cui, Z. Gong, and H.-M. Shen, "The role of autophagy in liver cancer: molecular mechanisms and potential therapeutic targets.," *Biochim. Biophys. Acta*, vol. 1836, no. 1, pp. 15–26, Aug. 2013.

[61] W. Martinet, J.-P. Timmermans, and G. R. Y. De Meyer, "Methods to assess autophagy in situ--transmission electron microscopy versus immunohistochemistry.," *Methods Enzymol.*, vol. 543, pp. 89–114, Jan. 2014.

[62] W. J. Kwanten, W. Martinet, P. P. Michielsen, and S. M. Francque, "Role of autophagy in the pathophysiology of nonalcoholic fatty liver disease: a controversial issue.," *World J. Gastroenterol.*, vol. 20, no. 23, pp. 7325–38, Jun. 2014.

[63] J. Kubisch, D. Türei, L. Földvári-Nagy, Z. A. Dunai, L. Zsákai, M. Varga, T. Vellai, P. Csermely, and T. Korcsmáros, "Complex regulation of autophagy in cancer - integrated

approaches to discover the networks that hold a double-edged sword.," *Semin. Cancer Biol.*, vol. 23, no. 4, pp. 252–61, Aug. 2013.

[64] S. Periyasamy-Thandavan, M. Jiang, P. Schoenlein, and Z. Dong, "Autophagy: molecular machinery, regulation, and implications for renal pathophysiology.," *Am. J. Physiol. Renal Physiol.*, vol. 297, no. 2, pp. F244–56, Aug. 2009.

[65] D. M. Benbrook and A. Long, "Integration of autophagy, proteasomal degradation, unfolded protein response and apoptosis.," *Exp. Oncol.*, vol. 34, no. 3, pp. 286–97, Oct. 2012.

[66] A.-H. Lee, G. C. Chu, N. N. Iwakoshi, and L. H. Glimcher, "XBP-1 is required for biogenesis of cellular secretory machinery of exocrine glands.," *EMBO J.*, vol. 24, no. 24, pp. 4368–80, Dec. 2005.

[67] M. Ogata, S. Hino, A. Saito, K. Morikawa, S. Kondo, S. Kanemoto, T. Murakami, M. Taniguchi, I. Tanii, K. Yoshinaga, S. Shiosaka, J. A. Hammarback, F. Urano, and K. Imaizumi, "Autophagy is activated for cell survival after endoplasmic reticulum stress.," *Mol. Cell. Biol.*, vol. 26, no. 24, pp. 9220–31, Dec. 2006.

[68] Y. Wei, S. Pattingre, S. Sinha, M. Bassik, and B. Levine, "JNK1-mediated phosphorylation of Bcl-2 regulates starvation-induced autophagy.," *Mol. Cell*, vol. 30, no. 6, pp. 678–88, Jun. 2008.

[69] A. C. Kimmelman, "The dynamic nature of autophagy in cancer.," *Genes Dev.*, vol. 25, no. 19, pp. 1999–2010, Oct. 2011.

[70] Y. Kouroku, E. Fujita, I. Tanida, T. Ueno, A. Isoai, H. Kumagai, S. Ogawa, R. J. Kaufman, E. Kominami, and T. Momoi, "ER stress (PERK/eIF2alpha phosphorylation) mediates the polyglutamine-induced LC3 conversion, an essential step for autophagy formation.," *Cell Death Differ.*, vol. 14, no. 2, pp. 230–9, Feb. 2007.

[71] K. Zhu, K. Dunner, and D. J. McConkey, "Proteasome inhibitors activate autophagy as a cytoprotective response in human prostate cancer cells.," *Oncogene*, vol. 29, no. 3, pp. 451–62, Jan. 2010.

[72] S. Lépine, J. C. Allegood, M. Park, P. Dent, S. Milstien, and S. Spiegel, "Sphingosine-1-phosphate phosphohydrolase-1 regulates ER stress-induced autophagy.," *Cell Death Differ.*, vol. 18, no. 2, pp. 350–61, Feb. 2011.

[73] A. Paridaens, D. Laukens, Y.-P. Vandewynckel, S. Coulon, H. Van Vlierberghe, A. Geerts, and I. Colle, "Endoplasmic reticulum stress and angiogenesis: is there an interaction between them?," *Liver Int.*, Jan. 2014.

[74] S. Coulon, F. Heindryckx, A. Geerts, C. Van Steenkiste, I. Colle, and H. Van Vlierberghe, "Angiogenesis in chronic liver disease and its complications.," *Liver Int.*, vol. 31, no. 2, pp. 146–62, Feb. 2011.

[75] K. R. Sampat and B. O'Neil, "Antiangiogenic therapies for advanced hepatocellular carcinoma.," *Oncologist*, vol. 18, no. 4, pp. 430–8, Jan. 2013.

[76] E. R. Pereira, N. Liao, G. A. Neale, and L. M. Hendershot, "Transcriptional and post-transcriptional regulation of proangiogenic factors by the unfolded protein response.," *PLoS One*, vol. 5, no. 9, Jan. 2010.

[77] M. M. Hickey and M. C. Simon, "Regulation of angiogenesis by hypoxia and hypoxia-inducible factors.," *Curr. Top. Dev. Biol.*, vol. 76, pp. 217–57, Jan. 2006.

[78] X. Yang, Y. Zhang, Y. Yang, S. Lim, Z. Cao, J. Rak, and Y. Cao, "Vascular endothelial growth factor-dependent spatiotemporal dual roles of placental growth factor in modulation of angiogenesis and tumor growth.," *Proc. Natl. Acad. Sci. U. S. A.*, vol. 110, no. 34, pp. 13932–7, Aug. 2013.

[79] E. Dufey, H. Urra, and C. Hetz, "ER proteostasis addiction in cancer biology: Novel concepts.," *Semin. Cancer Biol.*, Apr. 2015.

[80] Y. Wang, G. N. Alam, Y. Ning, F. Visioli, Z. Dong, J. E. Nör, and P. J. Polverini, "The unfolded protein response induces the angiogenic switch in human tumor cells through the PERK/ATF4 pathway.," *Cancer Res.*, vol. 72, no. 20, pp. 5396–406, Oct. 2012.

[81] E. Karali, S. Bellou, D. Stellas, A. Klinakis, C. Murphy, and T. Fotsis, "VEGF Signals through ATF6 and PERK to Promote Endothelial Cell Survival and Angiogenesis in the Absence of ER Stress.," *Mol. Cell*, Apr. 2014.

[82] D. Dong, M. Ni, J. Li, S. Xiong, W. Ye, J. J. Virrey, C. Mao, R. Ye, M. Wang, L. Pen, L. Dubeau, S. Groshen, F. M. Hofman, and A. S. Lee, "Critical role of the stress chaperone GRP78/BiP in tumor proliferation, survival, and tumor angiogenesis in transgene-induced mammary tumor development.," *Cancer Res.*, vol. 68, no. 2, pp. 498–505, Jan. 2008.

[83] N. Ferrara, H.-P. Gerber, and J. LeCouter, "The biology of VEGF and its receptors.," *Nat. Med.*, vol. 9, no. 6, pp. 669–76, Jun. 2003.

[84] D. Maglione, V. Guerriero, G. Viglietto, P. Delli-Bovi, and M. G. Persico, "Isolation of a human placenta cDNA coding for a protein related to the vascular permeability factor.," *Proc. Natl. Acad. Sci. U. S. A.*, vol. 88, no. 20, pp. 9267–71, Oct. 1991.

[85] P. Carmeliet, L. Moons, A. Luttun, V. Vincenti, V. Compernolle, M. De Mol, Y. Wu, F. Bono, L. Devy, H. Beck, D. Scholz, T. Acker, T. DiPalma, M. Dewerchin, A. Noel, I. Stalmans, A. Barra, S. Blacher, T. VandenDriessche, A. Ponten, U. Eriksson, K. H. Plate, J. M. Foidart, W. Schaper, D. S. Charnock-Jones, D. J. Hicklin, J. M. Herbert, D. Collen, and M. G. Persico, "Synergism between vascular endothelial growth factor and placental growth factor contributes to angiogenesis and plasma extravasation in pathological conditions.," *Nat. Med.*, vol. 7, no. 5, pp. 575–83, May 2001.

[86] L. Tudisco, F. Della Ragione, V. Tarallo, I. Apicella, M. D'Esposito, M. R. Matarazzo, and S. De Falco, "Epigenetic control of hypoxia inducible factor-1α-dependent expression of placental growth factor in hypoxic conditions.," *Epigenetics*, vol. 9, no. 4, pp. 600–10, Apr. 2014.

[87] A. Luttun, M. Tjwa, L. Moons, Y. Wu, A. Angelillo-Scherrer, F. Liao, J. A. Nagy, A. Hooper, J. Priller, B. De Klerck, V. Compernolle, E. Daci, P. Bohlen, M. Dewerchin, J.-M. Herbert, R. Fava, P. Matthys, G. Carmeliet, D. Collen, H. F. Dvorak, D. J. Hicklin, and P. Carmeliet, "Revascularization of ischemic tissues by PlGF treatment, and inhibition of tumor angiogenesis, arthritis and atherosclerosis by anti-Flt1.," *Nat. Med.*, vol. 8, no. 8, pp. 831–40, Aug. 2002.

[88] M. Dewerchin and P. Carmeliet, "Placental growth factor in cancer.," *Expert Opin. Ther. Targets*, vol. 18, no. 11, pp. 1339–54, Nov. 2014.

[89] S. De Falco, "The discovery of placenta growth factor and its biological activity.," *Exp. Mol. Med.*, vol. 44, no. 1, pp. 1–9, Jan. 2012.

[90] M. Snuderl, A. Batista, N. D. Kirkpatrick, C. Ruiz de Almodovar, L. Riedemann, E. C. Walsh, R. Anolik, Y. Huang, J. D. Martin, W. Kamoun, E. Knevels, T. Schmidt, C. T. Farrar, B. J. Vakoc, N. Mohan, E. Chung, S. Roberge, T. Peterson, C. Bais, B. H. Zhelyazkova, S. Yip, M. Hasselblatt, C. Rossig, E. Niemeyer, N. Ferrara, M. Klagsbrun, D. G. Duda, D. Fukumura, L. Xu, P. Carmeliet, and R. K. Jain, "Targeting placental growth factor/neuropilin 1 pathway inhibits growth and spread of medulloblastoma.," *Cell*, vol. 152, no. 5, pp. 1065–76, Feb. 2013.

[91] S. Van de Veire, I. Stalmans, F. Heindryckx, H. Oura, A. Tijeras-Raballand, T. Schmidt, S. Loges, I. Albrecht, B. Jonckx, S. Vinckier, C. Van Steenkiste, S. Tugues, C. Rolny, M. De Mol, D. Dettori, P. Hainaud, L. Coenegrachts, J.-O. Contreres, T. Van Bergen, H. Cuervo, W.-H. Xiao, C. Le Henaff, I. Buysschaert, B. Kharabi Masouleh, A. Geerts, T. Schomber, P. Bonnin, V. Lambert, J. Haustraete, S. Zacchigna, J.-M. Rakic, W. Jiménez, A. Noël, M. Giacca, I. Colle, J.-M. Foidart, G. Tobelem, M.

Morales-Ruiz, J. Vilar, P. Maxwell, S. A. Vinores, G. Carmeliet, M. Dewerchin, L. Claesson-Welsh, E. Dupuy, H. Van Vlierberghe, G. Christofori, M. Mazzone, M. Detmar, D. Collen, and P. Carmeliet, "Further pharmacological and genetic evidence for the efficacy of PlGF inhibition in cancer and eye disease.," *Cell*, vol. 141, no. 1, pp. 178–90, Apr. 2010.

[92] C. Fischer, B. Jonckx, M. Mazzone, S. Zacchigna, S. Loges, L. Pattarini, E. Chorianopoulos, L. Liesenborghs, M. Koch, M. De Mol, M. Autiero, S. Wyns, S. Plaisance, L. Moons, N. van Rooijen, M. Giacca, J.-M. Stassen, M. Dewerchin, D. Collen, and P. Carmeliet, "Anti-PlGF inhibits growth of VEGF(R)-inhibitor-resistant tumors without affecting healthy vessels.," *Cell*, vol. 131, no. 3, pp. 463–75, Nov. 2007.

[93] F. Heindryckx, S. Coulon, E. Terrie, C. Casteleyn, J.-M. Stassen, A. Geerts, L. Libbrecht, J. Allemeersch, P. Carmeliet, I. Colle, and H. Van Vlierberghe, "The placental growth factor as a target against hepatocellular carcinoma in a diethylnitrosamine-induced mouse model.," *J. Hepatol.*, vol. 58, no. 2, pp. 319–28, Feb. 2013.

[94] M. P. Crespo-Ortiz and M. Q. Wei, "Antitumor activity of artemisinin and its derivatives: from a well-known antimalarial agent to a potential anticancer drug.," *J. Biomed. Biotechnol.*, vol. 2012, p. 247597, Jan. 2012.

[95] T. Efferth, H. Dunstan, A. Sauerbrey, H. Miyachi, and C. R. Chitambar, "The anti-malarial artesunate is also active against cancer.," *Int. J. Oncol.*, vol. 18, no. 4, pp. 767–73, Apr. 2001.

[96] C. A. Morris, S. Duparc, I. Borghini-Fuhrer, D. Jung, C.-S. Shin, and L. Fleckenstein, "Review of the clinical pharmacokinetics of artesunate and its active metabolite dihydroartemisinin following intravenous, intramuscular, oral or rectal administration.," *Malar. J.*, vol. 10, p. 263, Jan. 2011.

[97] W. E. Ho, H. Y. Peh, T. K. Chan, and W. S. F. Wong, "Artemisinins: Pharmacological actions beyond anti-malarial.," *Pharmacol. Ther.*, vol. 142, no. 1, pp. 126–139, Dec. 2013.

[98] T. Efferth, A. Benakis, M. R. Romero, M. Tomicic, R. Rauh, D. Steinbach, R. Häfer, T. Stamminger, F. Oesch, B. Kaina, and M. Marschall, "Enhancement of cytotoxicity of artemisinins toward cancer cells by ferrous iron.," *Free Radic. Biol. Med.*, vol. 37, no. 7, pp. 998–1009, Oct. 2004.

[99] T. Efferth, A. Sauerbrey, A. Olbrich, E. Gebhart, P. Rauch, H. O. Weber, J. G. Hengstler, M.-E. Halatsch, M. Volm, K. D. Tew, D. D. Ross, and J. O. Funk, "Molecular modes of action of artesunate in tumor cell lines.," *Mol. Pharmacol.*, vol. 64, no. 2, pp. 382–94, Aug. 2003.

[100] J.-J. Lu, S.-M. Chen, X.-W. Zhang, J. Ding, and L.-H. Meng, "The anti-cancer activity of dihydroartemisinin is associated with induction of iron-dependent endoplasmic reticulum stress in colorectal carcinoma HCT116 cells.," *Invest. New Drugs*, vol. 29, no. 6, pp. 1276–83, Dec. 2011.

[101] F. H. Jansen, I. Adoubi, K. C. J C, T. DE Cnodder, N. Jansen, A. Tschulakow, and T. Efferth, "First study of oral Artenimol-R in advanced cervical cancer: clinical benefit, tolerability and tumor markers.," *Anticancer Res.*, vol. 31, no. 12, pp. 4417–22, Dec. 2011.

[102] Z.-Y. Zhang, S.-Q. Yu, L.-Y. Miao, X.-Y. Huang, X.-P. Zhang, Y.-P. Zhu, X.-H. Xia, and D.-Q. Li, "[Artesunate combined with vinorelbine plus cisplatin in treatment of advanced non-small cell lung cancer: a randomized controlled trial].," *Zhong Xi Yi Jie He Xue Bao*, vol. 6, no. 2, pp. 134–8, Feb. 2008.

[103] F. Heindryckx, I. Colle, and H. Van Vlierberghe, "Experimental mouse models for hepatocellular carcinoma research.," *Int. J. Exp. Pathol.*, vol. 90, no. 4, pp. 367–86, Aug. 2009.
[104] F. Heindryckx, K. Mertens, N. Charette, B. Vandeghinste, C. Casteleyn, C. Van Steenkiste, D. Slaets, L. Libbrecht, S. Staelens, P. Starkel, A. Geerts, I. Colle, and H. Van Vlierberghe, "Kinetics of angiogenic changes in a new mouse model for hepatocellular carcinoma," *Mol. Cancer*, vol. 9, no. 1, p. 219, 2010.
[105] J. S. Kang, H. Wanibuchi, K. Morimura, F. J. Gonzalez, and S. Fukushima, "Role of CYP2E1 in diethylnitrosamine-induced hepatocarcinogenesis in vivo.," *Cancer Res.*, vol. 67, no. 23, pp. 11141–6, Dec. 2007.
[106] G. M. Williams, M. J. Iatropoulos, and A. M. Jeffrey, "Mechanistic basis for nonlinearities and thresholds in rat liver carcinogenesis by the DNA-reactive carcinogens 2-acetylaminofluorene and diethylnitrosamine.," *Toxicol. Pathol.*, vol. 28, no. 3, pp. 388–95, Jan. .
[107] T. Troiani, C. Schettino, E. Martinelli, F. Morgillo, G. Tortora, and F. Ciardiello, "The use of xenograft models for the selection of cancer treatments with the EGFR as an example.," *Crit. Rev. Oncol. Hematol.*, vol. 65, no. 3, pp. 200–11, Mar. 2008.
[108] Y. Ma and L. M. Hendershot, "The role of the unfolded protein response in tumour development: friend or foe?," *Nat. Rev. Cancer*, vol. 4, no. 12, pp. 966–77, Dec. 2004.
[109] C. Jamora, G. Dennert, and A. S. Lee, "Inhibition of tumor progression by suppression of stress protein GRP78/BiP induction in fibrosarcoma B/C10ME.," *Proc. Natl. Acad. Sci. U. S. A.*, vol. 93, no. 15, pp. 7690–4, Jul. 1996.

Chapter 2

Aims of the work

1. **Aims of the work**

A role for ER stress signalling in cancer was initially proposed in 1996, introducing the concept that it could either be beneficial for tumour growth or play a guardian role to prevent cell transformation [108], [109]. Accumulating evidence in the course of the last decade indicated that all branches of the UPR contribute to the tumourigenesis, affecting diverse aspects of the disease including angiogenesis, cell differentiation, cell migration, tumour growth and the inflammatory microenvironment [41]. Also in human HCC, the UPR was shown to be activated [56].

- First, we aimed to determine the presence of ER stress and the temporal dynamics of UPR activation in the well-known diethylnitrosamine-induced mouse model for HCC. Additionally, we aimed to validate innovative imaging techniques for the functional assessment of experimental HCC burden (in collaboration with Infinity Lab, Ghent University).

- Secondly, we aimed to explore the effects of rational UPR modulation on HCC cell viability and proliferation *in vitro* and in the mouse model.

These objectives were assessed in the following manuscript:

Y.-P. Vandewynckel, D. Laukens, E. Bogaerts, A. Paridaens, A. Van den Bussche, X. Verhelst, C. Van Steenkiste, B. Descamps, C. Vanhove, L. Libbrecht, R. De Rycke, B. N. Lambrecht, A. Geerts, S. Janssens, H. Van Vlierberghe. **Modulation of the unfolded protein response impedes tumor cell adaptation to proteotoxic stress: a PERK for hepatocellular carcinoma therapy.** *Hepatol. Int.* 2014,9:93-104.

- Thirdly, we assessed the impact of ER stress in tumour initiation and progression by applying tauroursodeoxycholic acid (TUDCA), a bile acid with chaperone properties reducing ER stress, in the diethylnitrosamine-induced HCC model in preventive and therapeutic settings.

This objective was assessed in the following manuscript:

Y.-P. Vandewynckel, D. Laukens, L. Devisscher, A. Paridaens, E. Bogaerts, X. Verhelst, A. Van den Bussche, S. Raevens, C. Van Steenkiste, M. Van Troys, C. Ampe, B. Descamps, C. Vanhove, O. Govaere, A. Geerts, H. Van Vlierberghe. **Tauroursodeoxycholic acid dampens oncogenic apoptosis induced by endoplasmic reticulum stress during hepatocarcinogen exposure.** *Oncotarget* 2015,6:X. Accepted.

- Finally, we assessed the effect of established or potential HCC treatments possibly modulating the UPR, including sorafenib, artesunate, PlGF inhibition and proteasome inhibition, on the tumour growth and UPR signature in HCC and subsequently aimed to enhance the antitumour efficacy of these treatments by UPR modulation subverting ER stress towards apoptosis of the tumour cells.

These objectives were assessed in the following manuscripts:

Y.-P. Vandewynckel, I. Desaegher, D. Laukens, L. Devisscher, E. Bogaerts, A. Paridaens, S. Raevens, A. Van den Bussche, X. Verhelst, C. Van Steenkiste, B. Descamps, C. Vanhove, L. Libbrecht, A. Geerts, B. N. Lambrecht, S. Janssens, H. Van Vlierberghe. **Antitumor efficacy of sorafenib is potentiated by modulation of the interplay between the unfolded protein response and autophagy in hepatocellular carcinoma.** *Manuscript in preparation, patent application filed*.

Y.-P. Vandewynckel, D. Laukens, A. Geerts, C. Vanhove, B. Descamps, L. Devisscher, E. Bogaerts, A. Paridaens, X. Verhelst, C. Van Steenkiste, L. Libbrecht, I. Colle, B. Lambrecht, S. Janssens, H. Van Vlierberghe. **Therapeutic Effects of Artesunate in Hepatocellular Carcinoma: Repurposing an Ancient Antimalarial Agent.** *Eur. J. Gastroenterol. Hepatol.* 2014, 26:861-70.

Y.-P. Vandewynckel, D. Laukens, L. Devisscher, E. Bogaerts, A. Paridaens, A. Van den Bussche, S. Raevens, X. Verhelst, C. Van Steenkiste, B. Jonckx, L. Libbrecht, A. Geerts, P. Carmeliet, H. Van Vlierberghe. **Placental growth factor inhibition modulates the interplay between hypoxia and the unfolded protein response in hepatocellular carcinoma.** *Submitted for publication in BMC cancer.*

Y.-P. Vandewynckel, C. Coucke, D. Laukens, L. Devisscher, A. Paridaens, E. Bogaerts, A. Van den Bussche, S. Raevens, X. Verhelst, C. Van Steenkiste, L. Libbrecht, A. Geerts1, H. Van Vlierberghe. **Next-generation proteasome inhibitor oprozomib synergizes with modulators of endoplasmic reticulum stress in hepatocellular carcinoma.** *Manuscript in preparation, patent application filed*.

Chapter 3

Results

1. Identification and modulation of the ER stress phenotype in experimental hepatocellular carcinoma

1.1. Modulation of the unfolded protein response impedes tumor cell adaptation to proteotoxic stress: a PERK for hepatocellular carcinoma therapy

Yves-Paul Vandewynckel[1], Debby Laukens[1], Eliene Bogaerts[1], Annelies Paridaens[1], Anja Van den Bussche[1], Xavier Verhelst[1], Christophe Van Steenkiste[1], Benedicte Descamps[2], Chris Vanhove[3], Louis Libbrecht[4], Riet De Rycke[5], Bart N. Lambrecht[6], Anja Geerts[1], Sophie Janssens[6], Hans Van Vlierberghe[1].

[1]Department of Hepatology and Gastroenterology, Ghent University, De Pintelaan 185, 1K12 IE, 9000 Ghent, Belgium.

[2]Infinity Imaging Lab, Ghent University, De Pintelaan 185, 9000 Ghent, Belgium.

[3]Infinity Imaging Lab, Ghent University, De Pintelaan 185, 9000 Ghent, Belgium; GROUP-ID Consortium, Ghent University Hospital, Ghent University, De Pintelaan 185, 9000 Ghent, Belgium.

[4]Department of Pathology, Ghent University, De Pintelaan 185, 9000 Ghent, Belgium.

[5]GROUP-ID Consortium, Ghent University Hospital, Ghent University, De Pintelaan 185, 9000 Ghent, Belgium; Unit Immunoregulation and Mucosal Immunology, VIB Inflammation Research Center, Technologiepark 927, 9052 Ghent, Belgium.

[6]GROUP-ID Consortium, Ghent University Hospital, Ghent University, De Pintelaan 185, 9000 Ghent, Belgium ; Unit Immunoregulation and Mucosal Immunology, VIB Inflammation Research Center, Technologiepark 927, 9052 Ghent, Belgium; Department of Respiratory Medicine, Ghent University Hospital, Ghent University, De Pintelaan 185, 9000 Ghent, Belgium.

Modulation of the unfolded protein response impedes tumor cell adaptation to proteotoxic stress: a PERK for hepatocellular carcinoma therapy

1.1.1. Abstract

Background

Functional disturbances of the endoplasmic reticulum (ER) lead to activation of the unfolded protein response (UPR), which is involved in the consecutive steps of carcinogenesis. In human hepatocellular carcinoma (HCC), the UPR is shown to be activated; however, little is known about the UPR kinetics and effects of UPR modulation in HCC.

Methods

We sequentially monitored the UPR over time in an orthotopic mouse model for HCC and explored the effects of UPR modulation on cell viability and proliferation in vitro and in the mouse model.

Results

The expression of ER-resident chaperones peaked during tumor initiation and increased further during tumor progression, predominantly within the nodules. A peak in Ire1 signaling was observed during tumor initiation. The Perk pathway was activated during tumor progression, and the proapoptotic target Chop was upregulated from week 5 and continued to rise, especially in the tumors. The Atf6 pathway was modestly activated only after tumor initiation. Consistent with the UPR activation, electron microscopy demonstrated ER expansion and reorganization in HCC cells in vivo. Strikingly, under ER stress or hypoxia, the Perk inhibitor and not the Ire1 inhibitor reduced cell viability and proliferation via escalating proteotoxic stress in vitro. Notably, the Perk inhibitor significantly decreased tumor burden in the mouse model.

Conclusion

We provide the first evaluation of the UPR dynamics in a long-term cancer model and identified a small molecule inhibitor of Perk as a promising strategy for HCC therapy.

1.1.2. **Abbreviations**

HCC	Hepatocellular carcinoma
ER	Endoplasmic reticulum
GRP78	Glucose-regulated protein, 78 kDa
GRP94	Glucose-regulated protein, 94 kDa
PDIA4	Protein disulfide-isomerase A4
CANX	Calnexin
ERAD	ER-associated protein degradation
EDEM1	Degradation-enhancing a-mannosidase-like protein
UPR	Unfolded protein response
PKR	dsRNA-dependent protein kinase
PERK	PKR-like endoplasmic reticulum kinase
IRE1	Inositol requiring enzyme 1
ATF6	Activating transcription factor 6
eIF2a	Eukaryotic initiation factor 2a
ATF4	Activating transcription factor 4
CHOP	CCAAT/enhancer-binding protein homologous protein
NRF2	Nuclear factor erythroid 2-related factor 2
GCLC	Glutamate-cysteine ligase, catalytic subunit
GPX3	Glutathione peroxidase 3
ERDJ4	Endoplasmic reticulum DnaJ homolog 4
ERO1L	Endoplasmic oxidoreductin-1-like protein
XBP1u	Unspliced X-box-binding protein 1
HERPUD1	Homocysteine-responsive endoplasmic reticulum-resident ubiquitin-like domain member 1 protein
XBP1s	Spliced X-box-binding protein 1
DEN	Diethylnitrosamine

W	Week
PERKi	PERK inhibitor
GADD34	Growth arrest and DNA damage-inducible protein
TUDCA	Tauroursodeoxycholic acid

1.1.3. **Introduction**

Hepatocellular carcinoma (HCC) is the second leading cause of cancer-related mortality worldwide [1]. Conventional chemotherapy is ineffective, and targeted therapy for advanced HCC with sorafenib shows only a limited survival benefit [2].

The endoplasmic reticulum (ER) consists of a membranous network in which proteins are synthesized, posttranslationally modified and folded. Therefore, the ER lumen houses a large array of chaperones, including glucose-regulated protein-78 (GRP78) and -94 (GRP94), and protein disulfide-isomerase A4 (PDIA4), and contains stringent quality-control systems that selectively extract terminally misfolded proteins for degradation, a process known as ER-associated protein degradation (ERAD), which is accelerated by ER degradation-enhancing amannosidase-like 1 (EDEM1) [3]. Several perturbations in protein folding lead to the accumulation of unfolded proteins that trigger the unfolded protein response (UPR). The UPR engages a transcriptional response involved in protein quality control, ERAD, redox homeostasis and ER expansion. Paradoxically, the UPR also coordinates proapoptotic responses to ER stress [3, 4].

Three major ER stress sensors have been identified: PKR-like endoplasmic reticulum kinase (PERK), inositol-requiring enzyme 1 (IRE1) and activating transcription factor 6 (ATF6) [3]. Upon irremediable ER stress, the effect of ATF6 on cell fate is primarily cytoprotective, whereas the effect of IRE1 and PERK is presumed to be both proadaptive and proapoptotic [4, 5].

Following the release of GRP78, PERK phosphorylates eukaryotic initiation factor 2a (eIF2a), leading to the attenuation of global translation. However, the translation of certain transcripts, such as activating transcription factor 4 (ATF4), is favored. ATF4 induces genes involved in protein quality control, amino acid biosynthesis and the induction of apoptosis via CCAAT/enhancer-binding protein homologous protein (CHOP) [3]. PERK-regulated nuclear factor-(erythroid-derived-2)-like-2 (NRF2) promotes cell survival via antioxidant enzymes, such as glutamate-cysteine ligase, catalytic (GCLC) and glutathione peroxidase-3 (GPX3) [6]. IRE1 activation results in XBP1 mRNA splicing to generate a more active spliced XBP1 (XBP1s), which induces genes involved in protein folding, such as ERDJ4 and CANX, ERAD and redox homeostasis [7].

ATF6 is mobilized to the Golgi where it is cleaved, releasing a transcriptionally active fragment, which in turn induces the expression of chaperones, such as PDIA4 and endoplasmic oxidoreductin-1-like protein (ERO1L), unspliced XBP1 (XBP1u) and ERAD components, such as homocysteine-responsive endoplasmic reticulum-resident ubiquitin-like domain member 1 (HERPUD1) [3, 7]. Although each UPR pathway targets a specific set of genes, certain targets require the concomitant activation of two pathways, e.g., $P58^{IPK}$ and EDEM1 transcription require the cooperation of ATF6 and XBP1s [7].

Rapid tumor growth creates hypoxia, glucose deprivation and oxidative stress, activating the UPR in various solid tumor types [3]. In human HCC, elevated GRP78, ATF6 and IRE1 activation was observed [8–10]. The UPR demonstrates a specific time-dependent pattern of activation that determines its cytoprotective versus proapoptotic outcome [11]. However, these alterations have only been investigated in vitro during acute ER stress in a maximum time period of 48 h [3, 11], and it is unknown how tumor cells adapt to chronic ER stress in vivo. In the present study, we monitored the kinetics of the UPR, a potential tumoral Achilles' heel, in an orthotopic mouse model for hepatocarcinogenesis [12, 13]. Our data showed IRE1 signaling during tumor initiation and robust PERK activation once the tumors had been established. Furthermore, we explored the therapeutic potential of UPR modulation in vitro and in vivo. We observed that in contrast to the dogma stating that PERK induces apoptosis via CHOP accumulation, a small molecule inhibitor of PERK actually reduces HCC burden via proteotoxicity.

1.1.4. **Materials and methods**

Cell culture

HepG2, BWTG3 and Hepa1-6 (ATCC, Manassas, VA, USA) cells were cultured with DMEM supplemented with 10 % fetal bovine serum (Life Technologies, Ghent, Belgium). Cells were incubated for 48 h with tunicamycin (1.25 µg/ml), a PERK inhibitor (0.3 µM; GSK2656157, NoVi Biotechnology, Shandong, China), an IRE1 inhibitor (8 µM; 4µ8C, Calbiochem, Cambridge, MA, USA), salubrinal (50 µM; Tocris, Bristol, UK), tauroursodeoxycholic acid (1 µM), cycloheximide (5 µM), ascorbic acid (50 µM) or pretreated with N-acetylcysteine (2 h; 5 µM), SP600125 and SB203580 (30 min; 10 µM), and compared to equal volumes of solvent in normoxic and hypoxic (1 % oxygen; AnaeroGen, Oxoid, Hampshire, UK) conditions. All reagents were from Sigma (Diegem, Belgium) unless stated otherwise. Each experiment was performed in quadruplicate.

Animals

Wild-type 129S2/SvPasCrl mice (Charles River, Brussels, Belgium) were maintained as previously described [12]. Five-week-old males received weekly intraperitoneal saline or diethylnitrosamine (DEN; 35 mg/kg). Every 5 weeks (W) until W30 (12 groups with n = 12), a group of mice was euthanized. The mice were killed 1 week after the last DEN injection. By macroscopic and microscopic assessments, three liver tissue areas, non-HCC (no nodules in the close proximity), surrounding (perinodular ring of altered hepatic tissue) and HCC (nodules), were isolated by microdissection (Carl Zeiss, Bernreid, Germany) from W25 because at this time, nodules could be clearly distinguished from the surrounding tissue. The number of tumors with a minimum diameter of 2 mm was counted. In addition, 30 µg of tunicamycin was injected intraperitoneally in four untreated 30-week-old male mice 72 h before sacrifice. After randomizing mice treated for 25 W with DEN or saline, GSK2656157 (100 mg/kg bid) was administered intraperitoneally for 4 W and compared with the vehicle (4 groups with n = 12).

Blood was collected from the ophthalmic artery. All organs were fixed in 4 % phosphate-buffered formaldehyde and embedded in paraffin or snap frozen in liquid nitrogen. Hematoxylin & eosin and reticulin stainings were performed to assess the tumor burden as shown by the mean total tumor surface of six slides per liver and blindly evaluated by two independent observers. Interobserver reliability was substantial (intraclass correlation coefficient = 0.74). Mean intercapillary distance was measured on CD105-stained slides as previously described [12]. Sirius Red staining enabled fibrosis assessment by Metavir scoring. Serum alanine aminotransferase and glycemia were measured at Ghent University Hospital. All protocols were approved by the Ethics Committee of experimental animals, Ghent University (ECD 11/52).

Detailed information regarding RNA extraction, quantitative real-time PCR, Western blot analysis, immunohistochemistry, TUNEL immunofluorescence, WST-1 and caspase-3 activity assays, electron microscopy and positron emission tomography is provided in the Supplementary Materials and Methods.

Statistics

Statistical analysis was performed using SPSS 21 (SPSS, Chicago, IL, USA). Data are presented as the mean ± SD or as the fold change relative to the expression in the controls. Normally distributed data were subjected to unpaired Student's t test. Multiple groups were compared by one-way ANOVA with Bonferroni correction. Non-normally distributed data were tested using the Mann-Whitney U test. The Friedman test with Bonferroni correction was applied to compare non-HCC, surrounding and tumor tissues of the same liver. The chi-squared test was used to compare mortality. Reported p values were two sided and considered significant when lower than 0.05.

1.1.5. **Results**

Kinetics of chaperone expression in the HCC model

Every 5 weeks (W) after DEN administration, mice were killed for the analysis of tumor progression and the expression of the (co-)chaperones Grp78, Grp94 and $P58^{IPK}$ (Fig. 1a). At W25, tumor nodules were observed in a background of fibrosis (Fig. S1). The expression of Grp78 was upregulated at W10 (mRNA: $p<0.05$; protein: Fig. 1b) but reduced again at W15 (mRNA: $p<0.05$), and once tumors were established, Grp78 mRNA was elevated in the nodules compared to the surrounding ($p<0.05$) and non-HCC tissue ($p<0.01$). By immunohistochemistry, we demonstrated an inhomogeneous pattern of Grp78-positive HCC cells within the nodules, but only a few Grp78-positive cells in the surrounding tissue (Fig. 1c). Grp94 mRNA followed a similar temporal pattern, i.e., increased from W25 only in the surrounding and tumor tissue ($p<0.05$, Fig. 1a). Accordingly, in addition to a tendency to increase at W10, co-chaperone $P58^{IPK}$ exhibited upregulation in the surrounding tissue and nodules from W25 (Fig. 1a).

The Ire1 pathway is activated before tumor promotion

At W10, phospho-Ire1 levels (Fig. 1b), detected by the use of a phosphate-binding tag, and Xbp1 splicing ($p<0.05$, Fig. 1d) were increased. Two targets of Xbp1s (7), Canx mRNA and Erdj4 mRNA showed a similar evolution until W20, but in contrast to the Xbp1 splicing, they continued to rise in the tumor tissue ($p<0.05$, Fig. 1d). Additionally, Edem1 mRNA peaked at W5 ($p<0.05$) but not during tumor growth. Although splicing activity was not significantly altered in the DEN- compared with saline-treated mice at W30 (Fig. 1d), phospho-Ire1 levels were increased in the tumors (Fig. 1b), suggesting additional regulation of the Ire1 endoribonuclease, possibly by reduced oligomerization [3, 14].

The Perk pathway is robustly activated in HCC

At W25, during tumor progression, Atf4 mRNA upregulation was observed and limited to the nodules (Fig. 2a). At W30, expression expanded to the surrounding tissues (Fig. 2a, b).

Phosphorylation of eIf2a was increased in both surrounding and tumor tissue at W30 (Fig. 2b). Immunostaining for phospho-eIf2a showed a diffuse distribution in the surrounding tissue, intensifying toward the core of the nodules at W30. The expression of Chop, a presumed proapoptotic target of Perk [4], was increased from the beginning, then stable between W5 and W20 and from W25 continued to increase. Although expression was higher in HCC compared to non-HCC tissue ($p<0.05$), both Chop mRNA (Fig. 2a) and protein (Fig. 1b, 2b) levels were increased in all three isolated areas. Furthermore, caspase-3 activity, an indicator of apoptosis, was increased at W30 in the surrounding tissue and nodules ($p<0.01$, Fig. 2c). Growth arrest and DNA damage-inducible protein (Gadd34) demonstrated a similar pattern as Atf4, with a marked increase from W25, especially in the nodules ($p<0.05$; Fig. 2a, b), suggesting Perk activation in HCC. Concerning the Perk/Nrf2 axis, we observed the upregulation of Gpx3 mRNA at W5, W10 and W20, and Gclc mRNA showed a tendency to upregulation at these time points (Fig. S2). Surprisingly, in the tumors both these transcripts showed a tendency to downregulation compared to the non-tumor liver.

The Atf6 pathway is modestly activated after tumor initiation

To examine the Atf6 pathway, Pdia4, Herpud1 and Ero1L expressions were monitored [7]. The expression of Pdia4 mRNA ($p<0.05$; Fig. 2d) and protein (Fig. 1b) was modestly increased from W30 in the tumors compared with the surrounding tissue. In accordance, Ero1L and Herpud1 mRNA was upregulated in the nodules from W30 compared with saline-treated livers ($p<0.05$; Fig. 2d).

Murine HCC cells exhibit ultrastructural hallmarks of ER stress

Electron microscopy of the tumors in the mouse model at W30 revealed an extensive expanded ribosome-bound ER in a lamellar pattern (Fig. 3a, middle panel) in the HCC cells compared with the ER in the hepatocytes of saline-treated mice (Fig. 3a, left panel). The liver of mice treated with the ER stress inducer tunicamycin showed extremely dilated ER in the hepatocytes (Fig. 3a, right panel).

Interestingly, some HCC cells demonstrated a remarkable ER reorganization with disruption of ribosome-bound ER and extension of smooth ER (Fig. 3b). These observations provide structural evidence for the hypothesis that DEN-induced hepatocarcinogenesis leads to ER stress. Consistent with histological Metavir scoring of fibrosis (Fig. S1C), we observed the increased presence of collagen fibers in the extracellular matrix (data not shown).

PERK inhibition but not IRE1 inhibition diminishes the viability and proliferation of HCC cells under stressed conditions

To address whether interfering with the UPR affects tumor growth, we first validated the effect of the PERK inhibitor (PERKi) and IRE1 inhibitor on HepG2 cells under hypoxia and in the presence of tunicamycin-induced ER stress. The expression of ER stress markers was induced by tunicamycin and hypoxia (Fig. 4b).

PERKi induced no alterations in basal XBP1 splicing or on the basal expression of PERK targets (Fig. 4a, b). However, under hypoxia or ER stress, PERKi diminished the expression of chaperones GRP78 and PDIA4, the adaptive factor ATF4 and the proapoptotic factor CHOP and elevated IRE1 splicing activity (both $p<0.05$) compared with vehicle-treated cells (Fig. 4a, b). Under these conditions, PERKi decreased eIF2a phosphorylation, suggesting the unblocking of protein synthesis. Indeed, PERKi restored the tunicamycin-attenuated protein synthesis rate (Fig. S3A). The IRE1 inhibitor abolished basal and induced XBP1 splicing ($p<0.001$; Fig. 4a) and attenuated the induction of PDIA4 and GRP78, although to a lesser extent than in the presence of PERKi. ATF4 and CHOP were unchanged at the mRNA level but slightly increased at the protein level. We next defined the effect of these small molecules on the cell viability and proliferation rate in different HCC cell lines. Here, we also tested salubrinal, which is known to prevent eIF2a dephosphorylation, thus prolonging PERK activation.

Neither hypoxia nor tunicamycin affected cell viability (Fig. 4c), and under normal conditions, UPR modulation did not alter cell viability in HepG2 cells. However, following ER stress induction, PERKi, but not the IRE1 inhibitor, strikingly reduced cell viability ($p<0.001$), while salubrinal increased cell viability ($p<0.05$). PERKi also impaired cell viability under hypoxia ($p<0.01$). Accordingly, PERKi elevated caspase-3 activity under these stressed conditions ($p<0.001$, Fig. 4d).

To further confirm the potential of PERKi-induced cell death, cell proliferation was assessed by the incorporation of the thymidine analog bromodeoxyuridine into DNA. Under ER stress, PERKi ($p<0.01$) and the IRE1 inhibitor ($p<0.05$) reduced the cell proliferation rate. Hypoxia increased the proliferation rate ($p<0.001$; Fig. S3B), and only PERKi was able to temper the hypoxia-stimulated proliferation ($p<0.001$). Viability experiments were repeated in BWTG3 and Hepa1-6 cells with comparable results (Fig. S3C). These data suggest that PERKi is able to suppress HCC cell growth under conditions comparable to the tumor microenvironment.

Antitumor effect of the PERK inhibitor is mediated by proteotoxic stress and not oxidative stress

Because the PERK/NRF2 pathway is known to upregulate antioxidant enzymes [6], which were increased in our mouse model (Fig. S2), we examined whether the killing of HepG2 cells by PERKi depends on oxidative stress. Under ER stress, the co-incubation of PERKi with N-acetylcysteine (NAC) or ascorbic acid, which attenuate oxidative stress by directly scavenging ROS, was unable to counteract the PERKi-mediated reduction of cell viability (Fig. S3D) or the IRE1 hyperactivation (data not shown).

To examine whether the compensatory hyperactivation of the proapoptotic IRE1/JNK/p38 pathway [4] is involved in the antitumor effect of PERKi, cells were pretreated with the JNK inhibitor SP600125 or the p38 inhibitor SB203580 (validation not shown). Both compounds did not affect the PERKi-mediated reduction of cell viability (Fig. S3D).

Additionally, the combination of PERKi with the IRE1 inhibitor did not modify cell viability under ER stress compared with PERKi alone. These findings suggest that neither oxidative stress nor the observed IRE1 hyperactivation contribute to PERKi-induced cell death. In addition, we tested whether the PERKi-induced cell death was due to autophagy modulation by using inhibitors (3-methyladenine and chloroquine) or activators (rapamycin); however, despite validation by LC3 and P62 blotting, the effect of PERKi on viability was unaltered (data not shown).

PERK is known to inhibit protein synthesis in response to accumulation of misfolded proteins [3]. To check whether the cellular stress caused by PERKi was due to proteotoxicity, cycloheximide was used to inhibit protein synthesis.

Additionally, the chemical chaperone tauroursodeoxycholic acid (TUDCA) was applied to reduce the load of misfolded proteins. Both cycloheximide and TUDCA decreased PERKi-induced cell death under ER stress ($p<0.001$; Fig. S3D). These findings highlight a key role of proteotoxic stress in PERKi-induced cell death.

The PERK inhibitor disrupts the UPR and reduces tumor growth in vivo

Based on the in vitro data, we investigated the effects of PERKi in an orthotopic model of HCC. While the administration of PERKi in saline- or DEN-treated mice did not significantly alter weight or survival (Table 1), a tendency to increase the survival of the PERKi-treated HCC-bearing mice was observed (83 vs. 66 % in the vehicle-treated group). No other clinical signs of toxicity were observed in any of the PERKi-treated groups. Furthermore, PERKi induced no inherent hepatotoxicity, as the serum alanine aminotransferase levels were similar to those in the vehicle-treated control mice (35.6 ± 11 vs. 41.3 ± 14 U/l).

PERKi reduced PERK autophosphorylation in DEN-induced HCC, validating the in vivo activity of the small molecule used. Atf4 expression and eIf2a phosphorylation were only slightly reduced (Fig. 5a). The quantification analysis of HCC burden, characterized by the loss of normal reticulin staining, revealed that PERKi reduced the mean tumor number (10.5 ± 2.4 vs. 7.8 ± 3.4; $p<0.05$) and burden ($p<0.001$; Fig. 5b) of the DEN-treated mice and rendered the tumors more spongiform with increased intercellular spaces. Choline positron emission tomography, used to visualize cellular membrane biosynthesis, demonstrated a decreased number of loci with high mean standardized uptake values after PERKi compared with vehicle administration ($p<0.05$; Fig. 5c). In addition, TUNEL immunofluorescence showed that DEN administration significantly increased the hepatic apoptosis rate compared with saline-treated livers ($p<0.01$) and that the PERK inhibitor induced a tendency to further elevate the apoptosis rate (Fig. S4).

No abnormalities were found during the pathologic examinations of the heart, spleen and kidney. Because PERK is known to play an essential role in insulin biosynthesis [15], we examined the fasting blood sugar levels. Hyperglycemia was observed in the PERKi-treated mice (174 ± 43 vs. 118 ± 31 mg/dl, $p<0.01$). Taken together, PERKi decreased the tumor burden without inducing significant toxicity.

1.1.6. **Discussion**

HCC is the second leading cause of cancer-related mortality [1]. Hepatocarcinogenesis starts from the initial genotoxic insult, through the clonal expansion from a premalignant to a tumoral lesion (promotion) and finally to tumor progression [16]. In the present study, we monitored the UPR during hepatocarcinogenesis. We observed a differential induction of the UPR pathways with a strong activation of the PERK pathway in HCC. Initially, PERK induces eIF2a phosphorylation to globally attenuate translation, thus reducing the load of unfolded proteins entering the ER. Under irremediable ER stress, PERK induces CHOP accumulation and subsequently apoptosis. Interestingly, we found that a small molecule inhibitor of PERK leads to ER-stress-driven cell death and HCC regression via proteotoxicity.

The chaperones, which assist protein folding, were elevated early during tumor initiation and even more so later on in the tumors. In contrast, the Atf6 pathway, a cytoprotective fine-tuner of the UPR [7], was not activated until W30, suggesting that Atf6-mediated adaptation is not a prerequisite for HCC initiation. Interestingly, the increased expression of Grp78 and Pdia4 mRNA in the tumor nodules compared with the perinodular ring of hepatic tissue suggests that these targets are additionally upregulated by tumoral UPR fine-tuning.

Ire1 signaling peaked before tumor development at W5-15, indicating a possible modulatory role for the Ire1 pathway during tumor initiation. The rise in Xbp1s could be an adaptation to the environment created by DEN-mediated inflammation [4, 12]. Surprisingly, Edem1 and $P58^{IPK}$, both requiring the co-activation of Atf6 and Ire1, followed a different pattern. $P58^{IPK}$ was upregulated in the tumors, while Edem1, an ERAD accelerator [17], showed an early peak that faded thereafter.

In C57Bl/6J models of HCC induced by a single DEN injection, Chop expression was only found in the tumors and, in contrast to our model with repeated DEN injections, not in the surrounding tissue [18, 19]. Because Chop expression was increased from the first time point in the liver parenchyma without canonical UPR activation, Chop may be upregulated by an integrated stress response induced by DEN-mediated oxidative stress [20, 21].

To inhibit PERK, a recently developed small molecule (PERKi) was used and had no effect under normal conditions but potently diminished the viability of HCC cells under ER stress or hypoxia. In contrast, salubrinal treatment improved viability, suggesting a cytoprotective role of persistent eIF2a phosphorylation for attenuating protein synthesis [22]. In the mouse model, PERKi reduced the tumor burden. Collectively, these findings highlight the importance of the proadaptive outputs of PERK in HCC biology. Recently, the dogma of the proapoptotic PERK/ CHOP pathway was challenged by the observation that PERK-mediated eIF2a-phosphorylation-attenuated protein synthesis is crucial for cell survival [5] and that CHOP promotes inflammation-mediated hepatocarcinogenesis [18, 19]. Accordingly, in the present study, PERKi augmented UPR-mediated cell death despite reduced expression of CHOP.

PERKi decreased the expression of UPR-induced chaperones and the phospho-eIF2a/ATF4 pathway, which protect tumor cells from UPR-induced apoptosis [3, 23]. Furthermore, PERKi elevated global protein synthesis during ER stress, possibly escalating the unfolded protein load and ROS formation. Moreover, a protein synthesis inhibitor and a chemical chaperone were each able to hamper the cytotoxic effect of PERKi. Intriguingly, eIf2a phosphorylation was only modestly reduced *in vivo*, suggesting that other eIf2a kinases are able to bypass PERK inhibition [3]. Importantly, antioxidants were unable to limit PERKi-mediated cell death, suggesting that oxidative stress is not required for its cytotoxicity and that the inhibition of the PERK/NRF2 pathway, which promotes the antioxidant defense, is not the dominant antitumor action. Notably, PERKi enhanced IRE1 activation under ER stress, indicating a compensatory adaptation, consistent with the hyperactivity of the IRE1/XBP1 system in embryonic stem cells with defective PERK signaling [24]. However, because the inhibition of the IRE1/p38/JNK pathway did not affect cell death by PERKi, this pathway seems to be redundant for its antitumor effect. These findings reveal a pivotal survival role for the PERK pathway under stressed conditions as present in the tumor microenvironment.

PERK deficiency during development leads to Wolcott-Rallison syndrome [25]. However, in the therapeutic study with PERKi in adult mice, we observed no increased mortality or apparent toxicity with the exception of hyperglycemia, possibly due to reduced pancreatic b-cell mass [15]. In conclusion, our study sheds light on the UPR fine-tuning during hepatocarcinogenesis. Furthermore, our *in vitro* and *in vivo* results identified PERK inhibition as a novel approach to modulate the UPR in order to selectively kill ER-stressed HCC cells.

1.1.7. **References**

1. Ferlay J, Soerjomataram I, Ervik M, Dikshit R, Eser S, Mathers C, et al. GLOBOCAN 2012 v1.0, Cancer Incidence and Mortality Worldwide: IARC Cancer Base 11. International Agency for Research on Cancer. http://globocan.iarc.fr. Accessed on 23 May 2014
2. European Association for the Study of the Liver; European Organisation for Research and Treatment of Cancer. EASL-EORTC clinical practice guidelines: management of hepatocellular carcinoma. J Hepatol 2012;56:908–943
3. Vandewynckel YP, Laukens D, Geerts A, Bogaerts E, Paridaens A, Verhelst X, et al. The paradox of the unfolded protein response in cancer. Anticancer Res 2013;33:4683–4694
4. Hetz C. The unfolded protein response: controlling cell fate decisions under ER stress and beyond. Nat Rev Mol Cell Biol 2012;13:89–102
5. Han J, Back SH, Hur J, Lin YH, Gildersleeve R, Shan J, et al. ERstress-induced transcriptional regulation increases protein synthesis leading to cell death. Nat Cell Biol 2013;15:481–490
6. Bobrovnikova-Marjon E, Grigoriadou C, Pytel D, Zhang F, Ye J, Koumenis C, et al. PERK promotes cancer cell proliferation and tumor growth by limiting oxidative DNA damage. Oncogene 2010;29:3881–3895
7. Shoulders MD, Ryno LM, Genereux JC, Moresco JJ, Tu PG, Wu C, et al. Stress-independent activation of XBP1 s and/or ATF6 reveals three functionally diverse ER-proteostasis environments. Cell Rep 2013;3:1279–1292
8. Al-Rawashdeh FY, Scriven P, Cameron IC, Vergani PV, Wyld L. Unfolded protein response activation contributes to chemoresistance in hepatocellular carcinoma. Eur J Gastroenterol Hepatol 2010;22:1099–1105
9. Shuda M. Activation of the ATF6, XBP1 and grp78 genes in human hepatocellular carcinoma: a possible involvement of the ER stress pathway in hepatocarcinogenesis. J Hepatol 2003;38:605–614
10. Luk LM, Lam CT, Siu AF, Lam BY, Ng IO, Hu MY, et al. Proteomic profiling of hepatocellular carcinoma in Chinese cohort reveals heat-shock-proteins (Hsp27, Hsp70, GRP78) upregulation and their associated prognostic values. Proteomics 2006;6:1049–1057
11. Lin JH, Li H, Yasumura D, Cohen HR, Zhang C, Panning B, et al. IRE1 signaling affects cell fate during the unfolded protein response. Science 2007;318:944–949
12. Heindryckx F, Mertens K, Charette N, Vandeghinste B, Casteleyn C, Van Steenkiste C, et al. Kinetics of angiogenic changes in new mouse model for hepatocellular carcinoma. Mol Cancer 2010;9:219
13. Van de Veire S, Stalmans I, Heindryckx F, Oura H, Tijeras, Raballand A, Schmidt T, et al. Further pharmacological and genetic evidence for the efficacy of PlGF inhibition in cancer and eye disease. Cell 2010;141:178–190
14. Korennykh AV, Egea PF, Korostelev AA, Finer-Moore J, Zhang C, Shokat KM, et al. The unfolded protein response signals through high-order assembly of Ire1. Nature 2009;457:687–693
15. Harding HP, Zyryanova AF, Ron D. Uncoupling proteostasis and development in vitro with a small molecule inhibitor of the pancreatic endoplasmic reticulum kinase, PERK. J Biol Chem 2012;287:44338–44344
16. Kanzler S, Galle PR. Apoptosis and the liver. Semin Cancer Biol 2000;10:173–184
17. Hosokawa N, Wada I, Natsuka Y, Nagata K. EDEM accelerates ERAD by preventing aberrant dimer formation of misfolded alpha1-antitrypsin. Genes Cells 2006;11:465–476

18. Dezwaan-McCabe D, Riordan JD, Arensdorf AM, Icardi MS, Dupuy AJ, Rutkowski DT. The stress-regulated transcription factor CHOP promotes hepatic inflammatory gene expression, fibrosis, and oncogenesis. PLoS Genet 2013;9:e1003937
19. Scaiewicz V, Nahmias A, Chung RT, Mueller T, Tirosh B, Shibolet O. CCAAT/enhancer-binding protein homologous (CHOP) protein promotes carcinogenesis in the DEN-induced hepatocellular carcinoma model. PLoS ONE 2013;8:e81065
20. Ghosh D, Choudhury ST, Ghosh S, Mandal AK, Sarkar S, Ghosh A, et al. Nanocapsulated curcumin: oral chemopreventive formulation against diethylnitrosamine-induced hepatocellular carcinoma in rat. Chem Biol Interact 2012;195:206–214
21. Harding HP, Zhang Y, Zeng H, Novoa I, Lu PD, Calfon M, et al. An integrated stress response regulates amino acid metabolism and resistance to oxidative stress. Mol Cell 2003;11:619–633
22. Boyce M, Bryant KF, Jousse C, Long K, Harding HP, Scheuner D, et al. A selective inhibitor of eIF2alpha dephosphorylation protects cells from ER stress. Science 2005;307:935–939
23. Wang C, Jiang K, Gao D, Kang X, Sun C, Zhang Q, et al. Clusterin protects hepatocellular carcinoma cells from ER-stressinduced apoptosis through GRP78. PLoS ONE 2013;8:e55981
24. Harding HP, Zhang Y, Bertolotti A, Zeng H, Ron D. Perk is essential for translational regulation and cell survival during the unfolded protein response. Mol Cell 2000;5:897–904
25. Zhang P, McGrath B, Li S, Frank A, Zambito F, Reinert J, et al. The PERK eukaryotic initiation factor 2a kinase is required for the development of the skeletal system, postnatal growth, and function and viability of the pancreas. Mol Cell Biol 2002;22:3864–3874

1.1.8. **Figures**

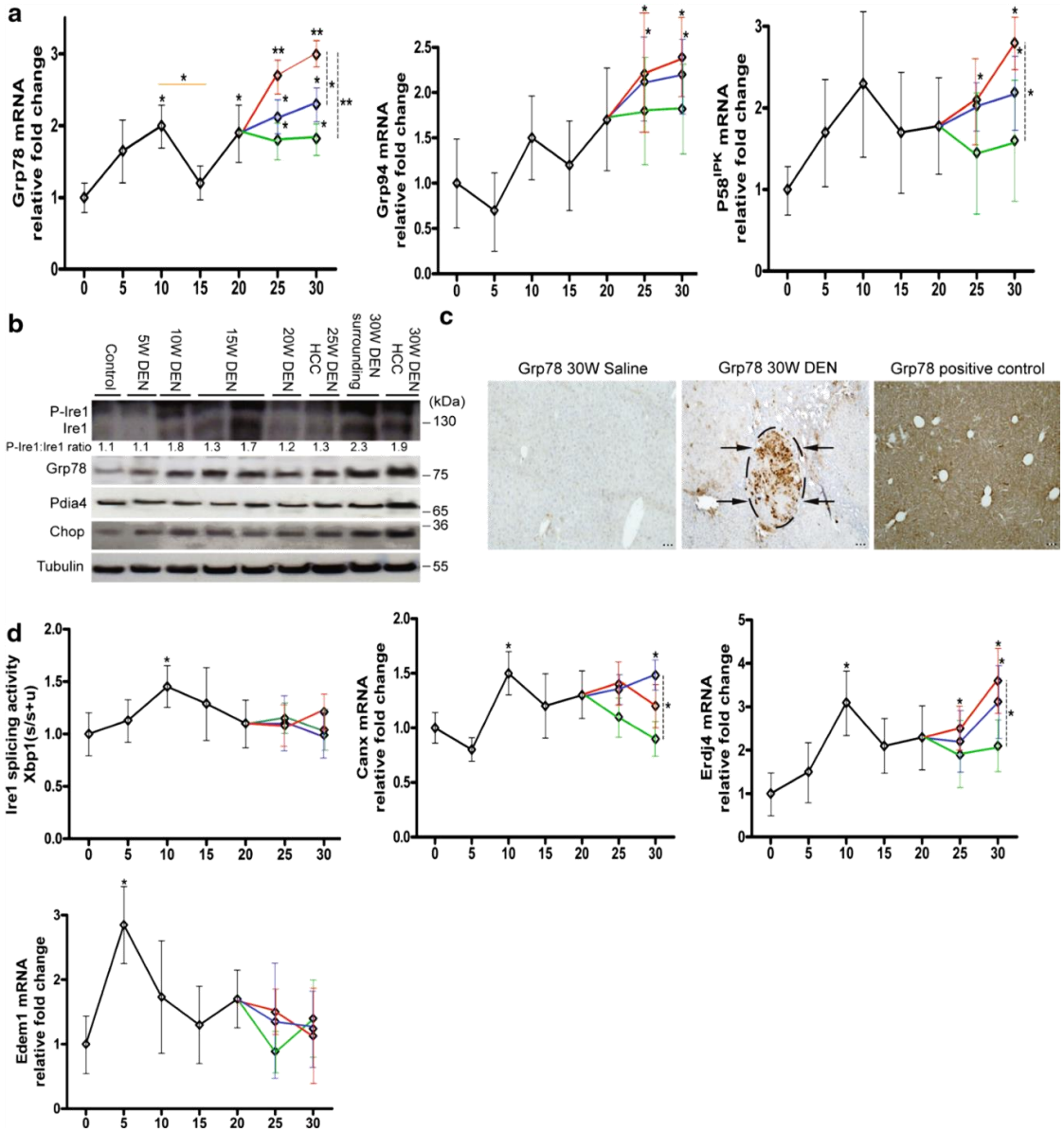

Fig. 1 Temporal dynamics of chaperones and the Ire1 pathway in the HCC model. a Real-time PCR of Grp78, Grp94 and P58^{IPK} during hepatocarcinogenesis. Orange line compares DEN-treated groups at different time points. From W25, different tissue compartments were isolated: green, non-HCC; blue, surrounding; red, tumors. Dashed lines compare these compartments at W30. Relative fold change was calculated using the DDCT method. b Immunoblotting for UPR-mediated proteins. Results are representative of two independent experiments. Densitometric analysis of the p-Ire1:Ire1 ratio is indicated. c Immunostaining for Grp78 in livers treated for 30 W. Arrows indicate tumor. Positive control received a single injection with tunicamycin. Scale bar 100 lm. d Real-time PCR of Ire1mediated splicing activity, Erdj4, Canx and Edem1. The Ire1mediated splicing of Xbp1 mRNA is calculated as the relative ratio of spliced Xbp1 mRNA over total Xbp1 mRNA. Horizontal axis in (a) and (d) indicates the number of weeks of DEN treatment. *p<0.05, **p<0.01.

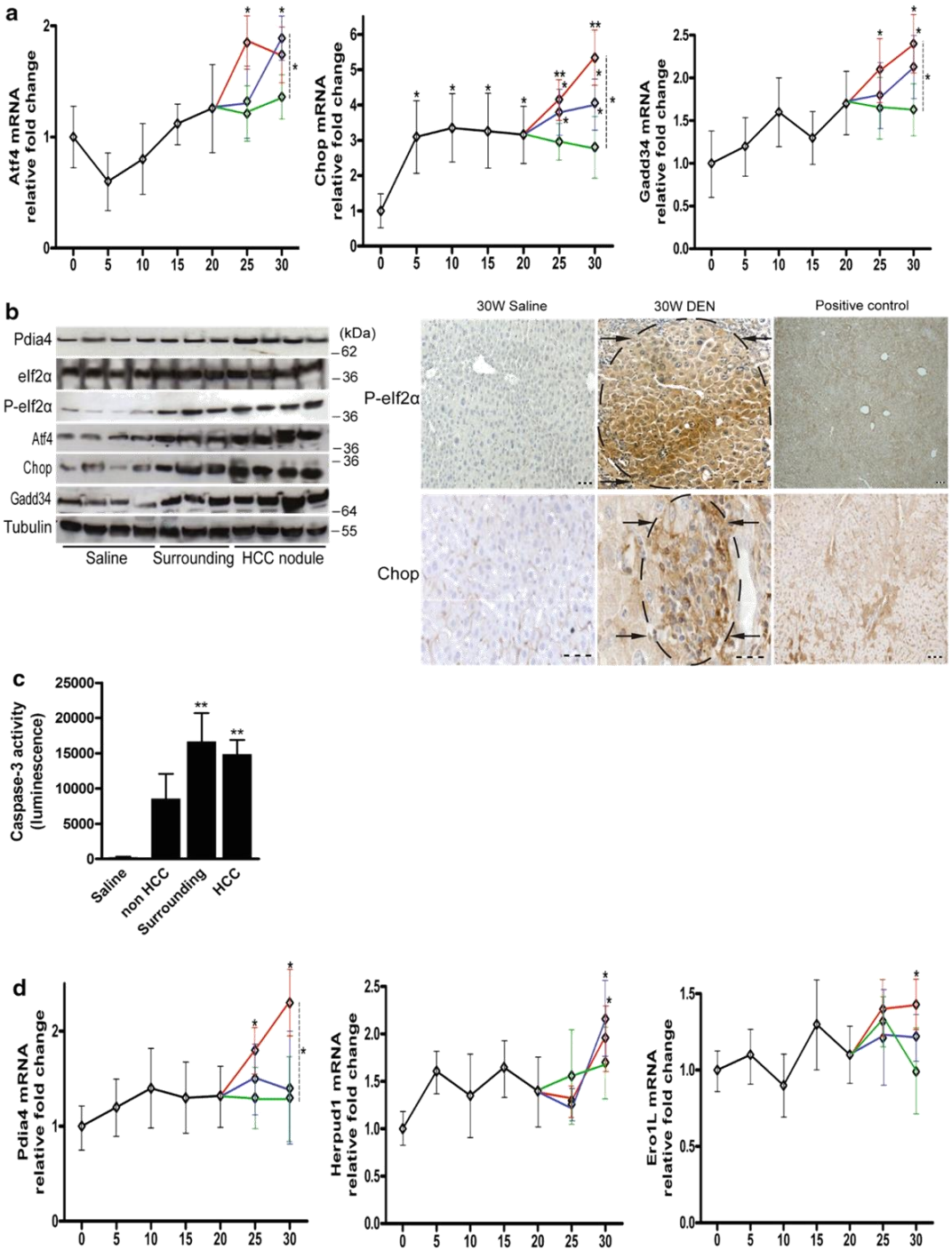

Fig. 2 Temporal dynamics of genes regulated by Perk or Atf6 in the HCC model. a Real-time PCR analysis of Perk-regulated genes. b Immunoblotting and immunostaining for Perk-regulated genes in livers treated for 30 W with DEN or saline. Positive control received tunicamycin for 72 h. Arrows indicate tumors. Scale bar 100 lm. c Caspase-3 activity of liver lysates of the indicated tissue after 30 weeks of saline or DEN administration. d Real-time PCR analysis of Atf6 target genes. Horizontal axis in (a) and (d) indicates the number of weeks of DEN treatment. Data are presented as the mean ± SD. One-way ANOVA was applied for statistical analysis. *p<0.05, **p<0.01.

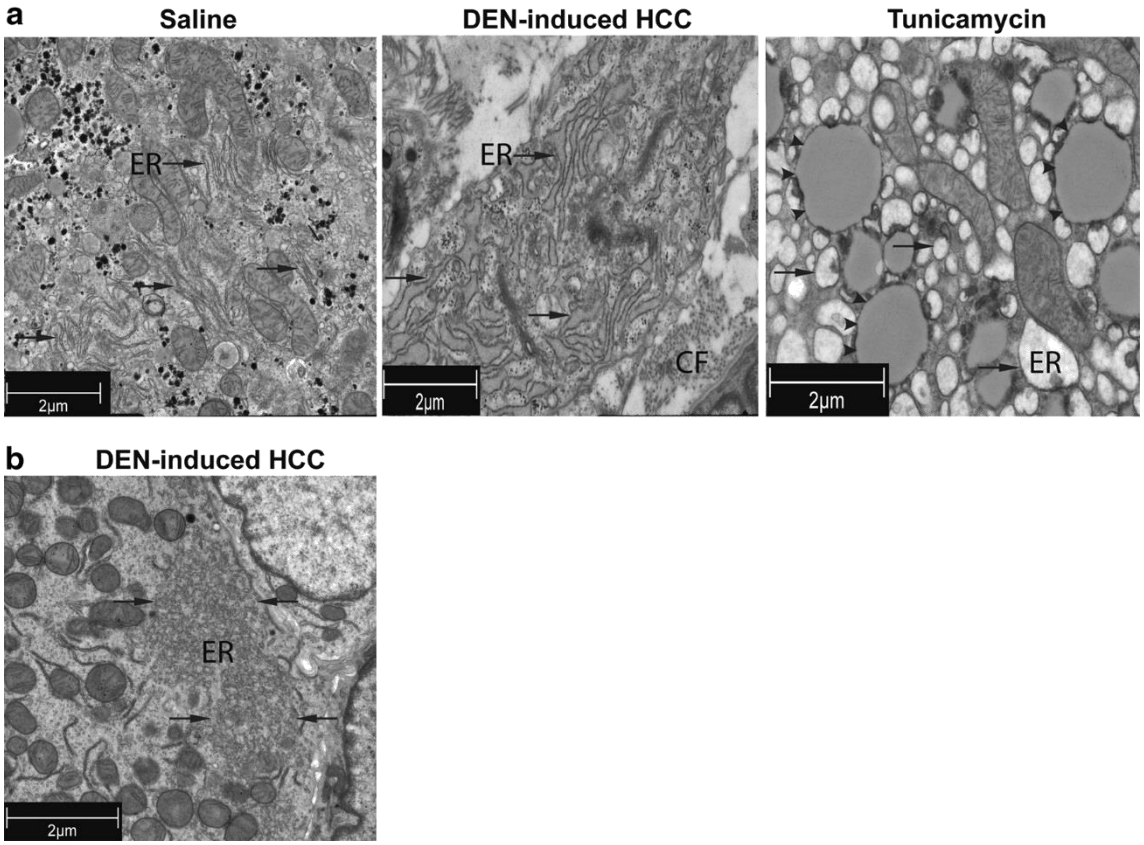

Fig. 3 Transmission electron microscopy of saline- and tunicamycin-treated livers and DEN-induced tumors of the mouse model. a Expansion of the endoplasmic reticulum (ER; arrows) in HCC cells (middle panel) compared with saline-treated livers (left panel). Dilated ER in the liver of mice that received tunicamycin for 72 h (right panel). CF, collagen fibers. Tunicamycin-induced lipid droplets are indicated by arrowheads. b Reorganization of the endoplasmic reticulum after 30 weeks of DEN administration. DEN-induced HCC: hepatocellular carcinoma nodules isolated from the diethylnitrosamine-treated mouse liver.

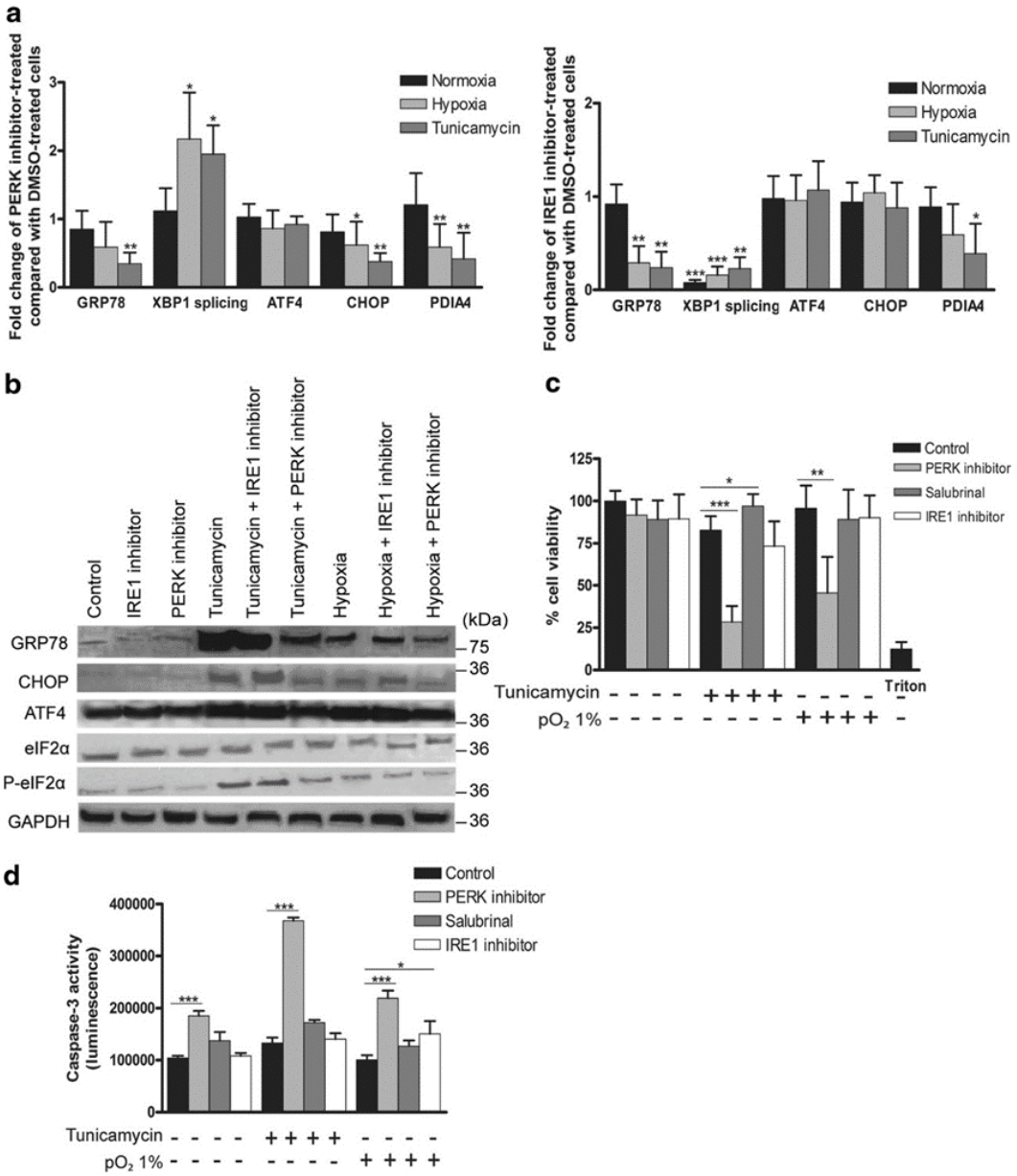

Fig. 4 Effect of salubrinal, PERK or IRE1 inhibitor on the UPR and cell viability in HepG2 cells. Cells were subjected to hypoxia or tunicamycin as indicated for 48 h. a Effect on UPR marker mRNA expression by a PERK inhibitor and by an IRE1 inhibitor compared with solvent-treated cells under the same condition. b Immunoblotting for UPR markers. c Cell viability of HepG2 cells was assessed by a WST-1 assay. d Caspase-3 activity of HepG2 cells treated with the indicated compounds. These experiments were repeated six times with similar results. *p<0.05, ***p<0.001.

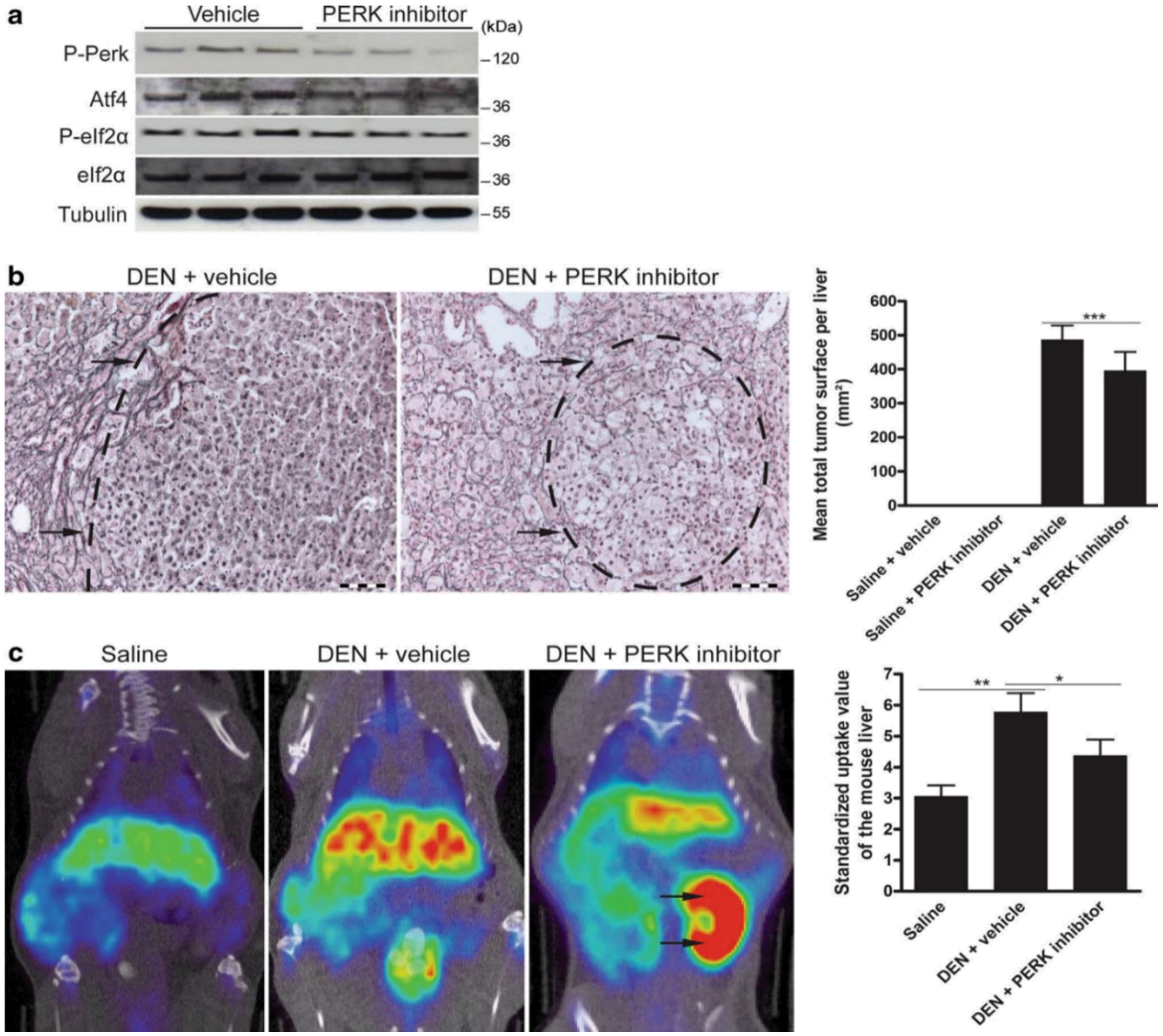

Fig. 5 A PERK inhibitor reduces HCC burden in the orthotopic mouse model. a Immunoblotting for phospho-Perk, Atf4 and phospho-eIf2a in the lysates of isolated tumors after 25 weeks of DEN followed by treatment with a PERK inhibitor or vehicle. Experiments were repeated twice with similar results. b Reticulin staining to quantify the tumor burden as shown by mean total tumor surface. Arrows indicate tumors. c ^{18}F-Choline positron emission tomography visualizes cell membrane synthesis after the indicated treatments. Arrows indicate the left kidney for reference density. Standardized uptake values of the mouse livers are presented as the mean ± SD. One-way ANOVA was applied for statistical analysis. *p<0.05, **p<0.01

1.1.9. **Tables**

Table 1 Mouse body weights (g) (mean ± SD) and survival rates (%)

Group	Mean body weight 25 weeks (g)	Mean body weight 30 weeks (g)	Survival (%)
Saline + vehicle	28.22 ± 2.10	27.03 ± 1.93	100
Saline + PERK inhibitor	27.42 ± 3.09	24.92 ± 3.38 NS	91.67
DEN + vehicle	21.75 ± 2.59***	19.41 ± 2.94	66.67
DEN + PERK inhibitor	20.36 ± 2.57	17.36 ± 3.07 NS	83.33 NS

NS not significant compared with vehicle
*** $p<0.001$: 25 weeks DEN versus saline

1.1.10. **Supplementary Figures**

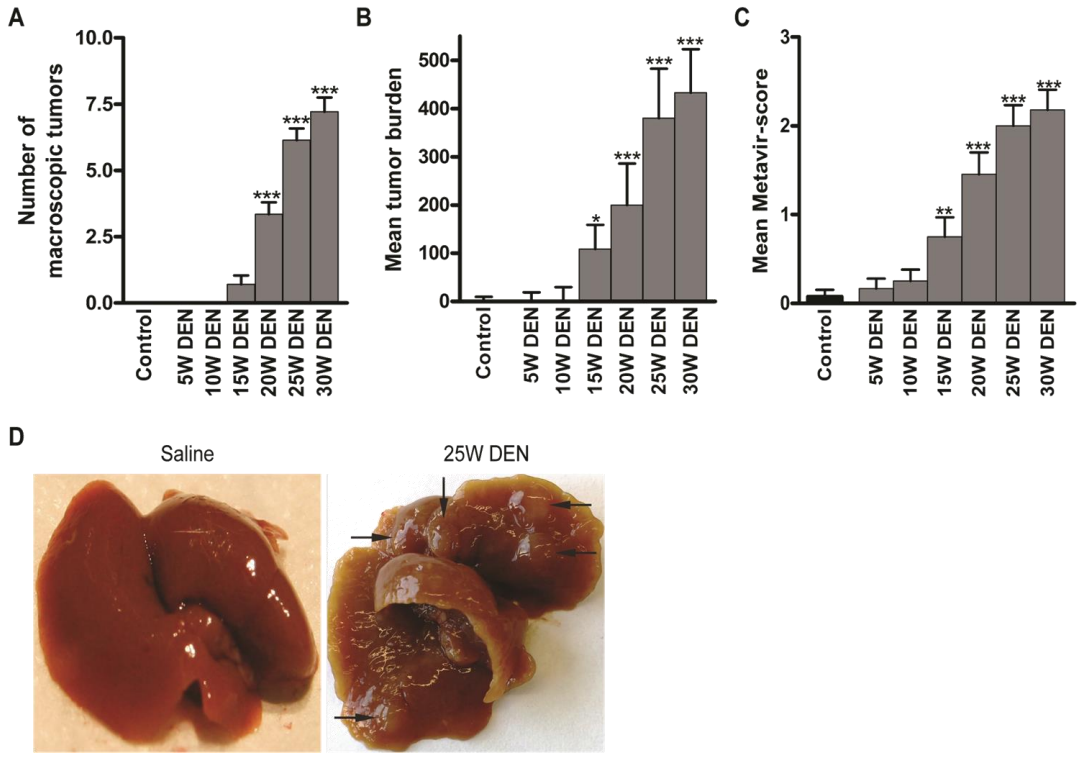

Fig. S1 Confirmation of the mouse model (A) Number of macroscopic tumors. (B) Mean tumor burden. (C) Fibrosis as shown by mean Metavir-score. Data are presented as the mean±SD of n=12. *p<0.05, **p<0.01, ***p<0.001. (D) Representative images of a 25 week saline- or DEN-treated liver. Arrows indicate tumors.

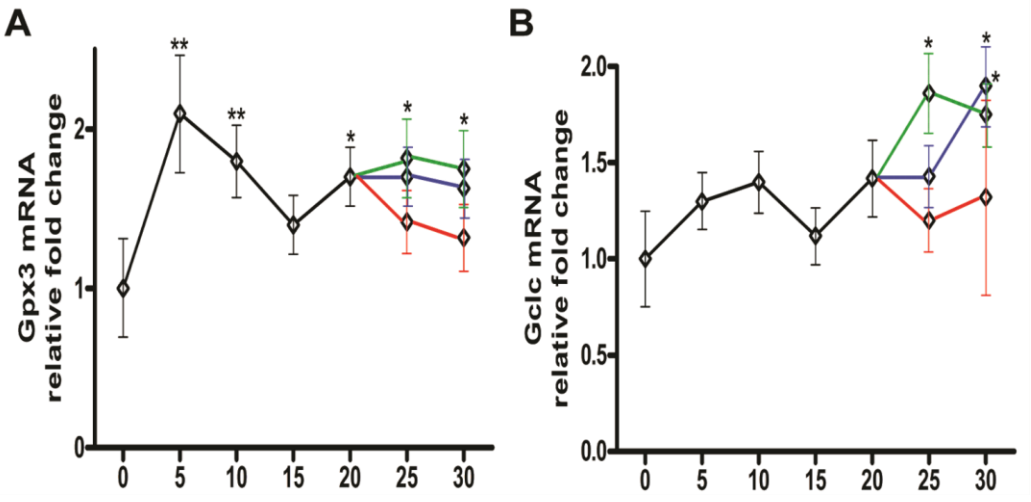

Fig. S2 Temporal dynamics of Nrf2-mediated genes (A) Real-time PCR analysis of *Gpx3* and (B) *Gclc*. Data are presented as the mean ± SD of n=12. *p<0.05, **p<0.01.

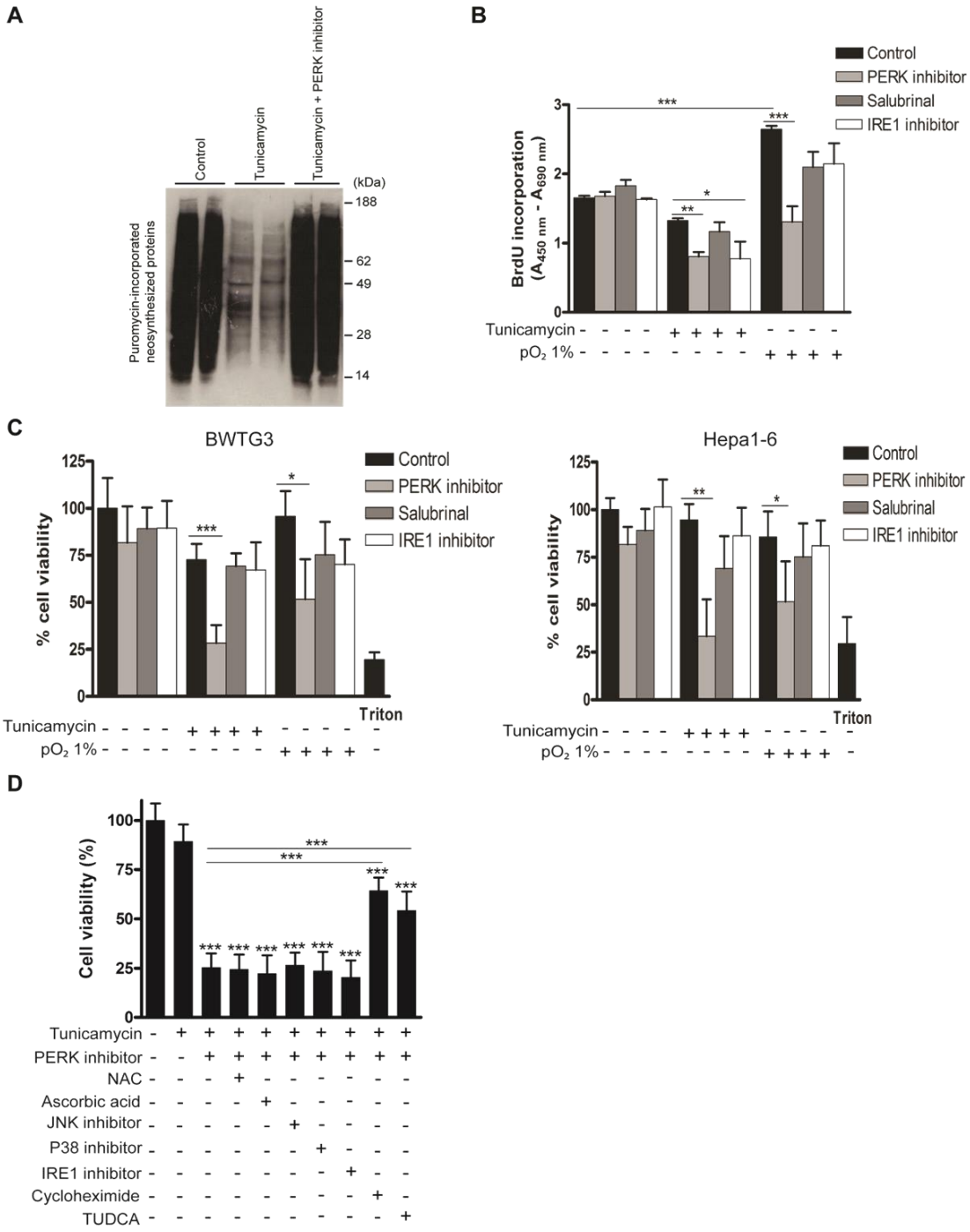

Fig. S3 Effect of UPR modulation on cell viability, proliferation and protein synthesis in HCC cells
(A) Protein synthesis rate as assessed by puromycin incorporation in HepG2 cells. (B) Proliferation rate was assessed by measurement of BrdU incorporation in HepG2 cells. (C) Cell viability of BWTG3 and Hepa1-6 cells, as assessed by a WST-1 assay. For cytotoxic control, 1% Triton X-100 was applied. (D) Effect of a PERK inhibitor on cell viability of HepG2 cells under ER stress in combination with the indicated compounds for 48 hours. Experiments were repeated twice with similar results. Data are presented as the mean ± SD. *p<0.05, **p<0.01, ***p<0.001.

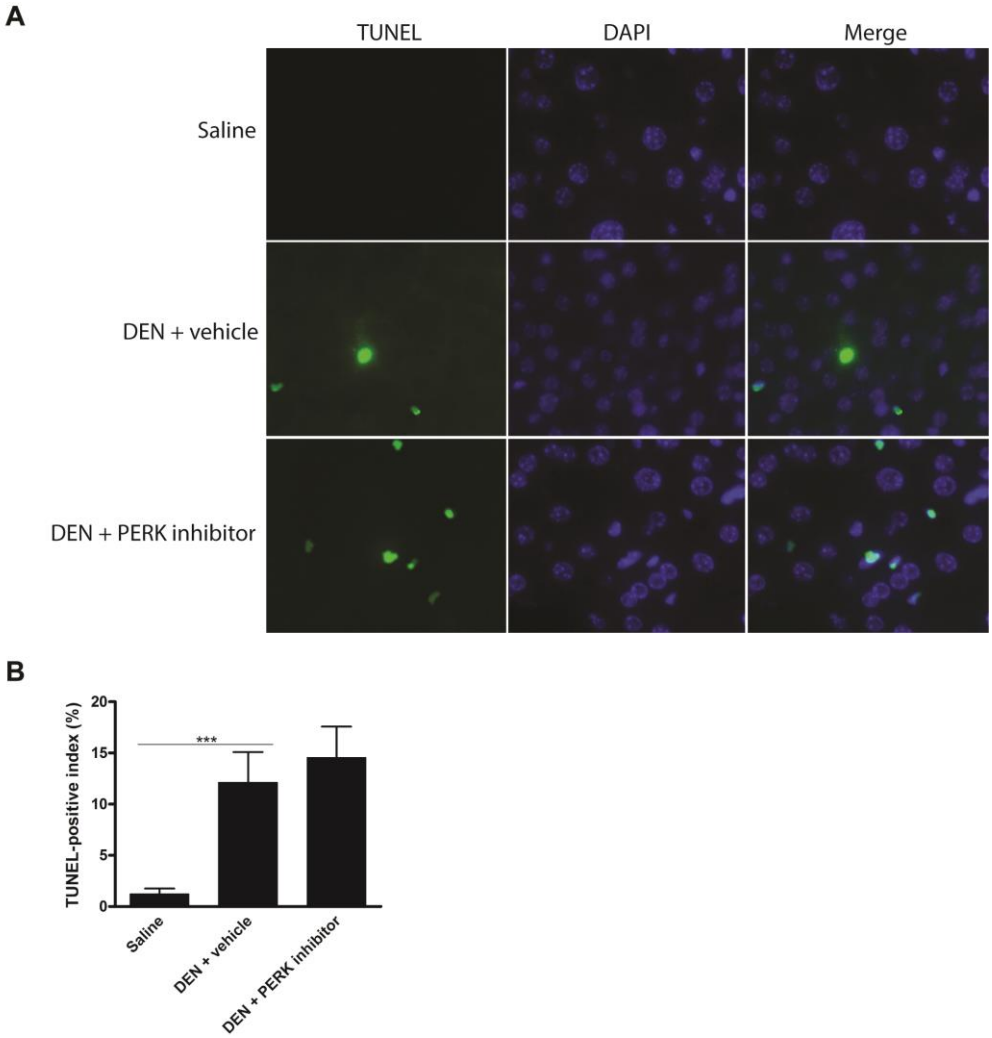

Fig. S4 The PERK inhibitor induces a tendency to increased hepatic apoptosis rate (A) Representative TUNEL immunofluorescence and (B) quantification of the TUNEL-positive index. *p< 0.05, **p<0.01.

1.2. Tauroursodeoxycholic acid dampens oncogenic apoptosis induced by endoplasmic reticulum stress during hepatocarcinogen exposure

Yves-Paul Vandewynckel[1], Debby Laukens[1], Lindsey Devisscher[1], Annelies Paridaens[1], Eliene Bogaerts[1], Xavier Verhelst[1], Anja Van den Bussche[1], Sarah Raevens[1], Christophe Van Steenkiste[1], Marleen Van Troys[2], Christophe Ampe[2], Benedicte Descamps[3], Chris Vanhove[3,4], Olivier Govaere[5], Anja Geerts[1], Hans Van Vlierberghe[1]

[1]Department of Hepatology and Gastroenterology, Ghent University, Ghent, Belgium

[2]Department of Biochemistry, Ghent University, Ghent, Belgium

[3]Infinity Imaging Lab, Ghent University, Ghent, Belgium

[4]GROUP-ID Consortium, Ghent University, Ghent, Belgium

[5]Translational Cell and Tissue Research, Department of Imaging and Pathology, University of Leuven, Belgium

Tauroursodeoxycholic acid dampens oncogenic apoptosis induced by endoplasmic reticulum stress during hepatocarcinogen exposure

1.2.1. Abstract

Hepatocellular carcinoma (HCC) is characterized by the accumulation of unfolded proteins in the endoplasmic reticulum (ER), which activates the unfolded protein response (UPR). However, the role of ER stress in tumor initiation and progression is controversial. To determine the impact of ER stress, we applied tauroursodeoxycholic acid (TUDCA), a bile acid with chaperone properties. The effects of TUDCA were assessed using a diethylnitrosamine-induced mouse HCC model in preventive and therapeutic settings. Cell metabolic activity, proliferation and invasion were investigated *in vitro*. Tumor progression was assessed in the HepG2 xenograft model. Administration of TUDCA in the preventive setting reduced carcinogen-induced elevation of alanine and aspartate aminotransferase levels, apoptosis of hepatocytes and tumor burden. TUDCA also reduced eukaryotic initiation factor 2α (eIf2α) phosphorylation, C/EBP homologous protein expression and caspase-12 processing. Thus, TUDCA suppresses carcinogen-induced pro-apoptotic UPR. TUDCA alleviated hepatic inflammation by increasing NF-κB inhibitor IκBα. Furthermore, TUDCA altered the invasive phenotype and enhanced metabolic activity but not proliferation in HCC cells. TUDCA administration after tumor development did not alter orthotopic tumor or xenograft growth. Taken together, TUDCA attenuates hepatocarcinogenesis by suppressing carcinogen-induced ER stress-mediated cell death and inflammation without stimulating tumor progression. Therefore, this chemical chaperone could represent a novel chemopreventive agent.

1.2.2. List of abbreviations

HCC, hepatocellular carcinoma; TUDCA, tauroursodeoxycholic acid; NFκB, nuclear factor kappa-B; ER, endoplasmic reticulum; UPR, unfolded protein response; Grp78, glucose-regulated protein, 78 kDa; eIf2α, eukaryotic initiation factor 2α; Chop, C/EBP homologous protein; DEN, diethylnitrosamine; LDH, lactate dehydrogenase; BrdU, bromodeoxyuridine; Gsta1, glutathione-S-transferase A1; Gsta2, glutathione-S-transferase A2; Nfe2l2, nuclear factor erythroid-derived 2, like 2; Gclc, glutamate-cysteine ligase

1.2.3. **Introduction**

Hepatocellular carcinoma (HCC) ranks as the second leading cause of cancer-related mortality worldwide and is frequently associated with liver cirrhosis [1,2]. Resection and transplantation are the only potentially curative treatments available following detection of a small HCC [1]. For the majority of patients with locally advanced disease, however, the multi-kinase inhibitor sorafenib and transarterial embolization are the only approved treatments. Unfortunately, both of these treatments provide a limited survival benefit [1]. Given that risk factors for HCC, such as liver cirrhosis, are fairly well established, chemopreventive strategies may help combat the disease. Ideally, these drugs should be safe for long-term use in the at-risk population. However, no chemopreventive drugs are currently available for HCC [3].

Tauroursodeoxycholic acid (TUDCA) is a hydrophilic bile acid that is produced endogenously in humans at very low levels [4]. TUDCA is synthesized in the conjugation pathway of ursodeoxycholic acid, which is effectively used for treating cholestatic liver diseases, including primary biliary cirrhosis, without major adverse reactions [4]. These hydrophilic bile acids act as bile secretagogues and immunomodulators that can prevent apoptosis induced by several agents, such as hydrophobic bile acids, alcohol, transforming growth factor β_1, and Fas ligand, in hepatic and non-hepatic cells [5,6]. In addition, TUDCA protects rat livers during long-term ethanol feeding [7] and human livers from ischemia-reperfusion injury during harvesting and cold storage [8]. The mechanisms involved in the antiapoptotic properties of TUDCA include targeting mitochondrial function and integrity and interactions with the nuclear factor kappa-B (NFκB) signaling pathways [9].

The endoplasmic reticulum (ER) is an important organelle required for cell survival and is highly sensitive to homeostatic alterations. Disruption of ER homeostasis leads to the accumulation of unfolded proteins, which disturb ER function and result in a state known as ER stress [10]. In resting cells, all ER stress receptors are maintained in an inactive state through association with the ER chaperone glucose-regulated protein, 78 kDa (Grp78). Upon ER stress, Grp78 dissociates and triggers the unfolded protein response (UPR), which orchestrates cellular adaptation to stress by inducing transcriptional programs and by repressing global translation by eukaryotic initiation factor 2α (eIf2α) phosphorylation [11].

However, if the stress is too severe, UPR signaling switches from a pro-survival to a pro-apoptotic state, leading to increased pro-apoptotic transcription factor C/EBP homologous protein (Chop) expression and the cleavage of procaspase-12 to its active caspase-12 form [11]. Interestingly, the UPR is activated in several liver diseases, including fatty liver disease, viral hepatitis, alcohol-induced liver injury and HCC [12,13].

Importantly, TUDCA has been shown to act as a chemical chaperone that decreases UPR signaling and protects hepatocytes against cytotoxicity caused by the ER stress inducer thapsigargin [14,15]. TUDCA has also been shown to abolish ER stress-induced caspase-12 processing and to subsequently inhibit effector caspases-3/7 activation and apoptosis [15].

Recent studies have demonstrated that hepatocyte apoptosis is a pathogenic event in several liver diseases [13,16]. Chronically increased hepatocyte apoptosis in genetic mouse models is carcinogenic and leads to compensatory liver regeneration, oxidative stress and DNA hypermethylation [16,17]. In this study, we investigated the preventive and therapeutic potential of TUDCA in HCC. Our data demonstrate that TUDCA reduces carcinogen-induced liver dysfunction and HCC incidence, likely through the prevention of ER stress-induced apoptosis and inflammation. Importantly, once HCC nodules are established, TUDCA does not modulate tumor growth.

1.2.4. **Results**

Preventive administration of TUDCA reduces HCC burden in an orthotopic mouse model

The ER stress-inducing hepatocarcinogen diethylnitrosamine (DEN) promotes multifocal HCC after 25 weeks of administration [18,19]. To explore the effects of TUDCA on hepatocarcinogenesis, we supplemented the animals with low or high dose TUDCA in their drinking water. Administration of DEN resulted in reduced body weights and 25% increased mortality ($p<0.001$; Table 1) compared to saline administration. TUDCA treatment did not affect the weight loss or mortality of DEN-treated mice, and no clinical signs of toxicity were observed in any of the TUDCA-treated groups.

DEN-treated mice that received low- or high-dose TUDCA developed fewer nodules per liver (all sizes: 18.9 ± 5.3 after vehicle versus 11.5 ± 3.9 after low-dose TUDCA [$p<0.01$] and 12.3 ± 4.1 after high-dose TUDCA [$p<0.05$]). HCC burden, quantified by the loss of reticulin staining, was reduced in DEN-treated mice following the co-administration of low- or high-dose TUDCA ($p<0.01$; Fig. 1A-C). Choline positron emission tomography, which visualizes cellular membrane biosynthesis, demonstrated that administration of low-dose TUDCA in DEN-treated mice resulted in fewer hepatic loci with high mean standardized uptake values compared with animals receiving vehicle alone ($p<0.05$; Fig. 1D-E). Repeated DEN administration induces HCC in a background of liver fibrosis [18]. However, no difference in grade of fibrosis, as determined by Sirius Red staining, was found between TUDCA- and vehicle-treated livers (data not shown).

DEN administration increased the levels of serum ALT and AST compared to saline administration ($p<0.001$; Fig. 2A). Importantly, serum ALT and AST levels were reduced in DEN-treated mice receiving TUDCA-supplemented drinking water compared to those receiving regular drinking water ($p<0.05$; Fig. 2A). This suggests that both low- and high-dose TUDCA protect the liver from DEN-induced hepatotoxicity. Collectively, these data indicate that TUDCA decreases the susceptibility of mice to DEN-induced hepatocarcinogenesis in a preventive setting.

TUDCA attenuates UPR-induced apoptosis in DEN-treated mice

Repeated DEN administration results in significant apoptosis and ER stress in hepatocytes [18,19]. We measured the activity of effector caspase-3/7 *ex vivo* and, as expected, observed increased levels in DEN-treated mouse livers ($p<0.001$, Fig. 2B).

Interestingly, the hepatic caspase-3/7 activity was lower in DEN/TUDCA-treated mice compared to DEN/vehicle-treated mice (Fig. 2B). In agreement with these data, TUNEL immunofluorescence demonstrated a significant reduction of TUNEL-positive hepatocytes following TUDCA supplementation ($p<0.05$, Fig. 2C-D), thus confirming reduced hepatocyte apoptosis upon DEN challenge.

Grp78 and Chop expression and eIf2α phosphorylation were increased in the mice treated with DEN, reflecting robust UPR activation (Fig. 3A-B). As a positive control, tunicamycin, a nucleoside antibiotic that inhibits protein glycosylation and thereby elicits acute ER stress [11], was administered to naive mice. These control mice showed significantly increased expression of Grp78 and Chop and eIf2α phosphorylation (Fig. 3B). Administration of TUDCA during the 25 weeks of carcinogen exposure consistently reduced the expression of Grp78 and Chop and inhibited eIf2α phosphorylation, thereby possibly restoring global translation (Fig. 3A-B). Caspase-12, the central player in ER stress-induced apoptosis [11], was markedly activated by both tunicamycin and DEN administration, whereas TUDCA reduced the DEN-induced cleavage of procaspase-12 ($p<0.05$; Fig. 3C). Overall, these data strongly suggest that TUDCA decreases carcinogen-induced ER stress and thereby attenuates caspase-12-mediated hepatocyte apoptosis.

TUDCA increases cellular metabolic activity independent of ER stress

To further explore the effect of TUDCA on cell viability and proliferation, HepG2, BWTG3 and Hepa1-6 cells were incubated with a dilution series of TUDCA. As shown by lactate dehydrogenase (LDH) activity in the cell supernatant, TUDCA at 0.1-1 mM did not induce cytotoxicity in HepG2 cells (Fig. S1A). At 10 mM, however, TUDCA increased the LDH activity ($p<0.001$). Next, we examined the effect of TUDCA on the MTT metabolic activity of cells under basal conditions. The reduction of tetrazolium salts such as MTT depends on both cellular metabolic activity and proliferation rate. Intriguingly, 0.1-1 mM TUDCA increased the MTT metabolic activity of HepG2 cells in a dose-dependent manner to supranormal levels of up to 150% ($p<0.001$; Fig. 3D).

Incorporation of the thymidine analogue bromodeoxyuridine (BrdU) into the DNA of HepG2 cells under basal conditions showed that TUDCA modestly decreased the cell proliferation rate at 1 mM ($p<0.05$, Fig. S1B). Furthermore, we directly counted HepG2 cells after 48 h of incubation with 0.1-1 mM TUDCA and found no difference in cell number compared to controls (data not shown). The MTT metabolic activity and BrdU incorporation experiments were repeated in BWTG3 and Hepa1-6 cells with similar results (Fig. S1C-F). These data suggest that, under basal conditions, TUDCA dose-dependently enhances cellular metabolic activity without increasing the absolute number of cells.

Next, we examined whether TUDCA would have the same effects in the presence of ER stress [11]. Tunicamycin (0.5 μg/ml) did not alter MTT metabolic activity or LDH release in HepG2 cells, suggesting no inherent cytotoxicity at the concentration used (Fig. 3D and S1A, respectively). However, tunicamycin did impair BrdU incorporation ($p<0.01$; Fig. S1B), confirming the well-known ER stress-mediated induction of cell cycle arrest [11]. Finally, TUDCA was able to enhance cellular metabolic activity even in the presence of acute ER stress (Fig. 3D and S1C-D); however, this had no effect on the antiproliferative effect of ER stress (Fig. S1B and S1E-F).

TUDCA does not reduce oxidative stress-induced cell death or DEN-induced oxidative stress

TUDCA has been shown to exert cytoprotective effects in different models by reducing oxidative stress [20], and ER stress is closely connected to the oxidative stress response [10]. Thus, we evaluated the effect of TUDCA on the cytotoxicity of H_2O_2-induced oxidative stress in HepG2 cells. Cell viability declined following the addition of 1-5 mM of H_2O_2 in a dose-dependent manner (Fig. S2A). In contrast to the established antioxidant properties of N-acetylcysteine, co-incubation with 0.1 or 1 mM TUDCA did not protect HepG2 cells against H_2O_2-induced cell death ($p<0.01$; Fig. S2A).

In the orthotopic HCC model, TUDCA supplementation did not alter the expression levels of DEN-induced antioxidant response genes such as glutathione-S-transferase A1 (*Gsta1*), glutathione-S-transferase A2 (*Gsta2*), nuclear factor erythroid-derived 2 like 2 (*Nfe2l2*) and glutamate-cysteine ligase (*Gclc*; Fig. S2B). Malondialdehyde (MDA) is a toxic product of reactions between reactive oxygen species (ROS) and polyunsaturated lipids that is commonly used as a biomarker to quantify oxidative stress.

DEN administration resulted in substantial accumulation of MDA protein adducts ($p<0.001$), and this was found to be unaltered by TUDCA supplementation (Fig. S2C). Thus, the chemopreventive action of TUDCA seems to be independent of oxidative stress.

TUDCA does not affect DEN-induced autophagic flux

ER stress is able to induce autophagy [21], which has been shown to protect against hepatocarcinogenesis [22]. We therefore tested whether TUDCA modulates autophagy *in vivo* (Fig. S3). DEN-treated liver tissue exhibited enhanced expression of Beclin-1 and increased conversion of LC3B-I to LC3B-II, indicating the activation of autophagic signals. The cellular content of p62, a receptor and substrate of selective autophagy, is a critical indicator of autophagic flux [23]. Immunoblotting for p62 showed that DEN slightly decreased the hepatic p62 content (Fig. S3A). TUDCA administration did not alter the stably elevated LC3 conversion and reduced p62 content. Thus, TUDCA was unable to alter the enhanced autophagic flux.

TUDCA attenuates DEN-induced hepatic inflammation

Human HCC usually develops in the background of chronic hepatic inflammation [1]. Repeated DEN-induced murine tumors share similar pathogenesis [18], where pro-inflammatory cytokines, such as interleukin-6 (IL-6) and tumor necrosis factor-α (Tnf-α), promote tumor development [24]. Indeed, accumulating evidence suggests extensive cross-talk between UPR and the inflammatory response [25]. Chop-deficient livers have been shown to exhibit reduced inflammation and hepatocarcinogenesis [26]. Because TUDCA abolished the DEN-induced Chop expression in our study, we hypothesized that TUDCA might alter DEN-induced hepatic inflammation.

Immunohistochemical staining demonstrated robust accumulation of F4/80+ macrophages in the livers of animals treated with DEN for 25 weeks (Fig. 4A-B). However, TUDCA significantly decreased the number of liver-infiltrating macrophages ($p<0.05$). Using multiplex microbead immunoassays, we observed that hepatic expression of inflammatory cytokines, including interleukin-1 beta (IL-1β), IL-6, keratinocyte-derived chemokine (KC), monocyte chemoattractant protein-1 (Mcp-1), and Tnf-α, was augmented following DEN administration. Importantly, IL-6 ($p<0.05$), KC ($p<0.05$) and Tnf-α ($p<0.01$) levels were reduced following TUDCA supplementation (Fig. 4C).

Elevated eIf2α phosphorylation leads to translational repression of the NF-κB inhibitor IκBα and thereby promotes NF-κB signaling [27], which exerts a pro-carcinogenic role in inflammation-related hepatocarcinogenesis [28]. Using salubrinal, which inhibits eIf2α de-phosphorylation, we confirmed that sustained eIf2α phosphorylation leads to translational repression of IκBα in HepG2 cells (data not shown). Because DEN-induced eIf2α phosphorylation was abolished by TUDCA supplementation (Fig. 3B), we assessed the effect of TUDCA on hepatic IκBα expression and NF-κB activation to investigate this potential mechanism of action. Interestingly, TUDCA supplementation restored IκBα expression and slightly decreased phospho-NFκB p65 levels, the active form of NF-κB, in the DEN-treated livers (Fig. 4D-E). These data indicate that TUDCA suppresses the immune response to DEN-induced liver injury by reducing phospho-eIf2α-mediated repression of IκBα translation.

TUDCA alters invasiveness in vitro

Because ER stress was previously linked to cell invasion [29,30], we questioned whether TUDCA could modify HCC cell invasion *in vitro*. Therefore, we examined the effect of TUDCA in a hepatocyte growth factor-induced invasion assay in which spheroids of the Hepa1-6 HCC cell line embedded in collagen matrix were observed over time (Fig. 5A-C). TUDCA decreased the sphere area after 60 h of incubation ($p<0.05$; Fig. 5A), whereas the perimeter of the TUDCA-treated spheres increased compared with controls after 24 ($p<0.001$) and 48 h ($p<0.05$) of incubation (Fig. 5B). Although TUDCA may have decreased sphere area by affecting cell proliferation in this context (e.g., as observed for HepG2 in Fig. 3B), the larger perimeter combined with a smaller area suggests an altered invasive phenotype. This result was also supported by the more irregular sphere shape observed upon invasion in the presence of TUDCA (Fig. 5C). However, in a Boyden chamber assay, addition of 1-2 mM of TUDCA induced no significant alterations in the hepatocyte growth factor-stimulated invasion of the HCC cells over a 48-hour period (Fig. 5D).

Degradation of the extracellular matrix is one pivotal step and occurs due to the actions of matrix metalloproteinases (MMP). MMP-2, MMP-9 and MMP-14 enzymes play important roles in the degradation of the extracellular matrix and exist extensively in HCC tissues. MMP profiling showed that addition of TUDCA did not alter the protein levels of MMP-2, -9 and -14 (Fig. 5E). Accordingly, we observed no changes in the extracellular MMP-2 and -9 activity in the concentrated conditioned medium (Fig. 5F). In conclusion, although TUDCA alters the invasive phenotype, TUDCA does not induce increased HCC cell invasion.

TUDCA did not affect tumor progression

Given our findings that TUDCA attenuated UPR-induced apoptosis and increased cellular metabolic activity, we evaluated whether TUDCA could stimulate tumor progression via its cytoprotective effect. To assess the effect of TUDCA on established tumors, we used orthotopic and xenograft mouse models of HCC. Following orthotopic HCC induction with 25 weeks of DEN, 5 weeks of low- or high-dose TUDCA supplementation had no significant effect on mortality (Table 1) or tumor number (all sizes: 17.4 ± 4.9 after vehicle versus 19.7 ± 4.5 after low-dose TUDCA and 18.8 ± 5.3 after high-dose TUDCA). Accordingly, microscopic quantification confirmed that TUDCA produced no significant effects on HCC burden (Fig. 6A-C). Next, we investigated the effects of 5 weeks of TUDCA supplementation following 25 weeks of DEN-induced tumor development on the UPR (Fig. 6D-E). TUDCA did not alter the protein levels of Chop or phospho-eIf2α in HCC-bearing livers (Fig. 6E). Moreover, no difference in the apoptosis rate was observed (data not shown). These results suggest that TUDCA was unable to restore ER function after prolonged hepatocarcinogen exposure.

In the HepG2 xenograft model, TUDCA supplementation for 5 weeks did not significantly modify tumor growth compared to control treatment (Fig. 6F-G), and no mortality occurred in any of these groups. Finally, no metastases were detected in any group of the preventive or therapeutic settings of the orthotopic or of the HepG2 xenograft model.

1.2.5. **Discussion**

There is an urgent need for innovative preventive and therapeutic options for HCC [3]. Previous studies have demonstrated that the chemical chaperone TUDCA serves as a cytoprotective agent by reducing ER stress and apoptosis [5,7,8,14]. In this study, we evaluated the preventive and therapeutic potential of TUDCA and its effect on carcinogen-induced ER stress in HCC. Our results reveal that TUDCA supplementation during carcinogen exposure reduces the carcinogen-induced apoptosis of hepatocytes and HCC incidence (Fig. 7). Furthermore, it does not stimulate the progression and invasion of established tumors.

A recent double-blind randomized trial demonstrated that daily TUDCA therapy (750 mg) for 6 months is safe and appears to be an effective liver cirrhosis treatment; in particular, it improved several biochemical parameters [31]. In addition, TUDCA therapy in cirrhotic patients awaiting liver transplantation supported their functional stability during the wait time [32]. Our results suggest that TUDCA therapy in patients with a high HCC risk, such as cirrhotic patients with continuous exposure to carcinogens, not only improved liver function but could also prevent HCC incidence.

We selected a low dosage (60 mg/kg/day), which corresponds to dosages administrable and tolerable for humans, and a high dosage (300 mg/kg/day) to assess dose-dependent effects and potential side effects. Both low- and high-dose TUDCA administration decreased tumor burden in our mouse models. However, the trend of reduced weight and survival was only observed in the high-dose TUDCA group. This reduction in body weight was also observed in a mouse model of retinitis pigmentosa, where animals were treated with high-dose TUDCA (500 mg/kg/day) [33]. Additionally, TUDCA has been shown to increase energy expenditure by promoting intracellular thyroid hormone activation [34]. Therefore, a low dose of TUDCA is advisable for chemoprevention.

Chemically improving the ER folding capacity by TUDCA administration was previously shown to protect from UPR signaling and ER stress-induced apoptosis, which are primarily regulated by the phospho-eIf2α\Chop cascade [10,15]. Although Chop plays critical pro-apoptotic roles, it was recently shown to promote carcinogenesis in a DEN-induced model of HCC [26]. Accordingly, TUDCA efficiently diminished Chop expression and tumorigenesis during carcinogen exposure in our study.

In hepatocytes, DEN is metabolized by cytochrome P450 2E1 through a ROS-generating reaction that induces liver injury and DNA damage [35,36].

Subsequently, danger signals released from injured hepatocytes induce liver inflammation. Accordingly, certain antioxidants, such as N-acetylcysteine [35] or lycopene [37], have been shown to attenuate DEN-induced hepatocarcinogenesis. Of note, N-acetylcysteine was recently shown to accelerate lung cancer progression in mice [38]. Because TUDCA did not affect oxidative stress-induced cytotoxicity *in vitro* or hepatic oxidative stress *in vivo*, we presume that the chemopreventive effect of TUDCA was not mediated by directly antagonizing oxidative stress but rather by modulating ER stress-induced apoptosis. Therefore, the combination of TUDCA with antioxidants could represent a dual-targeting chemopreventive strategy for HCC.

HCC has been characterized as a chronic inflammation-driven cancer, and chemically induced models have revealed the crucial roles of inflammatory signaling in disease onset and severity [35]. Therefore, we assessed whether TUDCA affected tumor-immune system crosstalk. TUDCA administration resulted in a decrease in hepatic macrophage infiltration and IL-6, KC and Tnf-α levels. These results suggest that TUDCA attenuates inflammation in response to DEN-induced liver injury and thus interrupts positive feedback from inflammation-induced ER stress and UPR-induced inflammation [13]. Interestingly, a similar effect of TUDCA on macrophage infiltration and Tnf-α expression was also recently observed in a model of ER stress-mediated steatohepatitis-induced HCC [39]. However, additional studies are needed to uncover the precise mechanism of the interaction between ER stress and inflammation and the effects of TUDCA on these signaling pathways.

Uncontrolled regeneration of hepatocytes, which occurs after repeated cycles of cell death and compensatory proliferation in chronic hepatitis, appears to be an important factor in hepatocarcinogenesis [16,40]. Apparently, increased hepatocyte apoptosis contributed to the development of HCC in our DEN-induced mouse model. TUDCA interrupts the positive feedback from UPR-mediated apoptosis-induced hepatocarcinogenesis, leading to UPR activation by tumor microenvironmental stresses [11].

Finally, an oral treatment option for preventing HCC would be highly beneficial for cirrhotic patients with high HCC risk. In this study, we showed that TUDCA could represent a clinically applicable chemopreventive agent for HCC. Whether hepatocyte susceptibility to other carcinogens, such as viral replication or alcohol, can be limited by chemical chaperones will be of great interest.In conclusion, our study demonstrates that supplementation with TUDCA diminishes carcinogen-induced hepatotoxicity and prevents tumor induction by, at least partially, alleviating positive feedback from ER stress, inflammation and apoptosis in carcinogen-injured liver tissue.

1.2.6. **Methods**

Animal studies

Ethics statement. The investigation was conducted in accordance with the ethical standards and according to the Declaration of Helsinki as well as the national and international guidelines. The investigation was also approved by the institutional review board of Ghent University (ECD 11/52).

Orthotopic model. Wild-type 129S2/SvPasCrl mice were purchased from Charles River (Belgium) and maintained as previously described [18]. In the preventive arm of the study, 5-week-old male mice were randomly divided into 4 groups (n=12 in each group). Three groups received weekly intraperitoneal DEN (35 mg/kg, in saline) injections for 25 weeks with either regular drinking water or drinking water supplemented with varying amounts of TUDCA (low dose of 60 mg/kg/day or high dose of 300 mg/kg/day). Mice in the control group received 25 weeks of saline injections and regular drinking water. In the therapeutic arm of the study, mice received DEN for 25 weeks before being treated with saline- or TUDCA-supplemented (low or high dose) drinking water for 5 weeks (n=12 in each group). In addition, 30 µg of tunicamycin was intraperitoneally injected in four naive 30-week-old male 129S2/SvPasCrl mice 72 h before sacrifice. Blood was collected from the retro-orbital sinus under isoflurane anesthesia. After macroscopic evaluation and quantification of hepatic tumor number, all organs were fixed in 4% phosphate-buffered formaldehyde (Klinipath) and embedded in paraffin or snap frozen in liquid nitrogen. Hematoxylin/eosin and reticulin staining were performed to assess tumor burden, and the results were evaluated by two independent observers. Sirius Red staining enabled fibrosis assessment according to Metavir scoring. Serum alanine and aspartate aminotransferase (ALT and AST, respectively) levels were measured at the Lab of Clinical Biology, Ghent University Hospital.

Xenograft model. HepG2 cells ($6x10^6$) were re-suspended in 100 µl of serum-free media and mixed with 100 µl of Matrigel (BD Biosciences, Bedford, MA, USA). The cell preparation was injected subcutaneously into the right flank of 8-week-old male athymic nude mice. Tumor volumes were calculated using the following formula: volume (mm^3) = $ab^2/2$; where b is the smaller dimension.

When the mean tumor volume reached 150 mm^3, animals were randomized into three groups (n=6 in each group) as follows: regular drinking water, low-dose (60 mg/kg/day) TUDCA-supplemented drinking water and high-dose (300 mg/kg/day) TUDCA-supplemented drinking water. Tumor dimensions were recorded two times per week with a digital caliper starting on the first day of treatment. Tumor weights were recorded at the time of sacrifice.

Cell culture

HepG2, BWTG3 and Hepa1-6 (ATCC, Virginia, USA) cells were cultured in DMEM supplemented with 10% fetal bovine serum (Life Technologies, Ghent, Belgium). Cells were incubated for 48 h with tunicamycin (0.5 μg/ml), TUDCA (0.1–10 mM, Calbiochem, MA, USA), salubrinal (50 μM, Tocris, Bristol, UK), N-acetylcysteine (5 mM), H_2O_2 (1-5 mM) or equal volumes of solvent. For direct cell counting, cells were trypsinised and counted in trypan blue. All reagents were obtained from Sigma (Diegem, Belgium) unless stated otherwise. Experiments were performed in quadruplicate and independently repeated three times.
Detailed information regarding choline positron emission tomography, caspase-3/7 activity, TUNEL apoptosis, RNA extraction, quantitative real-time PCR, western blot analysis, LDH, MTT, BrdU incorporation, lipid peroxidation, immunohistochemistry, multiplex microbead and spheroid invasion assays is provided in the Supporting Information.

Statistics

Statistical analyses were performed using SPSS version 21 (SPSS, Chicago, USA). Data are presented as the mean ± SD or fold change relative to expression in controls. Normally distributed data were subjected to unpaired student's t-tests. Multiple groups were compared by one-way analysis of variance (ANOVA) with Bonferroni correction. Non-normally distributed data were tested using the Mann-Whitney U test. The chi-squared test was used to compare mortality. Student's paired t-test was used to compare area or perimeter fold change. Reported p-values were two-sided and considered significant when less than 0.05.

1.2.7. **References**

1. EASL-EORTC clinical practice guidelines: management of hepatocellular carcinoma. J Hepatol. 2012; 56: 908–943.
2. International Agency for Research on Cancer. GLOBOCAN 2012: Estimated incidence, mortality and prevalence worldwide in 2012. 2012. http://globocan.iarc.fr/Pages/fact_sheets_cancer.aspx.
3. Lu SC. Where are we in the chemoprevention of hepatocellular carcinoma? Hepatology. 2010; 51: 734–736.
4. Lindor KD, Gershwin ME, Poupon R, Kaplan M, Bergasa NV, Heathcote EJ. AASLD practice guidelines: Management of primary biliary cirrhosis. Hepatology. 2009; 50: 291–308.
5. Poupon R. Ursodeoxycholic acid and bile-acid mimetics as therapeutic agents for cholestatic liver diseases: an overview of their mechanisms of action. Clin Res Hepatol. Gastroenterol 2012; 36 Suppl 1: S3–12.
6. Laukens D, Devisscher L, Van den Bossche L, Hindryckx P, Vandenbroucke R, Vandewynckel Y-P, Cuvelier C, Brinkman BM, Libert C, Vandenabeele P, De Vos M. Tauroursodeoxycholic acid inhibits experimental colitis by preventing early intestinal epithelial cell death. Lab Invest. 2014; 94: 1419-1430.
7. Colell A, Coll O, García-Ruiz C, París R, Tiribelli C, Kaplowitz N, Fernández-Checa JC. Tauroursodeoxycholic acid protects hepatocytes from ethanol-fed rats against tumour necrosis factor-induced cell death by replenishing mitochondrial glutathione. Hepatology. 2001; 34: 964–971.
8. Falasca L, Tisone G, Palmieri G, Anselmo A, Di Paolo D, Baiocchi L, Torri E, Orlando G, Casciani CU, Angelico M. Protective role of tauroursodeoxycholate during harvesting and cold storage of human liver: a pilot study in transplant recipients. Transplantation. 2001; 71: 1268–1276.
9. Perez M-J, Briz O. Bile-acid-induced cell injury and protection. World J Gastroenterol. 2009; 15: 1677–1689.
10. Walter P, Ron D. The unfolded protein response: from stress pathway to homeostatic regulation. Science. 2011; 334: 1081–1086.
11. Vandewynckel Y-P, Laukens D, Geerts A, Bogaerts E, Paridaens A, Verhelst X, Janssens S, Heindryckx F, Van Vlierberghe H. The paradox of the unfolded protein response in cancer. Anticancer Res. 2013; 33: 4683–4694.
12. Shuda M. Activation of the ATF6, XBP1 and grp78 genes in human hepatocellular carcinoma: a possible involvement of the ER stress pathway in hepatocarcinogenesis. J Hepatol. 2003; 38: 605–614.
13. Malhi H, Kaufman RJ. Endoplasmic reticulum stress in liver disease. J Hepatol. 2011; 54: 795–809.
14. Schoemaker MH, Conde de la Rosa L, Buist-Homan M, Vrenken TE, Havinga R, Poelstra K, Haisma HJ, Jansen PL, Moshage H. Tauroursodeoxycholic acid protects rat hepatocytes from bile acid-induced apoptosis via activation of survival pathways. Hepatology. 2004; 39: 1563–1573.
15. Xie Q, Khaoustov VI, Chung CC, Sohn J, Krishnan B, Lewis DE, Yoffe B. Effect of tauroursodeoxycholic acid on endoplasmic reticulum stress-induced caspase-12 activation. Hepatology. 2002; 36: 592–601.
16. Hikita H, Kodama T, Shimizu S, Li W, Shigekawa M, Tanaka S, Hosui A, Miyagi T, Tatsumi T, Kanto T, Hiramatsu N, Morii E, Hayashi N, et al. Bak deficiency inhibits liver carcinogenesis: a causal link between apoptosis and carcinogenesis. J Hepatol. 2012; 57: 92-100.

17. Hikita H, Tatsumi T, Saito Y, Tanaka S, Shimizu S, Li W, Sakamori R, Miyagi T, Hiramatsu N, Takehara T. Poster 1793: Oxidative stress induced by continuous hepatocyte apoptosis drives liver carcinogenesis independently of regeneration and DNA methylation status. Hepatology. 2013; 58: 92–207.
18. Heindryckx F, Mertens K, Charette N, Vandeghinste B, Casteleyn C, Van Steenkiste C, Slaets D, Libbrecht L, Staelens S, Starkel P, Geerts A, Colle I, Van Vlierberghe H. Kinetics of angiogenic changes in a new mouse model for hepatocellular carcinoma. Mol Cancer. 2010; 9: 219-230.
19. Vandewynckel Y-P, Laukens D, Bogaerts E, Paridaens A, Van den Bussche A, Verhelst X, Christophe Van Steenkiste, Descamps B, Vanhove C, Libbrecht L, De Rycke R, Lambrecht BN, Geerts A, et al. Modulation of the unfolded protein response impedes tumour cell adaptation to proteotoxic stress: a PERK for hepatocellular carcinoma therapy. Hepatol Int. 2014; 9: 93-104.
20. Oveson BC, Iwase T, Hackett SF, Lee SY, Usui S, Sedlak TW, Snyder SH, Campochiaro PA, Sung JU. Constituents of bile, bilirubin and TUDCA, protect against oxidative stress-induced retinal degeneration. J Neurochem. 2011; 116: 144–153.
21. Ma T, Li Y-Y, Zhu J, Fan L-L, Du W-D, Wu C-H, Sun GP, Li JB. Enhanced autophagic flux by endoplasmic reticulum stress in human hepatocellular carcinoma cells contributes to the maintenance of cell viability. Oncol Rep. 2013; 30: 433–440.
22. Lin H, Hua F, Hu Z-W. Autophagic flux, supported by toll-like receptor 2 activity, defends against the carcinogenesis of hepatocellular carcinoma. Autophagy. 2012; 8: 1859–1861.
23. Mizushima N, Yoshimori T, Levine B. Methods in mammalian autophagy research. Cell. 2010; 140: 313–326.
24. Park EJ, Lee JH, Yu G-Y, He G, Ali SR, Holzer RG, Osterreicher CH, Takahashi H, Karin M. Dietary and genetic obesity promote liver inflammation and tumourigenesis by enhancing IL-6 and TNF expression. Cell. 2010; 140: 197–208.
25. Zhang K, Kaufman RJ. From endoplasmic-reticulum stress to the inflammatory response. Nature. 2008; 454: 455–462.
26. Scaiewicz V, Nahmias A, Chung RT, Mueller T, Tirosh B, Shibolet O. CCAAT/enhancer-binding protein homologous (CHOP) Protein promotes carcinogenesis in the den-induced hepatocellular carcinoma model. PLoS One. 2013; 8: e81065.
27. Deng J, Lu PD, Zhang Y, Scheuner D, Kaufman RJ, Sonenberg N, Harding HP, Ron D. Translational repression mediates activation of nuclear factor kappa B by phosphorylated translation initiation factor 2. Mol Cell Biol. 2004; 24: 10161–10168.
28. Luedde T, Schwabe RF. NF-κB in the liver--linking injury, fibrosis and hepatocellular carcinoma. Nat Rev Gastroenterol Hepatol. 2011; 8: 108–118.
29. Li Y, Liu H, Huang YY, Pu LJ, Zhang XD, Jiang CC, Jiang ZW. Suppression of endoplasmic reticulum stress-induced invasion and migration of breast cancer cells through the downregulation of heparanase. Int J Mol Med. 2013; 31: 1234–1242.
30. Dejeans N, Pluquet O, Lhomond S, Grise F, Bouchecareilh M, Juin A, Meynard-Cadars M, Bidaud-Meynard A, Gentil C, Moreau V, Saltel F, Chevet E. Autocrine control of glioma cells adhesion and migration through IRE1α-mediated cleavage of SPARC mRNA. J Cell Sci. 2012; 125: 4278-4287.
31. Pan X, Zhao L, Li L, Li A, Ye J, Yang L, Xu KS, Hou XH. Efficacy and safety of tauroursodeoxycholic acid in the treatment of liver cirrhosis: a double-blind randomized controlled trial. J Huazhong Univ Sci Technolog Med Sci. 2013; 33: 189–194.
32. Caglieris S, Giannini E, Dardano G, Mondello L, Valente U, Testa R. Tauroursodeoxycholic acid administration as adjuvant therapy in cirrhotic patients on transplantation waiting lists. Hepatogastroenterology. 2000; 47: 1045-1047.

33. Drack AV, Dumitrescu AV, Bhattarai S, Gratie D, Stone EM, Mullins R, Sheffield VC. TUDCA slows retinal degeneration in two different mouse models of retinitis pigmentosa and prevents obesity in Bardet-Biedl syndrome type 1 mice. Invest Ophthalmol Vis Sci. 2012; 53: 100–106.
34. Watanabe M, Houten SM, Mataki C, Christoffolete MA, Kim BW, Sato H, Messaddeq N, Harney JW, Ezaki O, Kodama T, Schoonjans K, Bianco AC, Auwerx J. Bile acids induce energy expenditure by promoting intracellular thyroid hormone activation. Nature. 2006; 439: 484–489.
35. Lin H, Liu X, Yu J, Hua F, Hu Z. Antioxidant N-acetylcysteine attenuates hepatocarcinogenesis by inhibiting ROS/ER stress in TLR2 deficient mouse. PLoS One. 2013; 8: e74130.
36. Ghosh D, Choudhury ST, Ghosh S, Mandal AK, Sarkar S, Ghosh A, Saha KD, Das N. Nanocapsulated curcumin: oral chemopreventive formulation against diethylnitrosamine induced hepatocellular carcinoma in rat. Chem Biol Interact. 2012; 195: 206–214.
37. Ip BC, Liu C, Ausman LM, von Lintig J, Wang X-D. Lycopene attenuated hepatic tumorigenesis via differential mechanisms depending on carotenoid cleavage enzyme in mice. Cancer Prev Res. 2014; 7: 1219-1227.
38. Sayin VI, Ibrahim MX, Larsson E, Nilsson JA, Lindahl P, Bergo MO. Antioxidants accelerate lung cancer progression in mice. Sci Transl Med. 2014; 6: 221ra15.
39. Nakagawa H, Umemura A, Taniguchi K, Font-Burgada J, Dhar D, Ogata H, Zhong Z, Valasek MA, Seki E, Hidalgo J, Koike K, Kaufman RJ, Karin M. ER stress cooperates with hypernutrition to trigger tnf-dependent spontaneous HCC development. Cancer Cell. 2014; 26: 331–343.
40. Blagosklonny MV. Carcinogenesis, cancer therapy and chemoprevention. Cell Death Differ. 2005; 12: 592–602.

1.2.8. **Figures**

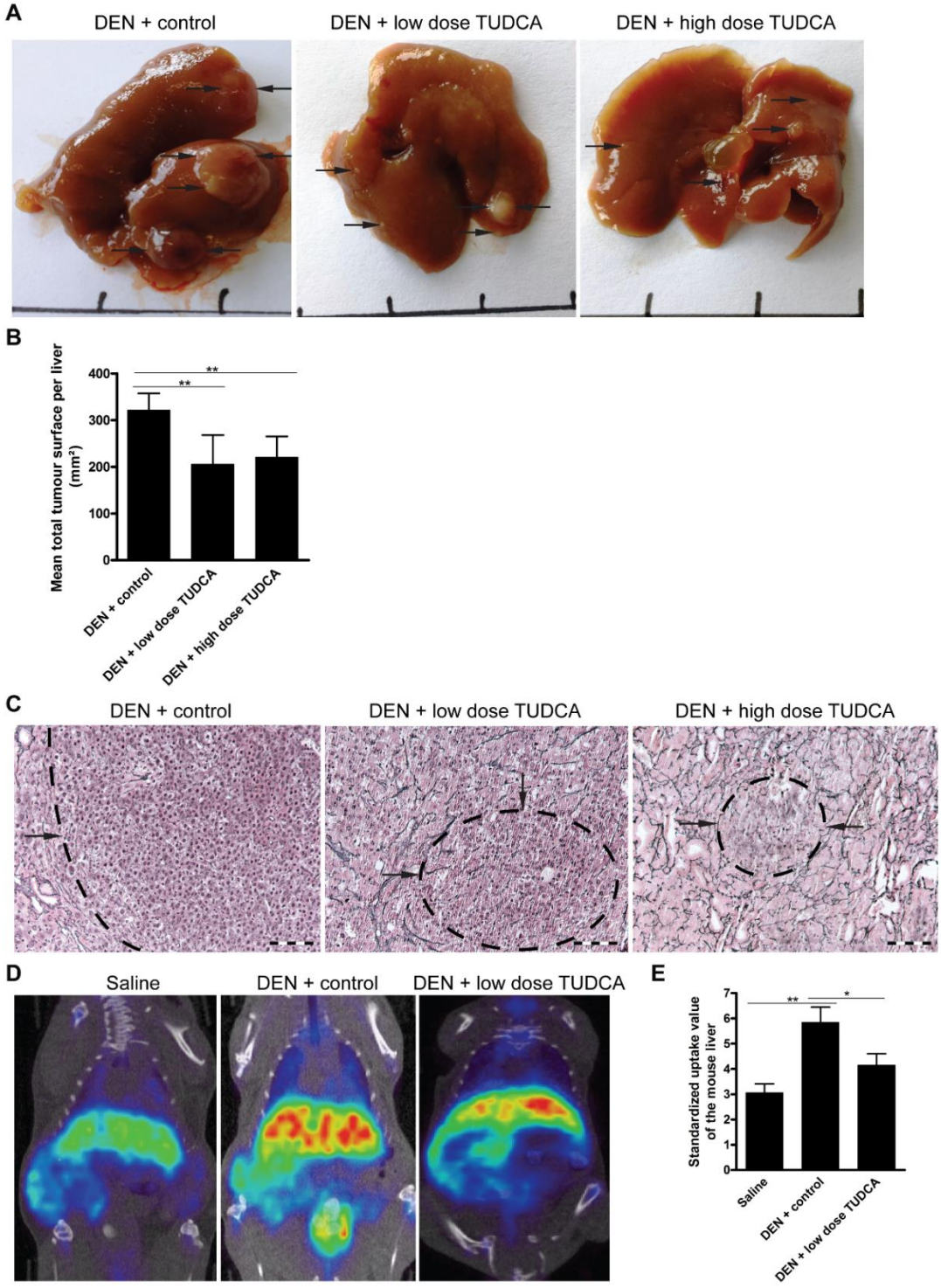

Fig. 1. TUDCA prevents the development of HCC during carcinogen exposure. (A) Representative images of livers treated for 25 weeks with the indicated treatments. (B) Quantitative analysis of the tumor burden as assessed by **(**C) Reticulin staining. Scale bar: 100 µm. (D) ^{18}F-Choline positron emission tomography was performed to visualize cell membrane synthesis after the indicated treatments (blue: low, red: high activity). (E) Quantification of ^{18}F-Choline positron emission tomography. Standardized uptake values of the mouse livers are presented as the mean ± SD. One-way ANOVA was applied for statistical analysis. *p<0.05, **p<0.01.

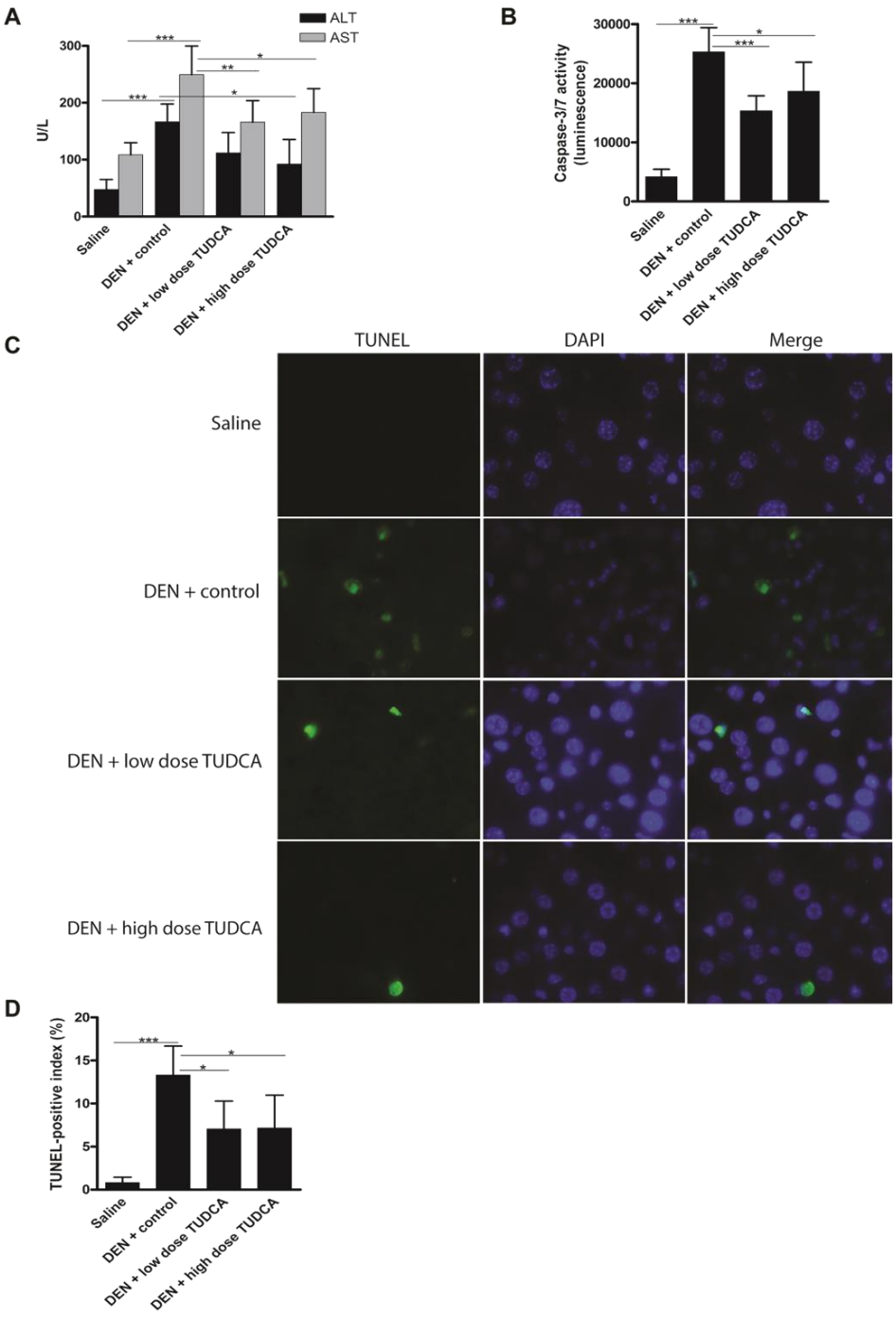

Fig. 2. TUDCA reduces DEN-induced apoptosis of hepatocytes. (A) Liver damage was assessed by measuring ALT and AST levels in the serum of mice after the indicated treatments. (B) Caspase-3/7 activity *ex vivo* (n=8). (C) TUNEL immunofluorescence and (D) quantification of the TUNEL-positive index. *p<0.05, **p<0.01, ***p<0.001.

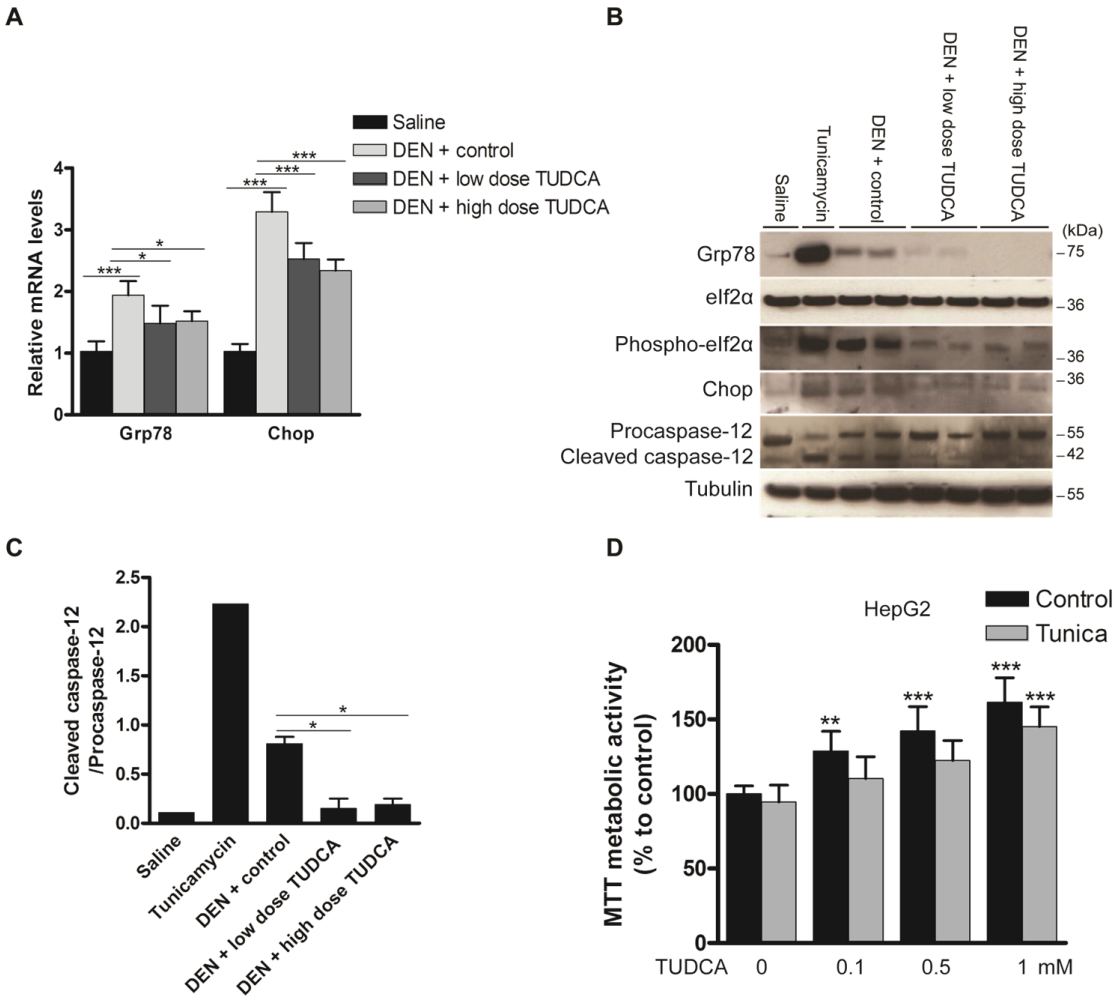

Fig. 3. Effect of TUDCA on the hepatic UPR pattern in the DEN-induced mouse model of HCC. (A) Real-time PCR analysis of the UPR targets Grp78 and Chop. (B) Expression of Grp78, eIf2α, phospho-eIf2α, Chop, procaspase-12 and cleaved caspase-12 was detected using Western blotting. Results are representative of 2 independent experiments. (C) Cleaved caspase-12/procaspase-12 ratio obtained using densitometric analysis of the Western blot shown in B. (D) Effect of TUDCA treatment on the MTT metabolic activity of HepG2 cells (treated with tunicamycin (Tunica) or not). *p<0.05, **p<0.01, ***p<0.001. Results are representative of 3 independent experiments.

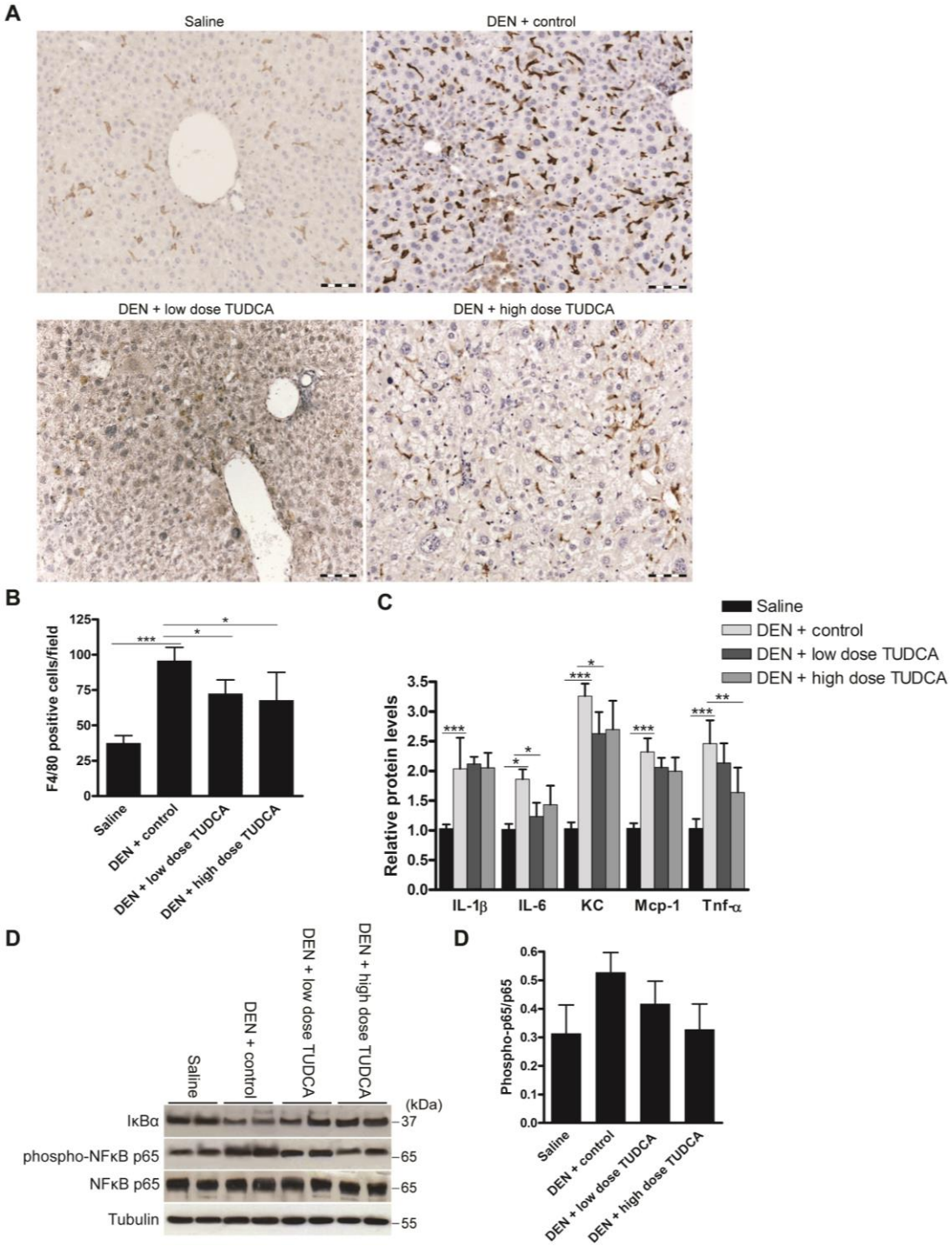

Fig. 4. Effect of TUDCA on DEN-induced hepatic inflammation. (A) Immunostaining for F4/80 and (B) quantification of F4/80-positive macrophages in the liver after the indicated treatments (n=5). (C) Determination of the indicated hepatic cytokine levels by multiplex microbead immunoassay (n=8). Values represent the mean ± SD. *p<0.05, **p<0.01, ***p<0.001. (D) Expression of IκBα, phospho-NFκB p65 and NFκB p65 was detected using Western blotting. Results are representative of 2 independent experiments. (E) Phospho-NFκB p65/ NFκB p65 ratio obtained using densitometric analysis of the Western blot shown in D.

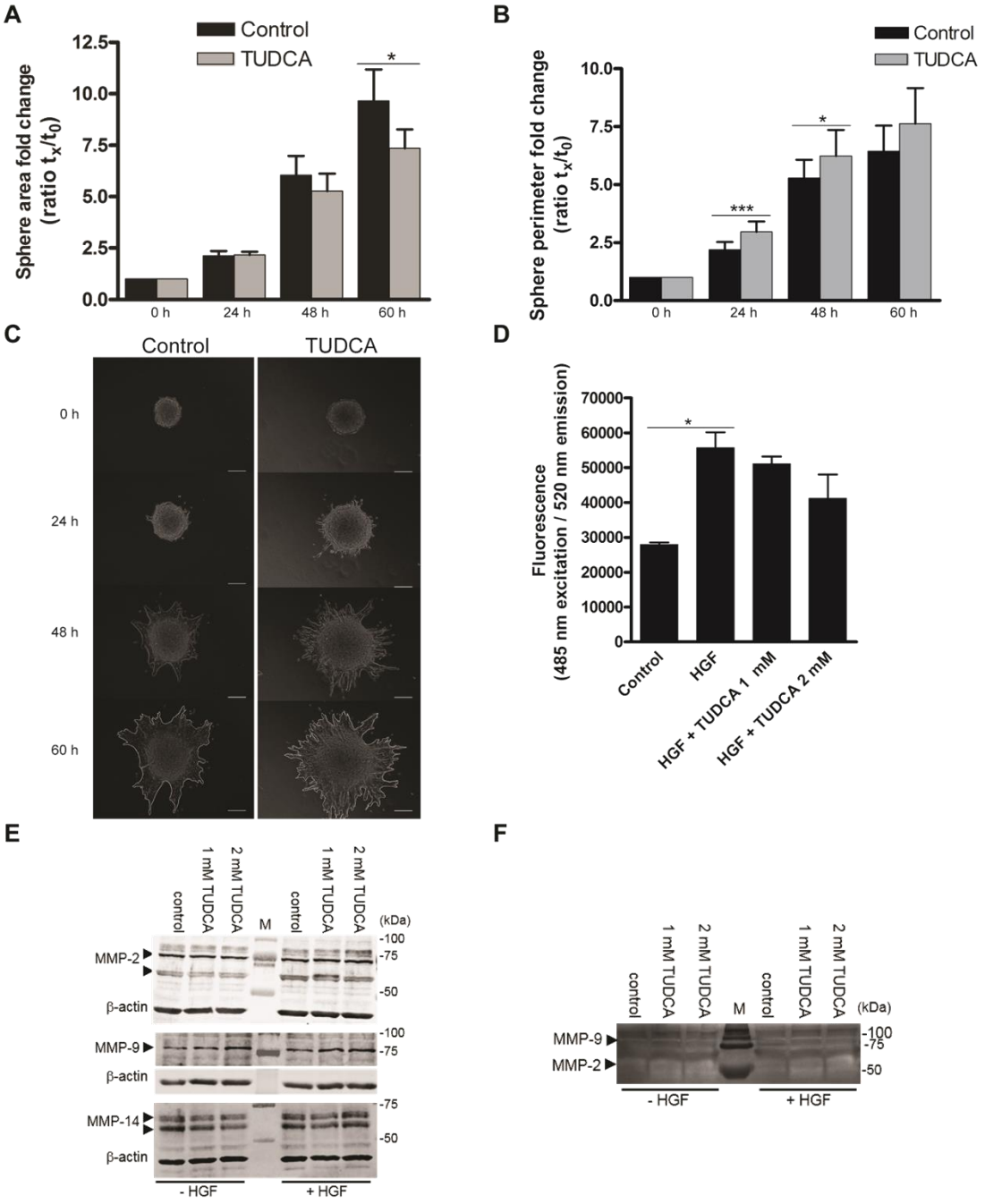

Fig. 5. Effects of TUDCA on HCC cell invasion. (A) The area and (B) length of the outside boundary (perimeter) of collagen-embedded Hepa1-6 spheroids (n=9) was measured at 0, 24, 48 and 60 h of incubation with 2 mM TUDCA or control medium. Results are representative of 2 independent experiments. (C) Representative images of invasive capacity of cells present in a collagen-embedded multicellular spheroid are shown at different time points. The multicellular spheroids are approx. 150 µm in diameter at start. At 60 h, the spheroid perimeter is marked. Scale bar is 50 µm. (D) Boyden chamber invasion assay with Hepa1-6 cells following 48 h of incubation with control medium, control medium with chemoattractant hepatocyte growth factor (HGF) without or with 1 or 2 mM TUDCA. Samples were run in quadruplicate. (E) Western blot analysis of MMP-2, -9 and -14 levels in Hepa1-6 cell lysates of control cells and cells treated with 1 or 2 mM TUDCA (48h), in the presence or absence of 50 ng/ml HGF stimulation. Arrows indicate MMP-2 (72 and 63-66 kDa), MMP-9 (78-82 kDa) and MMP-14 (66-57 kDa). The β-actin signal is used as loading control. (F) Gelatin zymography of concentrated culture medium of Hepa1-6 control cells or cells treated with 1 or 2 mM TUDCA (48 h), in the presence or absence of 50 ng/ml HGF stimulation. The white bands indicate MMP-activity; arrowheads: signal for MMP-9 (glycosylated, 92 kDa) and MMP-2 (58/62 kDa, active). Values represent the mean ± SD. *$p<0.05$, ***$p<0.001$.

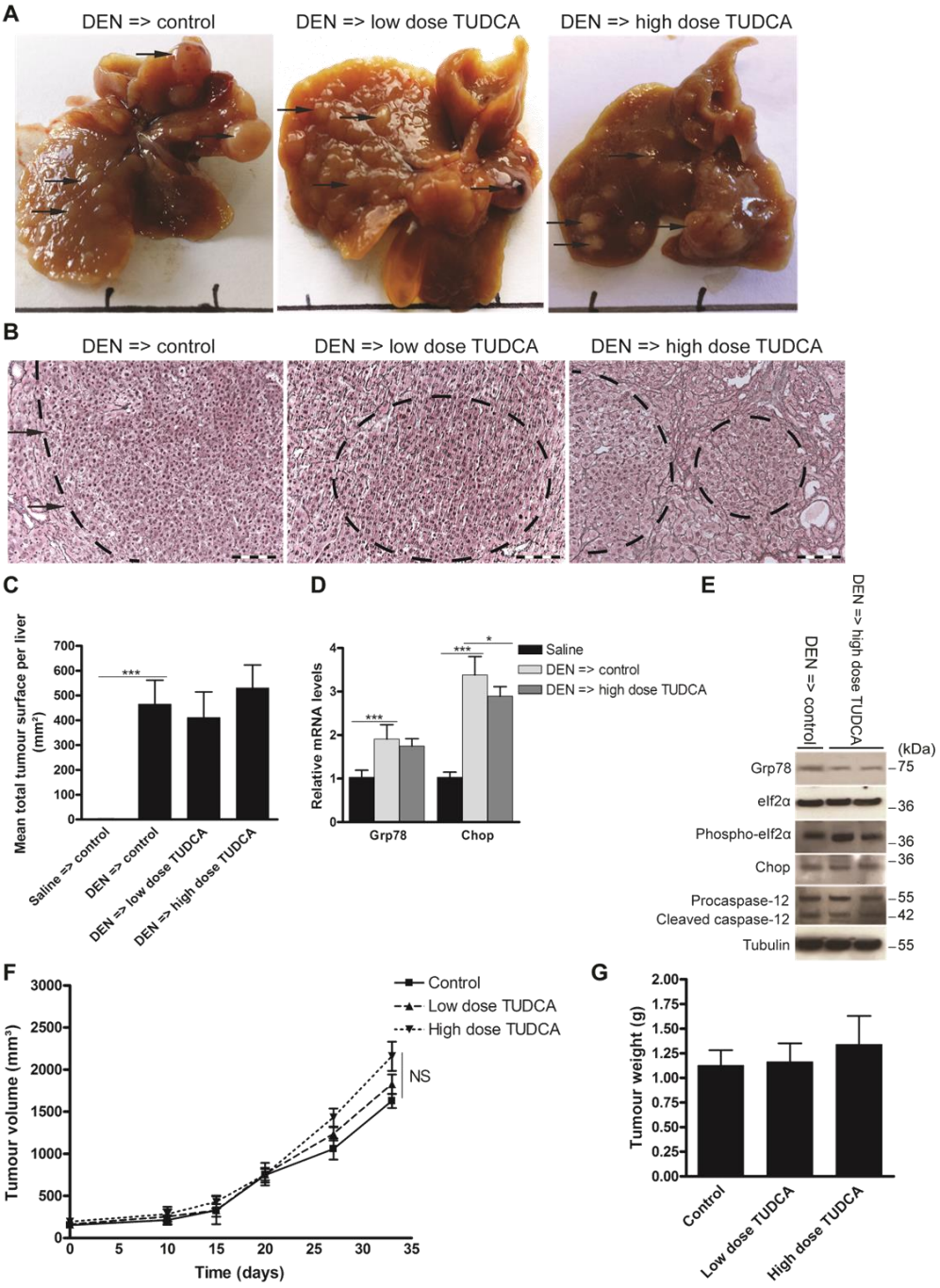

Fig. 6. Effect of TUDCA on the orthotopic and xenograft mouse models of HCC progression. (A) Representative images of murine livers treated for 25 weeks with DEN injections followed by 5 weeks of TUDCA-supplemented or control drinking water. (B) Reticulin staining of the DEN-treated livers for (C) quantification of tumor burden. Scale bar: 100 µm. (D) Real-time PCR analysis of the UPR targets Grp78 and Chop. (E) Expression of Grp78, eIf2α, phospho-eIf2α, Chop, procaspase-12 and cleaved caspase-12 was detected using Western blotting. Results are representative of 2 independent experiments. (F) Effect of indicated treatments on growth of HepG2 xenografts in athymic nude mice (n=6). The volume of each tumor was measured for 33 days. Values represent the mean ± SD. (G) At the end of the treatment period, animals were sacrificed and tumor weights were recorded. *p<0.05, **p<0.01.

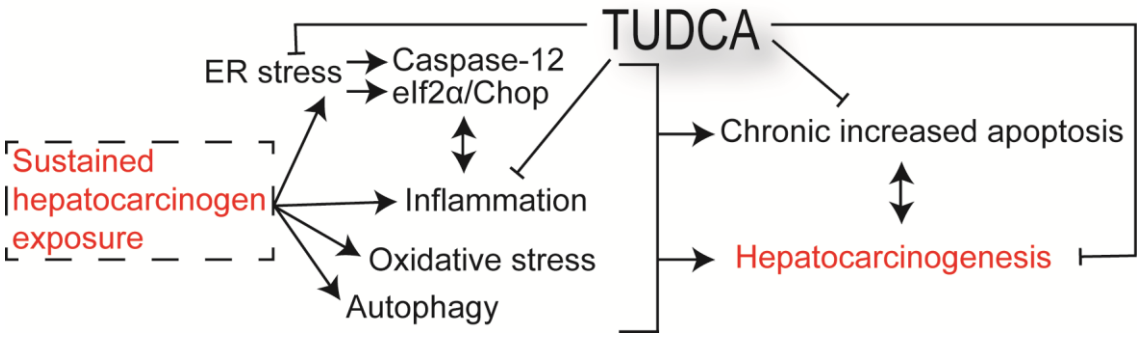

Fig. 7. Schematic overview outlining the mechanisms of the chemopreventive effects of TUDCA.

1.2.9. **Supplementary Figures**

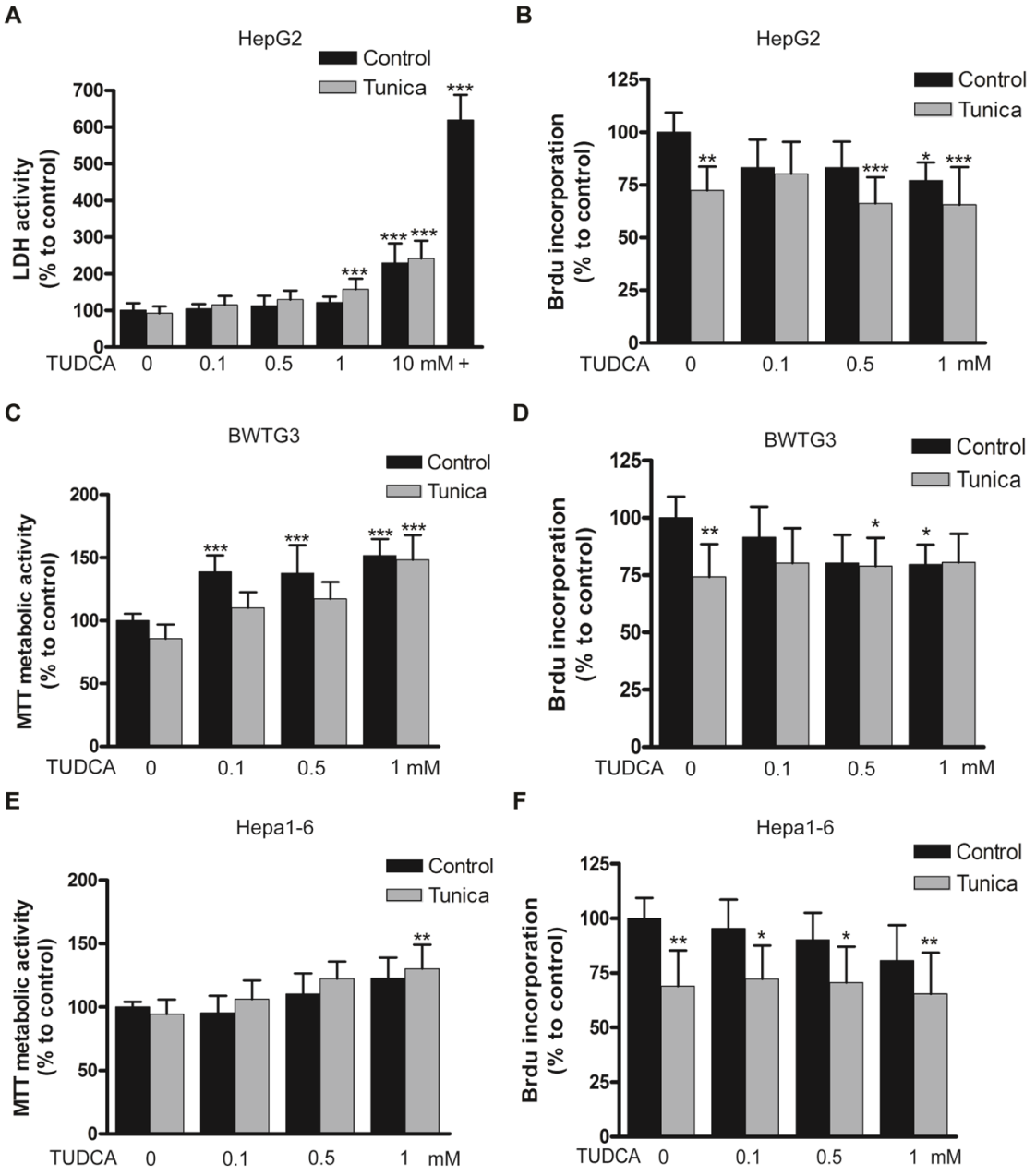

Fig. S1. Effect of TUDCA on viability and proliferation of HCC cells. Control cells or cells treated with 0.5 microgram/ml tunicamycin were treated with increasing concentrations of TUDCA as indicated. (A) LDH release in HepG2 cells. As positive control, TritonX 1% was applied. (B) Proliferation rate as assessed by BrdU incorporation in HepG2 cells. (C) MTT metabolic activity and (D) proliferation rate in BWTG3 cells. (E) MTT metabolic activity and (F) proliferation rate in Hepa1-6 cells. Data are presented as the mean ± SD of n=4. Statistical significance was determined by one-way analysis of variance (ANOVA) with Bonferroni correction. *p<0.05, **p<0.01, ***p<0.001.

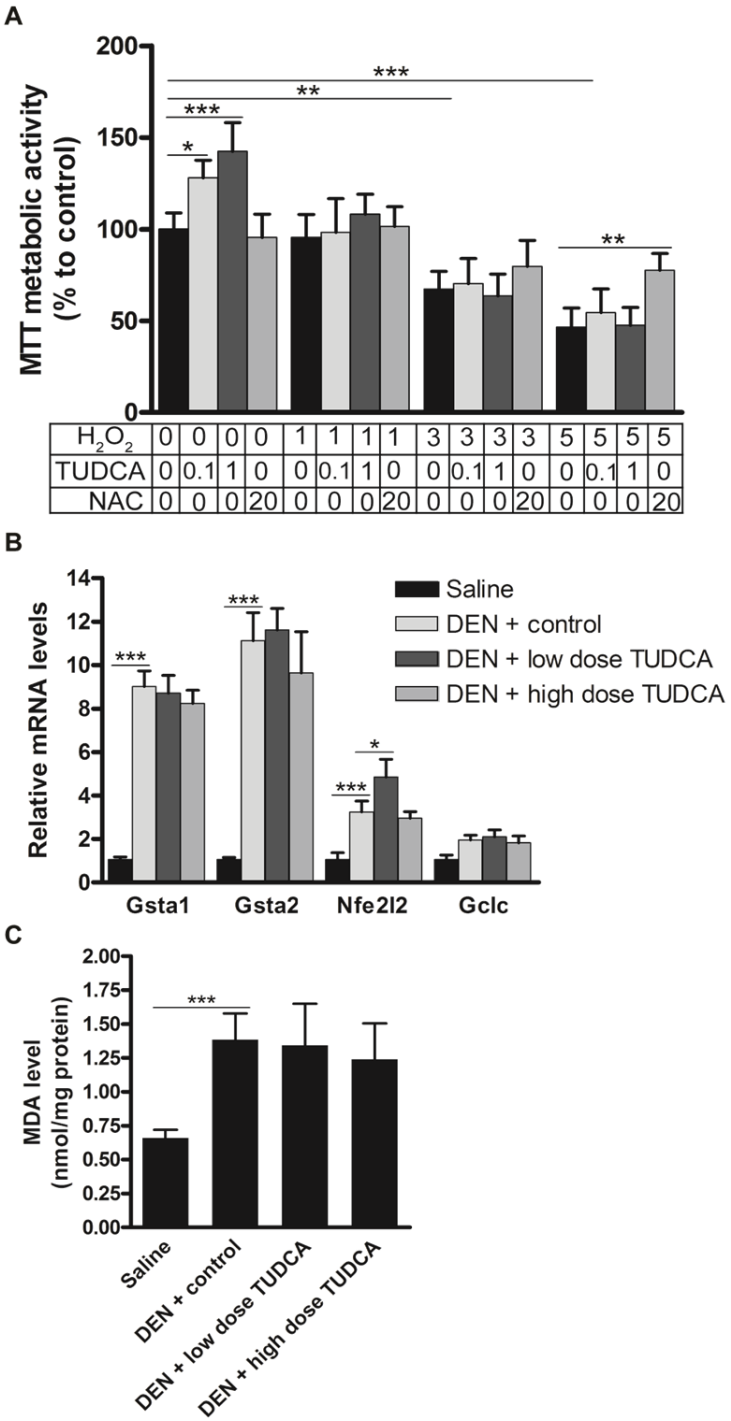

Fig. S2. Effect of TUDCA on oxidative stress-induced cytotoxicity in HepG2 cells. (A) MTT assay of HepG2 cells incubated for 48 h. Concentrations are indicated in mM. NAC, N-acetylcysteine. (B) Real-time PCR analysis of the indicated antioxidant genes after indicated cell treatments. (C) Malondialdehyde (MDA) levels were quantified as a measure of lipid peroxidation in the mouse livers after the indicated treatments. All the values are expressed as the mean ± SD, n=5. *p<0.05, **p<0.01, ***p<0.001.

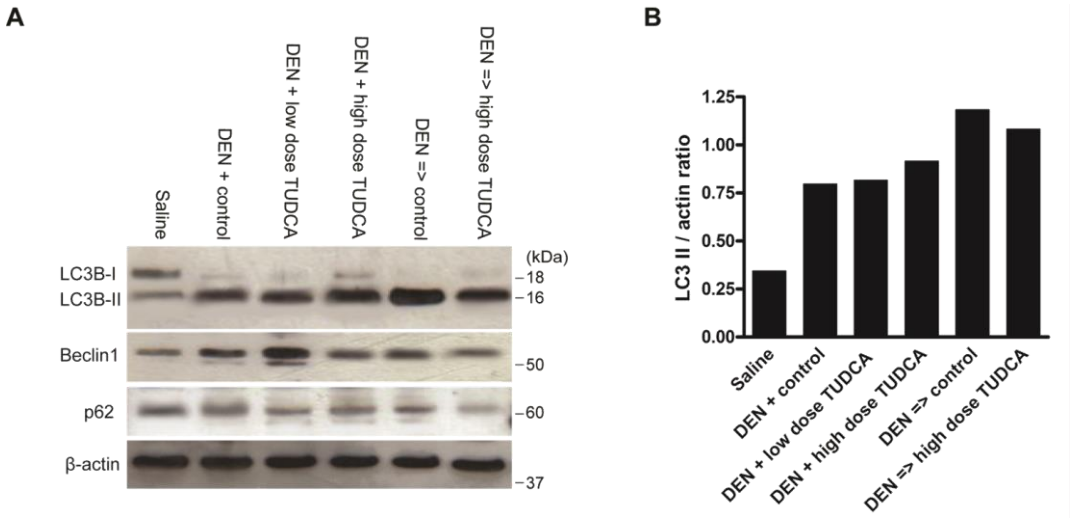

Fig. S3. Effect of TUDCA on DEN-induced autophagy. (A) The expression level of autophagy-associated proteins in the livers was analyzed by western blotting, β-actin: loading control. (B) Densitometric analysis of LC3 II/actin ratio.

1.2.10. **Tables**

Table 1: Mouse body weight (g) (mean ± SD)

Group	Average body weight 25 weeks (g)	Average body weight 30 weeks (g)	Survival (%)
Preventive study			
Saline	31.22 ± 1.39		100
DEN + control	26.75 ± 1.96***		75
DEN + low dose TUDCA	27.39 ± 1.45[#]		83
DEN + high dose TUDCA	24.64 ± 2.17[#]		67
Therapeutic study			
DEN => control	25.96 ± 3.65	22.92 ± 3.19	67
DEN => low dose TUDCA	23.86 ± 2.70	22.13 ± 2.57[¥]	75
DEN => high dose TUDCA	24.53 ± 2.13	23.43 ± 2.61[¥]	67

***p<0.001: 25 weeks DEN vs. saline. [#]not significant compared to DEN + control. [¥]not significant compared to DEN => control. DEN, diethylnitrosamine.

2. Sorafenib and the unfolded protein response in hepatocellular carcinoma

2.1. Antitumor efficacy of sorafenib is potentiated by modulation of the interplay between the unfolded protein response and autophagy in hepatocellular carcinoma

Manuscript in preparation, patent application filed

Yves-Paul Vandewynckel[1], Ine Desaegher[1], Debby Laukens[1], Lindsey Devisscher[1], Eliene Bogaerts[1], Annelies Paridaens[1], Sarah Raevens[1], Anja Van den Bussche[1], Xavier Verhelst[1], Christophe Van Steenkiste[1], Benedicte Descamps[2], Chris Vanhove[2,3], Louis Libbrecht[4], Anja Geerts[1], Bart N. Lambrecht[3,5,6], Sophie Janssens[3,5,6], Hans Van Vlierberghe[1]

[1]Department of Hepatology and Gastroenterology, Ghent University, Belgium
[2]Infinity Imaging Lab, Ghent University, Belgium
[3]GROUP-ID Consortium, Ghent University and University Hospital, Belgium
[4]Department of Pathology, Ghent University Hospital, Belgium
[5]Unit Immunoregulation and Mucosal Immunology, VIB Inflammation Research Centre, Belgium
[6]Department of Respiratory Medicine, Ghent University, Belgium

2.1.1. **Patent application: P2014-060**

Abstract of the patent

The present invention relates to compositions which can be used for the treatment of hepatocellular carcinoma. More in particular, the present invention discloses that the addition of both an endoplasmic reticulum stress inducer and an inhibitor of autophagy significantly improve the antitumoral efficacy of the kinase inhibitor sorafenib in a synergistic manner. Hence, the present invention relates to compositions comprising the kinase inhibitor sorafenib, an endoplasmic reticulum stress inducer -such as nelfinavir- and an inhibitor of autophagy -such as clarithromycin-. The present invention also discloses the combination of an endoplasmic reticulum stress inducer and an inhibitor of autophagy –without sorafenib- for the treatment of hepatocellular carcinoma.

Claims of the patent

1. A composition comprising the kinase inhibitor sorafenib, an endoplasmic reticulum stress inducer and an inhibitor of autophagy.
2. A composition according to claim 1 for use as a medicament.
3. A composition according to claim 1-2 for use to treat hepatocellular carcinoma.
4. A composition comprising an endoplasmic reticulum stress inducer and an inhibitor of autophagy for use to treat hepatocellular carcinoma.
5. A composition according to claims 3-4 wherein said hepatocellular carcinoma is advanced hepatocellular carcinoma.
6. A composition according to claims 1-5 wherein said endoplasmic reticulum stress inducer is a) the HIV protease inhibitor nelfinavir, saquinavir, fosamprenavir, atazanavir, darunavir, tipranavir, indinavir or liponavir, or b) the proteasome inhibitor bortezomib, carfilzomib or oprozomib, or c) quercetin, or any combination of said endoplasmic reticulum stress inducers.
7. A composition according to claims 1-6 wherein said inhibitor of autophagy is a) the neomacrolide clarithromycin, azithromycin or roxithromycin, or b) chloroquine or hydroxychloroquine, or, any combination of said inhibitors of autophagy.
8. A composition according to claims 1-2 and 4-7 comprising the kinase inhibitor sorafenib, the endoplasmic reticulum stress inducer nelfinavir and the inhibitor of autophagy clarithromycin.
9. A composition according to claims 1- and 4-7 comprising the kinase inhibitor sorafenib, the endoplasmic reticulum stress inducer nelfinavir and the inhibitor of autophagy chloroquine.

10. A composition according to claims 1-7 wherein said endoplasmic reticulum stress inducer is nelfinavir and wherein said inhibitor of autophagy is clarithromycin.
11. A pharmaceutical composition comprising a composition according to claims 1-10.
12. A process to treat hepatocellular carcinoma comprising administering a therapeutically effective amount of a pharmaceutical composition according to claim 11 to a person in need thereof.
13. A composition comprising the inhibitor of autophagy clarithromycin and the endoplasmic reticulum stress inducer nelfinavir for use to treat hepatocellular carcinoma wherein said nelfinavir is given at a dose of maximally 89,3 mg/kg.

Full patent application is provided in the Supplemental information.

Antitumor efficacy of sorafenib is potentiated by modulation of the interplay between the unfolded protein response and autophagy in hepatocellular carcinoma

2.1.2. Abstract

Hepatocellular carcinoma (HCC) is the second leading cause of cancer-related mortality and is resistant to cytotoxic and targeted therapies. Although sorafenib, a multi-kinase inhibitor, is the standard therapy, the antitumor effect is limited and average survival benefit is less than 3 months. Given the emerging importance of the unfolded protein response (UPR) and autophagy in HCC, we questioned whether the use of rationally designed combinations of sorafenib with clinically applicable modulators of the UPR and autophagy would be more effective than current sorafenib monotherapy. The UPR and autophagy and their relevance in cell viability and proliferation *in vitro* and in orthotopic and xenograft mouse models were assessed. Sorafenib activated the UPR and autophagy in HCC cells. Importantly, sorafenib induced inositol-requiring enzyme 1 (IRE1) RNase-mediated mRNA cleavage, a pro-apoptotic process called regulated IRE1-dependent decay. Moreover, sorafenib-mediated reduction in tumor cell proliferation was dependent on proteotoxicity and IRE1 RNase activity. Also autophagy induction by sorafenib was in part mediated by IRE1 activation. Targeting of the UPR or autophagy separately did not synergistically enhance the antitumor efficacy of sorafenib. However, combination with an UPR inducer and an inhibitor of adaptive protein refolding or autophagy potentiated the efficacy synergistically *in vitro* and in the used mouse models without significant toxicity.

Conclusion: Clinically applicable triple therapies of sorafenib with modulators of the UPR and autophagy seem to suppress intrinsic sorafenib resistance and open new avenues for a multi-target approach that may produce durable responses against HCC.

2.1.3. List of abbreviations

HCC, hepatocellular carcinoma; ER, endoplasmic reticulum; GRP78, glucose-regulated protein, 78 kDa; PDI, protein disulfide isomerases; ERAD, ER-associated protein degradation; UPR, unfolded protein response; PERK, PKR-like endoplasmic reticulum kinase; IRE1, inositol-requiring enzyme 1; ATF6, activating transcription factor 6; eIF2α, eukaryotic initiation factor 2α; ATF4, activating transcription factor 4; CHOP, CCAAT/enhancer-binding homologous protein; XBP1u, unspliced X-box-binding protein 1; XBP1s, spliced X-box-binding protein 1; RIDD, regulated IRE1-dependent decay; IP, intraperitoneal; IG, intragastric; ERDJ4, endoplasmic reticulum DnaJ homolog 4; DEN, diethylnitrosamine; GADD34, growth arrest and DNA damage inducible 34; HERPUD1, homocysteine-inducible, endoplasmic reticulum stress-inducible, ubiquitin-like domain member 1.

2.1.4. Introduction

Hepatocellular carcinoma (HCC) represents a major health problem that causes over 700,000 deaths annually worldwide [1]. Conventional chemotherapy is ineffective and targeted therapy for advanced HCC with sorafenib provides a limited and variable survival benefit [2]. Sorafenib was identified as a multi-kinase inhibitor, targeting Raf (serine/threonine-specific protein kinase), Fms-like tyrosine kinase 3,4 c-Kit, p38, stem cell growth factor receptor 1, vascular endothelial growth factor receptors, and platelet-derived growth factor receptor-β to induce growth arrest in a variety of tumors, including HCC [3]. Resistance may be either pre-existent (intrinsic resistance), or drug-induced (acquired resistance). So far, no clinical strategy has been found to overcome sorafenib resistance. Long-term exposure to sorafenib of HCC cells induces acquired resistance with epithelial-to-mesenchymal transition. The sensitivity for sorafenib after resistance development can partially be restored by inhibition of phosphatidylinositol 3-kinase/Akt, BCRP/ABCG2 or NF-κB-upregulated CD47 [4]–[6]. In addition, Rudalska et al. (2014) identified by *in vivo* shRNA screening the p38/ATF2 pathway as a potential mechanism of acquired sorafenib resistance in HCC [7]. However, the molecular mechanisms by which sorafenib exerts its effect or how intrinsic resistance to sorafenib is facilitated remain unclear [2].

Certain chemotherapeutic drugs provoke apoptosis through the mitochondrial pathway, whereas others, most notably the proteasome inhibitors, induce cell death via endoplasmic reticulum (ER) stress. The ER consists of a membranous network in which proteins are synthesized, post-translationally modified and folded.

Therefore, the ER lumen houses a large array of chaperones, including glucose-regulated protein-78 (GRP78) and protein disulfide isomerase A4 (PDIA4) and contains quality-control systems that extract terminally misfolded proteins for degradation, a process known as ER-associated protein degradation (ERAD) [8].

Disturbances in ER homeostasis activate the unfolded protein response (UPR), which initially compensates for damage, but will activate apoptosis during intense or persistent ER stress [9]. Three major ER stress transducers have been identified: PKR-like ER kinase (PERK), inositol-requiring enzyme 1 (IRE1) and activating transcription factor 6 (ATF6) [8]. Following release of GRP78, PERK phosphorylates eukaryotic initiation factor 2α (eIF2α) leading to attenuation of global translation. Accompanying this translational control, phosphorylated eIF2α selectively enhances translation of activating transcription factor 4 (ATF4), a transcriptional activator of genes involved in protein quality control, amino acid biosynthesis as well as induction of apoptosis such as CCAAT/enhancer-binding homologous protein (*CHOP*) [8]. Upon ER stress, ATF6 is mobilized to the Golgi where it is cleaved, which releases the transcriptionally active fragment and induces chaperones such as PDIA4, unspliced X-box-binding protein-1 (XBP1u) and ERAD components such as homocysteine-inducible, ER stress-inducible, ubiquitin-like domain member 1 (HERPUD1) [10]. Activation of IRE1 results in splicing of *XBP1u* mRNA to generate a more active spliced XBP1 (*XBP1s*), which induces genes involved in protein folding such as *ERDJ4* [10], [11]. Next to *XBP1* mRNA, also other mRNAs can be cleaved by IRE1, a process known as regulated IRE1-dependent decay (RIDD) [8], [12]. The effect of sorafenib on the UPR in HCC is controversial; both UPR inhibition [13] as activation [14]–[16] have been reported.

Besides canonical UPR activation, sustained ER stress can elicit autophagy, which allows cells to sequester cytoplasmic material by forming double-membrane vesicles and to target the material for degradation [17]. Interestingly, sorafenib was previously shown to generate cytoprotective autophagy in different types of tumor cells including HCC [16], [18].

We further investigated the effect of rationally designed combinations of clinically applicable UPR- and autophagy-modulating agents and human equivalent dose of sorafenib on HCC *in vitro* and validated these results in an orthotopic and xenograft mouse model. Our data indicate that the effect of sorafenib is in part mediated by proteotoxic stress, which activates compensatory mechanisms, such as adaptive protein refolding and autophagy. Inhibition of these survival mechanisms under amplified ER stress synergistically enhanced the antitumor efficacy.

2.1.5. **Materials and Methods**

Cell culture

Human HepG2 cells (HB-8065; ATCC, Virginia, USA) were cultured with Dulbecco's Modified Eagle's medium supplemented with 10% fetal bovine serum (Life Technologies, Ghent, Belgium). Cells were incubated for 24 hours with sorafenib (5-20 μM; Bay43-9006, Nexavar®), tunicamycin (1 μg/ml), thapsigargin (50 ng/ml), PERK inhibitor (0.5 μM; GSK2656157, Chengdu novi biotechnology, Shandong, China), IRE1 RNase inhibitor (8 μM; 4μ8C, Calbiochem, Massachusetts, USA), quercetin (25-100 μM), bacitracin (3 mM), nelfinavir (10 μM), chloroquine (10 μM), clarithromycin (50 μg/ml), bortezomib (50 nM; Santa Cruz, Heidelberg, Germany), tauroursodeoxycholic acid (1 mM), cycloheximide (5 μM) or MEK inhibitor PD98059 (30 minutes; 10 μM; Cell signaling) or equal volumes of solvent as control. All reagents were obtained from Sigma (Diegem, Belgium) unless stated otherwise. Each experiment was performed in quadruplicate.

Animals

Wild-type 129S2/SvPasCrl mice and athymic nude mice were purchased respectively from Charles River (L'Arbresle Cedex, France) and Harlan (Horst, The Netherlands) and maintained as previously described [19]. All protocols were approved by the Ethical Committee of experimental animals at the Faculty of Health Sciences, Ghent University, Belgium (ECD 11/52 and 13/39).

Orthotopic model. Five-week-old males received weekly intraperitoneal (IP) saline or diethylnitrosamine (DEN) (35 mg/kg, in saline). After 25 weeks, saline-treated mice were randomly divided into 2 groups: control (intragastric (IG) 100 μl of vehicle once daily) or sorafenib (IG 30 mg/kg once daily, as indicated by human equivalent plasma levels [20]); and DEN-treated into 5 groups (each n=12): control, sorafenib, sorafenib + clarithromycin (IG 50 mg/kg bid), sorafenib + nelfinavir (IP 50 mg/kg bid), sorafenib + nelfinavir + clarithromycin (idem) and nelfinavir (IP 250 mg/kg bid) + clarithromycin (idem). After 30 weeks, blood was collected from the retro-orbital sinus under isoflurane anaesthesia, and the mice were euthanized. All organs were fixed in 4% phosphate-buffered formaldehyde (Klinipath) and embedded in paraffin or snap frozen in liquid nitrogen. Hematoxylin/eosin and reticulin staining were performed and the results were blindly evaluated by two independent observers. Mean intercapillary distance was measured on CD105-stained slides as previously described [19].

Xenograft model. HepG2 cells ($6x10^6$) were mixed with 40% Matrigel (BD Biosciences, Bedford, MA, USA). The cell preparation was injected subcutaneously into the right flank of 8-week-old male athymic nude mice housed in filter-topped cages. Tumor dimensions were recorded three times per week with a digital caliper starting with the first day of treatment. Tumor volumes were calculated using the following formula: volume (mm^3)= $ab^2/2$, where b was the smaller dimension. When mean tumor volume reached 150 mm^3, animals were randomized into eight groups (n=6): sorafenib (IG 30 mg/kg once daily), sorafenib + clarithromycin (IG 50 mg/kg bid), sorafenib + nelfinavir (IP 50 mg/kg bid), sorafenib + nelfinavir + clarithromycin (idem), nelfinavir (IP 50 mg/kg bid) + clarithromycin (idem), nelfinavir (IP 250 mg/kg bid) + clarithromycin (idem), nelfinavir (IP 250 mg/kg bid) and control group. Final tumor weights were recorded at the time of sacrification.

Detailed information of total RNA extraction, quantitative real-time PCR, Western blotting, immunohistochemistry, MTT, bromodeoxyuridine (BrdU) incorporation and caspase-3 activity assays and positron emission tomography is provided in the Supplementary Materials and Methods.

Statistics

Statistical analyses were performed using SPSS 21 (SPSS, Chicago, USA). Data are presented as the mean ± SD or percentage relative to expression in controls. Variables were tested for normality using the Shapiro-Wilk test. Normally distributed data were subjected to the unpaired student's t-tests. Data involving more than two groups were assessed by one-way analysis of variance (ANOVA) with Bonferroni's post-hoc test. Non-normally distributed data were tested using the Mann-Whitney-U test. The chi-squared test was used to compare mortality. Continuous data (xenograft tumor volume changes) were evaluated using linear mixed models. CompuSyn program (ComboSyn, NJ, USA) was used to compute a combination index for drug combinations studied with cell proliferation assays. Reported p-values were two-sided and considered significant when less than 0.05.

2.1.6. **Results**

Sorafenib activates the IRE1/XBP1/RIDD and PERK/eIF2α/ATF4/GADD34 pathways in vitro

The effect of sorafenib on the UPR was assessed in HepG2 cells at concentrations achieved in clinical practice (between 1 and 10 μM [21], [22]). Sorafenib dose dependently increased the mRNA levels of chaperones GRP78 (5 μM: $p<0.05$; 10 μM: $p<0.001$) and PDIA4 (from 5 μM: $p<0.001$) compared to control (Fig. 1A). GRP78 protein levels were decreased by sorafenib, which is consistent with observations in sorafenib-treated human leukemia cells [14]. In contrast, sorafenib increased PDIA4 protein levels (Fig. 1A-B). In addition, sorafenib increased the mRNA levels of HERPUD1 (10 μM: $p<0.01$; Fig. 1A).

Expression of total IRE1 mRNA ($p<0.001$, Fig. 1A) and protein (Fig. 1B) was markedly increased by sorafenib. Through the use of Phos-tag (a reagent that selectively binds to phosphorylated amino acids), we readily detected the active phosphorylated form of IRE1 in sorafenib-treated cells (Fig. 1B) [23]. Accordingly, the IRE1-mediated splicing of XBP1 and expression of a target of XBP1s, ERDJ4 [10], were increased by sorafenib ($p<0.001$, Fig. 1A). 5 μM sorafenib decreased XBP1u mRNA levels ($p<0.05$). However, 10 μM sorafenib increased XBP1u mRNA ($p<0.001$; Fig. 1A). The IRE1 inhibitor attenuated induction of XBP1s and ERDJ4 mRNA and restored XBP1u levels ($p<0.001$; Fig. 1A). Surprisingly, the IRE1 inhibitor increased IRE1 mRNA ($p<0.001$), suggesting negative regulation of the sorafenib-induced IRE1 mRNA expression by the IRE1 RNase, possibly by RIDD [12].

Interestingly, liver-expressed transcripts which are known targets of RIDD were all downregulated by sorafenib (Fig. 1D) [24]. Addition of the IRE1 inhibitor abolished the sorafenib-mediated downregulation of the tested RIDD targets. These results confirm that sorafenib induced IRE1-mediated RIDD. Importantly, sorafenib-induced RIDD downregulated Glypican-3 (GPC3), which encodes a cell-surface heparan-sulfate proteoglycan expressed in HCC [25]. Chemical ER stress inducers, thapsigargin and tunicamycin [8], downregulated all tested RIDD targets, with exception of CYP2E1, which was upregulated by tunicamycin, although thapsigargin downregulated this transcript (Fig. 1D).

Next, we examined whether sorafenib also activates the PERK pathway. Sorafenib promoted phosphorylation of eIF2α and expression of PERK targets ATF4, CHOP and growth arrest and DNA damage inducible 34 (GADD34) (mRNA: Fig. 1A; protein: Fig. 1B). The PERK inhibitor decreased sorafenib-induced phosphorylation of eIF2α and expression of ATF4 and GADD34 (Fig. 1B). However, addition of the PERK inhibitor to sorafenib further upregulated GRP78, PDIA4 and HERPUD1 transcripts (Fig. 1A), which are primary regulated by ATF6 [10], suggesting enhanced cytoprotective ATF6 signaling upon pharmacological blockade of the PERK pathway. Interestingly, IRE1 inhibition modestly decreased sorafenib-induced expression of CHOP (Fig. 1B).

Since sorafenib is developed as an inhibitor of the RAF/MEK/ERK pathway, we examined the effect of the MEK inhibitor PD98059 on the UPR. Next to a slight decline in GRP78, PD98059 was unable to alter the expression of the UPR-mediated proteins (Fig. 1B), suggesting sorafenib induces ER stress in HCC cells independent of MEK inhibition.

Since sorafenib induces ER stress, we questioned whether pre-existent ER stress, as present in human HCC *in vivo* [26], modulates the effect of sorafenib on the UPR. Therefore, we examined the effect of sorafenib on the UPR in the presence of tunicamycin in HepG2 cells (Fig. 1C). Despite the presence of tunicamycin-induced ER stress, sorafenib was able to further enhance the expression of GRP78 ($p<0.001$), XBP1s ($p<0.05$), ERDJ4 ($p<0.001$), CHOP ($p<0.05$) and GADD34 ($p<0.001$) mRNA. At the protein level, addition of sorafenib to tunicamycin potentiated the PERK-mediated phosphorylation of eIF2α and expression of GADD34 and CHOP.

Sorafenib-mediated reduction in tumor cell proliferation is dependent on proteotoxic stress and IRE1 RNase activity

Sorafenib at 5-20 μM dose dependently reduced HepG2 cell viability and proliferation and triggered caspase-3 activation (Fig. S1A-C). Although tunicamycin alone did not affect cell viability, we observed slight enhancement of the sorafenib-mediated reduction in proliferation and induction of caspase-3 by addition of tunicamycin ($p<0.05$, Fig. S1A-C). In the next experiments, sorafenib was applied at 10 μM, since this was the lowest concentration significantly reducing cell viability in the range of the human intratumor concentration.

To demonstrate that proteotoxic stress caused by sorafenib originates during the synthesis of new proteins, cycloheximide (CX) was used to block protein synthesis. In addition, chemical chaperone tauroursodeoxycholic acid (TUDCA) was applied to reduce the load of misfolded proteins. Cell viability was reduced by CX and increased by TUDCA, confirming their effect on metabolic activity ($p<0.01$; Fig. 2A). Interestingly, CX increased the proliferation and TUDCA reduced the caspase-3 activity of sorafenib-challenged cells ($p<0.01$; Fig. 2B-C).
Next, we assessed the effect of inhibition of the sorafenib-activated IRE1 or PERK pathway on cell viability. The IRE1 inhibitor counteracted sorafenib-mediated suppression of viability ($p<0.05$, Fig. 2A), proliferation ($p<0.01$, Fig. 2B) and induction of caspase-3 activity ($p<0.001$, Fig. 2C), possibly by downregulating CHOP and inhibition of pro-apoptotic RIDD (Fig. 1). Inhibition of IRE1-activated JNK [8] by SP600125 did not alter the effect of sorafenib (data not shown). The PERK inhibitor did not alter sorafenib-induced cell death (Fig. 2A-C). Thus, these data demonstrate that IRE1 is partly responsible for the cytotoxicity of sorafenib, likely through induction of CHOP and RIDD.

Sorafenib induces autophagy in part via induction of IRE1

Sorafenib at 10 μM induced autophagy-related genes ATG5, ATG7 and BECLIN1 (Fig. S3A), LC3 conversion and P62 degradation (Fig. S3B) in HepG2 cells. Addition of the IRE1 inhibitor attenuated the induction of ATG5 and -7 ($p<0.01$) and LC3 conversion in sorafenib-challenged cells. The PERK inhibitor did not affect sorafenib-induced LC3 II (Fig. S3B). Chloroquine inhibits autophagy by increasing lysosomal pH [17]. Sorafenib-induced conversion of LC3 and P62 degradation in HepG2 cells was inhibited by chloroquine (Fig. S3B), suggesting sorafenib promotes autophagic flux. Additionally, we confirmed that neomacrolide antibiotic clarithromycin [27] was able to inhibit sorafenib-induced autophagic flux (Fig. S3B).
Further, we evaluated the effect of sorafenib in combination with autophagy inhibition. Surprisingly, chloroquine was unable to potentiate the effect of sorafenib (Fig. 3A-C). Addition of clarithromycin to sorafenib further reduced the proliferation rate ($p<0.01$; Fig. 3B) and enhanced the caspase-3 activity ($p<0.01$; Fig. 3C) compared to sorafenib alone. Again, this rather seems to be an additive effect because clarithromycin monotherapy was able to induce both effects compared to control (Table S1). Thus, combination of sorafenib with autophagy inhibitors did not induce synergistic effects to HCC cells.

Autophagy inhibition together with IRE1 hyperactivation enhanced the efficacy of sorafenib

Because the activation of the IRE1 pathway was critical for the sorafenib-induced antiproliferative effect, we questioned whether IRE1 hyperactivity could enhance its efficacy. Therefore, we used the clinically applicable flavonoid quercetin which is known to directly bind and activate IRE1 [28]. Indeed, in HepG2 cells, quercetin dose dependently downregulated the RIDD targets (Fig. 1D) and induced XBP1 splicing without affecting ATF6 targets such as HERPUD1 (Fig. S2A). Surprisingly, quercetin decreased sorafenib-induced CHOP expression (Fig. S2A and 1B) and caspase-3 activity ($p<0.001$; Fig. S2B-D).

In order to find a clinically applicable efficacy-enhancing combination with sorafenib, we evaluated the combination of sorafenib with general ER stress inducers. Therefore, we selected the proteasome inhibitor bortezomib [8], [29] and the HIV protease inhibitor nelfinavir [30]. Surprisingly, combination of sorafenib with bortezomib did not show additive effects, although both demonstrated in monotherapy significant antitumor effects ($p<0.001$; Fig. 3A-C). Addition of nelfinavir at a noncytotoxic but ER stress-inducing concentration of 10 μM (data not shown) to sorafenib reduced the proliferation rate ($p<0.05$; Fig. 3B) and increased the caspase-3 activity ($p<0.001$; Fig. 3C) compared to sorafenib alone, however, this did not represent a synergistic effect (Table S1).

Since intensification of ER stress was insufficient to increase the efficacy of sorafenib, we questioned whether the observed induction of resistance mechanisms, such as autophagy and adaptive protein refolding by upregulating chaperones, such as PDIA4, which help in relieving ER stress, enables tumor cell survival under ER stress. To modulate protein refolding, we applied bacitracin, which is known to affect PDI activity [31]. Although the efficacy of sorafenib was unaltered by addition of bacitracin, the efficacy of sorafenib/bortezomib was enhanced by triple therapy with bacitracin (Fig. 3A-C), indicating that adaptive protein refolding is an essential response to proteotoxic stress induced by sorafenib/bortezomib. Similar results on cell viability were obtained by triple therapy with sorafenib/nelfinavir and bacitracin compared to sorafenib/nelfinavir ($p<0.05$; Fig. 3A).

The efficacy of sorafenib with autophagy inhibition was synergistically enhanced by addition of ER stress inducers nelfinavir or bortezomib ($p<0.001$; Fig. 3A-C and Table S1), confirming the need for a triple therapy approach tackling cellular adaptation. In contrast to the autophagy inhibitors, addition of bacitracin to sorafenib/nelfinavir was unable to change the antitumor effect, suggesting autophagy is a more important survival mechanism instigated by sorafenib/nelfinavir than adaptive refolding. In addition, triple therapy with sorafenib, quercetin, and autophagy inhibition synergistically decreased tumor cell proliferation ($p<0.001$; Fig. S2E and Table S1), suggesting a pivotal role for IRE1 in this strategy.

In addition, testing of this combination in HepG2 cells with acquired sorafenib resistance obtained by slowly increasing sorafenib concentrations, as described in [4], is ongoing. Interestingly, UPR-regulated CHOP mRNA was significantly upregulated in the sorafenib-resistant compared to sorafenib-sensitive HepG2 cells ($p<0.001$).

The antitumor efficacy of sorafenib is potentiated by combination with nelfinavir and clarithromycin in mouse models of HCC

Since triple therapy with sorafenib, nelfinavir and clarithromycin demonstrated the strongest synergistic effects *in vitro* (combination index: 0.63, Table S1), we tested this triple therapy in an orthotopic and a xenograft mouse model.

In saline-treated and DEN-treated mice, sorafenib administration did not alter body weight or mortality (Table S2). In the DEN-treated mice, sorafenib reduced the hepatic tumor burden ($p<0.01$, Fig. 4A-B and S4A-B). Addition of nelfinavir, and not clarithromycin, to sorafenib, augmented the sorafenib-mediated antitumor effect ($p<0.01$). Moreover, triple therapy with sorafenib/nelfinavir/clarithromycin synergistically reduced tumor burden ($p<0.001$) and showed a tendency to reduce mortality ($p=0.17$, Table S2). Visualization of the cellular membrane biosynthesis by ^{18}F-choline positron emission tomography demonstrated a decreased number of loci with high mean standardized uptake values after triple therapy compared to vehicle-treated mice (Fig. S4D).

Hematoxylin/eosin staining demonstrated intense cytoplasmic vacuolization, which is related to ER stress [32], by sorafenib and, even more, by triple therapy (Fig. S4A). Sorafenib decreased tumor angiogenesis ($p<0.05$), however, addition of nelfinavir or clarithromycin did not alter vessel density (data not shown). Triple therapy increased caspase-3 activity, measured in lysates of HCC-bearing livers compared to vehicle-treated mice ($p<0.05$; Fig. S4C).

Analysis of HepG2 xenograft tumors from the control- and sorafenib-treated mice showed that 30 mg/kg/day sorafenib did not significantly reduce HCC growth *in vivo* (Fig. 4C-D). However, triple therapy demonstrated strong antitumor efficacy ($p<0.001$, Fig. 4C-D). Taken together, tackling the interplay between sorafenib-induced adaptation mechanisms strikingly suppressed HCC growth (Fig. 4E).

Finally, we tested the possibility to omit sorafenib, which can induce serious adverse events in clinical use [3], from the triple therapy of sorafenib, nelfinavir and clarithromycin. At the dose of 50 mg/kg bid of nelfinavir, omitting sorafenib dramatically reduced the antitumor effect in the HepG2 xenograft model, however, increasing the dose of nelfinavir to 250 mg/kg bid resulted in a comparable antitumor action compared to the triple therapy, while 250 mg/kg bid nelfinavir without clarithromycin did not suppress tumor growth (Fig. 4C-D). Based on these results, we evaluated the combination of 250 mg/kg bid nelfinavir and clarithromycin in the orthotopic model. Importantly, this combination was superior in inhibiting tumor progression compared to treatment with sorafenib monotherapy ($p<0.001$).

These data indicate that the threshold for ER stress-induced cell death during autophagy inhibition in HCC cells is elevated by omission of sorafenib from the triple therapy, which can be overcome by increasing the dose of nelfinavir.

2.1.7. **Discussion**

While sorafenib heralded a major breakthrough in HCC therapy, the clinical benefit is at best modest and transient [3]. HCC is a complex disease which needs multi-targeting approaches for effective therapy. ER stress and autophagy are two basic cell survival mechanisms often occurring in concert. In this study, we assessed the effect of sorafenib on the UPR and autophagy and on HCC growth in combination with modulation of these cellular adaptation processes.

Sorafenib activates the IRE1/XBP1/RIDD and PERK/eIF2α/ATF4/GADD34 pathways, but reduced GRP78 protein expression. Since IRE1 knockdown increased induction of apoptosis by 20 μM sorafenib in MHCC97-L and PLC/PRF/5 HCC cells [16], we hypothesized that IRE1 inhibition could boost the effect of sorafenib. Surprisingly, a small molecule inhibitor binding the IRE1 RNase domain [33] attenuated the antiproliferative effect of sorafenib in HepG2 cells. In this experiments, IRE1 is still present, upregulated and able to mediate the well-known protein-protein interactions, such as the IRE1-TRAF2 interaction [8]. Another difference is the concentration used, we applied 1-10 μM sorafenib, which is in the range of mean intratumor concentration of 8 μM in case of the recommended oral dose of 400 mg bid [21], [22]. For example, XBP1u mRNA levels decreased from 1 to 5 μM sorafenib, probably by depletion via IRE1-mediated splicing. However, 10 μM sorafenib increased XBP1u mRNA, which might suggest that XBP1s-mediated induction of XBP1u mRNA overruled the IRE1 splicing capacity [9]. Next to the known cytoprotective effects of IRE1 signaling [8], sustained XBP1 splicing is able to induce CHOP expression, cell dysfunction and apoptosis [9], [34]. In addition, the IRE1 RNase performs RIDD on specific target transcripts, a pro-apoptotic process activated by sorafenib [24].

Inhibition of protein synthesis increased cell survival of sorafenib-treated cells, while tunicamycin slightly increased the antiproliferative effect of sorafenib, suggesting ER stress plays a significant role in the effect of sorafenib. Next, we selected two clinically applicable ER stress inducers: the proteasome inhibitor bortezomib and the HIV protease inhibitor nelfinavir. Interestingly, only nelfinavir induces an additive effect in combination with sorafenib in HCC. This effect was also observed in leukemia cells [35]. Because sorafenib was shown to induce apoptosis through induction of growth arrest and DNA damage 45β (GADD45β) and mitochondrial fragmentation [36], which both can be induced by ER stress [37], [38], it would be interesting to investigate whether sorafenib-induced mitochondrial fragmentation and GADD45β expression is dependent on UPR activation.

Sorafenib promotes adaptive autophagy in HCC cells, as shown previously [39]. To inhibit autophagy, we used antimalarial chloroquine and neomacrolide antibiotic clarithromycin [27]. However, combination of sorafenib with these autophagy inhibitors again induces only additive, but no synergistic, effects.

Since sorafenib activates the UPR and thereby induces adaptive protein refolding and autophagy, we evaluated whether triple therapies could improve the antitumor efficacy of sorafenib. Combination of sorafenib with an ER stress inducer and an inhibitor of the observed compensatory mechanisms, adaptive protein refolding or autophagy, synergistically potentiated the antitumor efficacy of sorafenib *in vitro.* Of these multiple combinations, we tested the combination with nelfinavir and clarithromycin in different HCC models, which showed the strongest antiproliferative effects *in vitro*. Nelfinavir and clarithromycin synergized with sorafenib to reduce tumor growth *in vivo* without toxicity.

The p38/ATF2 pathway was recently identified as a mechanism of sorafenib resistance in HCC [7]. Investigating the effect of the proposed triple therapy modulating the induced UPR/autophagy on this sorafenib-resistance pathway may uncover downstream interconnections. For example, oligomerized IRE1 binds TNF receptor-associated factor 2 (TRAF2), activating apoptosis signal-regulating kinase 1 (ASK1) and downstream kinases that activate p38 [8], [40]. Therefore, an altered IRE1 pathway activation pattern may modulate the p38/ATF2 pathway and thereby sorafenib resistance.

A recent phase I trial of the HIV protease inhibitor nelfinavir in adults with solid tumors showed an ER stress-inducing maximum tolerated dose of 6250 mg/day or, for a person of 70 kg, 89 mg/kg/day, which is 2.5 fold over the doses typically used in HIV patients [41]. This human dose correspond to a dose of 1094 mg/kg/day in mice [42], which highly exceeds the dose used in this study. The threshold for ER stress-induced cell death during autophagy inhibition in HCC cells is elevated by omission of sorafenib, however, this can be counterbalanced by increasing the dose of nelfinavir without increased toxicity given its high maximum tolerated dose. Further investigation needs to determine whether daily administration of this dual therapy is feasible and sufficient for sustained antitumor response, as evidenced for sorafenib [3].

Clarithromycin and nelfinavir are inhibitors of cytochrome P450 CYP3A4, which is involved in the metabolism of sorafenib [20], and could thereby increase the tissue concentration of sorafenib *in vivo*. However, combination of clarithromycin with another CYP3A4 substrate and multi-kinase inhibitor sunitinib showed no effect on the pharmacokinetics of sunitinib [43].

Combined therapy with multiple drugs is a common practice in cancer therapy and can achieve better therapeutic effects than a single drug. Furthermore, the utility of combining approved drugs by rational drug repositioning may be rapidly implemented in HCC patients. Therefore, clinical evaluation of the investigated combinations subverting ER stress towards apoptosis is indicated.

2.1.8. **References**

[1] International Agency for Research on Cancer, "GLOBOCAN 2012," *Estimated Incidence, Mortality and Prevalence Worldwide in 2012*, 2012. [Online]. Available: http://globocan.iarc.fr/Pages/fact_sheets_cancer.aspx.

[2] "EASL-EORTC clinical practice guidelines: management of hepatocellular carcinoma.," *J. Hepatol.*, vol. 56, no. 4, pp. 908–43, Apr. 2012.

[3] J. M. Llovet, S. Ricci, V. Mazzaferro, P. Hilgard, E. Gane, J.-F. Blanc *et al.*"Sorafenib in advanced hepatocellular carcinoma.," *N. Engl. J. Med.*, vol. 359, no. 4, pp. 378–90, Jul. 2008.

[4] H. van Malenstein, J. Dekervel, C. Verslype, E. Van Cutsem, P. Windmolders, F. Nevens, *et al.* "Long-term exposure to sorafenib of liver cancer cells induces resistance with epithelial-to-mesenchymal transition, increased invasion and risk of rebound growth.," *Cancer Lett.*, vol. 329, no. 1, pp. 74–83, Feb. 2013.

[5] B. Zhai, F. Hu, X. Jiang, J. Xu, D. Zhao, B. Liu *et al.* Inhibition of Akt reverses the acquired resistance to sorafenib by switching protective autophagy to autophagic cell death in hepatocellular carcinoma.," *Mol. Cancer Ther.*, vol. 13, no. 6, pp. 1589–98, Jun. 2014.

[6] W.-C. Huang, Y.-L. Hsieh, C.-M. Hung, P.-H. Chien, Y.-F. Chien, L.-C. Chen *et al.* BCRP/ABCG2 inhibition sensitizes hepatocellular carcinoma cells to sorafenib.," *PLoS One*, vol. 8, no. 12, p. e83627, Jan. 2013.

[7] R. Rudalska, D. Dauch, T. Longerich, K. McJunkin, T. Wuestefeld, T.-W. Kang, A. *et al.* In vivo RNAi screening identifies a mechanism of sorafenib resistance in liver cancer.," *Nat. Med.*, vol. 20, no. 10, pp. 1138–46, Sep. 2014.

[8] Y.-P. Vandewynckel, D. Laukens, A. Geerts, E. Bogaerts, A. Paridaens, X. Verhelst, *et al.* The paradox of the unfolded protein response in cancer.," *Anticancer Res.*, vol. 33, no. 11, pp. 4683–94, Nov. 2013.

[9] C. Hetz, "The unfolded protein response: controlling cell fate decisions under ER stress and beyond.," *Nat. Rev. Mol. Cell Biol.*, vol. 13, no. 2, pp. 89–102, Feb. 2012.

[10] M. D. Shoulders, L. M. Ryno, J. C. Genereux, J. J. Moresco, P. G. Tu, C. Wu, *et al.* Stress-Independent Activation of XBP1s and/or ATF6 Reveals Three Functionally Diverse ER Proteostasis Environments.," *Cell Rep.*, vol. 3, no. 4, pp. 1279–92, Apr. 2013.

[11] K. Zhang, S. Wang, J. Malhotra, J. R. Hassler, S. H. Back, G. Wang, *et al.* The unfolded protein response transducer IRE1α prevents ER stress-induced hepatic steatosis.," *EMBO J.*, vol. 30, no. 7, pp. 1357–75, Apr. 2011.

[12] W. Tirasophon, "The endoribonuclease activity of mammalian IRE1 autoregulates its mRNA and is required for the unfolded protein response," *Genes Dev.*, vol. 14, no. 21, pp. 2725–2736, Nov. 2000.

[13] Y. Honma and M. Harada, "A new therapeutic strategy for hepatocellular carcinoma by molecular targeting agents via inhibition of cellular stress defense mechanisms.," *J. UOEH*, vol. 36, no. 4, pp. 229–35, Dec. 2014.

[14] M. Rahmani, E. M. Davis, T. R. Crabtree, J. R. Habibi, T. K. Nguyen, P. Dent, and S. Grant, "The kinase inhibitor sorafenib induces cell death through a process involving induction of endoplasmic reticulum stress.," *Mol. Cell. Biol.*, vol. 27, no. 15, pp. 5499–513, Aug. 2007.

[15] P. Yi, A. Higa, S. Taouji, M. G. Bexiga, E. Marza, D. Arma *et al.* Sorafenib-mediated targeting of the AAA^+ ATPase p97/VCP leads to disruption of the secretory pathway, endoplasmic reticulum stress, and hepatocellular cancer cell death.," *Mol. Cancer Ther.*, vol. 11, no. 12, pp. 2610–20, Dec. 2012.

[16] Y.-H. Shi, Z.-B. Ding, J. Zhou, B. Hui *et al.*Targeting autophagy enhances sorafenib lethality for hepatocellular carcinoma via ER stress-related apoptosis.," *Autophagy*, vol. 7, no. 10, pp. 1159–72, Oct. 2011.

[17] J. Cui, Z. Gong, and H.-M. Shen, "The role of autophagy in liver cancer: molecular mechanisms and potential therapeutic targets.," *Biochim. Biophys. Acta*, vol. 1836, no. 1, pp. 15–26, Aug. 2013.

[18] Y. Zhang, D. Xue, X. Wang, M. Lu, B. Gao, and X. Qiao, "Screening of kinase inhibitors targeting BRAF for regulating autophagy based on kinase pathways.," *Mol. Med. Rep.*, vol. 9, no. 1, pp. 83–90, Jan. 2014.

[19] F. Heindryckx, K. Mertens, N. Charette, B. Vandeghinste, C. Casteleyn, C. Van Steenkiste *et al.* Kinetics of angiogenic changes in a new mouse model for hepatocellular carcinoma," *Mol. Cancer*, vol. 9, no. 1, p. 219, 2010.

[20] E. A. Kuczynski, C. R. Lee, S. Man, E. Chen, and R. S. Kerbel, "Effects of sorafenib dose on acquired reversible resistance and toxicity in hepatocellular carcinoma.," *Cancer Res.*, Apr. 2015.

[21] M. Labots, M. Neerincx, J. Van der Mijn, H. Dekker, R. Honeywell, M. Rovithi *et al.* Tumor, skin, and plasma concentrations of protein kinase inhibitors (PKIs) in patients with advanced cancer. | 2013 ASCO Annual Meeting | Abstracts | Meeting Library," *J Clin Oncol*, vol. 31, no. 35, p. suppl abstr 11087, 2013.

[22] D. Strumberg, H. Richly, R. A. Hilger, N. Schleucher, S. Korfee, M. Tewes *et al.* Phase I clinical and pharmacokinetic study of the Novel Raf kinase and vascular endothelial growth factor receptor inhibitor BAY 43-9006 in patients with advanced refractory solid tumors.," *J. Clin. Oncol.*, vol. 23, no. 5, pp. 965–72, Feb. 2005.

[23] F. Osorio, S. J. Tavernier, E. Hoffmann, Y. Saeys, L. Martens, J. Vetters *et al.* The unfolded-protein-response sensor IRE-1α regulates the function of CD8α+ dendritic cells.," *Nat. Immunol.*, vol. 15, no. 3, pp. 248–57, Mar. 2014.

[24] M. Maurel, E. Chevet, J. Tavernier, and S. Gerlo, "Getting RIDD of RNA: IRE1 in cell fate regulation.," *Trends Biochem. Sci.*, Mar. 2014.

[25] M. Suzuki, K. Sugimoto, J. Tanaka, M. Tameda, Y. Inagaki, S. Kusagawa *et al.* Up-regulation of glypican-3 in human hepatocellular carcinoma.," *Anticancer Res.*, vol. 30, no. 12, pp. 5055–61, Dec. 2010.

[26] M. Shuda, "Activation of the ATF6, XBP1 and grp78 genes in human hepatocellular carcinoma: a possible involvement of the ER stress pathway in hepatocarcinogenesis," *J. Hepatol.*, vol. 38, no. 5, pp. 605–614, May 2003.

[27] S. Moriya, X.-F. Che, S. Komatsu, A. Abe, T. Kawaguchi, A. Gotoh *et al.* Macrolide antibiotics block autophagy flux and sensitize to bortezomib via endoplasmic reticulum stress-mediated CHOP induction in myeloma cells.," *Int. J. Oncol.*, vol. 42, no. 5, pp. 1541–50, May 2013.

[28] R. L. Wiseman, Y. Zhang, K. P. K. Lee, H. P. Harding, C. M. Haynes, J. Price *et al.* Flavonol activation defines an unanticipated ligand-binding site in the kinase-RNase domain of IRE1.," *Mol. Cell*, vol. 38, no. 2, pp. 291–304, Apr. 2010.

[29] K. Vaeteewoottacharn, R. Kariya, K. Matsuda, M. Taura, C. Wongkham, S. Wongkham, and S. Okada, "Perturbation of proteasome function by bortezomib leading to ER stress-induced apoptotic cell death in cholangiocarcinoma.," *J. Cancer Res. Clin. Oncol.*, vol. 139, no. 9, pp. 1551–62, Sep. 2013.

[30] A. Brüning, "Analysis of nelfinavir-induced endoplasmic reticulum stress.," *Methods Enzymol.*, vol. 491, pp. 127–42, Jan. 2011.

[31] C. Muller, J. Bandemer, C. Vindis, C. Camaré, E. Mucher, F. Guéraud *et al.* Protein disulfide isomerase modification and inhibition contribute to ER stress and apoptosis

induced by oxidized low density lipoproteins.," *Antioxid. Redox Signal.*, vol. 18, no. 7, pp. 731–42, Mar. 2013.

[32] M. Fuest, K. Willim, S. MacNelly, N. Fellner, G. P. Resch, H. E. Blum, and P. Hasselblatt, "The transcription factor c-Jun protects against sustained hepatic endoplasmic reticulum stress thereby promoting hepatocyte survival.," *Hepatology*, vol. 55, no. 2, pp. 408–18, Feb. 2012.

[33] B. C. S. Cross, P. J. Bond, P. G. Sadowski, B. K. Jha, J. Zak, J. M. Goodman *et al.* The molecular basis for selective inhibition of unconventional mRNA splicing by an IRE1-binding small molecule.," *Proc. Natl. Acad. Sci. U. S. A.*, Feb. 2012.

[34] F. Allagnat, F. Christulia, F. Ortis, P. Pirot, S. Lortz, S. Lenzen *et al.* Sustained production of spliced X-box binding protein 1 (XBP1) induces pancreatic beta cell dysfunction and apoptosis.," *Diabetologia*, vol. 53, no. 6, pp. 1120–30, Jun. 2010.

[35] A. Brüning, M. Rahmeh, A. Gingelmaier *et al.* The mitochondria-independent cytotoxic effect of nelfinavir on leukemia cells can be enhanced by sorafenib-mediated mcl-1 downregulation and mitochondrial membrane destabilization.," *Mol. Cancer*, vol. 9, p. 19, Jan. 2010.

[36] D.-L. Ou, Y.-C. Shen, S.-L. Yu, K.-F. Chen, P.-Y. Yeh, H.-H. Fan *et al.* Induction of DNA damage-inducible gene GADD45beta contributes to sorafenib-induced apoptosis in hepatocellular carcinoma cells.," *Cancer Res.*, vol. 70, no. 22, pp. 9309–18, Nov. 2010.

[37] K. Hamamura, M. B. Goldring, and H. Yokota, "Involvement of p38 MAPK in regulation of MMP13 mRNA in chondrocytes in response to surviving stress to endoplasmic reticulum.," *Arch. Oral Biol.*, vol. 54, no. 3, pp. 279–86, Mar. 2009.

[38] X. Zhao, C. Tian, W. M. Puszyk, O. O. Ogunwobi, M. Cao, T. Wang *et al.* OPA1 downregulation is involved in sorafenib-induced apoptosis in hepatocellular carcinoma.," *Lab. Invest.*, vol. 93, no. 1, pp. 8–19, Jan. 2013.

[39] S. Shimizu, T. Takehara, H. Hikita, T. Kodama, H. Tsunematsu, T. Miyagi *et al.* Inhibition of autophagy potentiates the antitumor effect of the multikinase inhibitor sorafenib in hepatocellular carcinoma.," *Int. J. Cancer*, vol. 131, no. 3, pp. 548–57, Aug. 2012.

[40] D. Ron and P. Walter, "Signal integration in the endoplasmic reticulum unfolded protein response.," *Nat. Rev. Mol. Cell Biol.*, vol. 8, no. 7, pp. 519–29, Jul. 2007.

[41] G. M. Blumenthal, J. J. Gills, M. S. Ballas, W. B. Bernstein, T. Komiya, R. Dechowdhury *et al.* A phase I trial of the HIV protease inhibitor nelfinavir in adults with solid tumors.," *Oncotarget*, vol. 5, no. 18, pp. 8161–72, Sep. 2014.

[42] U.S. Department of Health and Human Services and Food and drug administration (FDA), "Guidance for Industry Estimating the Maximum Safe Starting Dose in Initial Clinical Trials for Therapeutics in Adult Healthy Volunteers.," 2005.

[43] E. Szałek, A. Karbownik, W. Połom, M. Matuszewski, K. Sobańska, H. Urjasz *et al.* Sunitinib in combination with clarithromycin or azithromycin - is there a risk of interaction or not?," *Pharmacol. Rep.*, vol. 64, no. 6, pp. 1554–9, Jan. 2012.

2.1.9. **Figures**

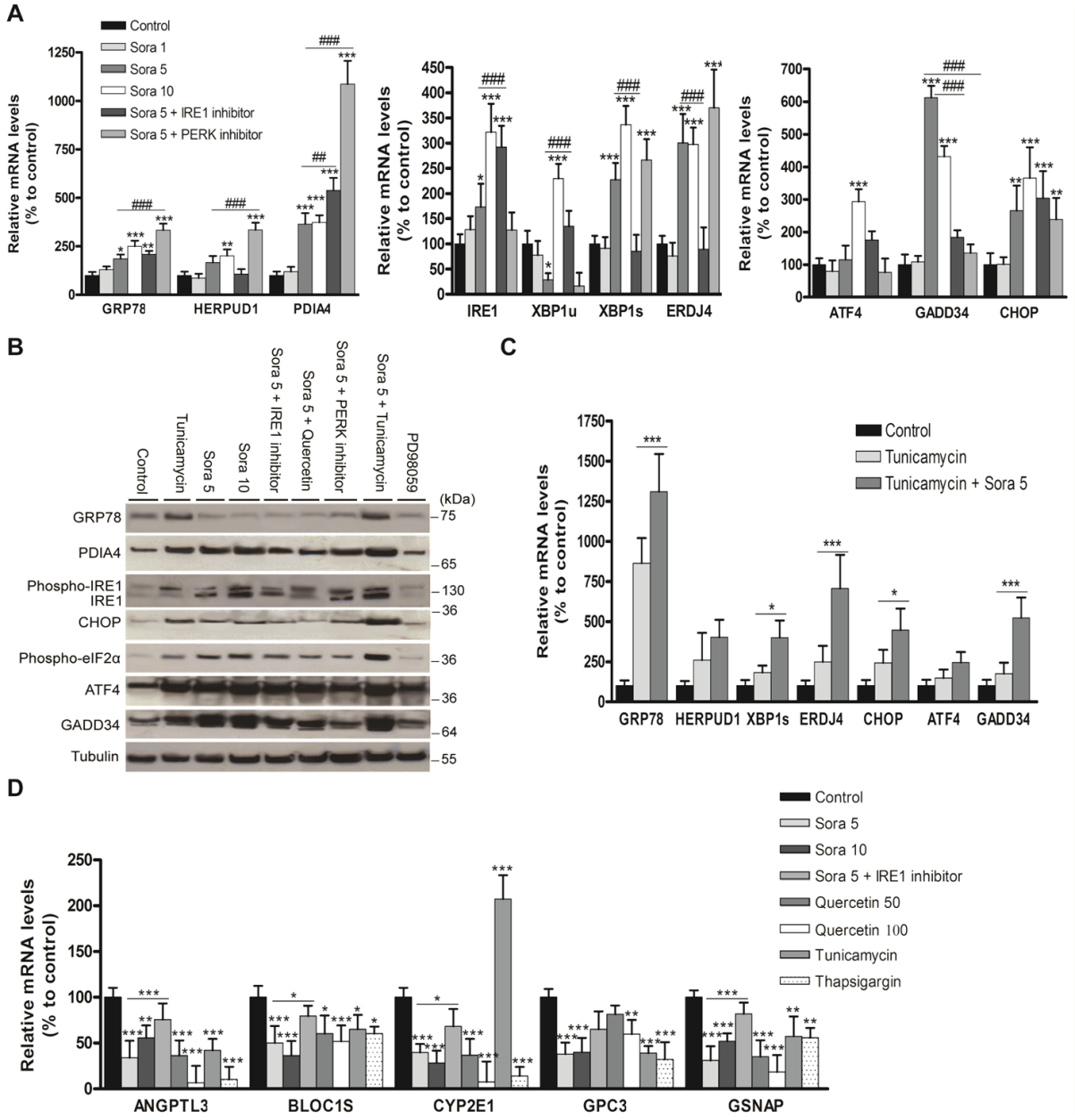

Fig. 1. Sorafenib activates the UPR in HepG2 cells irrespective of pre-existent ER stress. (A) Real-time PCR analysis of chaperones, IRE1 targets and PERK targets. (B) Cells receiving the indicated treatments were harvested for Western blot analysis, and probed for indicated UPR-mediated proteins. Quercetin concentration: 100 μM. (C) Real-time PCR analysis of UPR-mediated genes in the presence of tunicamycin. (D) Real-time PCR analysis of RIDD targets. One way ANOVA test was applied for statistical analysis. Data are presented as mean ± SD of n=4. All experiments were repeated three times with similar results. Concentrations are indicated in μM. Sora= sorafenib. *p<0.05, **p<0.01, ***p<0.001 compared to control. $^{\#}$p<0.05, $^{\#\#}$p<0.01, $^{\#\#\#}$p<0.001 compared to 5 μM sorafenib.

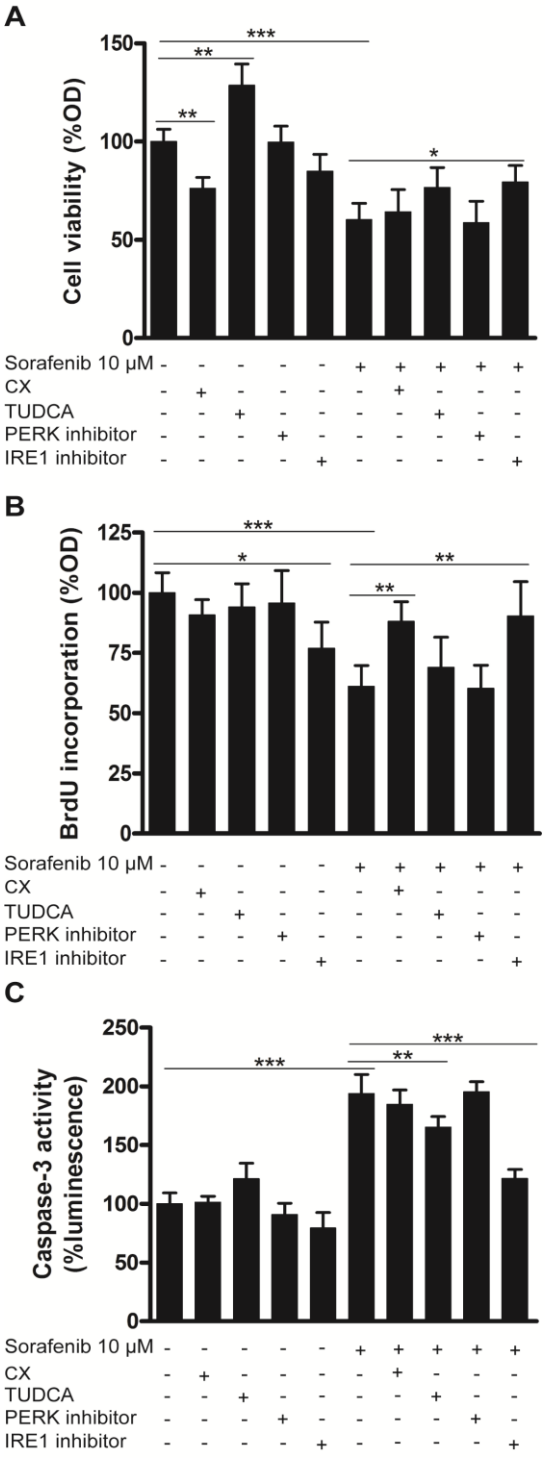

Fig. 2. Sorafenib-mediated reduction in tumor cell viability and proliferation depends on proteotoxic stress and the IRE1 RNase. (A) Cell viability as shown by MTT assay. (B) Cell proliferation was assessed by BrdU incorporation. (C) Caspase-3 activity of HepG2 cells treated with the indicated compounds. Data are presented as mean ± SD. These experiments were repeated three times with similar results. One way ANOVA test was applied for statistical analysis. CX= cycloheximide. *p<0.05, **p<0.01, ***p<0.001.

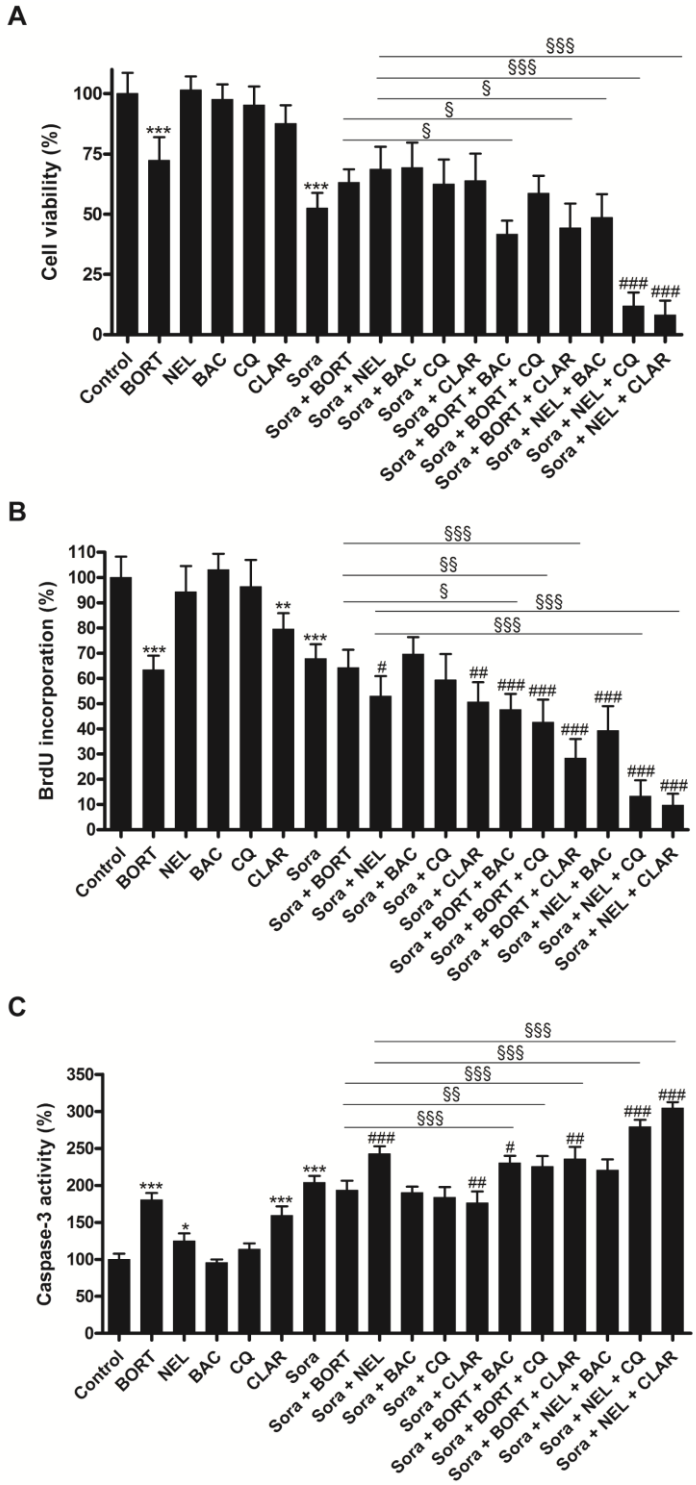

Fig. 3. Combination of sorafenib with an ER stress inducer and an inhibitor of adaptive protein refolding or autophagy potentiates the antitumor activity *in vitro*. (A) Cell viability, (B) proliferation rate and (C) caspase-3 activity of HepG2 cells. *p<0.05, **p<0.01, ***p<0.001 compared to control; $^{\#}$p<0.05, $^{\#\#}$p<0.01, $^{\#\#\#}$p<0.001 compared to 10 μM sorafenib alone; §p<0.05, §§p<0.01, §§§p<0.001 compared to the indicated group. Sora= sorafenib, BORT= bortezomib, NEL= nelfinavir, BAC= bacitracin, CQ= chloroquine, CLAR= clarithromycin.

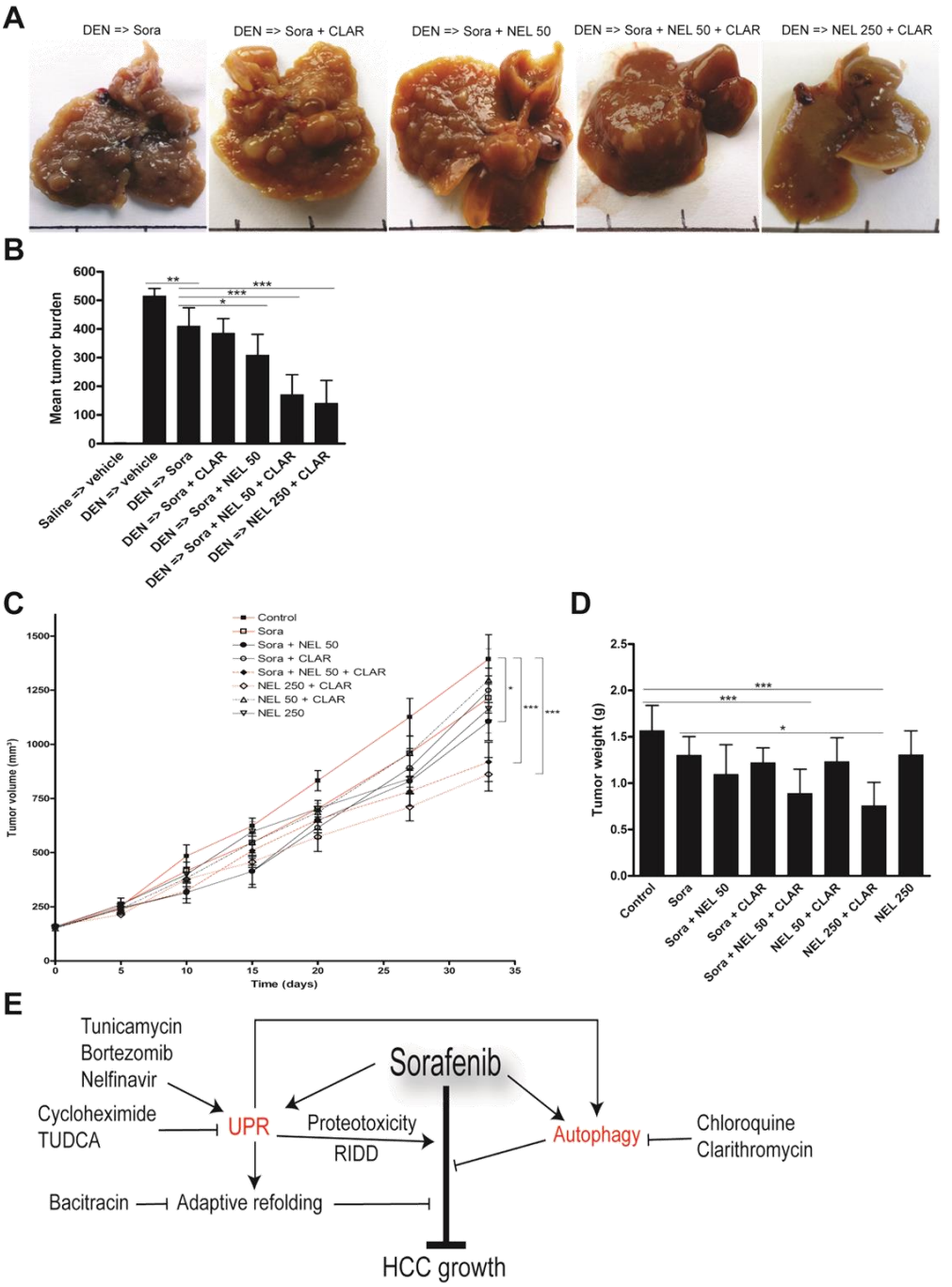

Fig. 4. Combination of sorafenib with an ER stress inducer and an inhibitor of autophagy potentiates the antitumor activity *in vivo*. (A) Representative photographs of the DEN-treated livers. (B) Tumor burden as assessed by reticulin staining in randomly selected high-power fields. *p<0.05, **p<0.01, ***p<0.001. (C) Effect of indicated treatments on growth of HepG2 xenografts in athymic nude mice (n=6). The tumor volume was measured three times per week for 4 weeks. Values represent the mean ± SD. (D) At the end of the treatment period, animals were sacrificed and xenograft tumor weights were recorded. (E) Schematic model outlining the modulation of sorafenib-induced resistance mechanisms. Sora= sorafenib, NEL 50= nelfinavir 50 mg/kg bid, NEL 250= nelfinavir 250 mg/kg bid, CLAR= clarithromycin.

2.1.1. **Supplementary figures**

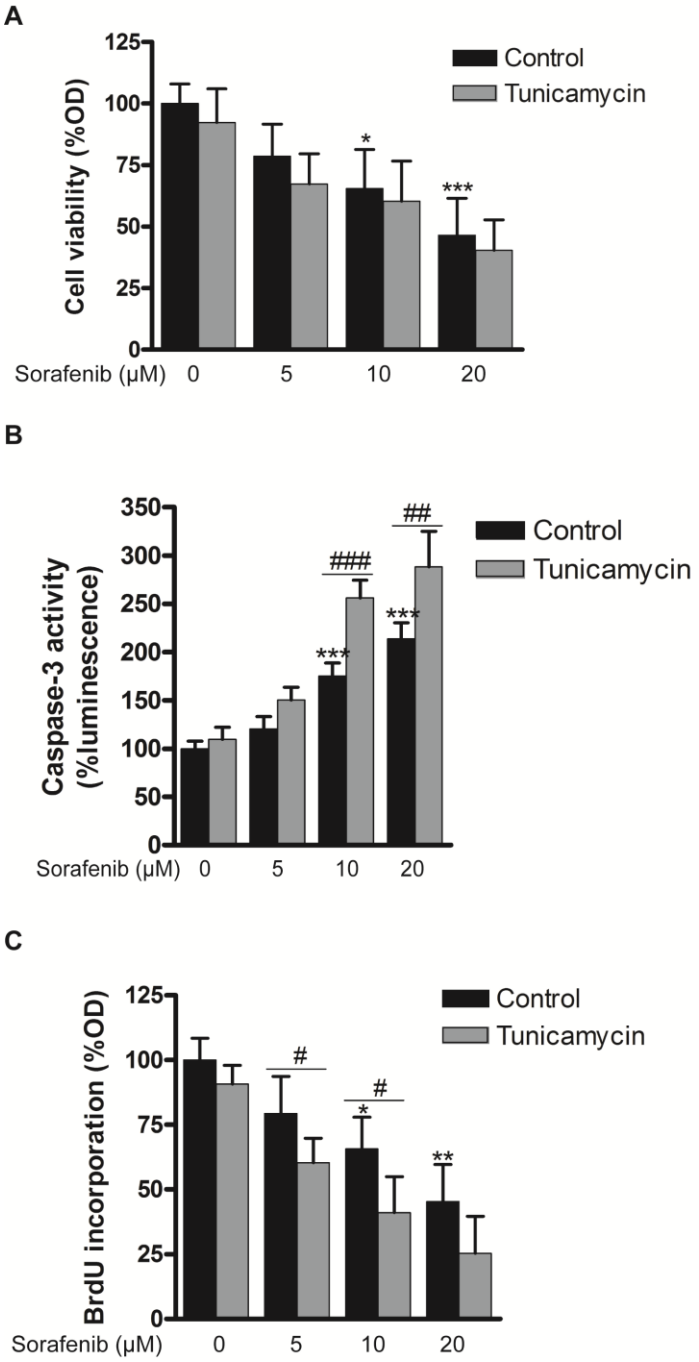

Fig. S1. Sorafenib induces apoptosis and reduces proliferation in human and murine HCC cells irrespective of pre-existent ER stress. (A) Cell viability, (B) caspase-3 activity and (C) proliferation assessment in HepG2, BWTG3 and Hepa1-6 cells. Data are expressed as the percentage of control and presented as the mean ± SD of three separate experiments, each of which was performed in triplicate. *$p<0.05$, **$p<0.01$, ***$p<0.001$ compared to 0 μM sorafenib in control conditions. $^{\#}p<0.05$, $^{\#\#}p<0.01$, $^{\#\#\#}p<0.001$ compared to indicated sorafenib concentration.

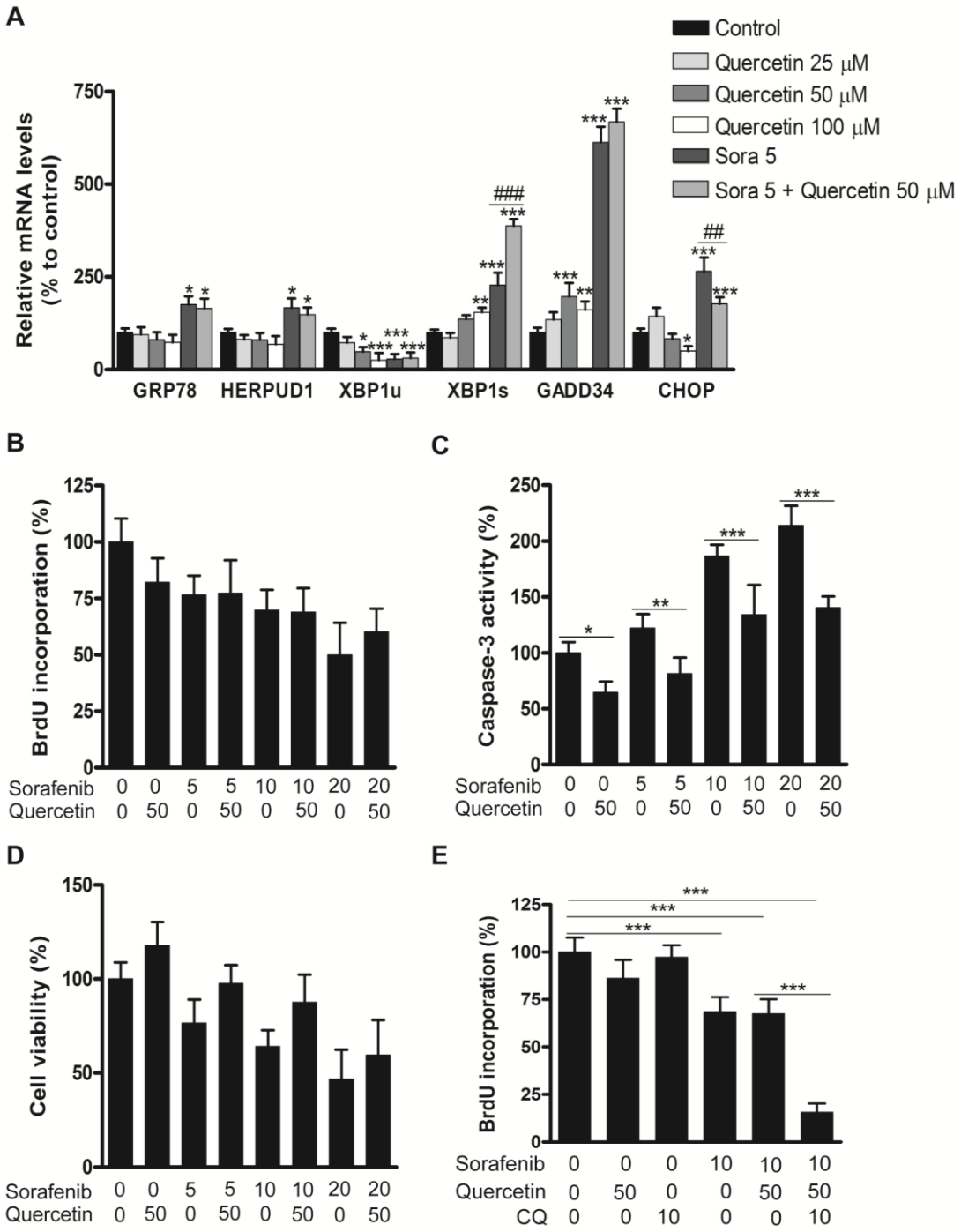

Fig. S2. IRE1 activator quercetin induces no synergistic antitumor effects in sorafenib-treated HepG2 cells. (A) Effect of 25-100 μM quercetin on the mRNA expression of UPR-mediated genes with and without sorafenib. (B) Proliferation rate. (C) Caspase-3 activity. (D) Cell viability. (E) Proliferation rate. Concentrations are indicated in μM. *p<0.05, **p<0.01, ***p<0.001 compared to sorafenib. Sora 5=sorafenib 5 μM. CQ=chloroquine.

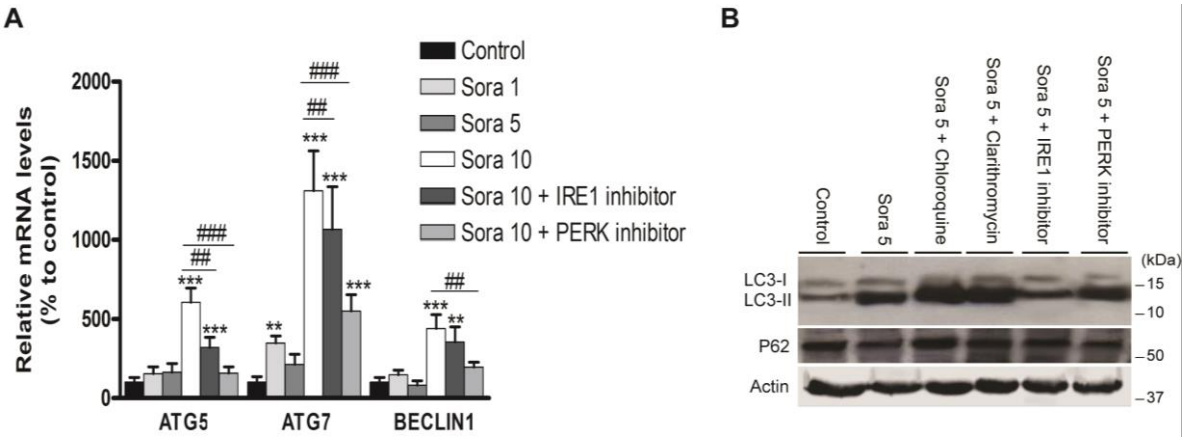

Fig. S3. Sorafenib dose dependently induces autophagy in part via ER stress modulation. (A) mRNA expression of autophagy-related genes and (B) Western blotting for LC3 and P62 in HepG2 cells. Blots are representative of three independent experiments. *p<0.05, **p<0.01, ***p<0.001 compared to saline.

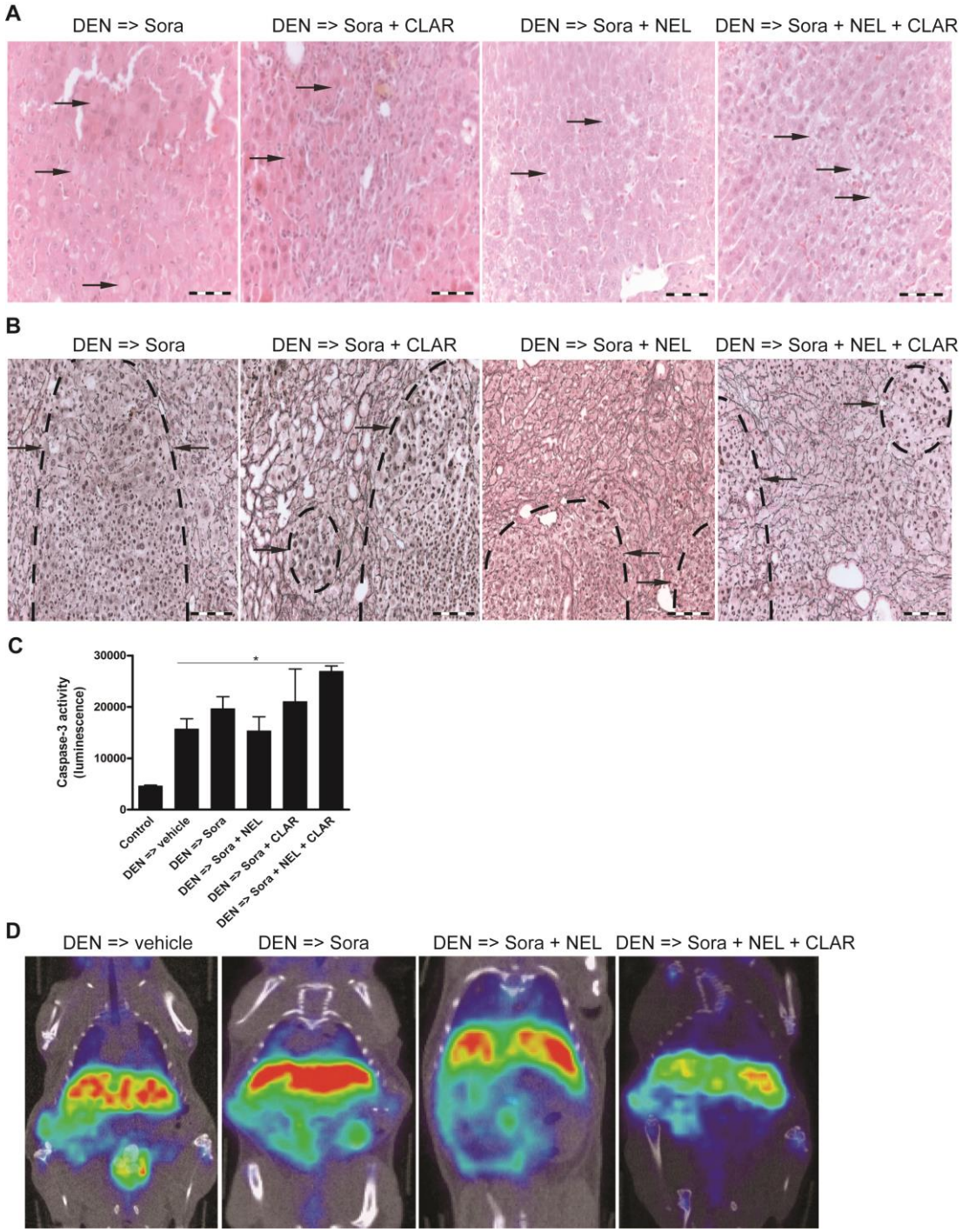

Fig. S4. Antitumor efficacy of sorafenib is potentiated by combination with nelfinavir and clarithromycin in xenograft and orthotopic models for HCC. (A) Hematoxylin/eosin and (B) Reticulin staining of HCC-bearing livers. Scale bar: 100 µm. Arrows indicate cytoplasmic vacuolization. (C) Caspase-3 activity in lysates of HCC-bearing livers, *p<0.05. (D) ^{18}F-Choline positron emission tomography visualizes cell membrane synthesis.

3. Antimalarial Artesunate and the unfolded protein response in hepatocellular carcinoma

3.1. Therapeutic effects of artesunate in hepatocellular carcinoma: repurposing an ancient antimalarial agent

Yves-Paul Vandewynckel[1], Debby Laukens[1], Anja Geerts[1], Chris Vanhove[2, 3], Benedicte Descamps[2], Isabelle Colle[1], Lindsey Devisscher[1], Eliene Bogaerts[1], Annelies Paridaens[1], Xavier Verhelst[1], Christophe Van Steenkiste[1], Louis Libbrecht[4], Bart Lambrecht[3,5,6], Sophie Janssens[3,5,6], Hans Van Vlierberghe[1]

[1]Department of Hepatology and Gastroenterology
[2]Infinity Imaging Lab, Medisip, iMinds
[3]GROUP-ID Consortium, Ghent University
[4]Department of Pathology, Ghent University Hospital
[5]Department of Respiratory Medicine
[6]Unit Immunoregulation and Mucosal Immunology, VIB Inflammation Research Center, Ghent, Belgium

Therapeutic effects of artesunate in hepatocellular carcinoma: repurposing an ancient antimalarial agent

3.1.1. Abstract

Objectives

Artemisinins are antimalarial drugs that exert potent anticancer activity. We evaluated the effects of artesunate, a semisynthetic derivative of artemisinin, on tumor growth, angiogenesis, the unfolded protein response, and chemoresistance in hepatocellular carcinoma.

Materials and methods

The effect of artesunate was examined in HepG2 and BWTG3 cells under normoxic and hypoxic conditions and in a diethylnitrosamine-induced mouse model. Histology was performed with hematoxylin/ eosin and reticulin staining. The expression of chemoresistance-related transporters and angiogenic and unfolded protein response factors was determined. Cytotoxicity was assessed by alanine and aspartate transaminase, lactate dehydrogenase, water-soluble tetrazolium salt, and caspase-3 activity assays. Small animal imaging was performed using dynamic contrastenhanced MRI and choline PET to assess tumor progression.

Results

Artesunate dose dependently reduced cell viability (from 50 μmol/l; $P< 0.05$) and increased caspase-3 activity ($P< 0.05$) in HepG2 and BWTG3 cells. These effects were enhanced by hypoxia (from 12.5 μmol/l; $P< 0.01$). Moreover, artesunate downregulated vascular endothelial growth factor and placental growth factor expression in vitro (both $P< 0.05$) and in vivo (both $P< 0.01$). In mice, artesunate decreased vessel density and tumor burden (both $P< 0.05$). These in-vivo effects were enhanced by combination with sorafenib ($P< 0.05$ and $P= 0.07$, respectively), without apparent hepatotoxicity. Furthermore, artesunate modulated the unfolded protein response in vitro and in vivo, increasing proapoptotic signaling, and did not induce doxorubicin chemoresistance.

Conclusion

These findings indicate that artesunate could offer a new approach to the therapy of hepatocellular carcinoma. Clinical trials with artesunate as monotherapy or in combination with current hypoxia-inducing approaches are necessary.

3.1.2. **Introduction**

Hepatocellular carcinoma (HCC) remains a major health problem and is the third leading cause of cancer-related mortality worldwide. HCC is frequently associated with liver cirrhosis and dysfunction, complicating therapeutic strategies [1]. Resection and transplantation are the only curative treatments available. However, only ∼20% of patients with HCC are eligible for surgery, and recurrence rates are high [2,3]. Classical chemotherapy is ineffective because HCC cells are chemoresistant, partially because of the increased cellular efflux of cytostatic compounds, including doxorubicin, by transmembrane ATP-binding cassette (ABC) transporters [4–7]. To date, the antiangiogenic multikinase inhibitor sorafenib, which targets Raf and platelet-derived and vascular endothelial growth factor (VEGF) receptor tyrosine kinase signaling, and transarterial embolization are the only approved treatments for advanced disease. Unfortunately, both treatments provide only a limited survival advantage [3], necessitating the development of innovative compounds. A phase III trial of sorafenib showed prolonged survival but only minimal tumor shrinkage, thus increasing the use of functional imaging (e.g. PET) [8].

Artemisinins, compounds extracted from the herb Artemisia annua, are safe and effective antimalarial drugs. Recent studies have suggested that artemisinins also exert antiangiogenic and cytotoxic effects on cancer cells [9]. Dihydroartemisinin, the main active metabolite, exerts antitumor effects against various human cancers, including liver, lung, ovarian, and pancreatic cancer [9,10]. Artesunate (ART) is a water-soluble semisynthetic artemisinin with improved pharmacokinetic properties and is approved by the Food and Drug Administration for the treatment of malaria [11]. The mechanism through which artemisinins inhibit cancer growth is not fully understood, but ferrous iron is considered to induce cytotoxic radicals by reductive scission of the endoperoxide bridge of artemisinins [9]. Blocking the transferrin receptor by specific monoclonal antibodies abrogates the antitumoral activity of ART [9]. Because the liver serves as an iron storehouse, we expect ART to be active in hepatocytes. Moreover, continuous HCC cell growth requires high iron metabolism, and cancer cells show increased transferrin receptor expression. As transferrin receptors are responsible for the uptake and regulation of intracellular iron [12], ART may have greater efficacy in cancer cells.

In addition to oxidative stress, ART inhibits angiogenesis and causes calcium dysregulation [9,13]. These effects may induce the unfolded protein response (UPR), which stimulates cellular adaptation to stress or, if the stress is too severe, apoptosis. In addition, the UPR regulates chemoresistance and angiogenesis and is activated in HCC [14–16]. Three UPR transducers have been identified: PKR-like endoplasmic reticulum kinase (PERK), inositol-requiring enzyme 1 (IRE1), and activating transcription factor 6 (ATF6) [17]. In the absence of misfolded proteins, these stress sensors exist in an inactive state in association with binding immunoglobulin protein (BiP). During endoplasmic reticulum stress, misfolded proteins sequester BiP, allowing sensor activation. PERK phosphorylates eukaryotic initiation factor 2α (eIF2α), leading to transcription factor 4 (ATF4) and C/EBP homologous protein transcription factor (CHOP) activation, growth arrest, and DNA damage-inducible protein (GADD34) expression [17]. Furthermore, dihydroartemisinin induces CHOP in HepG2 cells [9]. The effects of ART on HCC growth, angiogenesis, UPR induction, and chemoresistance in vitro and in vivo are unknown.

In this study, we tested the hypothesis that ART has antitumor activity in HCC and elucidated potential modes of action, such as the induction of tumor hypoxia and endoplasmic reticulum stress. We then evaluated dual therapy with sorafenib (ART/Sora) and the effect of ART on chemoresistance.

3.1.3. **Materials and methods**

Cell culture

The human HepG2 (HB-8065; ATCC, Manassas, Virginia, USA) and mouse BWTG3 [18] cell lines were cultured in DMEM supplemented with 10% FBS (Life Technologies, Ghent, Belgium) and incubated at 37°C in a water-saturated atmosphere of 5% CO_2/95% air. Cells were seeded in six-well plates at 2.5×10^6 cells/well and incubated for 1 or 4 days with different ART concentrations (provided by Dafra Pharma Research, Turnhout, Belgium); equal volumes of PBS and ethanol were included as controls. Cell density was assessed daily. Selective PERK (Toronto Research Chemicals, Toronto, Canada) and IRE1 (4μ8C; Calbiochem, Billerica, Massachusetts, USA) inhibitors were applied at concentrations of 0.1 and 7 μmol/l, respectively. Each experiment was conducted in quadruplicate under normoxic and hypoxic conditions (1% oxygen in a hypoxia chamber, AnaeroGen; Oxoid, Basingstoke, UK). Subsequently, the cells were lysed for RNA extraction.

Animals

Wild-type 129S2/SvPasCrl mice were purchased from Charles River (Brussels, Belgium) and maintained as described previously [19]. Five-week-old males received weekly intraperitoneal saline or diethylnitrosamine (DEN) (35 mg/kg, in saline) injections [20]. After 25 weeks, the mice were divided randomly into six groups (each n=14) including two control groups [intraperitoneal injections with 100μl of saline once daily with or without ART (30mg/kg/day)] and four DEN-treated groups [saline, ART, intragastric sorafenib (Bayer, Diegem, Belgium) once daily (10 mg/kg/day) or ART/Sora]. After 30 weeks, blood was collected from the ophthalmic artery under isoflurane anesthesia and the mice were euthanized. Pimonidazole HCl (Hypoxyprobe-1; Natural Pharmacia International Inc., Burlington, Massachusetts) was administered intraperitoneally to four random mice per group at a single dose of 60 mg/kg 1 h before they were killed. After macroscopic and microscopic assessment, all organs were fixed in 4% phosphate-buffered formaldehyde (Klinipath, Olen, Belgium) and embedded in paraffin or snap frozen in liquid nitrogen. Hematoxylin/eosin and reticulin staining was performed to assess tumor burden (size×number) and evaluated by two independent observers. All animals received humane care, and all protocols were approved by the Ethical Committee of Experimental Animals at the Faculty of Health Sciences, Ghent University, Belgium (ECD 11/52).

WST-1 and LDH cytotoxicity assays

HepG2 cells were seeded in 96-well plates at 10^4 cells/ well in DMEM supplemented with 10% FBS and stimulated with an ART dilution series or 1% Triton X-100. After 24 h, 100 µl of supernatant was collected for lactate dehydrogenase (LDH) measurement according to the manufacturer's protocol (Biovision, Milpita, California, USA). Cell viability was determined using water-soluble tetrazolium salt 1 (WST-1) (Roche Diagnostics, Mannheim, Delaware, USA). After supernatant collection, the reagent was added and cells were incubated for 4 h at 37°C. The absorbance of the bioreduced WST-1 (formazan) was measured at 450 nm against a background control at 655 nm (Multiskan Ascent, Leuven, Belgium). Experiments were conducted in quadruplicate.

Detailed information on the caspase-3 activity assay, total RNA extraction, quantitative real-time PCR, western blotting, immunohistochemistry, enzyme-linked immunosorbent assay and dynamic contrast-enhanced MRI (DCE-MR), and choline PET imaging is provided in the Supplementary Materials and methods section.

Statistics

Statistical analysis was carried out using SPSS 21 (SPSS Inc., Chicago, Illinois, USA). Values are presented as the mean ± SEM or log 2[fold change (FC)] relative to the average expression in controls. Variables were tested for normality using the Shapiro–Wilk test. Normally distributed data were subjected to the unpaired Student's t-test. Non-normally distributed data were tested using the Mann-Whitney U-test. Two-tailed probabilities were calculated; a P-value less than 0.05 was considered statistically significant. Survival was analyzed using the log-rank test.

3.1.4. **Results**

Dose-dependent and time-dependent inhibitory effects of ART on tumor cell viability

To assess the effects of ART on HCC cells, cell viability, cytotoxicity, and caspase-3 activity were assessed in HepG2 and BWTG3 cells treated with different ART concentrations. The WST-1 assay indicated that ART dose dependently decreased HepG2 cellular metabolic activity and, thus, cell viability (Fig. 1a, $P<0.05$ at 50 μmol/l). Because liver tumors rapidly outgrow their vascular supply and become hypoxic, all experiments were conducted under normoxic and hypoxic conditions [21]. In HepG2 and BWTG3 cells, hypoxia enhanced the reduction in cell viability [Fig. 1b ($P<0.05$ at 12.5 μmol/l) and Fig. 1Sb ($P<0.001$ at 12.5 μmol/l), respectively].

Dose-dependent cellular cytotoxicity was measured by LDH released into the supernatant and observed at 25 and 50 μmol/l ART in HepG2 cells (Fig. 1c; $P<0.01$ and $P<0.001$, respectively) and 50 μmol/l ART in BWTG3 cells (Fig. 1Sc, $P<0.05$).

The activity of caspase-3, a downstream effector of the intrinsic and extrinsic apoptotic pathways, time dependently increased after 24 and 48 h of incubation with 50 μmol/l ART in HepG2 cells, indicating induction of apoptosis (Fig. 1e, $P<0.05$ after 24 h). All of these effects led to a significant reduction in the number of HepG2 cells by 25 and 50 μmol/l ART after 4 days of incubation ($P<0.01$, Fig. 1f).

ART monotherapy and ART/Sora show antitumor efficacy in a mouse model of HCC

To confirm the antitumor activity of ART observed in our in-vitro studies, we evaluated its antitumor activity in an HCC mouse model. Twenty-five weeks of DEN administration reduced the body weight of mice when compared with controls ($P<0.001$). Subsequent treatment with ART or ART/Sora for 5 weeks did not significantly alter the average body weight when compared with vehicle (Table 1). ART did not increase mortality in saline-injected mice; in DEN-injected mice with HCC, survival rates were slightly, but not significantly, increased by ART or ART/Sora therapy ($P>0.05$, 71.43, 85.71, and 82.62%; Fig. 2a). Furthermore, neither ART nor sorafenib induced apparent hepatotoxicity as the serum alanine aminotransferase and aspartate aminotransferase levels were equally increased compared with vehicle-treated mice after administration of DEN (Fig. 2b). Macroscopic evaluation (Fig. 3a) and tumor burden quantification (size×number), as determined by reticulin staining (Fig. 2c), showed reduced tumor number (Fig. 2d) and burden (Fig. 2e) in ART-treated mice (both $P<0.05$).

In addition, although sorafenib did not enhance the ART-induced reduction in HCC nodules (P=0.76, Fig. 2c), a borderline significant additive effect on tumor burden was observed microscopically (P=0.07, Fig. 2e). Interestingly, 25 weeks of DEN administration significantly increased transferrin receptor mRNA levels (1.93 FC compared with 25 weeks of saline, P<0.01) and protein levels (Fig. 2Sg).

Caspase-3 activity levels were increased by administration of DEN (Fig. 2f, P<0.05) and significantly increased in HCC livers after ART monotherapy compared with controls (P<0.01). Administration of sorafenib also increased caspase-3 activity (P<0.05) and an additive effect was observed after ART/Sora (P<0.001).

Functional choline PET and DCE-MRI studies were used to visualize cellular membrane biosynthesis [22] and time-dependent contrast uptake, respectively. Choline PET showed a reduced number of loci with high mean standardized uptake values according to the PERCIST criteria [23] after the administration of ART and ART/Sora compared with saline (Fig. 3b). DCE-MRI showed smaller and reduced numbers of nodules with low vascularization following the administration of ART and ART/Sora (Fig. 3c).

ART decreases tumor angiogenesis in HCC

In addition to its direct effect on tumor cell viability, the antitumor efficacy of ART has been associated with antiangiogenic activity [9,13]. Therefore, we assessed the effects of ART on the expression of key angiogenic factors VEGF and placental growth factor (PlGF), intratumoral hypoxia, and vessel density in this HCC model. After 25 weeks of DEN administration, Vegf mRNA and protein levels were upregulated (P<0.001 and P<0.01, respectively; Fig. 2S and Fig. 4a). An increase in vessel density after the administration of DEN further led to neovascularization, as shown by CD105 immunohistochemistry (1.49 FC, P<0.001, Fig. 4b–d). However, pimonidazole binding showed reduced oxygen levels within the tumor nodules, suggesting the formation of dysfunctional vessels.

Remarkably, Plgf and Vegf mRNA (P<0.01 and P<0.05, respectively; Fig. 2S) and protein levels (P<0.05 and P<0.01, respectively; Fig. 4a) were reduced after 5 weeks of ART treatment compared with controls. Moreover, ART decreased the vessel density in the tumor (Fig. 4b) and surrounding tissue (Fig. 4c) compared with vehicle (both P<0.05). ART/Sora reduced angiogenesis more than ART monotherapy, but the difference was significant only in the tumor tissue (P<0.05).

Reduced vascularization was associated with increased nodular hypoxia in ART-treated and ART/Sora-treated mice compared with vehicle-treated mice (Fig. 4e). Finally, the addition of 25 μmol/l ART for 24 h to HepG2 cells under hypoxia reduced VEGF and PlGF secretion (both $P<0.05$) (Fig. 2Sb), suggesting that these effects are cell intrinsic.

ART modulates the UPR and ABC transporter induction in vitro and in vivo

Because the induction of endoplasmic reticulum stress is a proposed ART mechanism of action [9], we evaluated the expression of key markers of the three UPR pathways in vitro and in vivo. In HepG2 cells, ART upregulated ATF4 and CHOP mRNA (both $P<0.05$, Fig. 3Sa) and protein (Fig. 2Sf) under normoxia. In addition, induction of these PERK targets was observed in BWTG3 cells (Fig. 4Sa). In mice, ART increased the levels of Atf4 mRNA ($P<0.01$, Fig. 3Sa) and phospho-eIf2α ($P<0.01$, Fig. 3Sb), Atf4 ($P<0.01$), Chop ($P<0.05$), and Gadd34 ($P=0.12$) protein expression (Fig. 3Sc). No changes were observed in IRE1-mediated X-box-binding protein 1 (XBP1) splicing activity in vitro or in vivo. Remarkably, in HepG2 cells, 25 μmol/l ART reduced the mRNA levels of BiP and other ATF6 pathway targets, protein disulfide isomerase family A, member 4 (PDIA4), and unspliced XBP1. Western blot analysis showed reduction of BiP by ART therapy in vitro (Fig. 2Sf) and in vivo (Fig. 3Sc). Importantly, VEGF and PlGF expression and the reduced cell viability induced by ART were not altered by an IRE1 or a PERK inhibitor in HepG2 cells despite their effective inhibition of XBP1 splicing and CHOP expression (Fig. 2Sb–f). Therefore, ART attenuates the expression of chaperones, including BiP and PDIA4, and the cytoprotective ATF6 pathway, and increases certain PERK targets (e.g. the proapoptotic protein CHOP).

ABC transporters determine cell viability following chemotherapy, and doxorubicin is the most commonly used chemotherapeutic agent for HCC [6,24,25]. Because hypoxia is a well-known ABC transporter inducer and because reduced oxygen levels were observed after ART therapy, we examined the effects of ART on the chemoresistance profile in HCC, which is primarily determined by the ABCB1 and ABCG2 levels [24,26]. Furthermore, we examined the effects of the ART-induced expression pattern by exposing HepG2 cells to ART for 4 h before incubation with doxorubicin for 24 h. In HepG2 cells, ABCB1 and ABCG2 were decreased by ART under normoxia, but not hypoxia ($P<0.01$, Fig. 3Sd). In BWTG3 cells, only Abcg2 was decreased ($P<0.05$, Fig. 4Sb).

In addition, the expression of other ABC transporters implicated in chemoresistance, for example ABCC10, was altered [6]. ART pretreatment did not alter doxorubicin cytotoxicity (Fig. 2Sc), excluding direct resistance induction.

In mice, ART decreased Abcg2 and did not alter Abcb1 at the mRNA (Figs 3Sd and 4Sb) and protein levels [ABCG2: $P<0.05$; ABCB1 (Fig. 3Se): NS]. Only Abcc6 mRNA was upregulated ($P<0.05$).

3.1.5. **Discussion**

To date, only sorafenib has provided limited benefits for advanced HCC. ART is an approved treatment option for malaria and is well tolerated by patients at therapeutic doses of ~5 mg/kg/day [27,28]. The antitumor activity of ART has been described [9,29,30], but its biological activity has not been completely elucidated. In this study, ART (30 mg/kg/day) exerted potent cytotoxic effects on HCC in vitro and in vivo without inducing body weight reduction, hepatotoxicity, or increased mortality in an orthotopic mouse model of HCC.

The effects of ART on angiogenesis and VEGF downregulation have been reported in other cell types [31,32]. We showed that ART reduced the angiogenic factors VEGF and PlGF in vitro and in vivo and decreased tumor angiogenesis in a mouse model [19]. Because the UPR is crucial for angiogenesis regulation and hypoxia is a well-known endoplasmic reticulum stress inducer, we evaluated the effects of ART on the UPR and, consequently, angiogenic factors [33]. ART fortified the PERK pathway in HCC. However, the addition of a selective PERK inhibitor did not counteract the ART-mediated reduction of VEGF or PlGF. In addition, ART did not affect the IRE1 pathway, and in-vitro IRE1 inhibition did not alter its effects on angiogenic factors or cell viability. These data suggest that ART-induced reductions in tumor angiogenesis could be dependent on the UPR, but upstream selective pathway inhibition was insufficient, confirming the known functional redundancy of the UPR. Validation in knockout models of downstream UPR factors is required.

Remarkably, the antitumor activity of ART was increased under hypoxia. In addition, because hypoxic conditions are more distinctly present in intratumoral regions than in healthy livers [34], this finding also allows for dual therapy with ART and conventional hypoxia-inducing therapeutic strategies, for example transarterial embolization [34] and sorafenib therapy [35]. Because we previously showed the antitumor efficacy of sorafenib in DEN-induced HCC [36], we investigated combined ART/Sora and showed that it exerted an additive effect on the microscopic tumor burden and further reduced tumor neovascularization compared with monotherapy.

Notably, macroscopic tumor counting in the ART/Sora group could have been biased by difficulty in identifying smaller nodules in contrast to the quantification of tumor burden determined by reticulin staining. In addition, no significant alterations were observed in the vascularization of the nontumoral liver tissue by ART/Sora compared with ART monotherapy. Apparently, the different modes of action of ART and sorafenib allow them to act in parallel. Further investigation to determine downstream interactions is needed.

In the mouse model, ART decreased tumor neovascularization. Moreover, enhanced antiproliferative activity was observed under hypoxia in HCC cell lines. Consequently, we hypothesize that a positive feedback loop exists: repeated ART administration reduces angiogenesis, increasing intratumoral hypoxia and thus enhancing ART efficacy (Fig. 4f).
Given the modest effects of ART on ABC transporters in the mouse model and the unaltered doxorubicin cytotoxicity after pretreatment with ART in vitro, there is no indication for combining ART with chemotherapeutics such as doxorubicin for HCC therapy or to presume enhanced chemoresistance after ART therapy. Moreover, although doxorubicin is a substrate, the relevance of the only in-vivo upregulated ABC transporter, Abcc6, to chemoresistance is questionable [4]. Finally, in line with findings in non-small-cell lung cancer [37], Abcg2 was significantly reduced by ART. In this study, the effect of ART on ABC transporter expression was examined. Future studies should also investigate efflux pump activity.

3.1.6. **Conclusion**

ART, as a monotherapy or in combination with sorafenib, exerted antitumor effects in experimental HCC models, and ART/Sora therapy was more effective than sorafenib alone and did not show cumulative toxicity. Experience in the use of ART and sorafenib in clinical practice is a considerable advantage. Furthermore, as a safe and low cost drug, ART might be of particular interest for developing countries with a high incidence of HCC [3, 38]. These results collectively suggest that ART could be a promising candidate drug for HCC treatment.

3.1.7. **Acknowledgements**

The authors thank the Department of Biostatistics, Ghent University, for support with statistical analysis.

3.1.8. **Funding**

This study was supported by the Research Foundation Flanders project 3G015612. H.V.V. is a senior clinical investigator of the Research Foundation Flanders. Y.V. and L.D. are sponsored by a grant from the Special Research Fund (B/12531/01, 01D20510), Ghent University. D.L. is funded by an FWO grant (1298213N) and E.B. received an ‘Emmanuel van der Schueren’ grant from the Flemish League against Cancer.

3.1.9. **References**

1 Blachier M, Leleu H, Peck-Radosavljevic M, Valla DC, Roudot-Thoraval F. The burden of liver disease in Europe: a review of available epidemiological data. J Hepatol 2013; 58:593–608.

2 Yamamoto J, Kosuge T, Takayama T, Shimada K, Yamasaki S, Ozaki H, et al. Recurrence of hepatocellular carcinoma after surgery. Br J Surg 1996; 83:1219–1222.

3 European Association for the Study of the Liver; European Organisation for Research and Treatment of Cancer. EASL-EORTC clinical practice guidelines: management of hepatocellular carcinoma. J Hepatol 2012; 56:908–943.

4 Chen ZS, Tiwari AK. Multidrug resistance proteins (MRPs/ABCCs) in cancer chemotherapy and genetic diseases. FEBS J 2011; 278:3226–3245.

5 Moustafa MA, Ogino D, Nishimura M, Ueda N, Naito S, Furukawa M, et al. Comparative analysis of ATP-binding cassette (ABC) transporter gene expression levels in peripheral blood leukocytes and in liver with hepatocellular carcinoma. Cancer Sci 2004; 95:530–536.

6 Borel F, Han R, Visser A, Petry H, van Deventer SJ, Jansen PL, Konstantinova P. Réseau Centre de Ressources Biologiques Foie (French Liver Biobanks Network), France. Adenosine triphosphate-binding cassette transporter genes up-regulation in untreated hepatocellular carcinoma is mediated by cellular microRNAs. Hepatology 2012; 55:821–832.

7 Bonin S, Pascolo L, Crocé LS, Stanta G, Tiribelli C. Gene expression of ABC proteins in hepatocellular carcinoma, peraneoplastic tissue, and liver diseases. Mol Med 2002; 8:318–325.

8 Llovet JM, Ricci S, Mazzaferro V, Hilgard P, Gane E, Blanc JF, et al. SHARP Investigators Study Group. Sorafenib in advanced hepatocellular carcinoma. N Engl J Med 2008; 359:378–390.

9 Crespo-Ortiz MP, Wei MQ. Antitumor activity of artemisinin and its derivatives: from a well-known antimalarial agent to a potential anticancer drug. J Biomed Biotechnol 2012; 2012:247597.

10 Zhang CZ, Zhang H, Yun J, Chen GG, Lai PB. Dihydroartemisinin exhibits antitumor activity toward hepatocellular carcinoma in vitro and in vivo. Biochem Pharmacol 2012; 83:1278–1289.

11 Haynes RK. From artemisinin to new artemisinin antimalarials: biosynthesis, extraction, old and new derivatives, stereochemistry and medicinal chemistry requirements. Curr Top Med Chem 2006; 6:509–537.

12 Pascale RM, De Miglio MR, Muroni MR, Simile MM, Daino L, Seddaiu MA, et al. Transferrin and transferrin receptor gene expression and iron uptake in hepatocellular carcinoma in the rat. Hepatology 1998; 27:452–461.

13 Chen HH, Zhou HJ, Wu GD, Lou XE. Inhibitory effects of artesunate on angiogenesis and on expressions of vascular endothelial growth factor and VEGF receptor KDR/flk-1. Pharmacology 2004; 71:1–9.

14 Shuda M, Kondoh N, Imazeki N, Tanaka K, Okada T, Mori K. Activation of the ATF6, XBP1 and grp78 genes in human hepatocellular carcinoma: a possible involvement of the ER stress pathway in hepatocarcinogenesis. J Hepatol 2003; 38:605–614.

15 Malhi H, Kaufman RJ. Endoplasmic reticulum stress in liver disease. J Hepatol 2011; 54:795–809.

16 Dong D, Ni M, Li J, Xiong S, Ye W, Virrey JJ, et al. Critical role of the stress chaperone GRP78/BiP in tumor proliferation, survival, and tumor angiogenesis in transgene-induced mammary tumor development. Cancer Res 2008; 68:498–505.

17 Walter P, Ron D. The unfolded protein response: from stress pathway to homeostatic regulation. Science 2011; 334:1081–1086.

18 Szpirer C, Szpirer J. A mouse hepatoma cell line which secretes several serum proteins including albumin and alpha-foetoprotein. Differentiation 1975; 4:85–91.

19 Van de Veire S, Stalmans I, Heindryckx F, Oura H, Tijeras-Raballand A, Schmidt T, et al. Further pharmacological and genetic evidence for the efficacy of PlGF inhibition in cancer and eye disease. Cell 2010; 141:178–190.

20 Heindryckx F, Mertens K, Charette N, Vandeghinste B, Casteleyn C, Van Steenkiste C, et al. Kinetics of angiogenic changes in a new mouse model for hepatocellular carcinoma. Mol Cancer 2010; 9:219.

21 Heindryckx F, Kuchnio A, Casteleyn C, Coulon S, Olievier K, Colle I, et al. Effect of prolyl hydroxylase domain-2 haplodeficiency on the hepatocarcinogenesis in mice. J Hepatol 2012; 57:61–68.

22 Kuang Y, Salem N, Corn DJ, Erokwu B, Tian H, Wang F, Lee Z. Transport and metabolism of radiolabeled choline in hepatocellular carcinoma. Mol Pharm 2010; 7:2077–2092.

23 Wahl RL, Jacene H, Kasamon Y, Lodge MA. From RECIST to PERCIST: evolving considerations for PET response criteria in solid tumors. J Nucl Med 2009; 50 (Suppl 1):122S–150S.

24 Sun Z, Zhao Z, Li G, Dong S, Huang Z, Ye L, et al. Relevance of two genes in the multidrug resistance of hepatocellular carcinoma: in vivo and clinical studies. Tumori 2010; 96:90–96.

25 Li G, Chen X, Wang Q, Xu Z, Zhang W, Ye L. The roles of four multi-drug resistance proteins in hepatocellular carcinoma multidrug resistance. J Huazhong Univ Sci Technolog Med Sci 2007; 27:173–175.

26 Zhu H, Chen XP, Luo SF, Guan J, Zhang WG, Zhang BX. Involvement of hypoxia-inducible factor-1-alpha in multidrug resistance induced by hypoxia in HepG2 cells. J Exp Clin Cancer Res 2005; 24:565–574.

27 Efferth T, Kaina B. Toxicity of the antimalarial artemisinin and its derivatives. Crit Rev Toxicol 2010; 40:405–421.

28 Taylor W, Terlouw DJ, Olliaro PL, White NJ, Brasseur P, ter Kuile FO. Use of weight-for-age-data to optimize tablet strength and dosing regimens for a new fixed-dose artesunate-amodiaquine combination for treating falciparum malaria. Bull World Health Organ 2006; 84:956–964.

29 Aquino I, Tsuboy MS, Marcarini JC, Mantovani MS, Perazzo FF, Maistro EL. Genotoxic evaluation of the antimalarial drugs artemisinin and artesunate in human HepG2 cells and effects on CASP3 and SOD1 gene expressions. Genet Mol Res 2013; 12:2517–2527.

30 Jin M, Shen X, Zhao C, Qin X, Liu H, Huang L, et al. In vivo study of effects of artesunate nanoliposomes on human hepatocellular carcinoma xenografts in nude mice. Drug Deliv 2013; 20:127–133.

31 Zhou HJ, Wang WQ, Wu GD, Lee J, Li A. Artesunate inhibits angiogenesis and downregulates vascular endothelial growth factor expression in chronic myeloid leukemia K562 cells. Vascul Pharmacol 2007; 47:131–138.

32 Dell'Eva R, Pfeffer U, Vené R, Anfosso L, Forlani A, Albini A, Efferth T. Inhibition of angiogenesis in vivo and growth of Kaposi's sarcoma xenograft tumors by the anti-malarial artesunate. Biochem Pharmacol 2004; 68:2359–2366.

33 Ghosh R, Lipson KL, Sargent KE, Mercurio AM, Hunt JS, Ron D, Urano F. Transcriptional regulation of VEGF-A by the unfolded protein response pathway. PloS One 2010; 5:e9575.

34 Wu XZ, Xie GR, Chen D. Hypoxia and hepatocellular carcinoma: the therapeutic target for hepatocellular carcinoma. J Gastroenterol Hepatol 2007; 22:1178–1182.

35 Liang Y, Zheng T, Song R, Wang J, Yin D, Wang L, et al. Hypoxia-mediated sorafenib resistance can be overcome by EF24 through VHL dependent HIF-1α inhibition in hepatocellular carcinoma. Hepatology 2013; 57:1847–1857.

36 Heindryckx F, Coulon S, Terrie E, Casteleyn C, Stassen JM, Geerts A, et al. The placental growth factor as a target against hepatocellular carcinoma in a diethylnitrosamine-induced mouse model. J Hepatol 2013; 58:319–328.

37 Ma H, Yao Q, Zhang AM, Lin S, Wang XX, Wu L, et al. The effects of artesunate on the expression of EGFR and ABCG2 in A549 human lung cancer cells and a xenograft model. Molecules 2011; 16: 10556–10569.

38 El-Serag HB. Epidemiology of viral hepatitis and hepatocellular carcinoma. Gastroenterology 2012; 142:1264–1273.e1.

3.1.10. **Figures**

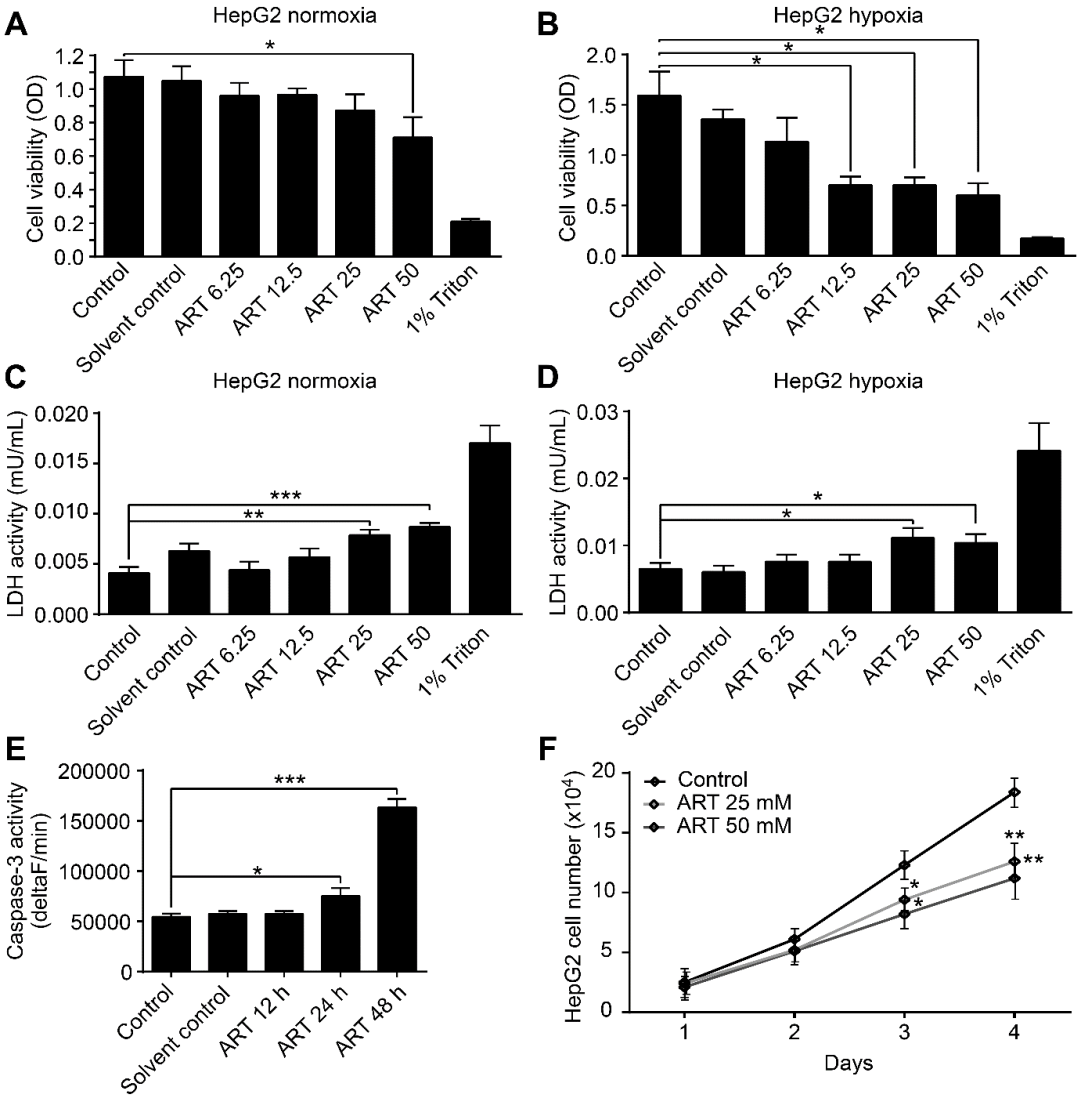

Fig. 1 Artesunate (ART) reduces proliferation and increases cytotoxicity in HepG2 cells. Cells were incubated for 24 h with 6.25–50 µmol/l ART or PBS or ethanol as a control. (a) Assessment of cell viability by optical density (OD) under normoxia and (b) hypoxia in HepG2 cells. (c) Assessment of cytotoxicity by LDH release in HepG2 under normoxia and (d) hypoxia. 1% Triton X-100 =positive control. (e) Assessment of caspase-3 activity over time in HepG2 cells treated with 50 µmol/l ART. (f) Incubation of HepG2 cells with ART for 4 days with a daily assessment of cell density. *P< 0.05,**P <0.01, ***P <0.001.

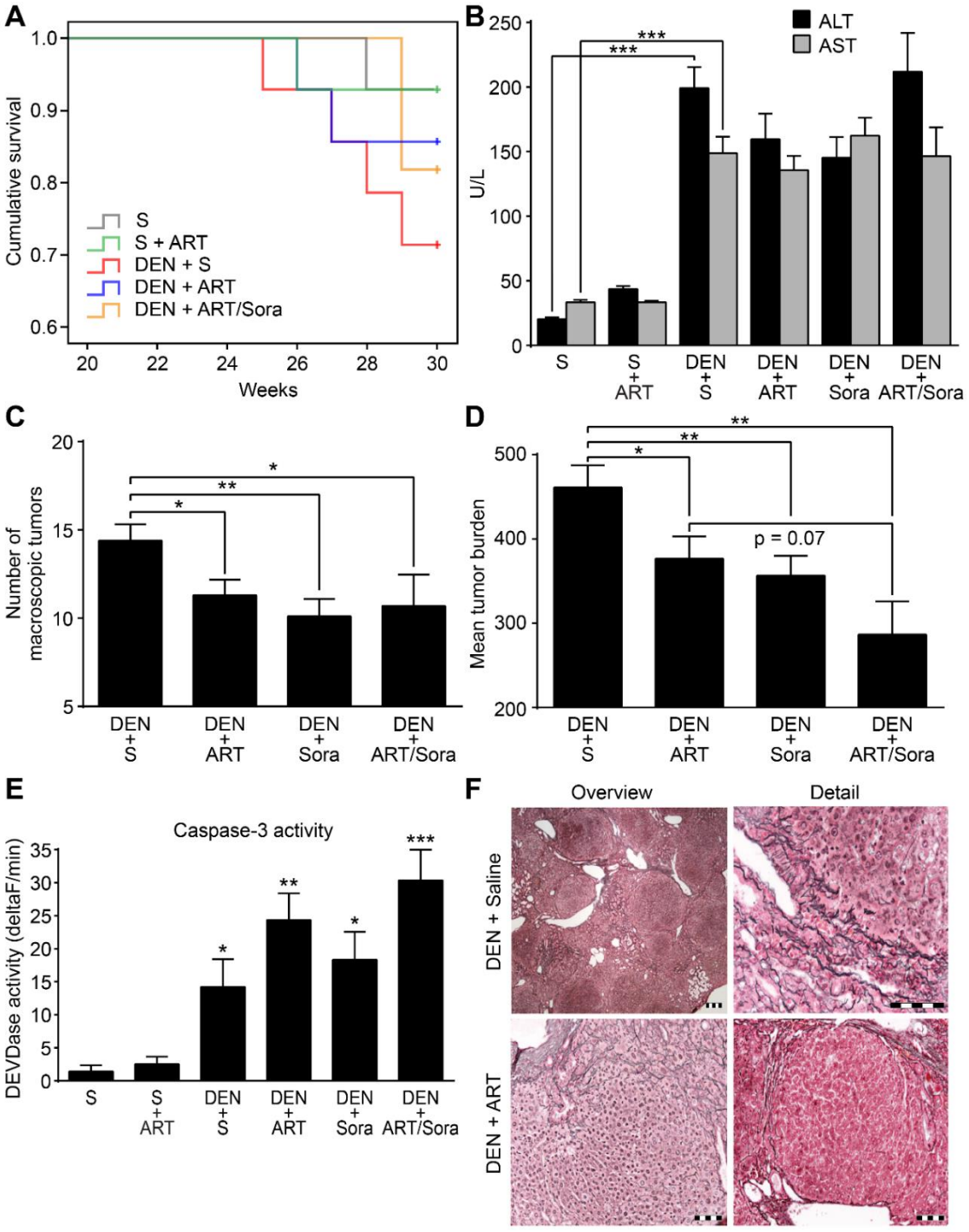

Fig. 2 Artesunate (ART) shows antitumor activity in an hepatocellular carcinoma (HCC) mouse model. (a) Kaplan–Meier survival curve. (b) Alanine aminotransferase (ALT) and aspartate aminotransferase (AST) levels. (c) Tumor number and (d) tumor burden. (e) Caspase-3 activity in saline (S)-treated mouse liver tissue and tumor nodules from diethylnitrosamine (DEN)-treated mice. (f) Representative reticulin-stained slides showing the absence of reticulin in HCC. Following ART, smaller nodules with less defined tumor borders were observed. Scale bars =100 μm. *P < 0.05, **P <0.01, ***P <0.001. Sora, sorafenib.

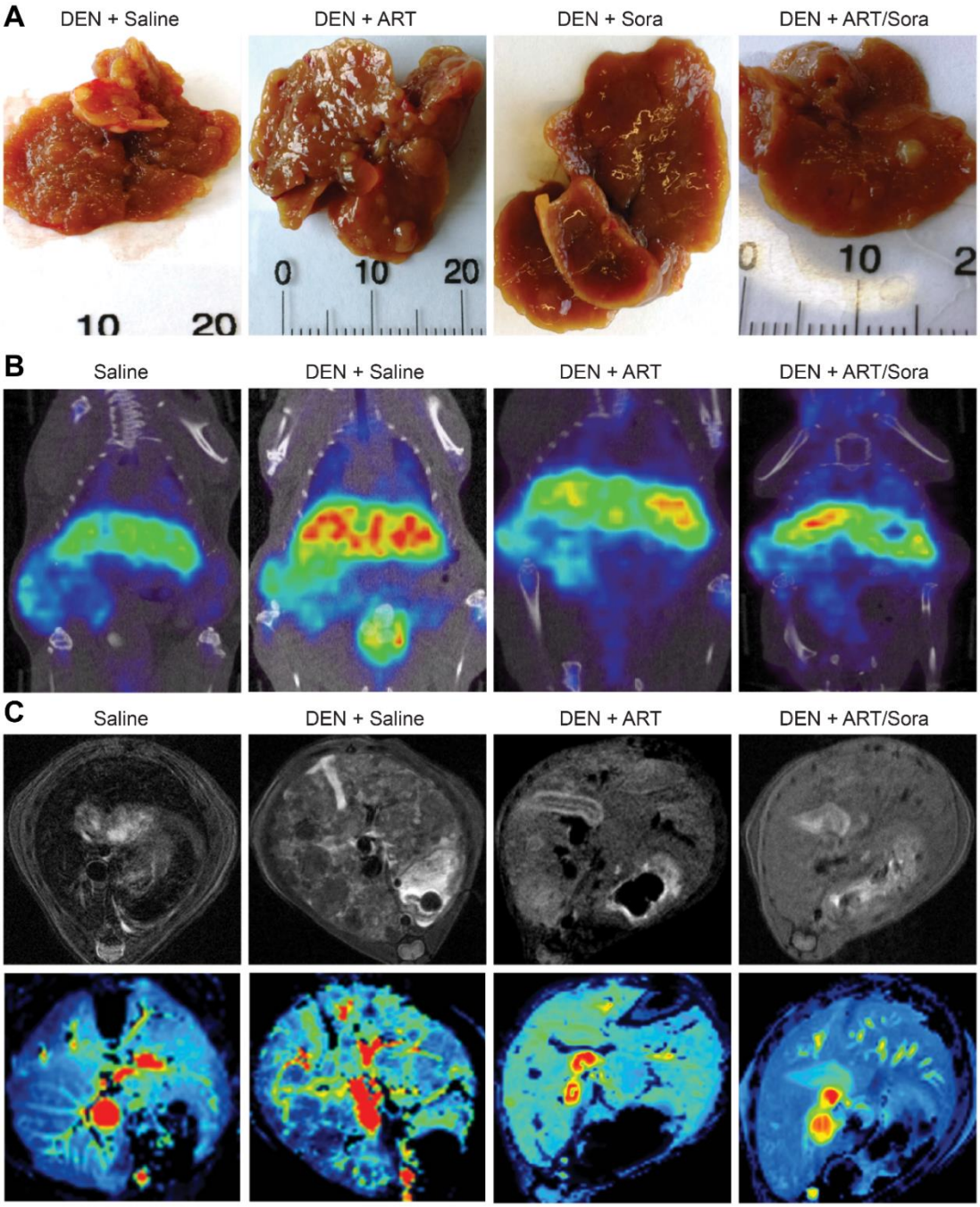

Fig. 3 Structural and functional imaging of the hepatocellular carcinoma model. (a) Representative liver images. (b) Representative images of choline PET and (c) DCE-MRI. ART, artesunate; DEN, diethylnitrosamine; Sora, sorafenib.

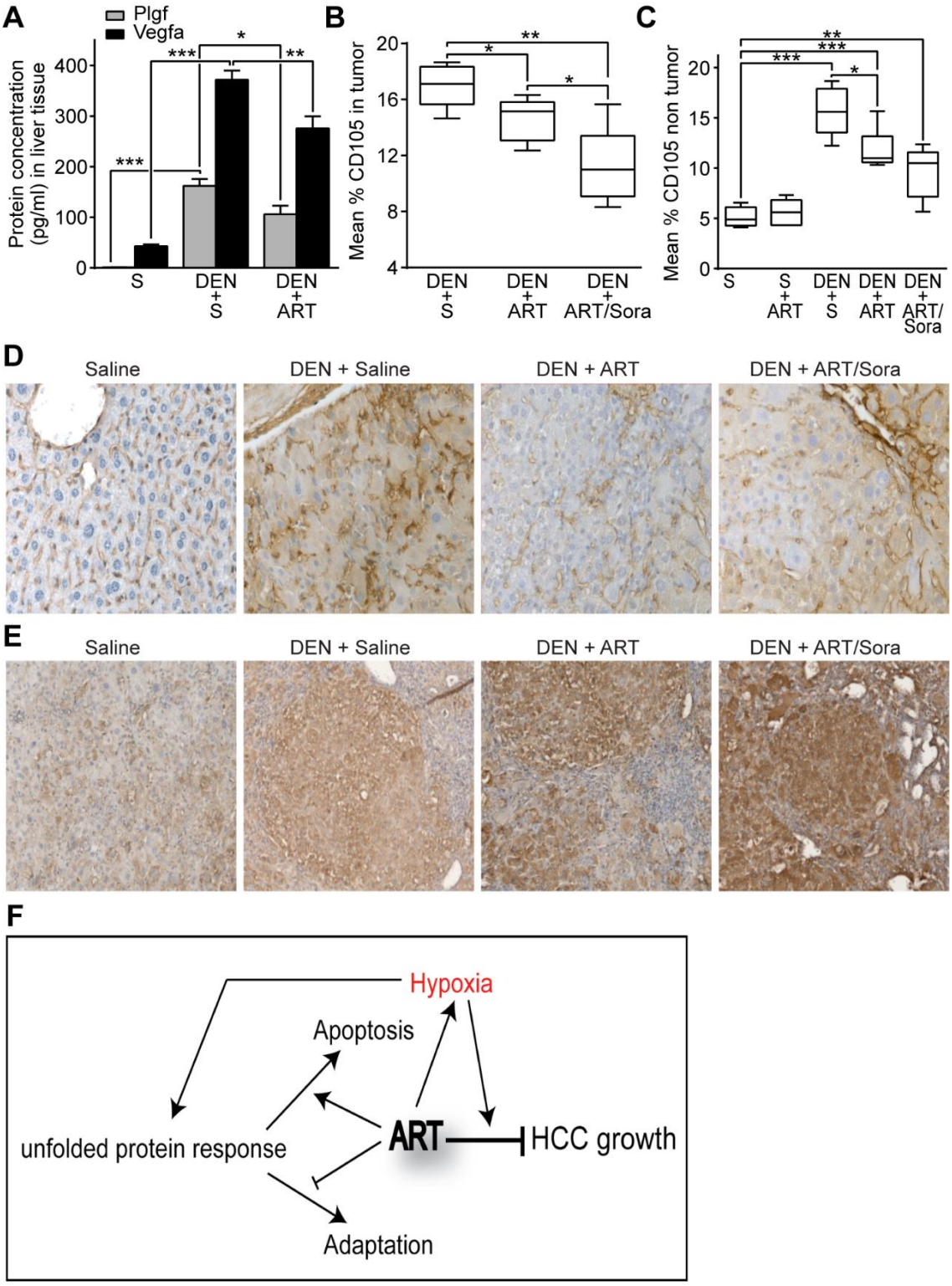

Fig. 4 Artesunate (ART) shows antiangiogenic properties in the hepatocellular carcinoma (HCC) model. (a) Protein concentrations of Vegf and Plgf (pg/ml) in liver lysates. (b) Assessment of vessel density by CD105 staining in tumor nodules and (c) surrounding tissue. (d) Representative CD105 staining of liver tissue after different treatments. (e) Pimonidazole staining. Scale bars =100 µm; S, saline; *P < 0.05, **P <0.01 and ***P <0.001. (f) Schematic representation of the modes of action of ART related to modulation of the unfolded protein response and hypoxia. DEN, diethylnitrosamine; Sora, sorafenib.

3.1.11. **Table**

Table 1 Mouse body weights (g) (mean ± SEM)

Groups	Average body weight 25 weeks (g)	Average body weight 30 weeks (g)
Saline	27.22 ± 1.32	26.03 ± 1.61
Saline + ART	26.31 ± 2.28	25.62 ± 2.03
DEN + saline	19.75 ± 1.76***	18.30 ± 1.92
DEN + ART	20.86 ± 1.45	19.17 ± 2.10 (NS)
DEN + sorafenib	22.96 ± 3.65	17.92 ± 3.19 (NS)
DEN + ART/sorafenib	18.53 ± 2.13	17.43 ± 3.61 (NS)

ART, artesunate; DEN, diethylnitrosamine; NS, not significant compared with DEN + saline.
***$P < 0.001$: 25 weeks DEN versus saline.

3.1.12. **Supplementary figures**

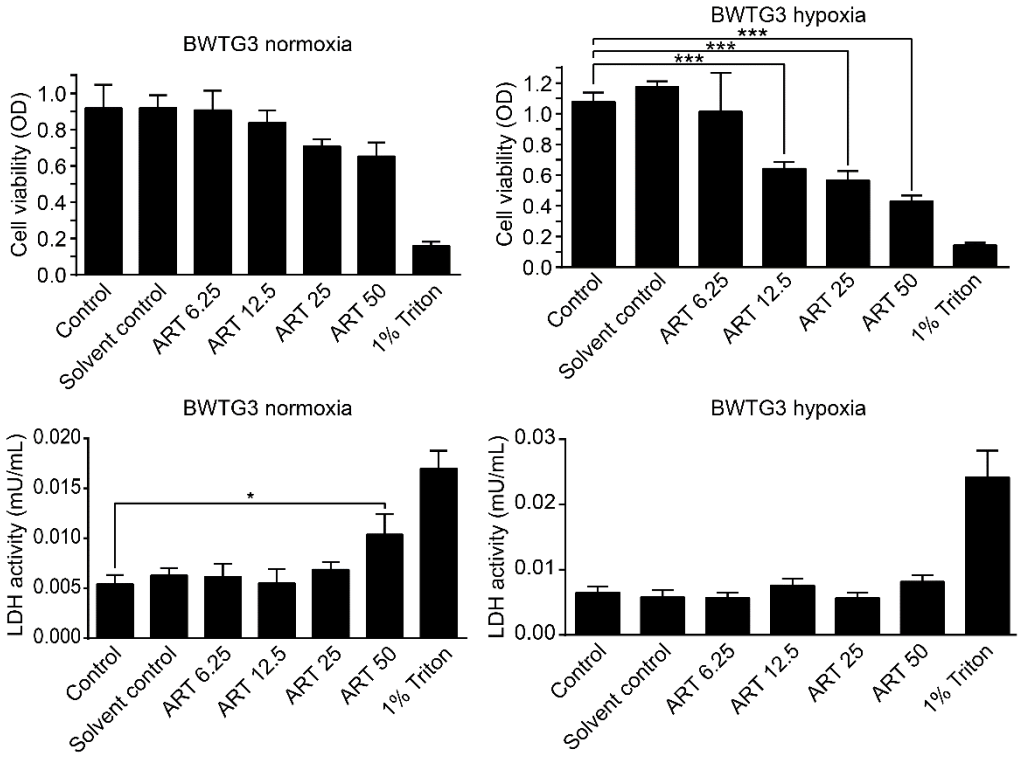

Fig. 1S: ART dose dependently reduces proliferation and increases cytotoxicity in BWTG3 cells. Cells were incubated for 24 hours with 6.25-50 μM of ART or PBS or ethanol as a control. (A) Assessment of cell viability under normoxia and (B) hypoxia. (C) Assessment of LDH release under normoxia and (D) hypoxia. 1% Triton-X100= positive control. *p<0.05, ***p<0.001.

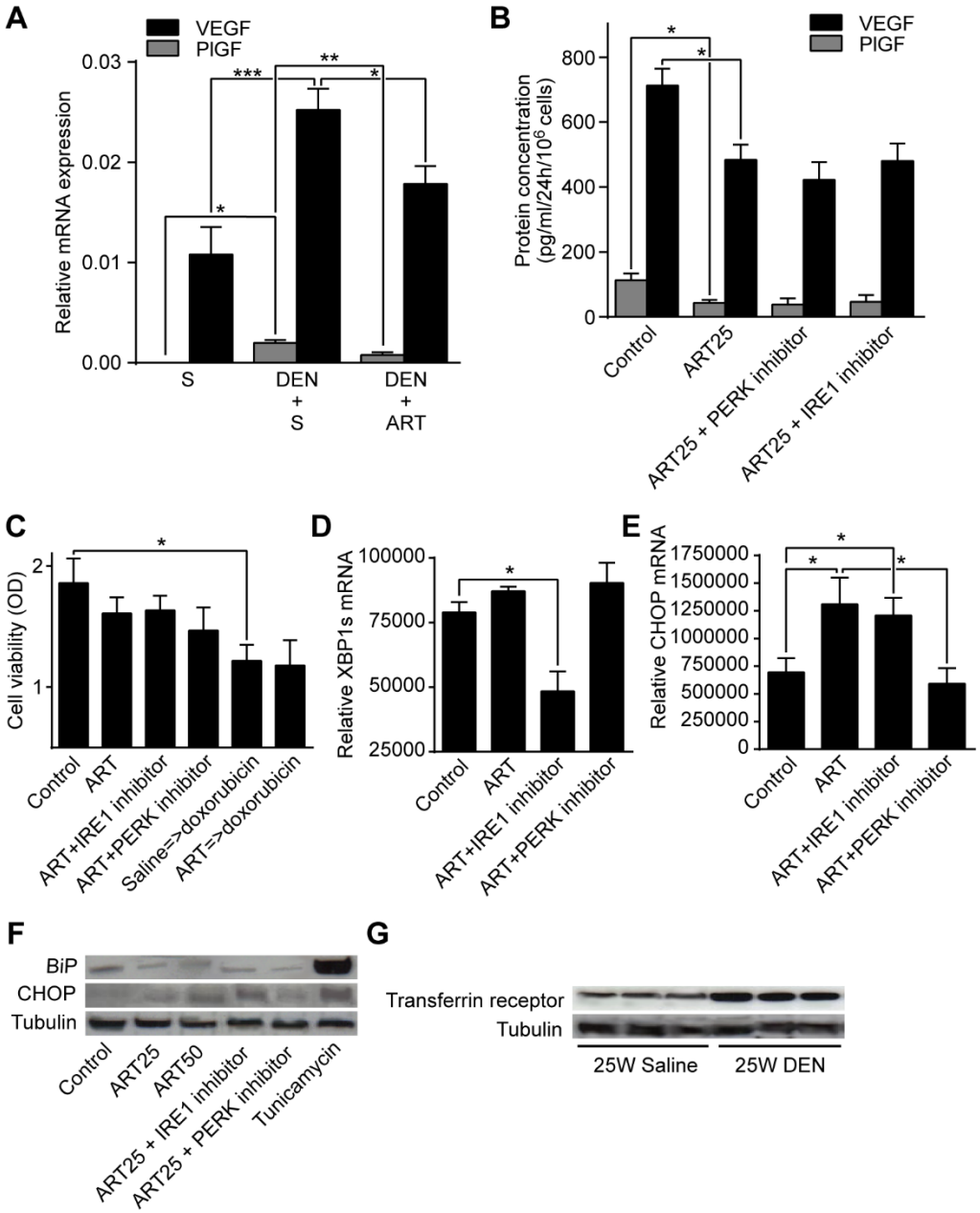

Fig. 2S: The effect of ART on angiogenic factors and cell viability is independent of PERK and IRE1 signaling. (A) Relative VEGF and PlGF mRNA expression in the mouse model. (B) Protein concentrations of VEGF and PlGF in supernatant from HepG2 cells incubated with ART and a PERK or IRE1 inhibitor. (C) Assessment of cell viability. Relative mRNA levels of (D) XBP1s and (E) CHOP in HepG2 cells. (F) Western blotting of lysates from HepG2 cells with anti-BiP and anti-CHOP antibodies. ART=Artesunate; S=Saline; *p<0.05, **p<0.01 and ***p<0.001.

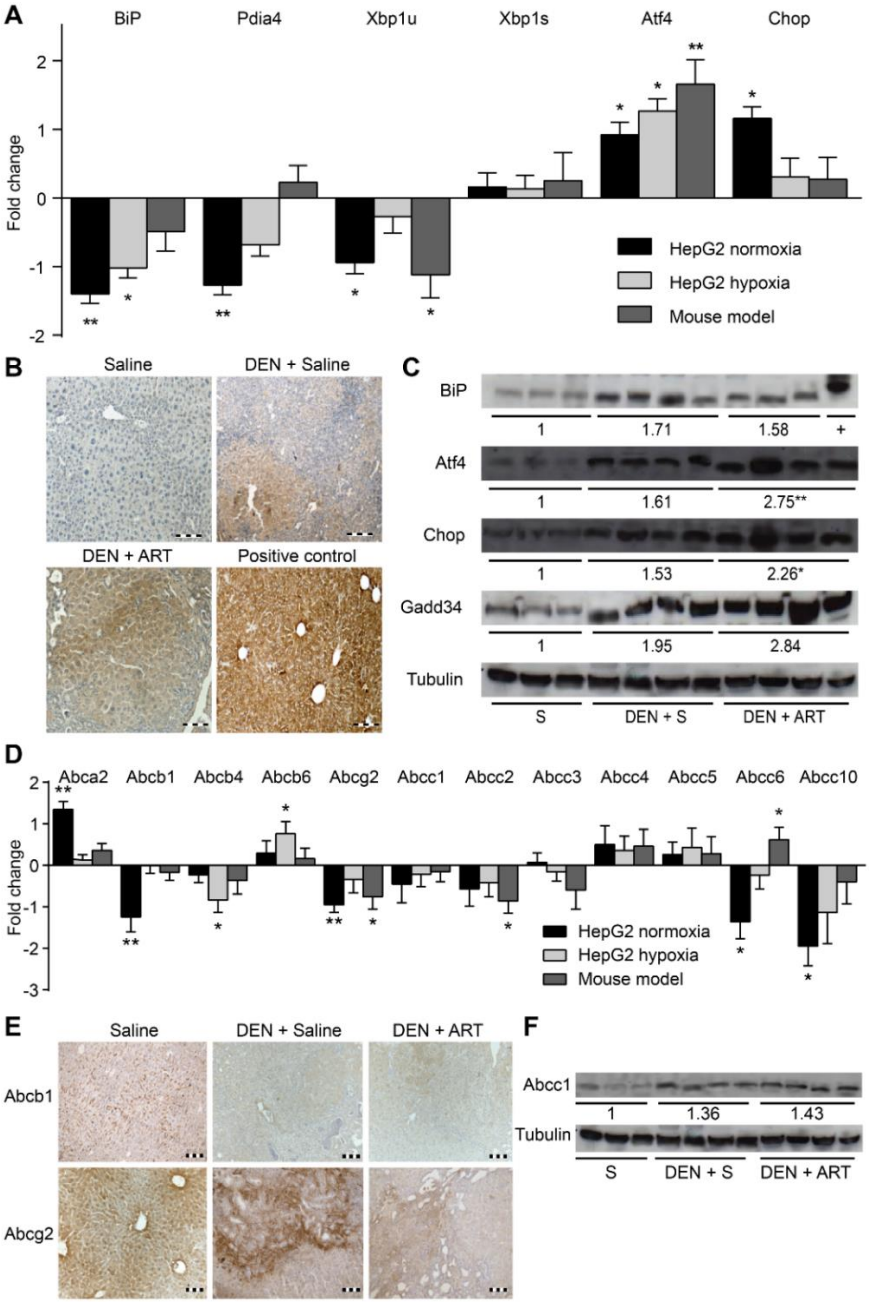

Fig. 3S: The mRNA and protein levels of UPR- and chemoresistance-related proteins. (A) The mRNA log2(fold change) of UPR-related genes in HepG2 cells following 25 μM ART compared with saline treatment, and the mRNA log2(fold change) of UPR-related genes in the mouse HCC model following 5 weeks of 30 mg/kg per day ART compared with saline administration. (B) Representative immunohistochemistry images of phospho-eIf2α, which was increased ($p<0.01$) by ART treatment. Positive controls received only intraperitoneal tunicamycin for 72 hours. (C) Western blotting of lysates from liver tissue after saline administration or tumors after DEN administration, as described in the Materials and Methods. The outer right lane in the blot for BiP represents a positive control. The mean densitometric values are shown below each group. (D) mRNA log2(fold change) of chemoresistance-related genes compared with those following saline administration. (E) Abcb1 expression was unaltered, whereas Abcg2 expression was decreased ($p<0.05$) by ART. Scale bars: 100 μm. (F) Western blot of Abcc1. Experiments were repeated twice with similar results. *$p<0.05$ and **$p<0.01$.

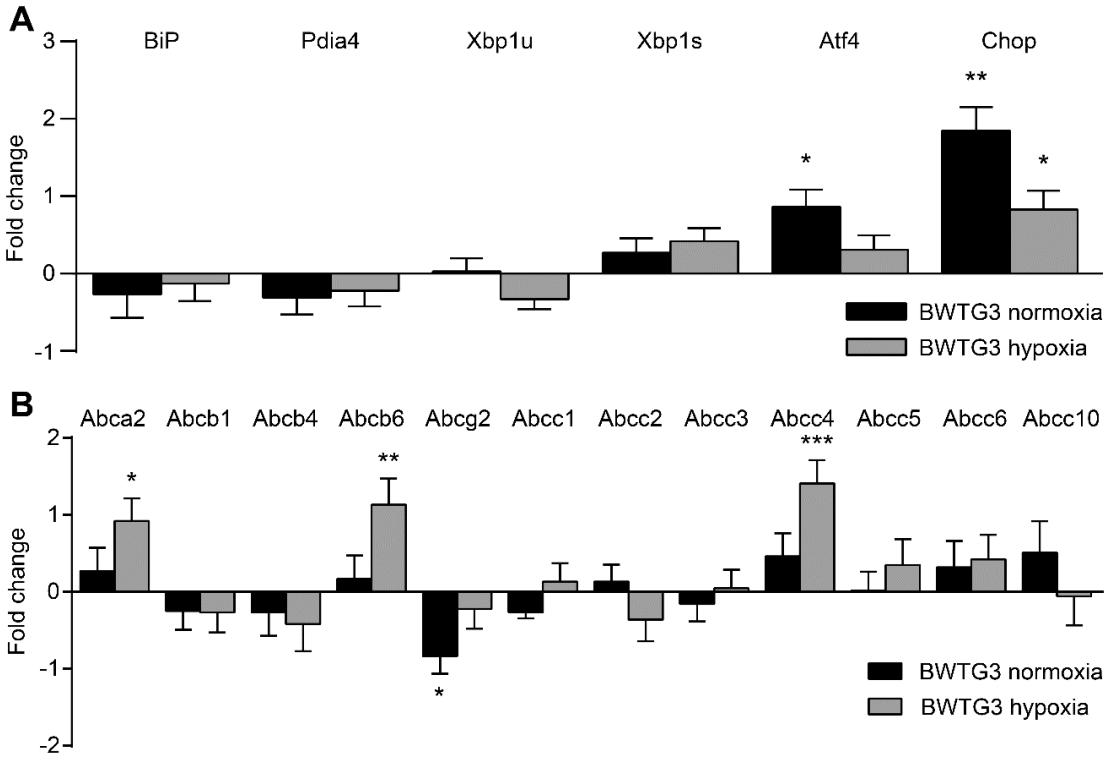

Fig. 4S: The mRNA and protein levels of UPR- and chemoresistance-related proteins in BWTG3 cells. (A) The mRNA log2(fold change) of UPR- and (B) chemoresistance-related genes following 25 μM ART compared with saline treatment. *p<0.05, **p<0.01 and ***p<0.001.

4. PlGF inhibition and the UPR in hepatocellular carcinoma.

4.1. Placental growth factor inhibition modulates the interplay between hypoxia and the unfolded protein response in hepatocellular carcinoma.

Submitted for publication in BMC cancer (23 March 2015)

Yves-Paul Vandewynckel[1], Debby Laukens[1], Lindsey Devisscher[1], Eliene Bogaerts[1], Annelies Paridaens[1], Anja Van den Bussche[1], Sarah Raevens[1], Xavier Verhelst[1], Christophe Van Steenkiste[1], Bart Jonckx[2], Louis Libbrecht[3], Anja Geerts[1], Peter Carmeliet[4,5], Hans Van Vlierberghe[1]

[1]Department of Hepatology and Gastroenterology, Ghent University, Ghent, Belgium

[2]ThromboGenics NV, Heverlee, Belgium

[3]Department of Pathology, Ghent University Hospital, Ghent, Belgium

[4]Laboratory of Angiogenesis and Neurovascular link, Vesalius Research Centre, KU Leuven, Leuven, Belgium

[5]Laboratory of Angiogenesis & Neurovascular Link, Vesalius Research Centre, VIB, Leuven, Belgium

Placental growth factor inhibition modulates the interplay between hypoxia and unfolded protein response in hepatocellular carcinoma

4.1.1. Abstract

Background. Hepatocellular carcinoma (HCC) is a leading cause of cancer-related mortality. We previously showed that the inhibition of placental growth factor (PlGF) exerts antitumour effects and induces vessel normalisation, possibly reducing hypoxia. However, the exact mechanism underlying these effects remains unclear. Because hypoxia and endoplasmic reticulum stress, which activates the unfolded protein response (UPR), have been implicated in HCC progression, we assessed the interactions between PlGF and these microenvironmental stresses.

Methods. PlGF knockout mice and validated monoclonal anti-PlGF antibodies were used in a diethylnitrosamine-induced mouse model for HCC. We examined the interactions among hypoxia, UPR activation and PlGF induction in HCC cells.

Results. Both the genetic and pharmacological inhibitions of PlGF reduced the chaperone levels and the activation of the PKR-like endoplasmic reticulum kinase (PERK) pathway of the UPR in diethylnitrosamine-induced HCC. Furthermore, we identified that tumour hypoxia was attenuated, as shown by reduced pimonidazole binding. Interestingly, hypoxic exposure markedly activated the PERK pathway in HCC cells *in vitro*, suggesting that PlGF inhibition may diminish PERK activation by improving oxygen delivery. We also found that PlGF expression is upregulated by different chemical UPR inducers via activation of the inositol-requiring enzyme 1 pathway in HCC cells.

Conclusions. PlGF inhibition attenuates PERK activation, likely by tempering hypoxia in HCC via vessel normalisation. The UPR, in turn, is able to regulate PlGF expression, suggesting the existence of a feedback mechanism for hypoxia-mediated UPR that promotes the expression of the angiogenic factor PlGF. These findings have important implications for our understanding of the effect of therapies normalising tumour vasculature.

4.1.2. **Background**

Hepatocellular carcinoma (HCC) ranks as the second leading cause of cancer-related mortality worldwide [1]. Conventional chemotherapy is ineffective, and targeted therapy for advanced HCC with sorafenib, which targets Raf and platelet-derived and vascular endothelial growth factor (VEGF) receptor tyrosine kinase signalling, shows only a limited survival benefit [2].

The VEGF signalling pathways play central roles in angiogenesis [3]. VEGF-A binds to two tyrosine kinase receptors, VEGFR-1 and VEGFR-2. Most of the biological effects of VEGF-A are mediated by VEGFR-2 [3]. The placental growth factor (PlGF, four isoforms: PlGF-1-4) binds to VEGFR-1 and induces responses in endothelial, malignant, and immune cells [4]. VEGFR-1 has weak tyrosine kinase activity but a substantially higher binding affinity for VEGF-A than VEGFR-2. Although VEGFR-1 may act as a trap for VEGF-A, it also transmits signals in response to PlGF via its tyrosine kinase domains [4], [5]. A role for VEGFR-1 during tumour angiogenesis has been suggested [5], [6]. VEGFR-1 expression in HCC tissues is higher than that in peritumoural tissues and correlates with worse survival after resection [7], [8].

Importantly, genetic or pharmacological inhibition of PlGF reduces tumour growth and induces vessel normalisation in different preclinical models, including the diethylnitrosamine-induced HCC model [5], [9], [10]. Although anti-PlGF antibodies are controversial [11], evidence for the dose and specificity of the anti-PlGF-2 antibody clone 5D11D4 was previously provided [5]. Furthermore, disease stabilization for 12 months has been observed with anti-human PlGF monoclonal antibody TB403 in 2 out of 23 patients with advanced solid tumours refractory to standard therapy, confirming the need for a better understanding of the effect of PlGF inhibition on tumour biology [12].

The endoplasmic reticulum (ER) consists of a membranous network in which proteins are synthesised, post-translationally modified and folded. Therefore, the lumen houses chaperones, including protein disulfide isomerase A4 (PDIA4), calnexin (CANX), glucose-regulated protein-78 (GRP78) and -94 (GRP94) [12–14]. Several perturbations in the protein folding, such as hypoxia, glucose deprivation and oxidative stress, lead to the accumulation of unfolded proteins in the ER, a phenomenon called ER stress. ER stress triggers the unfolded protein response (UPR), which leads to an adaptive transcriptional response involved in protein quality control, redox homeostasis and angiogenesis. Paradoxically, the UPR also coordinates pro-apoptotic responses to ER stress [13], [14]. Interestingly, ER stress is present in human and experimental HCC, and modulating the UPR could hold important therapeutic potential [16], [17].

Three major ER stress sensors have been identified, as follows: PKR-like ER kinase (PERK), inositol-requiring enzyme 1 (IRE1) and activating transcription factor 6 (ATF6) [13]. The effect of ATF6 on cell fate is primarily cytoprotective, whereas the effect of IRE1 and PERK is presumed to be both pro-adaptive and pro-apoptotic [13], [14], [18]. However, inhibition of the PERK pathway induces antitumour effects in experimental HCC [14]. Following the release of GRP78, PERK phosphorylates the eukaryotic initiation factor 2α (eIF2α), leading to the attenuation of global translation. However, the translation of certain transcripts, such as activating transcription factor 4 (ATF4), is favoured. ATF4 induces genes involved in protein quality control, amino acid biosynthesis and the induction of apoptosis via C/EBP homologous protein (CHOP) [13]. IRE1 activation results in X-box-binding protein 1 (XBP1) mRNA splicing to generate a more active spliced XBP1 (XBP1s), which induces the genes involved in protein folding, such as endoplasmic reticulum DnaJ homolog 4 (ERDJ4) and CANX [19]. ATF6 is mobilised to the Golgi, where it is cleaved, releasing a transcriptionally active fragment, which in turn induces the expression of homocysteine-responsive ER-resident ubiquitin-like domain member 1 (HERPUD1), unspliced XBP1 (XBP1u) and chaperones including PDIA4 [12, 18].

In this study, we investigated whether vessel normalisation induced by PlGF blockade modulates the activation of the UPR or oxygen levels in experimental HCC and whether PlGF expression is regulated by ER stress. Collectively, we revealed that PlGF inhibition reduced hypoxia and the activation of the PERK pathway of the UPR in the tumour nodules of the carcinogen-induced mouse model. Furthermore, PlGF expression was upregulated by divergent ER stress stimuli in vitro. These results provide important insight into the reciprocal interactions between PlGF and the tumour microenvironment.

4.1.3. **Materials and Methods**

Animals

Wild type 129S2/SvPasCrl mice were purchased from Charles River (Belgium), and $PlGF^{-/-}$ knockout (PlGFKO) 129S2/SvPasCrl mice were obtained from the laboratory of Angiogenesis & Neurovascular link (Leuven, Belgium). Both were maintained as previously described [5]. All mice were genotyped by PCR before the start of the experiments. PlGF-deficient mice are born at normal Mendelian ratios and do not show any obvious vascular anomalities [20]. Five-week-old males received weekly intraperitoneal saline or diethylnitrosamine (DEN) (35 mg/kg, in saline) injections [21]. A murine anti-PlGF monoclonal antibody (validated clone 5D11D4 [5]; referred to as aPlGF) was obtained from Thrombogenics (Leuven, Belgium). Wild type mice that received DEN for 25 weeks were subsequently treated for 5 weeks with aPlGF (intraperitoneally, 25 mg/kg; 2x/week) or IgG (same regimen, n=10 in each group). Wild type mice that received saline for 25 weeks were subsequently treated for 5 weeks with aPlGF (same regimen) or IgG (same regimen, n=10 in each group). Pimonidazole HCl (Hypoxyprobe-1 Inc., Burlington, MA, USA) was intraperitoneally administered to 4 random mice per group in a single dose of 60 mg/kg one hour before sacrifice. Male PlGFKO mice and their wild type littermates received DEN for 30 weeks (n=12 in each group). After 30 weeks, blood was collected from the retro-orbital sinus under isoflurane anaesthesia. After macroscopic evaluation and the quantification of the number of hepatic tumours with a minimum diameter of 2 mm, the livers were fixed in 4% phosphate-buffered formaldehyde (Klinipath) and embedded in paraffin or snap frozen in liquid nitrogen. Tumour nodules were isolated by microdissection (Carl Zeiss, Bernreid, Germany) for expression analysis. Haematoxylin/eosin and reticulin staining were performed to assess the tumour burden, and the results were assessed by 2 independent observers. All protocols were approved by the Ethical Committee of experimental animals at the Faculty of Health Sciences, Ghent University, Belgium (ECD 11/52).

Cell culture

HepG2 cells (HB-8065; ATCC, Virginia, USA) were cultured in DMEM supplemented with 10% foetal bovine serum (Life Technologies, Ghent, Belgium).

Cells were incubated for 24 h or 48 h with a PERK inhibitor (0.3 μM; GSK2656157, NoVi Biotechnology, Shandong, China), an IRE1 inhibitor (8 μM; 4μ8C, Calbiochem, Massachusetts, USA), tauroursodeoxycholic acid (TUDCA, 1 mM), tunicamycin (1 μM), thapsigargin (150 nM) or quercetin (100-300 μM) and compared to equal volumes of solvent. All reagents were obtained from Sigma (Diegem, Belgium) unless stated otherwise. Hypoxic atmosphere (1% oxygen) was established in a hypoxic chamber (AnaeroGen; Oxoid, Basingstoke, UK). Experiments were carried out in quadruplicate and independently repeated three times.

Detailed information regarding total RNA extraction, quantitative real-time PCR, Western blotting, and immunohistochemistry is provided in the Supplementary Materials and Methods.

Statistics

Statistical analyses were performed using SPSS 21 (SPSS, Chicago, USA). Values are presented as the means ± SD or fold change relative to the mean expression in controls. Kolmogorov-Smirnov test was used to test for normality. Normally distributed data were subjected to the unpaired Student's t-tests. Multiple groups were compared by one-way analysis of variance (ANOVA) with Bonferroni correction. Non-normally distributed data were tested using the Mann-Whitney U-test. Two-tailed probabilities were calculated; a p-value less than 0.05 was considered statistically significant.

4.1.4. **Results**

PlGF inhibition induces antitumour effects and vessel normalisation in experimental HCC

First, we validated the previously reported antitumour effects and vessel normalisation induced by PlGF blockage [5, 9]. When wild type mice with established HCC were treated with aPlGF (n=10) or IgG (n=10) from 25 weeks onward for 5 weeks, 20% of mice receiving control IgG died, whereas only 10% died in the aPlGF group. Additionally, aPlGF-treated mice developed fewer nodules per liver (all sizes: 17.6 ± 4.9 after IgG versus 12.7 ± 3.2 after aPlGF; $p<0.05$). After 30 weeks of DEN administration to wild type (n=12) or PlGFKO (n=12) mice, 25% of wild type mice compared to 16% of PlGFKO mice succumbed, and fewer tumour nodules per liver were observed in PlGFKO mice (22.4 ± 4.8 in wild type versus 15.8 ± 6.2 in PlGFKO; $p<0.05$). Furthermore, several capillaries in control HCC nodules had an abnormal shape and size (Fig. S1A). In PlGF-blocked tumours, fewer capillaries, as shown by endoglin staining, were tortuous (aPlGF: $p<0.05$ and PlGFKO: $p<0.01$; Fig. S1B). These results confirm that PlGF blockage induces antitumour effects and partially normalises the abnormal tumour vessel structure.

PlGF inhibition reduced chaperone expression and activation of the Perk pathway in experimental HCC

We among others previously described the UPR pattern in DEN-induced HCC [16]. Here, we evaluated the effect of PlGF inhibition on this pattern in isolated tumours. The administration of aPlGF downregulated the mRNA expression of the ER stress-induced chaperones Grp78 and Grp94 in the tumours, compared to the IgG group ($p<0.05$; Fig. 1A). Additionally, the PlGFKO mice that received DEN for 30 weeks showed reduced levels of Grp78 ($p<0.05$) and Grp94 ($p<0.05$) in the tumours compared to their wild type littermates. Western blotting demonstrated reduced protein expression of Grp78 in the tumours of the aPlGF-treated and PlGFKO mice compared to those of the IgG-treated and wild type control group, respectively (Fig. 1B).
The Ire1-mediated splicing of Xbp1 was unaltered by PlGF inhibition (Fig. 1C). Accordingly, the targets of Xbp1s, Canx and Erdj4, showed a similar expression level compared to the corresponding controls.

Western blot analysis showed that the Perk-mediated phosphorylation of eIf2α was reduced in the HCC tissues of aPlGF-treated and PlGFKO mice compared to IgG-treated and wild type controls resp. (Fig. 1B and S2). Atf4 mRNA (aPlGF: $p<0.05$ and PlGFKO: $p<0.01$; Fig. 1D) and protein (Fig. 1B) expression in the nodules were decreased by PlGF inhibition. Further, Chop mRNA ($p<0.05$; Fig. 1D) and protein (Fig. 1B) levels were decreased. Next, we assessed the expression of Growth arrest and DNA damage-inducible protein (Gadd34), which initiates eIf2α dephosphorylation leading to a negative feedback loop of the Perk pathway [13]. Gadd34 levels were unaltered (Fig. 1B and 1D), indicating that PlGF inhibition did not enhance this negative feedback loop. Also, the mRNA and protein levels of the UPR sensor Perk itself were unaltered, excluding a direct effect of PlGF on Perk expression (Fig. S3A-B). Overall, these data indicate that PlGF inhibition indirectly diminished Perk signalling in HCC.

To examine the Atf6 pathway, Pdia4 and Herpud1 mRNA expression was monitored (Fig. 1A). Only Pdia4 mRNA was downregulated in the tumours of PlGFKO mice compared to their wild type littermates ($p<0.05$).

Importantly, wild type mice that received saline for 25 weeks and were subsequently treated with aPlGF for 5 weeks demonstrated no significant differences in the hepatic mRNA expression of the selected UPR targets compared to those receiving control IgG treatment (data not shown). Thus, these results demonstrate that PlGF inhibition reduces the intratumour expression of chaperones, such as Grp78, Grp94 and Pdia4, as well as the activation of the Perk pathway.

PlGF inhibition reduces intratumour hypoxia

We previously showed that PlGF inhibition induces vessel normalisation (Fig. S1; [5]). To investigate whether these vascular changes were functionally relevant or, in other words, whether PlGF inhibition effectively increased the oxygen levels in the hepatic tumours of the used mouse model, we applied pimonidazole, a molecule that binds only hypoxic areas *in vivo* and can be detected after sacrifice by immunohistochemistry (Fig. 2A). Indeed, administration of aPlGF significantly reduced tumoural pimonidazole binding ($p<0.05$; Fig. 2A-B). To improve the quantification method of the binding of pimonidazole, Western blotting for detection of pimonidazole adducts in isolated DEN-induced tumours was performed (Fig. 2C). Densitometry analysis confirmed that the liver tumours were characterized by increased pimonidazole binding and that administration of aPlGF reduced pimonidazole binding in the tumours ($p<0.05$; Fig. 2C-D).

Finally, aPlGF downregulated the expression of hypoxia-inducible genes *Glut1* ($p<0.05$) and *Pfk* ($p=0.07$) in the DEN-induced HCC (Fig. 2E). Thus, aPlGF effectively tempered the induction of tumour hypoxia.

Hypoxia activates the PERK pathway

Because PlGF inhibition reduced tumour hypoxia and PERK activation *in vivo*, we questioned whether hypoxia mediates PERK activation in HCC cells. Therefore, we examined the effect of hypoxia (<1% O_2 or 7.6 mmHg [24]) for 24 h or 48 h on the expression of PERK targets in HepG2 cells (Fig. 3A-B). Hypoxic exposure upregulated the mRNA expression of GRP78 ($p<0.001$), ATF4 ($p<0.05$), CHOP ($p<0.001$) and GADD34 ($p<0.001$). Furthermore, hypoxic exposure also increased the phosphorylation of eIF2α (24 h: $p<0.05$ and 48 h: $p<0.01$; Fig. 3B-C) and protein expression of ATF4 and CHOP (Fig. 3B). These data indicate that hypoxic exposure causes potent activation of the PERK pathway in HCC cells.

Activation of the IRE1 pathway promotes PlGF expression

Because the UPR is activated in HCC and PlGF inhibition is able to reduce activation of at least the Perk branch of the UPR, we next analysed the effect of ER stress on PlGF expression *in vitro*. Therefore, we used two different ER stress inducers: tunicamycin, an inhibitor of protein glycosylation, and thapsigargin, an inhibitor of sarcoplasmic/endoplasmic reticulum Ca^{2+} ATPases [13], [25]. Both significantly increased the mRNA levels of PlGF (Fig. 4A). As shown in Fig. 4B, an increase in the expression of faster-migrating unglycosylated PlGF was detected in HepG2 cells treated with tunicamycin.

The addition of the chemical chaperone TUDCA to tunicamycin-treated cells attenuated the ER stress-mediated induction of PlGF mRNA ($p<0.01$), whereas the addition of TUDCA to untreated cells had no effect on the PlGF mRNA levels (Fig. 4A). Quercetin, an IRE1 activator [26] (Fig. S4A), induced PlGF expression (300 μM: $p<0.01$; Fig. 4A-B). Accordingly, the addition of a small-molecule inhibitor of the IRE1 pathway reduced the tunicamycin-mediated upregulation of PlGF mRNA ($p>0,001$, Fig. 4A) and protein (Fig. 4B) levels. In contrast, the addition of a small-molecule inhibitor of the PERK pathway did not affect PlGF expression. These data show that the ER stress-mediated upregulation of PlGF is primary regulated by the IRE1 pathway of the UPR.

4.1.5. **Discussion**

Growing tumours are often subjected to deficiencies in vital nutrients and oxygen. These inadequate extracellular conditions can adversely affect the environment of the ER and impinge on the maturation of nascent proteins. We recently reported that PlGF inhibition induces vessel normalisation, potentially supporting the delivery of nutrients and oxygen to tumour cells [5], [27].

In this study, we found that PlGF inhibition reduced intratumour hypoxia and ER stress levels (Fig. 5). In fact, PlGF inhibition attenuates the carcinogen-induced upregulation of chaperones, such as Grp78 and Grp94, and the activation of the Perk pathway without affecting Ire1 activation. These chaperones and Perk activation are pro-survival and pro-proliferative modulators in tumour cells [13]–[15]. Probably, the aPlGF-mediated reduction of these UPR factors tempers the aggressive growth of HCC cells.

Recently, hypoxia-inducible factor-1α (HIF-1α), a key transcription factor in the cellular response to hypoxia, was shown to be an important driver of HCC growth [28]. In this study, we showed that PlGF inhibition reduced tumour hypoxia and PERK activation *in vivo* and that hypoxia activates the PERK/phospho-IF2α/ATF4 cascade in HCC cells, suggesting that tumour hypoxia mediates the observed PERK activation in HCC. Possibly, tumour hypoxia is also involved in the pronounced activation of PERK in other tumour types, such as glioma [29]. Finally, because PERK is, next to hypoxia, able to stimulate tumour growth [13], [30], the normalisation of tumoural oxygen levels by PlGF inhibition is able to dually target pro-survival signalling via reduced activation of the HIF-1α and PERK pathway.

Because PlGF inhibition was previously reported to reduce experimental liver fibrosis [31], the contribution of hypoxia and ER stress modulation, which both have been implicated in fibrogenesis [32], [33], to this outcome requires further investigation.

Whereas the UPR has previously been shown to upregulate several angiogenic factors, including VEGF [34], this is, to our knowledge, the first report to demonstrate the induction of PlGF by ER stress in tumour cells. Because studies on transgenic mice have revealed that PlGF expression is restricted to pathological conditions [35], the further investigation of the role of ER stress in the selectivity of PlGF expression to pathological conditions, potentially characterised by ER stress, is indicated. Finally, the role of the UPR in vessel abnormalisation induced by excessive production of angiogenic factors requires further investigation [35].

Vice versa, the effect of therapies modulating tumour angiogenesis on the UPR activation pattern, which affects tumour growth, is currently unknown. To our knowledge, this is the first study to provide evidence that vessel normalisation regulates the UPR in cancer cells. We speculate that anti-VEGF therapies may exert their therapeutic effect in part by UPR modulation.

The promising preclinical findings of anti-PlGF in HCC but also in other tumour types such as medulloblastoma [36], together with the acceptable safety profile of anti-PlGF administration in Phase I clinical trials, have attracted attention to PlGF as a potential target for therapy. However, improved understanding of the effect on tumour biology is required. This study indicates that anti-PlGF modulates the tumour microenvironment and cell adaptation mechanisms, which have been linked to tumour behavior [13], [37].

4.1.6. **Conclusions**

In summary, we have shown that inhibition of PlGF tempers UPR activation in HCC, most likely by improved oxygen delivery via the induced normalisation of tumour vessels. Moreover, we revealed that the UPR, in turn, regulates the expression of PlGF in HCC cells. Thus, our study sheds light on the reciprocal interactions between PlGF, hypoxia and the UPR and suggests that the antitumour effects of angiogenesis-modulating therapy could be mediated by modifying the tumour microenvironmental stresses in HCC.

4.1.7. List of abbreviations

HCC, hepatocellular carcinoma; VEGF, vascular endothelial growth factor; PlGF, placental growth factor; ER, endoplasmic reticulum; PDIA4, protein disulfide isomerase family A, member 4; CANX, calnexin; GRP78, glucose-regulated protein 78; GRP94, glucose-regulated protein 94; UPR, unfolded protein response; PERK, PKR-like endoplasmic reticulum kinase; IRE1, inositol-requiring enzyme 1; ATF6, activating transcription factor 6; eIF2α, eukaryotic initiation factor 2α; ATF4, activating transcription factor 4; CHOP, C/EBP homologous protein; XBP1, X-box-binding protein 1; XBP1s, spliced XBP1; ERDJ4,endoplasmic reticulum DnaJ homolog 4; XBP1u, unspliced XBP1; HERPUD1, homocysteine-responsive endoplasmic reticulum-resident ubiquitin-like domain member 1 protein; PlGFKO, PlGF knockout; DEN, diethylnitrosamine; aPlGF, anti-PlGF monoclonal antibody; TUDCA, tauroursodeoxycholic acid; GADD34, growth arrest and DNA damage-inducible protein; HIF-1α, hypoxia-inducible factor-1α.

4.1.8. Competing interests:

Bart Jonckx is an employee of Thrombogenics NV. The other authors have no conflicts of interest to declare.

4.1.9. Acknowledgements

The authors thank I. Desaegher and P. Vanwassenhove (Ghent University) for their expert technical assistance. The authors would also like to thank Dr. Sc. F. Heindryckx (Uppsala University, Department of Medical Biochemistry and Microbiology, Sweden) for sharing materials. This study was supported by the Research Foundation Flanders project 3G015612. HVV is senior clinical investigator of the Research Foundation Flanders. PC is Department Director, VIB Vesalius Research Center, K.U. Leuven, Belgium. YV is sponsored by a grant from the Special Research Fund (01D20012), Ghent University. DL, XV and SR are sponsored by the Research Foundation Flanders (1298213N, 1700214N and 11W5715N, respectively), and EB received an ‘Emmanuel van der Schueren’ grant from the Flemish League against Cancer. The funders had no role in study design, data collection and analysis, decision to publish, or preparation of the manuscript.

4.1.10. **References**

[1] International Agency for Research on Cancer. GLOBOCAN 2012. Estimated Incidence, Mortality and Prevalence Worldwide in 2012. Available at http://globocan.iarc.fr/Pages/fact_sheets_cancer.aspx. Accessed 12 December 2014.

[2] European Association For The Study Of The Liver, European Organisation For Research And Treatment Of Cancer. EASL-EORTC clinical practice guidelines: management of hepatocellular carcinoma. J Hepatol. 2012;56:908–43.

[3] Coulon S, Heindryckx F, Geerts A, Van Steenkiste C, Colle I, Van Vlierberghe H. Angiogenesis in chronic liver disease and its complications. Liver Int. 2011;31:146–62.

[4] De Falco S. The discovery of placenta growth factor and its biological activity. Exp Mol Med. 2012;44:1–9.

[5] Van de Veire S, Stalmans I, Heindryckx F, Oura H, Tijeras-Raballand A, Schmidt T, et al. Further pharmacological and genetic evidence for the efficacy of PlGF inhibition in cancer and eye disease. Cell. 2010;141:178–90.

[6] Fischer C, Jonckx B, Mazzone M, Zacchigna S, Loges S, Pattarini L, et al. Anti-PlGF inhibits growth of VEGF(R)-inhibitor-resistant tumors without affecting healthy vessels. Cell. 2007;131:463–75.

[7] Li T, Zhu Y, Qin C, Yang Z, Fang A, Xu S, et al. Expression and prognostic significance of vascular endothelial growth factor receptor 1 in hepatocellular carcinoma. J Clin Pathol. 2012;65:808–14.

[8] Ng IO, Poon RT, Lee JM, Fan ST, Ng M, Tso WK. Microvessel density, vascular endothelial growth factor and its receptors Flt-1 and Flk-1/KDR in hepatocellular carcinoma. Am J Clin Pathol. 2001;116:838–45.

[9] Heindryckx F, Coulon S, Terrie E, Casteleyn C, Stassen J-M, Geerts A, et al. The placental growth factor as a target against hepatocellular carcinoma in a diethylnitrosamine-induced mouse model. J Hepatol 2013;58:319–28.

[10] Fischer C, Mazzone M, Jonckx B, Carmeliet P. FLT1 and its ligands VEGFB and PlGF: drug targets for anti-angiogenic therapy? Nat Rev Cancer. 2008;8:942–56.

[11] Bais C, Wu X, Yao J, Yang S, Crawford Y, McCutcheon K, et al. PlGF blockade does not inhibit angiogenesis during primary tumor growth. Cell. 2010;141,166–77.

[12] Lassen U, Nielsen DL, Sørensen M, Winstedt L, Niskanen T, Stenberg Y, et al. A phase I, dose-escalation study of TB-403, a monoclonal antibody directed against PlGF, in patients with advanced solid tumours. Br J Cancer. 2012;106:678–84.

[13] Vandewynckel Y-P, Laukens D, Geerts A, Bogaerts E, Paridaens A, Verhelst X, et al. The paradox of the unfolded protein response in cancer. Anticancer Res. 2013;33:4683–94.

[14] Hetz C. The unfolded protein response: controlling cell fate decisions under ER stress and beyond. Nat Rev Mol Cell Biol. 2012;13:89–102.

[15] Rachidi S, Sun S, Wu BX, Jones E, Drake RR, Ogretmen B, et al. Endoplasmic reticulum heat shock protein gp96 maintains liver homeostasis and promotes hepatocellular carcinogenesis. J Hepatol. 2014;62:879-88.

[16] Vandewynckel Y-P, Laukens D, Bogaerts E, Paridaens A, Van den Bussche A, Verhelst X, et al. Modulation of the unfolded protein response impedes tumor cell adaptation to proteotoxic stress: a PERK for hepatocellular carcinoma therapy. Hepatol Int. 2014;9:93-104.

[17] Shuda M. Activation of the ATF6, XBP1 and grp78 genes in human hepatocellular carcinoma: a possible involvement of the ER stress pathway in hepatocarcinogenesis. J Hepatol. 2003;38:605–14.

[18] Han J, Back SH, Hur J, Lin Y-H, Gildersleeve R, Shan J, et al. ER-stress-induced transcriptional regulation increases protein synthesis leading to cell death. Nat Cell Biol. 2013;15:481–90.

[19] Shoulders MD, Ryno LM, Genereux JC, Moresco JJ, Tu PG, Wu C, et al. Stress-independent activation of XBP1s and/or ATF6 reveals three functionally diverse ER proteostasis environments. Cell Rep. 2013;3:1279–92.

[20] Carmeliet P, Moons L, Luttun A, Vincenti V, Compernolle V, De Mol M, et al. Synergism between vascular endothelial growth factor and placental growth factor contributes to angiogenesis and plasma extravasation in pathological conditions. Nat Med. 2001;7:575–83.

[21] Heindryckx F, Mertens K, Charette N, Vandeghinste B, Casteleyn C, Van Steenkiste C, et al. Kinetics of angiogenic changes in a new mouse model for hepatocellular carcinoma. Mol Cancer. 2010;9:219.

[22] Yang X, Zhang Y, Yang Y, Lim S, Cao Z, Rak J, et al. Vascular endothelial growth factor-dependent spatiotemporal dual roles of placental growth factor in modulation of angiogenesis and tumor growth. Proc Natl Acad Sci U S A. 2013;110:13932–7.

[23] Hedlund E-ME, Yang X, Zhang Y, Yang Y, Shibuya M, Zhong W, et al. Tumor cell-derived placental growth factor sensitizes antiangiogenic and antitumor effects of anti-VEGF drugs. Proc Natl Acad Sci U S A. 2013;110:654–9.

[24] Riedl CC, Brader P, Zanzonico PB, Chun YS, Woo Y, Singh P, et al. Imaging hypoxia in orthotopic rat liver tumors with iodine 124-labeled iodoazomycin galactopyranoside PET. Radiology. 2008;248:561–70.

[25] Errico M, Riccioni T, Iyer S, Pisano C, Acharya KR, Persico MG, et al. Identification of placenta growth factor determinants for binding and activation of Flt-1 receptor. J Biol Chem. 2004;279:43929–39.

[26] Wiseman RL, Zhang Y, Lee KPK, Harding HP, Haynes CM, Price J, et al. Flavonol activation defines an unanticipated ligand-binding site in the kinase-RNase domain of IRE1. Mol Cell. 2010;38:291–304.

[27] Maes H, Kuchnio A, Peric A, Moens S, Nys K, De Bock K, et al. Tumor vessel normalization by chloroquine independent of autophagy. Cancer Cell. 2014;26:190–206.

[28] Choi SH, Kwon O-J, Park JY, Kim DY, Ahn SH, Kim SU, et al. Inhibition of tumour angiogenesis and growth by small hairpin HIF-1α and IL-8 in hepatocellular carcinoma. Liver Int. 2014;34:632–42.

[29] Hou X, Liu Y, Liu H, Chen X, Liu M, Che H, et al. PERK silence inhibits glioma cell growth under low glucose stress by blockage of p-AKT and subsequent HK2's mitochondria translocation. Sci Rep. 2015;12:9065.

[30] Mujcic H, Nagelkerke A, Rouschop KMA, Chung S, Chaudary N, Span PN, et al. Hypoxic activation of the PERK/eIF2α arm of the unfolded protein response promotes metastasis through induction of LAMP3. Clin Cancer Res. 2013;19:6126–37.

[31] Van Steenkiste C, Ribera J, Geerts A, Pauta M, Tugues S, Casteleyn C, et al. Inhibition of placental growth factor activity reduces the severity of fibrosis, inflammation, and portal hypertension in cirrhotic mice. Hepatology. 2011;53:1629–40.

[32] Zhan L, Huang C, Meng X-M, Song Y, Wu XQ, Yang Y, et al. Hypoxia-inducible factor-1alpha in hepatic fibrosis: A promising therapeutic target. Biochimie. 2015;108C:1–7.

[33] Li X, Wang Y, Wang H, Huang C, Huang Y, Li J. Endoplasmic reticulum stress is the crossroads of autophagy, inflammation, and apoptosis signaling pathways and participates in liver fibrosis. Inflamm Res. 2015;64:1–7.

[34] Pereira ER, Liao N, Neale GA, Hendershot LM. Transcriptional and post-transcriptional regulation of proangiogenic factors by the unfolded protein response. PLoS One. 2010;5:e12521.

[35] Autiero M, Luttun A, Tjwa M, Carmeliet P. Placental growth factor and its receptor, vascular endothelial growth factor receptor-1: novel targets for stimulation of ischemic tissue revascularization and inhibition of angiogenic and inflammatory disorders. J Thromb Haemost. 2003;1:1356–70.

[36] Snuderl M, Batista A, Kirkpatrick ND, Ruiz de Almodovar C, Riedemann L, Walsh EC, et al. Targeting placental growth factor/neuropilin 1 pathway inhibits growth and spread of medulloblastoma. Cell. 2013;152:1065–76.

[37] Fels DR and Koumenis C. The PERK/eIF2alpha/ATF4 module of the UPR in hypoxia resistance and tumor growth. Cancer Biol Ther. 2006;5:723–8.

4.1.11. **Figures**

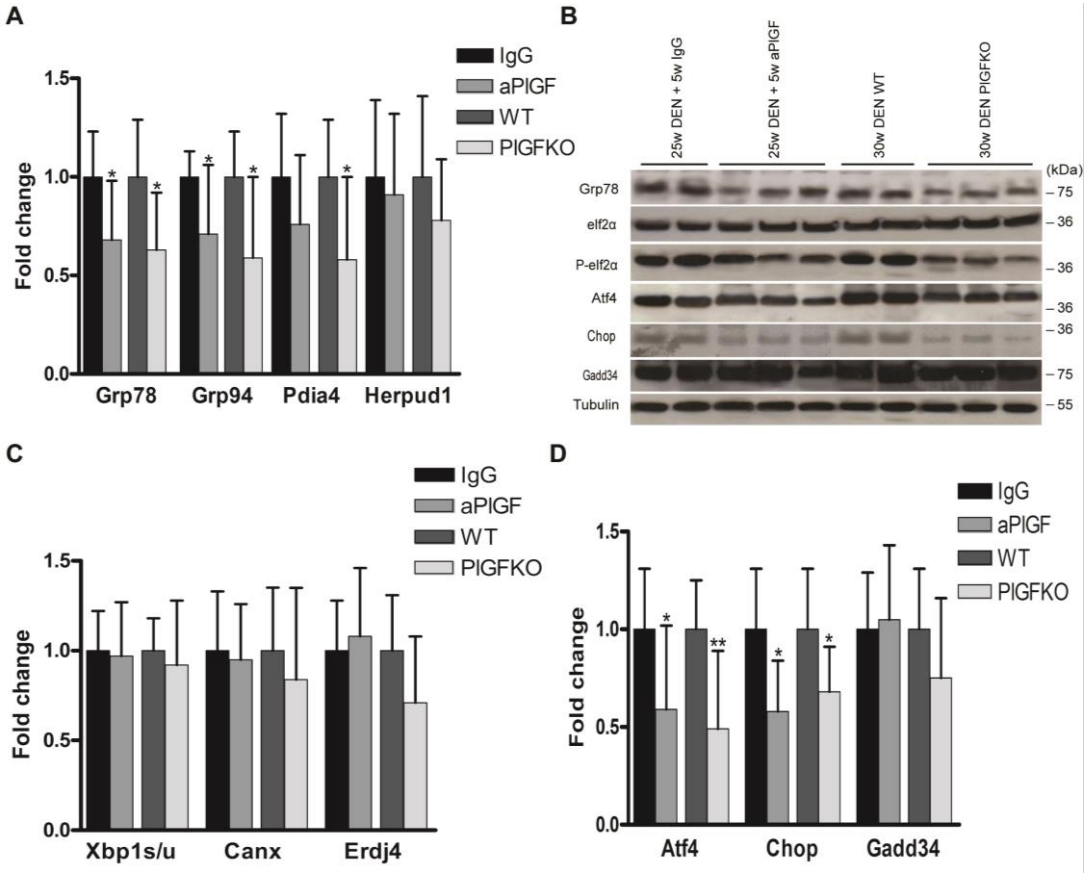

Fig. 1. PlGF inhibition tempers the activation of the UPR in an orthotopic mouse model of HCC. (A) Quantitative real-time PCR analysis of the ER chaperones *Grp78*, *Grp94* and *Pdia4* and *Herpud1* in aPlGF-treated and PlGFKO mice. Relative fold changes were calculated using the ΔΔCT method. (B) Immunoblotting for UPR-mediated proteins. (C) Quantitative real-time PCR analysis of ER chaperones of Ire1-mediated splicing of *Xbp1* and Ire1 targets *Canx* and *Erdj4*, (D) Perk-related genes *Atf4*, *Chop* and *Gadd34*. *p<0.05, **p<0.01, ***p<0.001. IgG= 25w DEN + 5w IgG, aPlGF= 25w DEN + 5w aPlGF, WT= 30w DEN in wild type (WT) mice, PlGFKO= 30w DEN in $PlGF^{-/-}$ knockout mice.

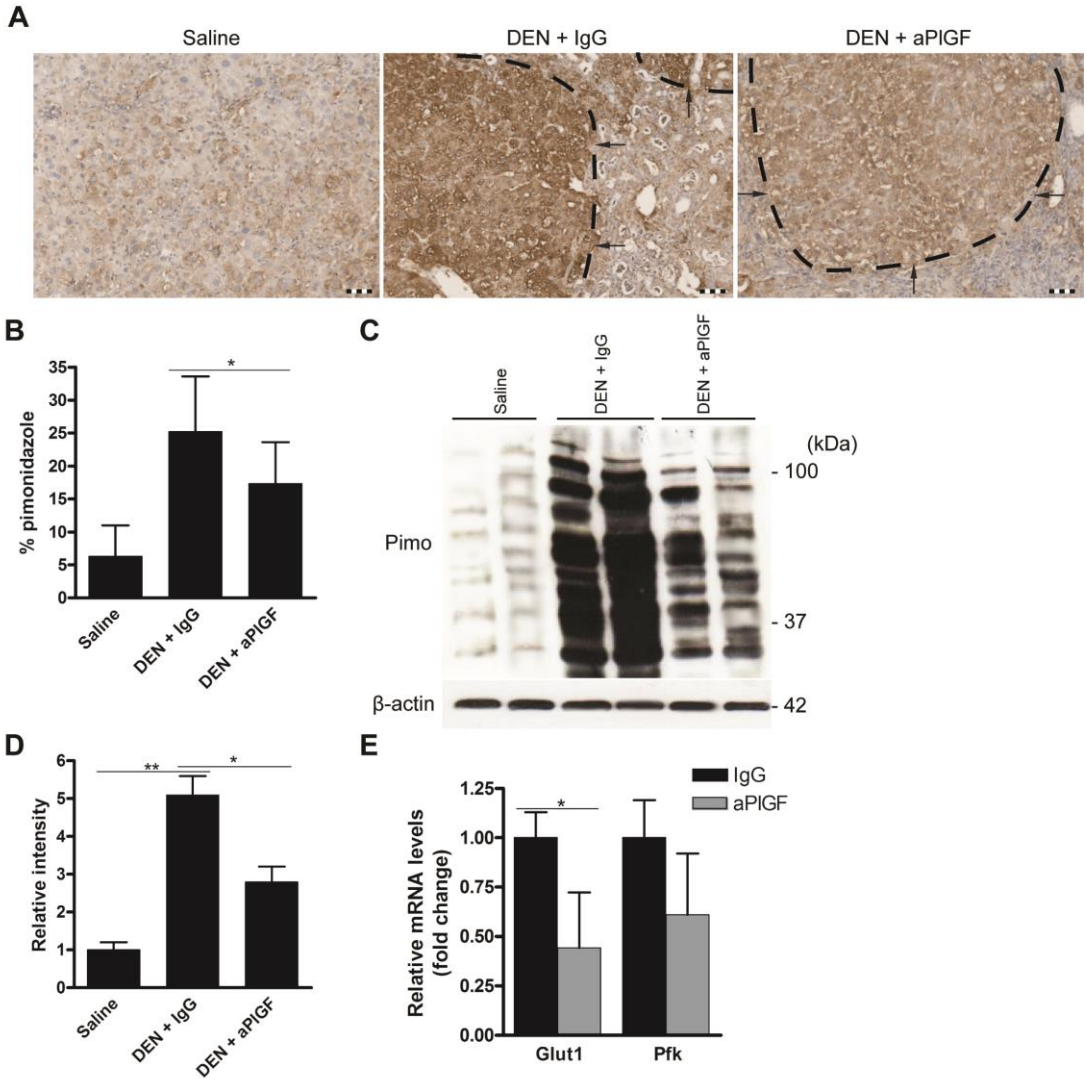

Fig. 2. PlGF inhibition reduces intratumour hypoxia in experimental HCC. (A) Immunostaining for pimonidazole in mouse livers following the indicated treatment. Arrows indicate tumours. Scale bars: 100 µm. (B) Quantification of the immunostaining for pimonidazole. (C) Lysates of control liver tissue or isolated DEN-induced tumours were subjected to Western blotting for detection of pimonidazole adducts (Pimo). Blotting of β-actin is shown as a loading control. (D) Densitometry analysis of the pimonidazole blot in (C). (E) Real-time PCR analysis of *Glut1* and *Pfk* mRNA levels in tumour tissues. IgG= 25w DEN + 5w IgG, aPlGF= 25w DEN + 5w aPlGF. Data are presented as the means ± SD. *p<0.05.

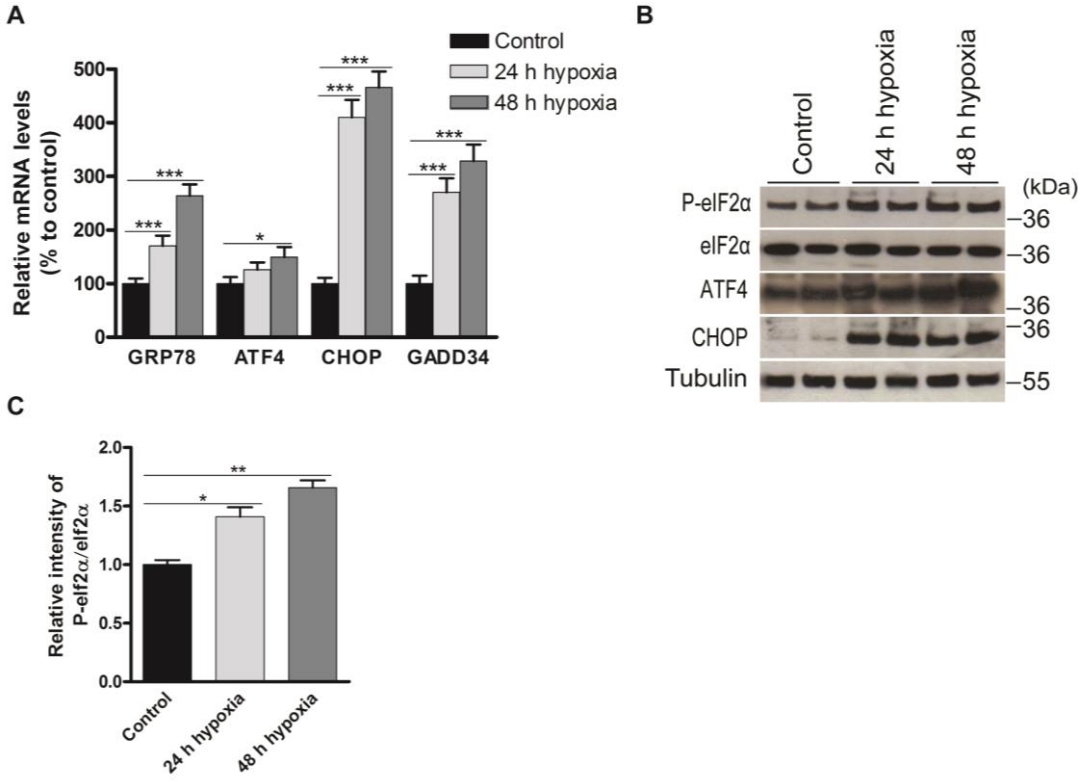

Fig. 3. Hypoxia activates the PERK pathway in HCC cells. (A) HepG2 cells were cultured in normoxia or hypoxia for 24 h or 48 h. The PERK targets, *GRP78*, *ATF4*, *CHOP* and *GADD34* mRNA were detected by Real-time PCR analysis. (B) Expressions of phospho-eIF2α, eIF2α, ATF4, and CHOP protein were detected using Western blotting. All experiments were repeated three times with similar results. (C) Densitometry analysis of the ratio of phosphorylated eIf2α to total eIf2α bands normalised to tubulin and relative to the corresponding control. Quantitative results of the phosphorylation of eIf2α are presented as the mean ± SD. *p<0.05, **p<0.01, ***p<0.001.

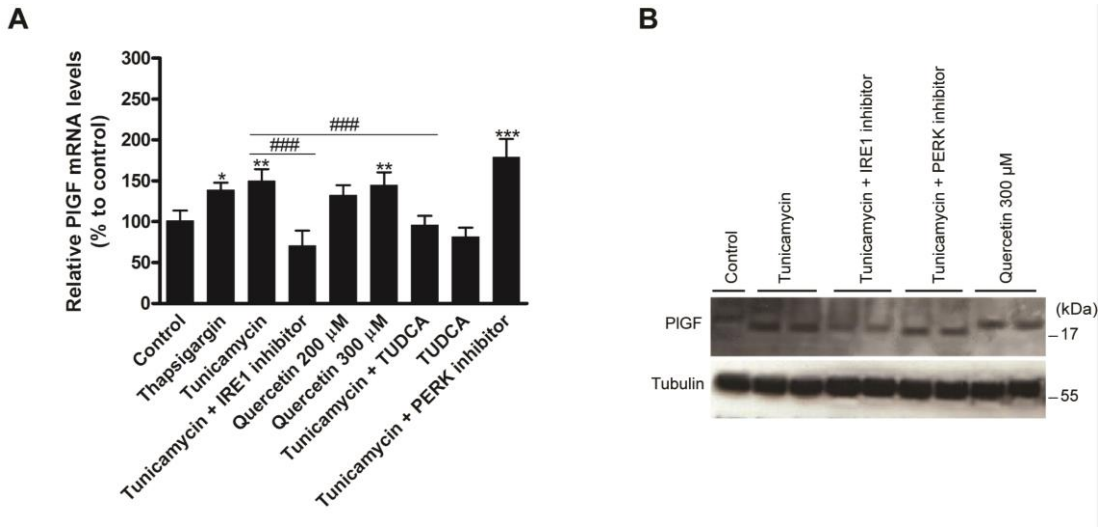

Fig. 4. ER stress induces PlGF expression in HepG2 cells. (A) Relative *PlGF* mRNA levels in HepG2 cells treated for 48 hours with the indicated treatments. *p<0.05, **p<0.01, ***p<0.001 compared to control. $^{\#}$p<0.05, $^{\#\#}$p<0.01, $^{\#\#\#}$p<0.001 compared to the indicated group. TUDCA: tauroursodeoxycholic acid. (B) Immunoblotting of cell lysates was performed to detect PlGF protein levels. All experiments were repeated three times with similar results.

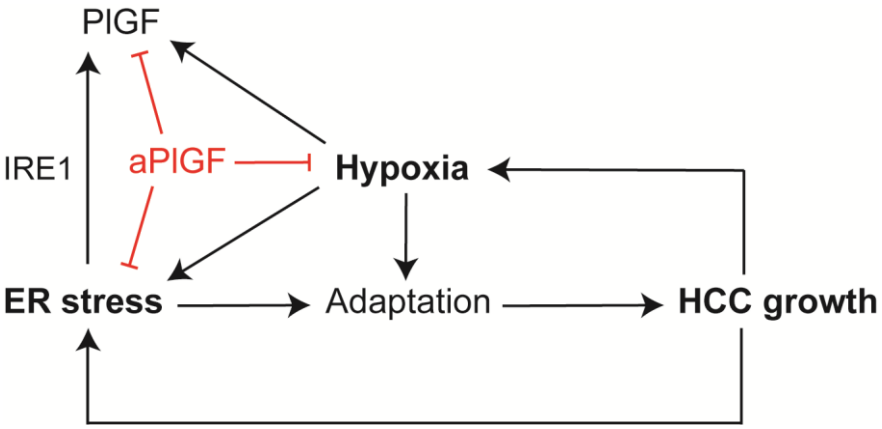

Fig. 5. Schematic model outlining the interactions among PlGF, ER stress and hypoxia and their effects on HCC growth.

4.1.12. **Supplementary Figures**

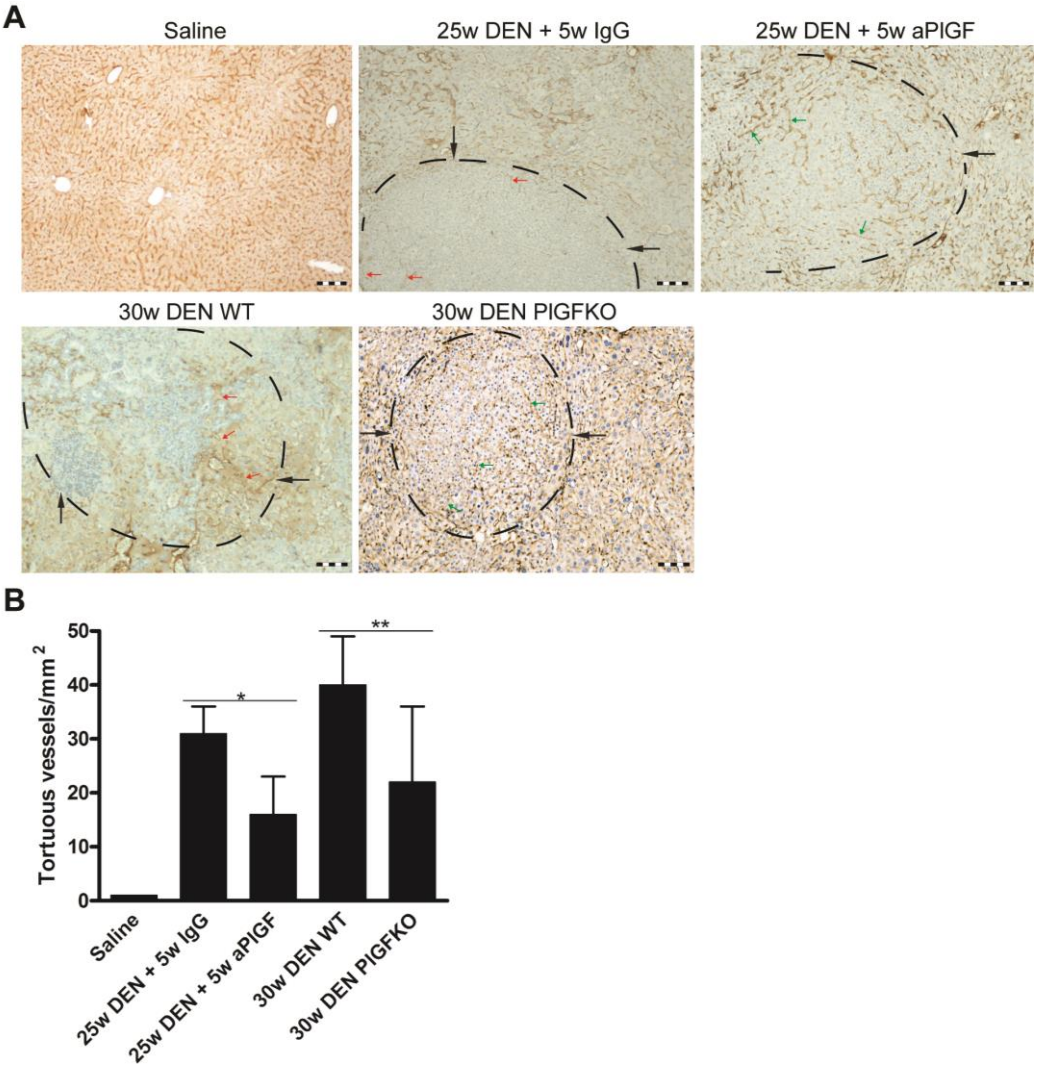

Fig. S1. PlGF blockage induces vessel normalization. (A) Immunostaining for the endothelial marker endoglin (CD105). In HCC nodules, the capillary network is chaotically organized with tortuous vessels (indicated by red arrows) laying at large distances from each other. However, the capillaries in HCC after aPlGF treatment or in PlGFKO mice have a more normal appearance with regular pattern, size, and shape (indicated by green arrows). Black arrows and dashed lines indicate tumours. (B) Quantification of tortuous vessels per mm^2; n= 5; *p<0.05, **p<0.01.

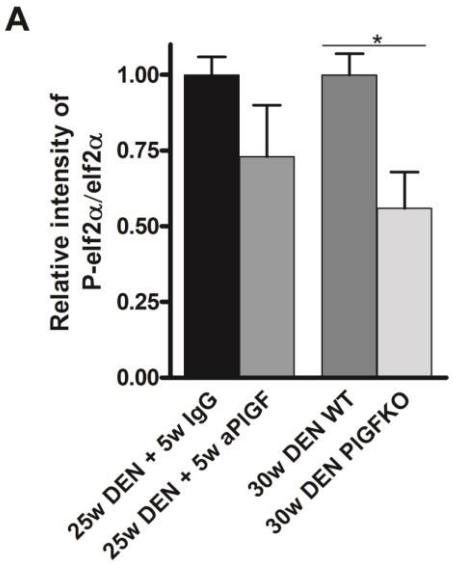

Fig. S2. Densitometry analysis of the phosphorylation of eIf2α in isolated HCC. (A) Densitometry analysis of the ratio of phosphorylated eIf2α to total eIf2α bands normalized to tubulin and relative to the corresponding control. Quantitative results of phosphorylation of eIf2α are presented as the mean ± SD. *p<0.05.

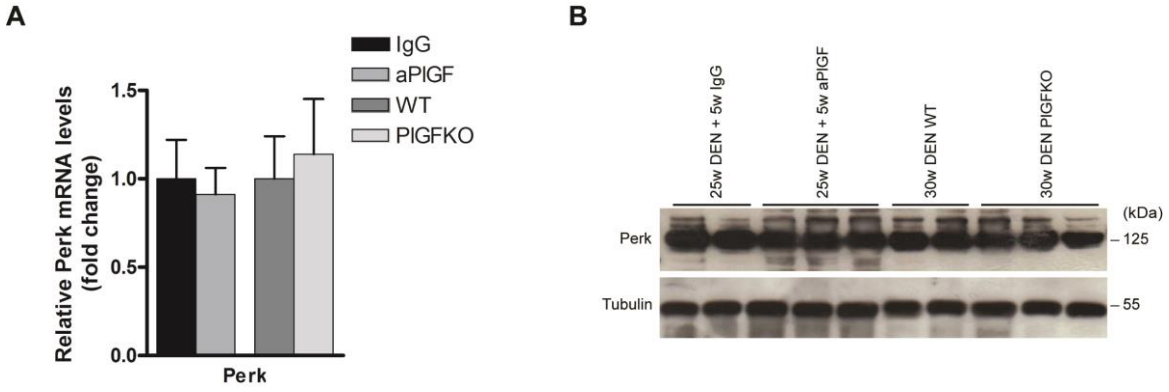

Fig. S3. Effect of PlGF inhibition on the expression of the UPR sensor Perk. (A) Quantitative real-time PCR analysis of Perk. Relative fold changes were calculated using the ΔΔCT method. IgG= 25w DEN + 5w IgG, aPlGF= 25w DEN + 5w aPlGF, WT= 30w DEN in wild type (WT) mice, PlGFKO= 30w DEN in PlGF$^{-/-}$ knockout mice. (B) Immunoblotting for Perk protein.

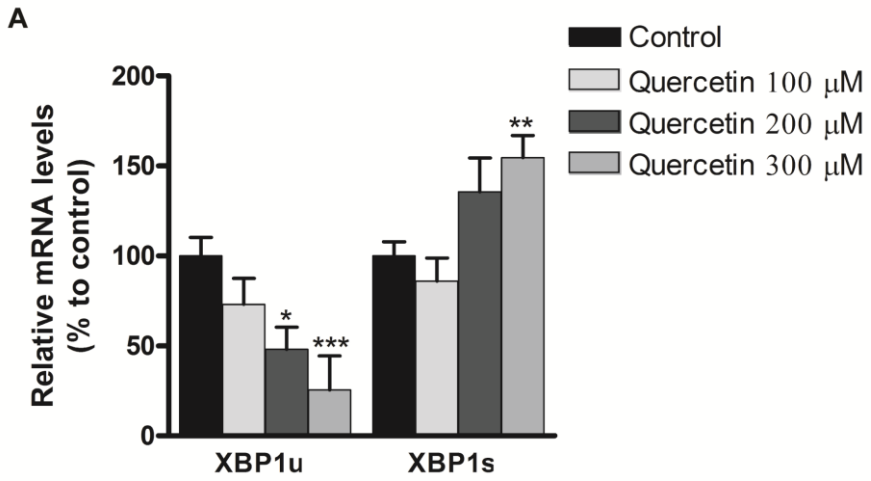

Fig. S4. Validation of quercetin as activator of the IRE1 RNase. (A) Quantitative real-time PCR analysis of unspliced and spliced XBP1 mRNA to evaluate the effect of 100-300 μM quercetin for 24 hours on HepG2 cells. Results are representative of 2 independent experiments. *p<0.05, **p<0.01, ***p<0.001.

5. Proteasome inhibition and the UPR in hepatocellular carcinoma

5.1. Next-generation proteasome inhibitor oprozomib synergizes with modulators of endoplasmic reticulum stress in hepatocellular carcinoma

Manuscript in preparation, patent application filed.

Yves-Paul Vandewynckel[1], Céline Coucke[1], Debby Laukens[1], Lindsey Devisscher[1], Annelies Paridaens[1], Eliene Bogaerts[1], Anja Van den Bussche[1], Sarah Raevens[1], Xavier Verhelst[1], Christophe Van Steenkiste[1], Louis Libbrecht[2], Anja Geerts[1], Hans Van Vlierberghe[1]

[1]Department of Hepatology and Gastroenterology, Ghent University, Belgium

[2]Department of Pathology, Ghent University Hospital, Belgium

Next-generation proteasome inhibitor oprozomib synergizes with modulators of endoplasmic reticulum stress in hepatocellular carcinoma

5.1.1. Abstract

Background & Aims:

Advanced hepatocellular carcinoma (HCC) responds poorly to conventional systemic therapies. The first-in-class proteasome inhibitor bortezomib has been approved in clinical use for hematologic malignancies and has shown modest activity in a variety of solid tumours including HCC. However, a considerable proportion of subjects fail to respond and experience adverse events. Recently, the next-generation orally bioavailable proteasome inhibitor oprozomib was developed. In this study, we assessed the efficacy of oprozomib and its effects on the unfolded protein response (UPR) in HCC.

Methods:

Oprozomib was evaluated in vitro and in diethylnitrosamine-induced and xenograft mouse models for HCC. Also, the role of the UPR in HCC cells treated with oprozomib was determined.

Results:

Oprozomib dose-dependently reduced the viability and proliferation of human HCC cells. Unexpectedly, oprozomib-treated cells displayed reduced cytoprotective ATF6-mediated transcription, whereas PERK and IRE1 pathway activation was not observed. However, oprozomib increased pro-apoptotic UPR-mediated protein levels, including CHOP, by prolonging their half-life. Supplementary boosting UPR activity improved the sensitivity of HCC cells to oprozomib, an effect that was blocked by inhibition of PERK. Oral oprozomib monotherapy displayed significant antitumour effects in the experimental HCC models, and importantly, the combination of oprozomib with different UPR activators further improved the antitumour efficacy in vitro and in vivo by stimulating UPR-induced apoptosis without cumulative toxicity.

Conclusion:

Next-generation proteasome inhibition by oprozomib significantly dysregulates UPR activation in HCC. This finding can be exploited to enhance the antitumour efficacy by combining oprozomib with UPR modulators for the treatment of advanced HCC.

5.1.2. **List of nonstandard abbreviations**

HCC, hepatocellular carcinoma; ER, endoplasmic reticulum; GRP78, glucose-regulated protein, 78 kDa; OZ, oprozomib; UPR , unfolded protein response; PERK, PKR-like endoplasmic reticulum kinase; IRE1, inositol-requiring enzyme-1; ATF6, activating transcription factor 6; eIF2α, eukaryotic initiation factor 2α; ATF4, activating transcription factor 4; CHOP, c/EBP-homologous protein; XBP1u, unspliced X-box-binding protein 1; XBP1s, spliced X-box-binding protein 1; ERDJ4, endoplasmic reticulum DnaJ homolog 4; RIP, intramembrane proteolysis; S1P, site-1 protease; S2P, site-2 protease; GRP94, glucose-regulated protein, 94 kDa; PDIA4, protein disulfide isomerase A4; CALR, calreticulin; ERO1L, endoplasmic oxidoreductin-1-like protein; HERPUD1, homocysteine-inducible, ER stress-inducible, ubiquitin-like domain member 1; DEN, diethylnitrosamine; NAC, N-acetyl-L-cysteine; GADD34, growth arrest and DNA damage inducible 34; SREBP-1, sterol regulatory element binding protein-1.

5.1.3. **Introduction**

Hepatocellular carcinoma (HCC) is the second leading cause of cancer-related mortality worldwide [1]. Resection and transplantation are the only potentially curative treatments available following detection of a small HCC [2]. For the majority of patients with locally advanced disease, however, the multi-kinase inhibitor sorafenib and transarterial embolization are the only approved treatments. Unfortunately, both provide a limited survival benefit [2].

The ubiquitin-proteasome pathway is responsible for the degradation of misfolded proteins as well as short-lived mediators of signalling cascades regulating cell proliferation and survival pathways [3]. Proteasome inhibition leads to accumulation of these substrates, resulting in concomitant activation of pro- and anti-proliferative signals, disruption of cell-cycle regulation, and, ultimately, apoptosis. Bortezomib is a first-in-class proteasome inhibitor clinically used for the treatment of multiple myeloma. Bortezomib-induced cell death is related with induction of endoplasmic reticulum (ER) stress, inhibition of nuclear factor kappa B, activation of caspase-8 and generation of oxidative stress [3], [4]. Multiple clinical trials have demonstrated that this small-molecule possesses antitumour activity in a variety of human cancers [5], [6]. Despite promising preclinical results [5], a multicentre, single-arm, phase II trial assessing the activity of bortezomib in HCC has demonstrated modest antitumour effects, indicating intrinsic or acquired resistance [4], [7]. In addition, the majority of the patients developed adverse events including peripheral neuropathy [7]. However, the good clinical outcome of bortezomib in myeloma led to the development of next-generation proteasome inhibitors, such as carfilzomib, that selectively and irreversibly bind to the proteasome aspiring to enhance inhibition, improve antitumour activity and decrease toxicity by reducing off-target effects, such as peripheral neuropathy [8], [9]. A phase III trial showed that intravenously administered carfilzomib improved progression-free survival in myeloma with a favourable risk-benefit profile [10]. Recently, an orally bioavailable analogue of carfilzomib, called oprozomib (OZ), was developed [9].

Proteasome inhibition is thought to trigger accumulation of misfolded proteins in the ER, which activates the unfolded protein response (UPR) [4]. Three major ER stress transducers have been identified: PKR-like endoplasmic reticulum kinase (PERK), inositol-requiring enzyme-1 (IRE1) and activating transcription factor 6 (ATF6) [11]. Following release of chaperone glucose-regulated protein, 78 kDa (GRP78), PERK phosphorylates eukaryotic initiation factor 2α (eIF2α) leading to attenuation of global translation. However, the phosphorylated form of this factor favours selective translation of activating transcription factor 4 (*ATF4*), which regulates genes involved in protein quality control, amino acid biosynthesis as well as apoptosis regulators such as c/EBP-homologous protein (*CHOP*) [11]. Activation of IRE1 results in splicing of unspliced X-box-binding protein 1 (*XBP1u*) mRNA to generate a more active spliced XBP1 (*XBP1s*), which induces genes involved in protein folding such as endoplasmic reticulum DnaJ homolog 4 (*ERDJ4*), protein degradation and redox homeostasis [11]. ATF6 is mobilized to the Golgi where it is cleaved by regulated intramembrane proteolysis (RIP), which involves the site-1 (S1P) and site-2 (S2P) proteases, releasing a transcriptionally active fragment, which in turn induces the expression of chaperones, such as GRP78, glucose-regulated protein, 94 kDa (GRP94), protein disulfide isomerase A4 (PDIA4), calreticulin (CALR) and endoplasmic oxidoreductin-1-like protein (ERO1L), XBP1u and of proteins stimulating protein degradation, such as homocysteine-inducible, ER stress-inducible, ubiquitin-like domain member 1 (HERPUD1) [12].

In this study, we provide a molecular clue to the how OZ might work and identified the therapeutic potential of OZ in monotherapy or in combination with modulators of the induced interplay with the UPR *in vitro* and in mouse models for HCC.

5.1.4. **Materials and Methods**

Cell culture

HepG2 (ATCC, Virginia, USA) and Huh7 cells (JCRB, Japan) were cultured in Dulbecco's Modified Eagle's medium supplemented with 10% foetal bovine serum (Life Technologies, Ghent, Belgium). Cells were incubated for 48 hours with oprozomib (100-400 nM; ApexBio, USA), tunicamycin (1 μg/ml; Sigma, Diegem, Belgium), PERK inhibitor (14 μM; GSK2656157, Chengdu novi, Shandong, China), salubrinal (50 μM; Sigma), IRE1 inhibitor (25 μM; 4μ8C, Calbiochem, Massachusetts, USA), cycloheximide (5 μM; Sigma), 1,10-phenanthroline (5-50 μM; Sigma), ascorbic acid (50 μM; Sigma), nelfinavir (10 μM; Sigma) or pre-treated with N-acetyl-L-cysteine (2 hours; 5 μM; Sigma) and compared to equal volumes of solvent as control. Each condition was performed in quadruplicate.

Animals

Wild-type 129S2/SvPasCrl mice were purchased from Charles River, Belgium, and were housed as previously described [13]. The animals had free access to water and to a commercial chow (mice maintenance chow, Carfil Labofood, Pavan Service, Belgium). Five-week-old male mice received weekly intraperitoneal injections with saline or diethylnitrosamine (DEN) (35 mg/kg, Sigma) for 25 weeks. Then, 4 DEN-treated groups (n=12) were treated for 4 weeks with oprozomib (intragastric 30 mg/kg/day for 3 consecutive days per week) alone or in combination with salubrinal (intraperitoneally 1 mg/kg/day) or nelfinavir (intraperitoneally 250 mg/kg/day) and compared to a similar volume of vehicle. Blood was collected from the retro-orbital sinus under isoflurane anaesthesia. After macroscopic evaluation and quantification of the number of hepatic tumours, all organs were fixed in 4% phosphate-buffered formaldehyde (Klinipath, Belgium) and embedded in paraffin or snap frozen in liquid nitrogen. Haematoxylin/eosin and reticulin stainings were performed to assess tumour burden and the results were blindly evaluated by two independent observers (YV and CC).

For the xenograft model, HepG2 cells ($6x10^6$) were resuspended in 100 µl serum-free media and mixed with 100 µl Matrigel (BD Biosciences, Bedford, MA, USA). Cell/Matrigel mixture was injected subcutaneously into the right flank of 8-week-old athymic nude ($Foxn1^{nu}/Foxn1^{nu}$) mice housed in filter-topped cages. Tumour dimensions were recorded three times per week with a digital calliper starting with the first day of treatment. Tumour volumes were calculated using the following formula: volume (mm^3) = $ab^2/2$, where b was the smaller dimension. When tumours reached 150 mm^3, animals were randomized into four groups (n=6) with the same treatment regime as the DEN-treated mice plus monotherapy with salubrinal (intraperitoneally 1 mg/kg/day) or nelfinavir (intraperitoneally 250 mg/kg/day). The ethical committee of experimental animals at Ghent University, Belgium, approved the protocols (ECD 13/39).

Detailed information of MTT, TUNEL, caspase-3/7 activity, bromodeoxyuridine (BrdU) incorporation assays, total RNA extraction, quantitative real-time PCR and Western blotting is provided in the Supplementary Materials and Methods.

Statistics

Statistical analyses were performed using SPSS 21 (SPSS, Chicago, USA). Data are presented as the mean ± SD or percentage relative to controls. Variables were tested for normality using the Shapiro-Wilk test. Normally distributed data were subjected to the unpaired student's t-tests. Data involving more than two groups were assessed by one-way analysis of variance (ANOVA) with Bonferroni's post-hoc test. Non-normally distributed data were tested using the Mann-Whitney-U test. The chi-squared test was used to compare mortality. The IC50 values were obtained using the Bliss method. Interpretation of combination index (CI) values, as calculated by the method of Chou and Talalay [14] using CompuSyn software (ComboSyn Inc., Paramus, NJ), is defined such that CI= 1 indicates an additive effect, and CI<1 and a CI>1 indicate synergism and antagonism, respectively. Reported p-values were two-sided and considered significant when less than 0.05.

5.1.5. **Results**

Supplementary ER stress improves the sensitivity of HCC cells to proteasome inhibition

In HepG2 cells, 48 hours of incubation with 100-400 nM OZ dose-dependently reduced cell viability, as shown by a tetrazolium MTT spectrophotometric assay ($p<0.001$; Fig. 1A and Table S1). Combination with the chemical ER stress inducer tunicamycin or with the recently developed small-molecules selectively inhibiting the IRE1 or PERK pathway or salubrinal, which inhibits eIF2α dephosphorylation, was evaluated. Addition of tunicamycin or salubrinal synergistically decreased cell viability ($p<0.05$, CI=0.71 and 0.60 respectively). As shown by BrdU incorporation, OZ decreased the proliferation rate ($p<0.001$; Fig. 1B), whereas the addition of tunicamycin or salubrinal further impeded cell proliferation ($p<0.05$). As revealed by activation of executioner caspase-3/7, OZ dose-dependently induced apoptosis in HepG2 cells ($p<0.001$; Fig. 1C). Again, addition of tunicamycin or salubrinal further increased caspase-3/7 activity ($p<0.001$). Although the IRE1 and PERK inhibitors were previously validated [15], these compounds did not affect the sensitivity of HCC cells to OZ. Since tunicamycin increased the sensitivity, but is not clinically applicable because of its toxicity, the HIV protease inhibitor nelfinavir, which represents one of the few clinically applicable ER stress-inducing agents [16], was tested. Interestingly, also addition of nelfinavir synergistically increased the sensitivity to OZ (CI=0.68). The MTT viability and BrdU incorporation experiments were repeated in Huh7 cells with similar results (Fig. S1A-B and Table S1).

Next, we questioned whether the efficacy of other proteasome inhibitors, such as the first-in-class bortezomib, could also be enhanced by combination with UPR inducers. Interestingly, a similar synergistic increase in antiproliferative efficacy was observed with 25 nM bortezomib in combination with tunicamycin, nelfinavir or salubrinal in HepG2 cells (Fig. S2A-B). Finally, we assessed whether OZ or bortezomib altered the chemosensitivity of HepG2 cells to 25-100 μM doxorubicin and observed that proteasome inhibition did not alter the chemosensitivity (data not shown). Together, these results indicate that the sensitivity of human HCC cells to proteasome inhibition is enhanced by ER stress.

Antiproliferative effect of oprozomib depends on the build-up of proteotoxic stress

After 24 hours of incubation, no significant alteration in proliferation rate, caspase-3 activity or cell viability is induced by 400 nM OZ (data not shown). However, after 48 hours, as stated above, OZ displayed robust growth-inhibitory effects, suggesting sufficient time is required to build-up proteotoxicity induced by proteasome inhibition in HCC cells. To demonstrate that proteotoxic stress caused by OZ originates during the synthesis of new proteins, cycloheximide was used to inhibit protein synthesis. Interestingly, treatment with cycloheximide readily increased proliferation ($p<0.001$; Fig. S3A) and cell viability ($p<0.01$; Fig. S3B) and reduced caspase-3 induction ($p<0.001$; Fig. S3C) of OZ-challenged HepG2 cells.

Since bortezomib generates oxidative stress, which is crucial for its antitumour activity [17] and is reported to induce ER stress [11], we investigated whether the antiproliferative effect of OZ is also dependent on oxidative stress. Therefore, we measured cell viability and proliferation after treatment with OZ only or in combination with the antioxidants N-acetyl-L-cysteine (NAC) or ascorbic acid in HepG2 cells. Surprisingly, addition of these antioxidants to OZ did not alter its antitumour action (Fig. S3A-C). Thus, these findings suggest that the build-up of proteotoxic, and not oxidative, stress is indispensable for the effects of OZ.

Oprozomib upregulates UPR-mediated proteins without induction of the transcriptional UPR program

First, we examined the induction of UPR targets at the mRNA level by 200 or 400 nM OZ in HepG2 cells. Surprisingly, incubation with 400 nM OZ downregulated the ATF6-mediated *GRP78* and *PDIA4* mRNA levels ($p<0.05$; Fig. 2A) [18]. In addition, incubation with 400 nM OZ repressed *CHOP* and *ATF4* transcription ($p<0.05$) but did not alter the mRNA levels of IRE1-generated *XBP1s* and its target *ERDJ4*. Even in presence of ER stress induced by tunicamycin, OZ reduced the transcription of *GRP78*, *PDIA4*, *XBP1u* and *CHOP* compared to cells treated with tunicamycin alone. Intriguingly, the levels of growth arrest and DNA damage inducible 34 (*GADD34*) mRNA, a downstream target of ATF4 and CHOP protein, were increased by incubation with OZ and tunicamycin compared to tunicamycin alone ($p<0.001$). Collectively, these data indicate that OZ impeded the transcriptional induction of target genes of the ATF6 and PERK pathway without altering the IRE1 RNase activity.

In contrast to the mRNA levels, 400 nM OZ triggered increased expression of GRP78, PDIA4, ATF4 and CHOP protein (Fig. 2B). In line with its transcriptional activation, also GADD34 protein levels were elevated. Based on these findings, we determined the protein half-life of the transcription factor CHOP in HepG2 cells by performing a time-course in the presence of cycloheximide blocking protein synthesis (Fig. 2C). The half-life of CHOP protein increased from 5.75 hours in vehicle-treated to 12.82 hours in OZ-treated cells (fold change: 2.23, $p<0.001$; Fig. 2D). Thus, OZ increased the UPR protein levels by inhibition of their proteasomal degradation and not by enhanced *de novo* synthesis following induction of the transcriptional UPR program.

OZ inhibits cytoprotective ATF6 signalling by direct RIP inhibition

Because OZ increased the levels of full ATF6 protein without any change in the levels of the transcriptionally active cleaved ATF6 fragment, consistent with inhibition of ATF6 activation (Fig. 2B), the effect of OZ on tunicamycin-induced ATF6 activation was evaluated (Fig. S4). First, we assessed the effect of OZ on the tunicamycin-mediated transcriptional induction of additional ATF6-regulated UPR targets, such as *GRP94*, *ERO1L*, *CALR* and *HERPUD1* mRNA (Fig. S4A) [12], [18]. As expected, upregulation of all ATF6 targets by tunicamycin was evident. Interestingly, addition of OZ to tunicamycin downregulated these selected ATF6 targets. To validate this hypothesis, the processing of another target of RIP, sterol regulatory element binding protein-1 (SREBP-1), was examined. Western blotting confirmed accumulation of precursor SREBP-1 in OZ-treated HepG2 cells (Fig. S4B). These results indicate that OZ inhibits ATF6 signalling by RIP inhibition.

RIP inhibition could be either directly by inhibition of the S1P or S2P expression or activity or indirectly by upregulation of a repressor of protease-mediated ATF6 activation. OZ does not alter the *S1P* or *S2P* mRNA levels (Fig. S4C), suggesting OZ functions through post-translational RIP inhibition without affecting *S1P* or *S2P* expression. Nucleobindin 1 is a reported ATF6 repressor [19]. While tunicamycin increased nucleobindin 1 expression, the expression in OZ-treated cells was indistinguishable from vehicle-treated cells (Fig. S4B).

Treatment of HepG2 cells with 25 μM 1,10-phenanthroline, a metalloprotease-specific S2P inhibitor [20], leads to accumulation of precursor SREBP-1 and to the absence of processed SREBP-1 detection and did not alter the nucleobindin 1 expression (Fig. S4B). In addition, 5 to 50 μM of 1,10-phenanthroline dose-dependently reduced the HepG2 cell viability (Fig. S4D), phenocopying the effects of OZ (Fig. 1 and S4B, respectively). Thus, OZ at an effective dose of 400 nM inhibits cytoprotective ATF6 signalling by RIP inhibition, probably, via off-target protease inhibition.

The PERK pathway regulates the nelfinavir-mediated increase in sensitivity to OZ

OZ slightly increased the eIF2α phosphorylation, which could not be inhibited by the PERK inhibitor (Fig. 2B), suggesting other eIF2α kinases such as heme-regulated inhibitor are involved, as previously reported for eIF2α phosphorylation induced by proteasome inhibitor MG-132 [21]. Importantly, addition of salubrinal or nelfinavir profoundly increased the OZ-induced eIF2α phosphorylation and pro-apoptotic CHOP protein levels (Fig. 2B), which may contribute to the increased sensitivity to OZ (Fig. 1). Indeed, addition of the PERK inhibitor increased the proliferation rate of HepG2 cells treated with the combination of OZ and nelfinavir ($p<0.05$; Fig. 2E), validating the role of the PERK pathway in the mechanism of this combination. Furthermore, addition of nelfinavir to OZ abolished the protein levels of the ATF6-dependent chaperones GRP78 and PDIA4 (Fig. 2B), possibly exacerbating the generated proteotoxicity. Interestingly, nelfinavir was previously reported to induce apoptosis in liposarcoma cells by direct S2P inhibition [22]. These data suggest that dysregulation of the transcriptional UPR program and decreased proteasomal degradation of short-lived pro-apoptotic UPR proteins are involved in OZ-induced HCC cell death and the observed synergy with PERK inducers.

OZ reduced tumour burden in orthotopic and xenograft mouse models for HCC

Prior to evaluating the antitumour activity of OZ in the DEN-induced mouse model characterized by severe liver dysfunction [23], several dosing regimens for 2 weeks were tested in 25 weeks saline-treated and DEN-treated mice (n=3, Table 1). We observed 100% mortality in the mice with liver dysfunction treated with 50 mg/kg/day for 5 consecutive days per week. At 30 mg/kg/day for 3 consecutive days per week, no mortality occurred. Therefore, this dosing regimen was applied in the following experiments.

OZ for 4 weeks did not affect mortality in saline- or DEN-injected mice (n=12, Table 2). Average body weight of mice was decreased following 25 weeks of DEN compared to saline administration ($p<0.001$, Table 2). Subsequent treatment with OZ did not alter the average body weight compared to vehicle. Although serum ALT and AST levels were elevated by DEN administration ($p<0.001$), treatment with OZ did not alter these levels in the surviving mice (Fig. S5A).

DEN-treated mice that received OZ developed fewer macroscopic nodules per liver (all sizes: 16.2 ± 4.5 after vehicle versus 11.1 ± 3.9 after OZ; $p<0.05$). HCC burden, microscopically quantified by the loss of reticulin staining, was reduced in OZ-treated compared to vehicle-treated mice ($p<0.01$, Fig. 3A-C). Hepatic caspase-3/7 activity levels *ex vivo* were elevated by DEN compared to saline administration ($p<0.001$, Fig. 3D). OZ monotherapy further increased these levels compared to vehicle-treated HCC-bearing mice ($p<0.05$), consistent with *in vivo* apoptosis induction. We previously reported the UPR pattern in the DEN-induced mouse model [15]. Here, OZ administration reduced the levels of *Grp78* mRNA ($p<0.05$) and induced a tendency to reduce *Pdia4* and *Chop* in the isolated tumours (Fig. 4A). However, immunoblotting of lysates of isolated tumours revealed that OZ promoted CHOP protein expression *in vivo* (Fig. 4B). Yet, UPR-regulated caspase-12 cleavage was only slightly increased by OZ. These observations provide evidence that the efficacy of OZ in inhibiting the growth of DEN-induced HCC is through similar mechanisms as those observed *in vitro*.

Secondly, the effect of OZ was assessed in a HepG2 xenograft model. No significant differences in body weight or appearance between control and OZ-treated animals were observed during the course of the xenograft study (data not shown). OZ administration suppressed the growth rate of the HepG2-derived tumours ($p<0.05$, Fig. 4E). Accordingly, TUNEL immunofluorescence demonstrated a significant increase of TUNEL-positive apoptotic HepG2 cells following OZ administration ($p<0.01$, Fig. 4C-D).

Nelfinavir and salubrinal potentiate the therapeutic efficacy of OZ in experimental HCC

Administration of nelfinavir or salubrinal did not alter the mean body weight compared to vehicle (Table 1). Although hepatic caspase-3/7 activity was not significantly increased (Fig. 3D), combining OZ with nelfinavir was more efficacious compared to OZ monotherapy in the orthotopic model (number of macroscopic nodules per liver: 11.1 ± 3.9 after OZ versus 7.2 ± 5.2 after OZ and nelfinavir; microscopic tumour burden: $p<0.05$; Fig. 3A-C).

Addition of salubrinal at 1 mg/kg/24 hrs similarly improved the effect of OZ (number of macroscopic nodules per liver: 6.7 ± 4.8 after OZ and salubrinal; microscopic tumour burden: $p<0.05$; Fig. 3A-C). Interestingly, addition of nelfinavir or salubrinal to OZ promoted eIf2α phosphorylation and downstream *Chop* mRNA and protein levels (Fig. 4A-B), suggesting intensified pro-apoptotic UPR signalling. Caspase-12 cleavage was indeed markedly increased by addition of nelfinavir or salubrinal to OZ treatment (Fig. 4B). In contrast, salubrinal at 1 mg/kg/72 hrs induced no detectable effects on the antitumour efficacy of OZ, eIf2α phosphorylation or Chop expression (data not shown).

Accordingly, in the HepG2 xenograft model, dual therapy with OZ and nelfinavir or OZ and salubrinal strikingly inhibited tumour growth compared to vehicle-treated (both $p<0.001$) and to OZ-treated mice (both $p<0.01$), whereas nelfinavir or salubrinal monotherapy did not alter the xenograft growth (Fig. S5B-C). Furthermore, addition of nelfinavir or salubrinal augmented the number of TUNEL-positive HepG2 cells in the xenograft tumours ($p<0.05$ and $p<0.01$ respectively, Fig. 4C-D), suggesting robust induction of apoptosis when UPR modulators are added. Thus, we identified that nelfinavir and salubrinal potentiate the therapeutic efficacy of OZ in different models for HCC, likely by increased UPR-mediated apoptosis via induction of Chop synthesis while OZ diminishes its proteasomal degradation.

5.1.6. **Discussion**

Proteasome inhibition could represent a novel therapeutic strategy for advanced HCC [5], [7]. The next-generation orally bio-available irreversible proteasome inhibitor oprozomib (OZ) is assumed to evoke less adverse events and improved antitumour activity compared to the first-in-class bortezomib [3]. Recently, OZ was shown to exert antitumour activity on myeloma and head and neck cancer xenograft models [3]. In this study, OZ exerted potent anti-tumour effects *in vitro* and in different *in vivo* models for HCC, supporting the potential value of irreversibly targeting the proteasome in the treatment of HCC. Moreover, we revealed a strategy to further enhance the efficacy of OZ by modulation of the UPR.

When unfolded proteins accumulate in the ER, the UPR is initiated to allow the cells to restore homeostasis by proteasomal degradation of unfolded proteins, translational arrest and increasing protein folding capacity [11]. The association between UPR activity and therapeutic efficacy of proteasome inhibition was first illustrated in myeloma, in which patient serum levels of XBP1 correlated with the clinical response towards bortezomib [24]. Theoretically, decreased protein degradation by proteasome inhibition could lead to oxidative stress and UPR activation. However, the effect on the UPR is not well understood. We showed that the cytotoxic effect of OZ depends on the build-up of proteotoxic stress without an important contribution of oxidative stress. Although OZ did not induce the transcriptional UPR program and even inhibited the protease-dependent activation of the cytoprotective ATF6 pathway, OZ increased the protein levels of different UPR markers. Notably, OZ increased the protein stability of the pro-apoptotic transcription factor CHOP and did induce CHOP-mediated transcription of *GADD34*. Thus, OZ increased the levels of the UPR-regulated proteins by abrogated proteasomal degradation of these rather than a general activation of the UPR program by increased unfolded protein load. Apparently, rapid proteasomal degradation of UPR proteins is a pivotal negative feedback mechanism following recovery of the ER proteostasis.

Consistent with the effect of OZ on the UPR, PERK or IRE1 inhibition did not alter its effect, whereas ER stress inducers, such as tunicamycin or nelfinavir, or an inhibitor of eIF2α dephosphorylation enhanced the growth-inhibitory effects of OZ in HCC cells. Interestingly, a similar synergy was observed with bortezomib, suggesting this concept can also be applied to other proteasome inhibitors. Since the maximum serum levels attained in patients are much higher (bortezomib: 0.16 μM (1.3 mg/m^2 intravenous); oprozomib: 3.8 μM (30 mg per os) [25]), the concentrations used *in vitro* are clinically relevant.

Based on these results, we evaluated the *in vivo* effects of the combination of nelfinavir or salubrinal and OZ in HCC. Both nelfinavir and salubrinal enhanced the growth-inhibitory effect without cumulative toxicity, suggesting this rational combination presents a safe strategy to potentiate the antitumour effects of proteasome inhibition in HCC. Experience in the use of proteasome inhibitors and nelfinavir in clinical practice and the oral bio-availability are considerable advantages for implementation.

Bortezomib resistance in myeloma cells was shown to be induced by attenuated eIF2α phosphorylation [26]. Salubrinal typically provides for enhanced resistance to stress conditions, such as those triggered by oxidizing or UPR-inducing agents [27], [28]. However, here we provide evidence that salubrinal renders HCC cells more susceptible to proteasome inhibition by activating the PERK/phospho-eIF2α/CHOP pathway. Of note, human HCC, in contrast to unaffected adjacent liver tissue, is characterized by increased CHOP staining [29].

Although a recent phase I trial with OZ demonstrated that OZ has an acceptable safety profile when given daily for 5 consecutive days every 2 weeks in patients with solid tumours [30], significant toxicity occurred when OZ was administrated for several consecutive days in mice with DEN-induced liver dysfunction. However, identification of sensitivity enhancers by UPR modulation could allow for dose and, possibly, toxicity reduction.

Because ER stress potentiates the antitumour efficacy of OZ, we assume a stronger effect on hypoxic ER-stressed tumour cells compared to the normal liver tissue [15]. Consequently, OZ could be more efficacious in combination with antiangiogenic treatments increasing tumour hypoxia-induced UPR [11], [31].

In conclusion, dysregulation of the transcriptional UPR program and reduced proteasomal degradation of pro-apoptotic UPR-mediated proteins are involved in OZ-induced cell death. Furthermore, modulation of the interplay between OZ and the UPR enhances its antitumour efficacy without cumulative toxicity. Therefore, OZ monotherapy or in combination with UPR modulators may present a novel and clinically applicable therapeutic strategy for HCC.

5.1.7. **Acknowledgements**

The authors thank P. Vanwassenhove at the Department of Gastroenterology and Dr. M. Bol at the Department of Basic Medical Sciences, Ghent University (Ghent, Belgium) for their expert technical assistance.

5.1.8. **References**

[1] International Agency for Research on Cancer, "GLOBOCAN 2012," *Estimated Incidence, Mortality and Prevalence Worldwide in 2012*, 2012. [Online]. Available: http://globocan.iarc.fr/Pages/fact_sheets_cancer.aspx.

[2] "EASL-EORTC clinical practice guidelines: management of hepatocellular carcinoma.," *J. Hepatol.*, vol. 56, no. 4, pp. 908–43, Apr. 2012.

[3] M.-V. Mateos, E. M. Ocio, and J. F. San Miguel, "Novel generation of agents with proven clinical activity in multiple myeloma.," *Semin. Oncol.*, vol. 40, no. 5, pp. 618–33, Oct. 2013.

[4] L. I. Aronson and F. E. Davies, "DangER: protein ovERload. Targeting protein degradation to treat myeloma.," *Haematologica*, vol. 97, no. 8, pp. 1119–30, Aug. 2012.

[5] I. Saeki, S. Terai, K. Fujisawa, T. Takami, N. Yamamoto, T. Matsumoto *et al.* Bortezomib induces tumor-specific cell death and growth inhibition in hepatocellular carcinoma and improves liver fibrosis.," *J. Gastroenterol.*, Sep. 2012.

[6] B. Boozari, B. Mundt, N. Woller, N. Strüver, E. Gürlevik, P. Schache *et al.* Antitumoural immunity by virus-mediated immunogenic apoptosis inhibits metastatic growth of hepatocellular carcinoma.," *Gut*, vol. 59, no. 10, pp. 1416–26, Oct. 2010.

[7] G. P. Kim, M. R. Mahoney, D. Szydlo, T. S. K. Mok, R. Marshke, K. Holen *et al.* An international, multicenter phase II trial of bortezomib in patients with hepatocellular carcinoma.," *Invest. New Drugs*, vol. 30, no. 1, pp. 387–94, Feb. 2012.

[8] N. Saini and A. Mahindra, "Therapeutic strategies for the treatment of multiple myeloma.," *Discov. Med.*, vol. 15, no. 83, pp. 251–8, Apr. 2013.

[9] H.-J. Zhou, M. A. Aujay, M. K. Bennett, M. Dajee, S. D. Demo, Y. Fang *et al.* Design and synthesis of an orally bioavailable and selective peptide epoxyketone proteasome inhibitor (PR-047).," *J. Med. Chem.*, vol. 52, no. 9, pp. 3028–38, May 2009.

[10] A. K. Stewart, S. V. Rajkumar, M. A. Dimopoulos, T. Masszi, I. Špička, A. Oriol *et al.* Carfilzomib, Lenalidomide, and Dexamethasone for Relapsed Multiple Myeloma," *N. Engl. J. Med.*, vol. 372, no. 2, p. 141206080130007, Dec. 2014.

[11] Y.-P. Vandewynckel, D. Laukens, A. Geerts, E. Bogaerts, A. Paridaens, X. Verhelst *et al.* The paradox of the unfolded protein response in cancer.," *Anticancer Res.*, vol. 33, no. 11, pp. 4683–94, Nov. 2013.

[12] S. Rachidi, S. Sun, B. X. Wu, E. Jones, R. R. Drake, B. Ogretmen, A. Cowart *et al.* Endoplasmic reticulum heat shock protein gp96 maintains liver homeostasis and promotes hepatocellular carcinogenesis.," *J. Hepatol.*, Nov. 2014.

[13] S. Van de Veire, I. Stalmans, F. Heindryckx, H. Oura, A. Tijeras-Raballand, T. Schmidt *et al.* Further pharmacological and genetic evidence for the efficacy of PlGF inhibition in cancer and eye disease.," *Cell*, vol. 141, no. 1, pp. 178–90, Apr. 2010.

[14] T.-C. Chou, "Drug combination studies and their synergy quantification using the Chou-Talalay method.," *Cancer Res.*, vol. 70, no. 2, pp. 440–6, Jan. 2010.

[15] Y.-P. Vandewynckel, D. Laukens, E. Bogaerts, A. Paridaens, A. Van den Bussche, X. Verhelst *et al.* Modulation of the unfolded protein response impedes tumor cell adaptation to proteotoxic stress: a PERK for hepatocellular carcinoma therapy," *Hepatol. Int.*, vol. 9, no. 1, pp. 93–104, 2015.

[16] A. Brüning, "Analysis of nelfinavir-induced endoplasmic reticulum stress.," *Methods Enzymol.*, vol. 491, pp. 127–42, Jan. 2011.

[17] Y.-H. Ling, L. Liebes, Y. Zou, R. Perez-Soler, "Reactive oxygen species generation and mitochondrial dysfunction in the apoptotic response to Bortezomib, a novel proteasome inhibitor, in human H460 non-small cell lung cancer cells.," *J. Biol. Chem.*, vol. 278, no. 36, pp. 33714–23, Sep. 2003.

[18] M. D. Shoulders, L. M. Ryno, J. C. Genereux, J. J. Moresco, P. G. Tu, C. Wu *et al.* Stress-Independent Activation of XBP1s and/or ATF6 Reveals Three Functionally Diverse ER Proteostasis Environments.," *Cell Rep.*, vol. 3, no. 4, pp. 1279–92, Apr. 2013.

[19] Y. Tsukumo, A. Tomida, O. Kitahara, Y. Nakamura, S. Asada, K. Mori, T. Tsuruo, "Nucleobindin 1 controls the unfolded protein response by inhibiting ATF6 activation.," *J. Biol. Chem.*, vol. 282, no. 40, pp. 29264–72, Oct. 2007.

[20] L. Feng, H. Yan, Z. Wu, N. Yan, Z. Wang, P. D. Jeffrey *et al.* Structure of a site-2 protease family intramembrane metalloprotease.," *Science*, vol. 318, 1608–12, 2007.

[21] A. Yerlikaya, S. R. Kimball, B. A. Stanley, "Phosphorylation of eIF2alpha in response to 26S proteasome inhibition is mediated by the haem-regulated inhibitor (HRI) kinase.," *Biochem. J.*, vol. 412, no. 3, pp. 579–88, Jun. 2008.

[22] M. Guan, K. Fousek, C. Jiang, S. Guo, T. Synold, B. Xi, *et al.* Nelfinavir induces liposarcoma apoptosis through inhibition of regulated intramembrane proteolysis of SREBP-1 and ATF6.," *Clin. Cancer Res.*, vol. 17, no. 7, pp. 1796–806, Apr. 2011.

[23] F. Heindryckx, K. Mertens, N. Charette, B. Vandeghinste, C. Casteleyn, C. Van Steenkiste *et al.* Kinetics of angiogenic changes in a new mouse model for hepatocellular carcinoma," *Mol. Cancer*, vol. 9, no. 1, p. 219, 2010.

[24] S. C. W. Ling, E. K. K. Lau, A. Al-Shabeeb, A. Nikolic, A. Catalano, H. Iland *et al.* "Response of myeloma to the proteasome inhibitor bortezomib is correlated with the unfolded protein response regulator XBP-1.," *Haematologica*, vol. 97, 64–72, 2012.

[25] K. P. Papadopoulos, D. S. Mendelson, A. W. Tolcher, A. Patnaik, H. A. Burris, D. W. Rasco, *et al.* A phase I, open-label, dose-escalation study of the novel oral proteasome inhibitor (PI) ONX 0912 in patients with advanced refractory or recurrent solid tumors.," *J Clin Oncol*, vol. 29, no. suppl, p. abstr 3075, 2011.

[26] D. M. Schewe and J. A. Aguirre-Ghiso, "Inhibition of eIF2alpha dephosphorylation maximizes bortezomib efficiency and eliminates quiescent multiple myeloma cells surviving proteasome inhibitor therapy.," *Cancer Res.*, vol. 69, no. 4, pp. 1545–52, Feb. 2009.

[27] M. Boyce, K. F. Bryant, C. Jousse, K. Long, H. P. Harding, D. Scheuner *et al.* A selective inhibitor of eIF2alpha dephosphorylation protects cells from ER stress.," *Science*, vol. 307, no. 5711, pp. 935–9, Feb. 2005.

[28] J. Lewerenz and P. Maher, "Basal levels of eIF2alpha phosphorylation determine cellular antioxidant status by regulating ATF4 and xCT expression.," *J. Biol. Chem.*, vol. 284, no. 2, pp. 1106–15, Jan. 2009.

[29] D. Dezwaan-McCabe, J. D. Riordan, A. M. Arensdorf, M. S. Icardi, A. J. Dupuy, D. T. Rutkowski, "The Stress-Regulated Transcription Factor CHOP Promotes Hepatic Inflammatory Gene Expression, Fibrosis, and Oncogenesis.," *PLoS Genet.*, vol. 9, no. 12, p. e1003937, Dec. 2013.

[30] H. Wang, F. Guan, D. Chen, Q. P. Dou, H. Yang, An analysis of the safety profile of proteasome inhibitors for treating various cancers. *Expert Opin. Drug.*, 13, 1043–54, 2014.

[31] A. Paridaens, D. Laukens, Y.-P. Vandewynckel, S. Coulon, H. Van Vlierberghe, A. Geerts *et al.* Endoplasmic reticulum stress and angiogenesis: is there an interaction between them?, *Liver Int.*, 2014.

5.1.9. **Tables**

Table 1. Mortality at different dosing regimens (n=3 in each group).

Consecutive-day dosing in weekly cycle	Mortality in saline-treated mice	Mortality in DEN-treated mice
50 mg/kg/day for 5 days	2/3	3/3
30 mg/kg/day for 5 days	1/3	1/3
30 mg/kg/day for 4 days	0/3	1/3
30 mg/kg/day for 3 days	0/3	0/3

Table 2. Average body weight (g) ± SD and survival of mice (n=12 in each group).

Group	Average body weight 25 weeks (g)	Average body weight 29 weeks (g)	Survival (%)
Saline => vehicle	27.22 ± 1.32	26.03 ± 1.61	100
DEN => vehicle	19.75 ± 1.76***	18.30 ± 2.92	58.33
DEN => OZ	20.86 ± 1.45	19.17 ± 2.10 NS	58.33
DEN => OZ + nelfinavir	22.96 ± 3.65	17.92 ± 3.19 NS	66.67
DEN => OZ + salubrinal	21.23 ± 5.89	18.09 ± 6.23 NS	66.67

***p<0.001: 25 weeks DEN vs. saline, NS= not significant compared to vehicle.

5.1.10. **Figures**

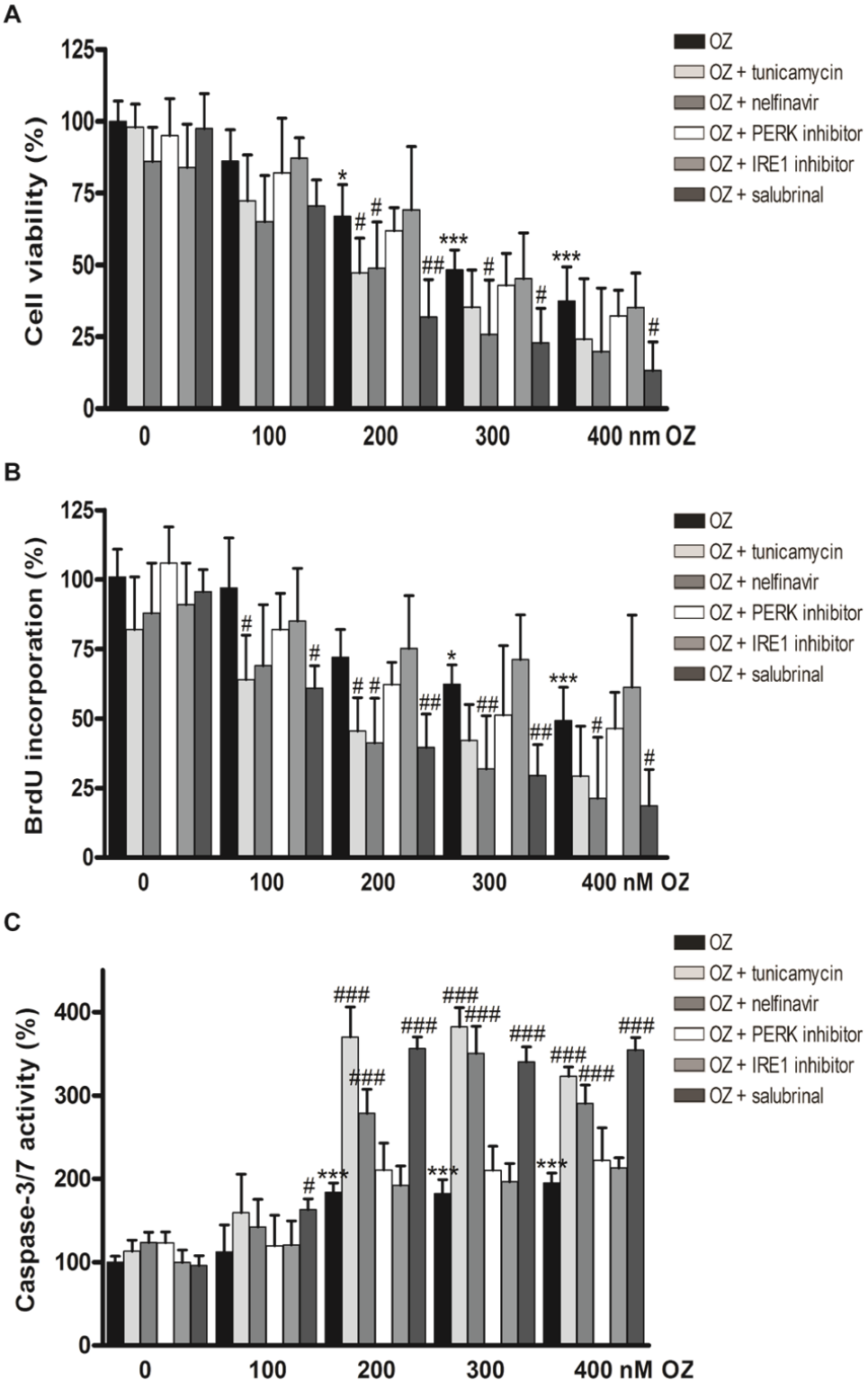

Fig. 1. Antiproliferative and pro-apoptotic effects of oprozomib in monotherapy or in combination with modulators of ER stress in human hepatoma HepG2 cells. (A) MTT assay (B) BrdU incorporation (C) Caspase-3/7 activity. OZ: oprozomib. *p<0.05, **p<0.01, ***p<0.001 compared to oprozomib 0 nM; $^{\#}$p<0.05, $^{\#\#}$p<0.01, $^{\#\#\#}$p<0.001 compared to respective concentration of oprozomib alone.

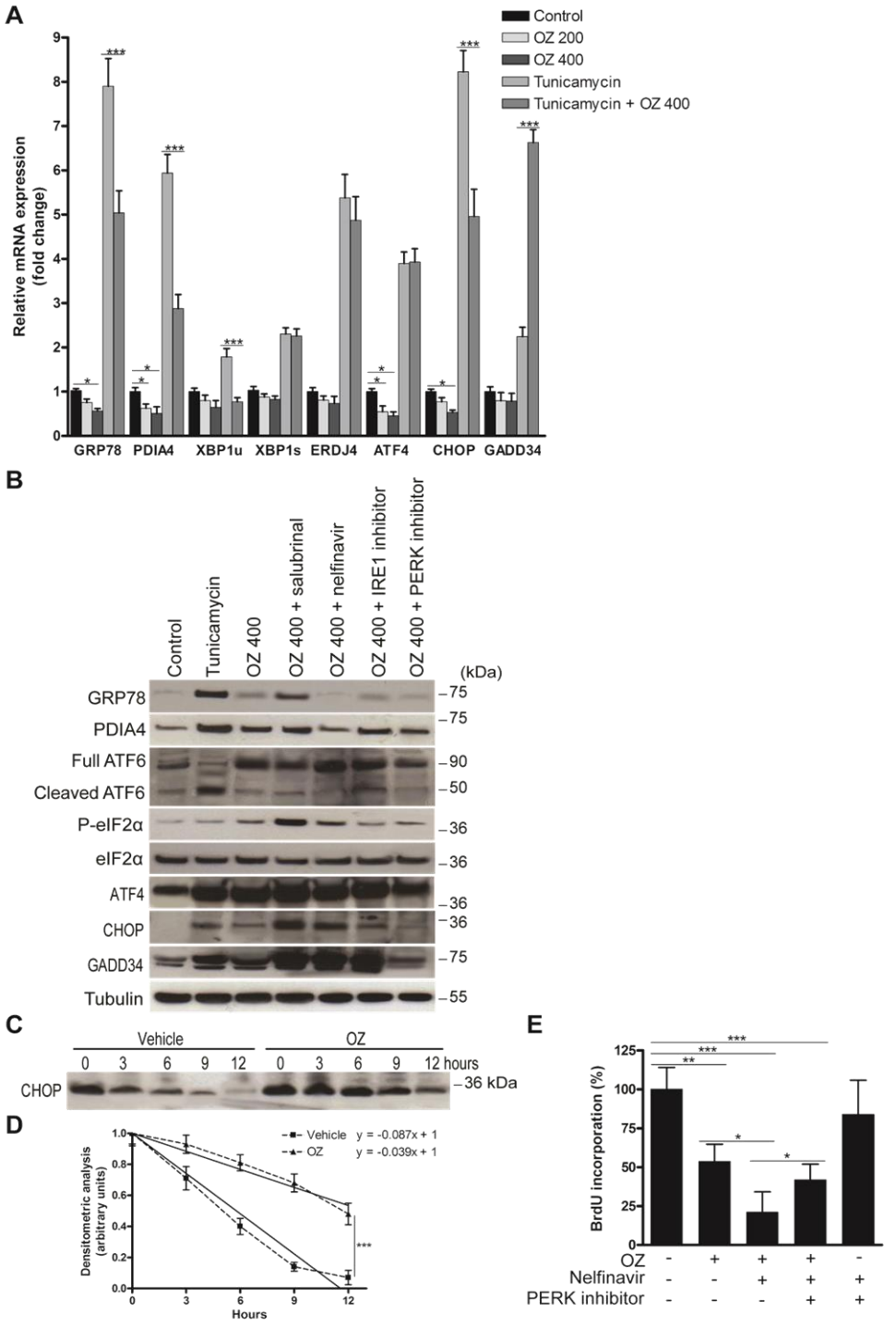

Fig. 2. Oprozomib modulates the UPR pattern in HepG2 cells. (A) Real-time PCR analysis of relative mRNA levels of UPR-mediated genes after 48 hours of incubation with the indicated treatments. (B) Immunoblotting of UPR-mediated proteins. (C) To measure the half-life of CHOP protein in HepG2 cells, cells were pre-treated for 1 hour with 1 μg/ml tunicamycin and a time-course in the presence of 50 μg/ml cycloheximide, which blocks protein synthesis, was performed. Band intensities were quantified using ImageJ software. (D) Half-life of CHOP protein was determined by plotting optical density (arbitrary unit) calculated from densitometric analysis of bands in panel C versus hours of treatment. Data represent the mean ± SD of three independent experiments. (E) BrdU incorporation of HepG2 cells incubated with indicated treatments for 48 hours. OZ: 400 nM oprozomib. *p<0.05, **p<0.01, ***p<0.001.

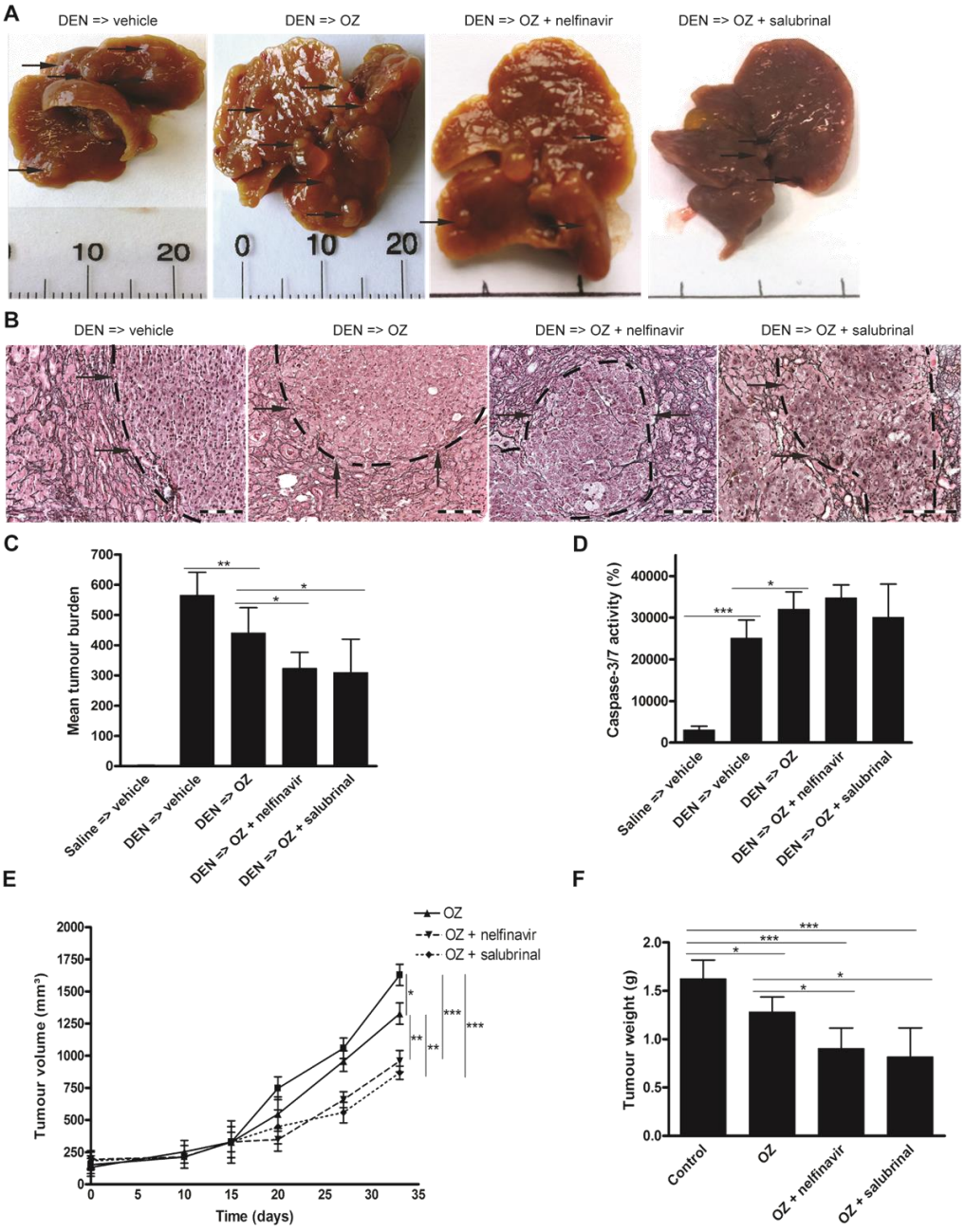

Fig. 3. Impact of oprozomib in monotherapy or in combination with ER stress modulators on an orthotopic and a xenograft model for HCC. (A) Photographs of representative livers after different treatments. (B) Reticulin staining. Scale bar: 100 µm. (C) Assessment of tumour burden in the carcinogen-induced mouse model in randomly selected high-power fields. (D) Hepatic caspase-3/7 activity *ex vivo*. (E) Evolution of tumour volume in mice bearing HepG2-derived xenograft tumours. (F) Final tumour weights. Values represent the mean ± SD. *p<0.05, **p<0.01, ***p<0.001.

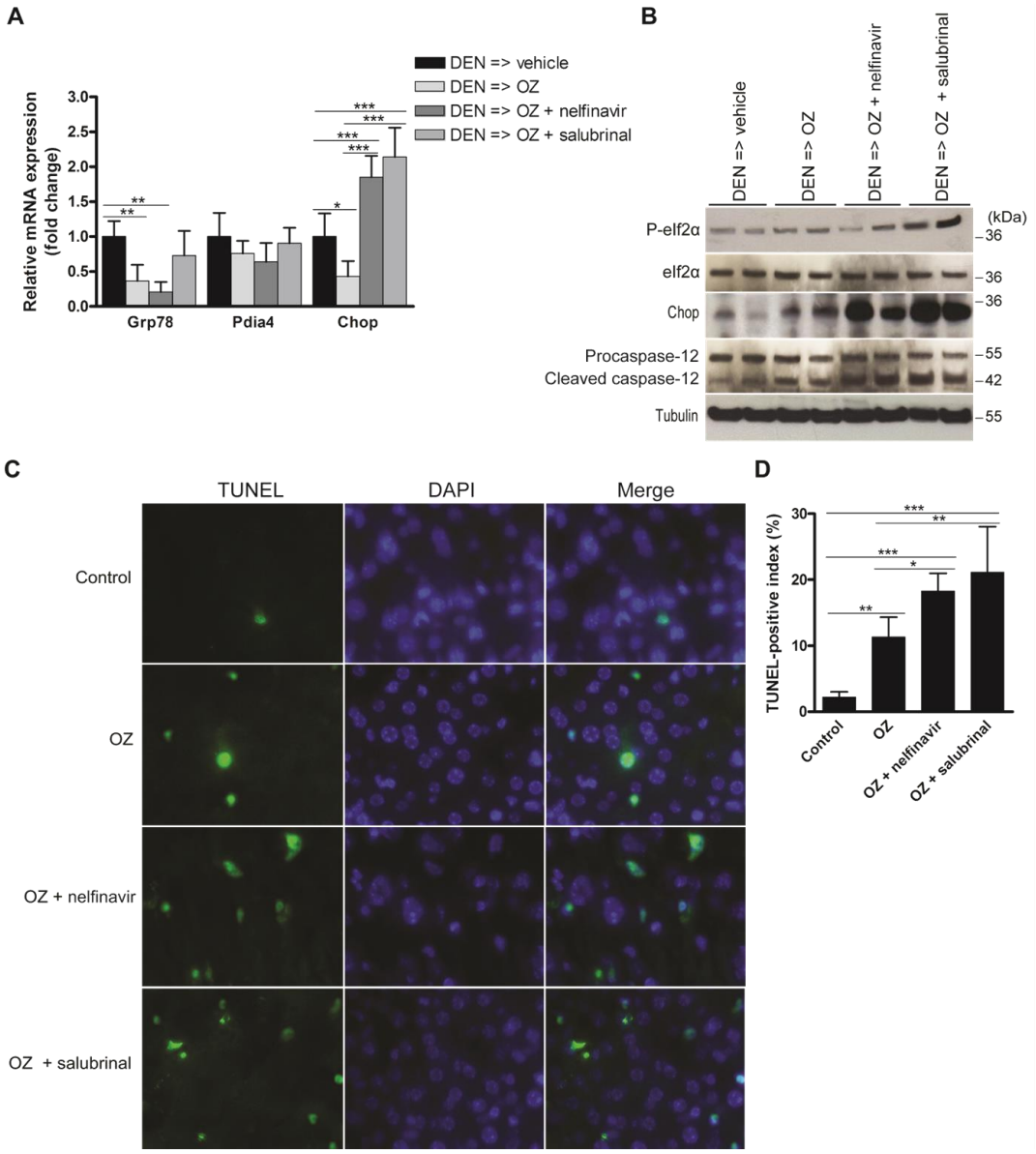

Fig. 4. Oprozomib and UPR modulation in experimental HCC. (A) Real-time PCR analysis and (B) Immunoblotting of UPR targets in isolated DEN-induced tumours following the indicated treatments. (C) TUNEL immunofluorescence in HepG2 xenografts and (D) quantification of TUNEL-positive index (n=6). OZ: oprozomib. *p<0.05, **p<0.01, ***p<0.001.

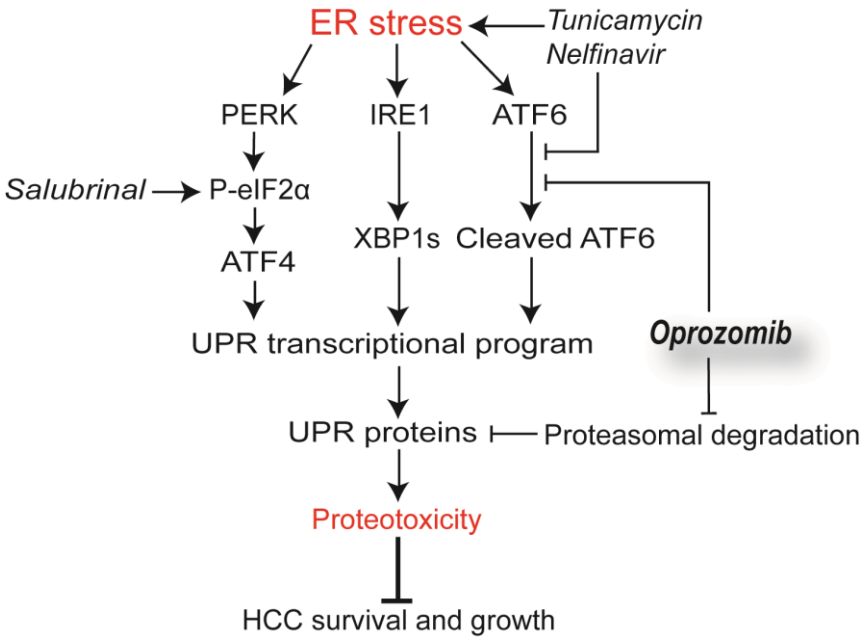

Fig. 5. Schematic model outlining the mechanisms of oprozomib with indication of the point of action of the applied products. Persistent ER stress activates the tripartite UPR-mediated transcriptional program followed by translation of these UPR proteins, which leads to proteotoxicity-mediated tumour cell death. Although oprozomib did not induce the UPR and even inhibited ATF6-mediated transcription, it increased the UPR-mediated protein levels by prolonging their half-life. This UPR dysregulation allows for enhanced proteotoxicity by supplementary boosting PERK activity by tunicamycin, nelfinavir (also inhibits ATF6) or salubrinal.

5.1.11. **Supplementary Figures**

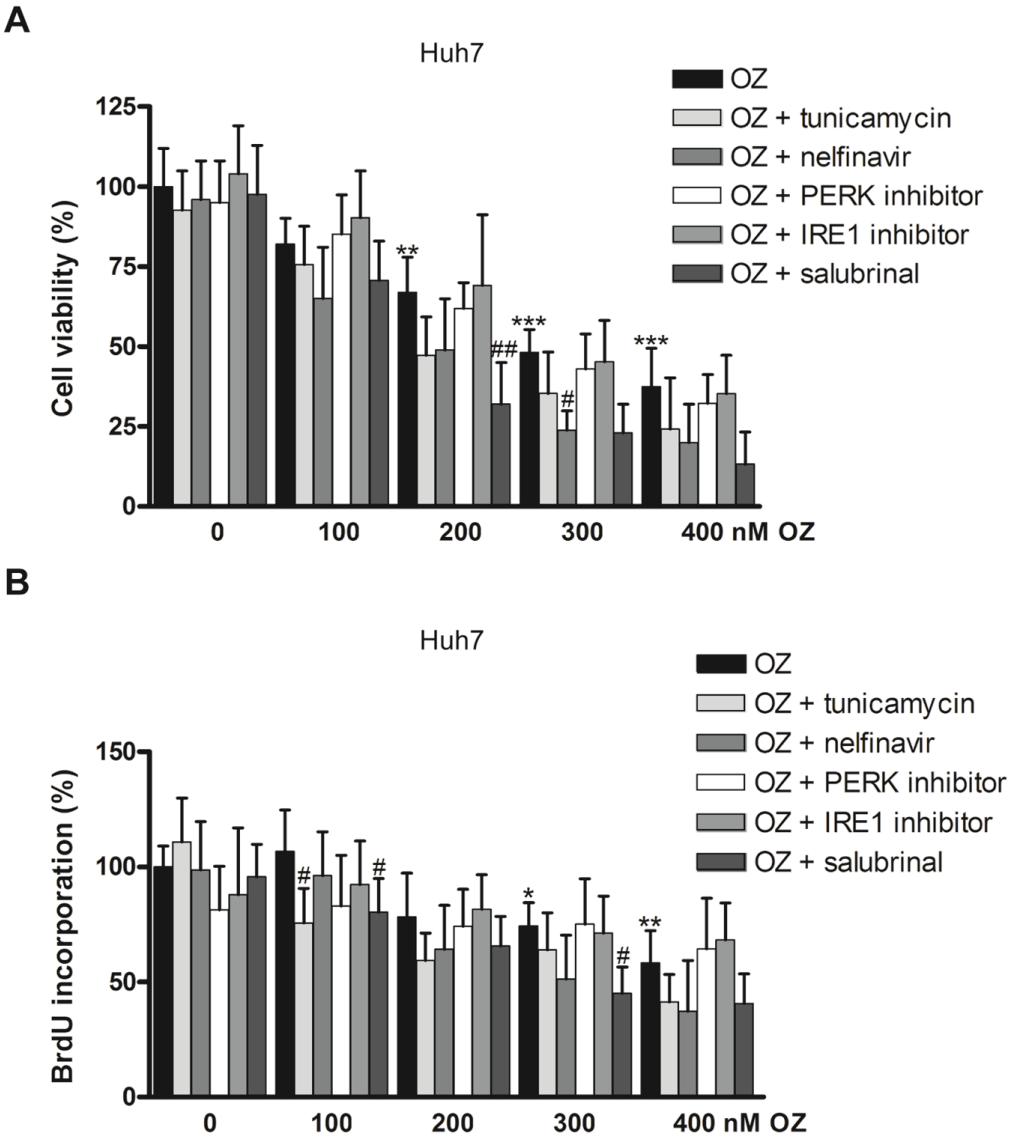

Fig. S1. Growth-inhibitory effects of oprozomib in Huh7 cells. (A) Assessment of cell viability by MTT assay. (B) Cell proliferation rate as assessed by BrdU incorporation in Huh7 cells. One-way ANOVA was applied for statistical analysis. *p<0.05, **p<0.01, ***p<0.001 compared to oprozomib 0 nM; $^{\#}$p<0.05, $^{\#\#}$p<0.01, $^{\#\#\#}$p<0.001 compared to respective concentration of oprozomib alone. OZ: oprozomib. Results are representative of 2 independent experiments.

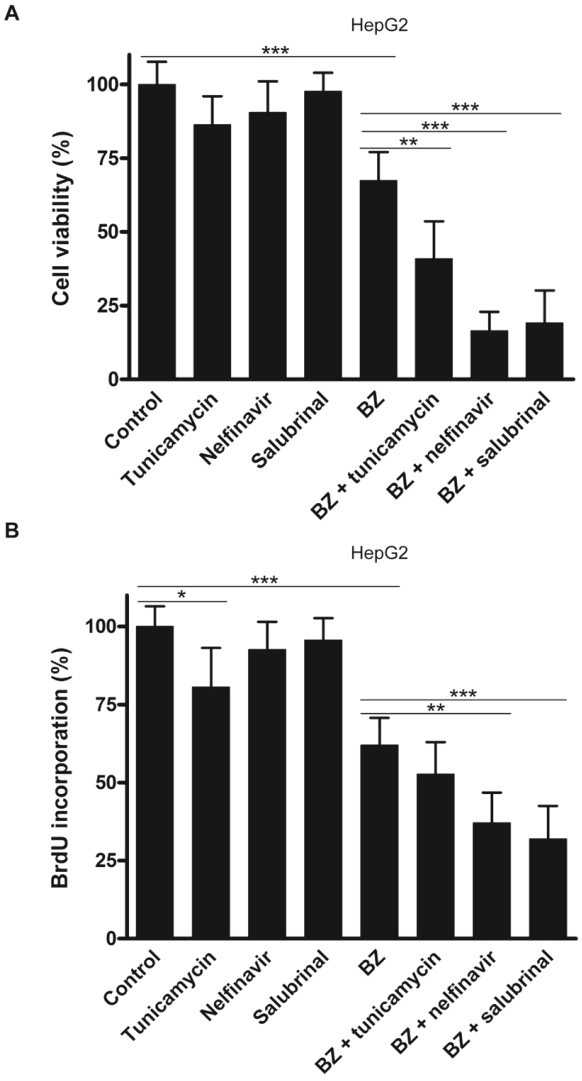

Fig. S2. Bortezomib and ER stress modulation in HepG2 cells. (A) Cell viability as assessed by MTT assay. (B) Cell proliferation rate as assessed by BrdU incorporation. *p<0.05, **p<0.01, ***p<0.001. BZ: bortezomib 25 nM. Results are representative of 3 independent experiments.

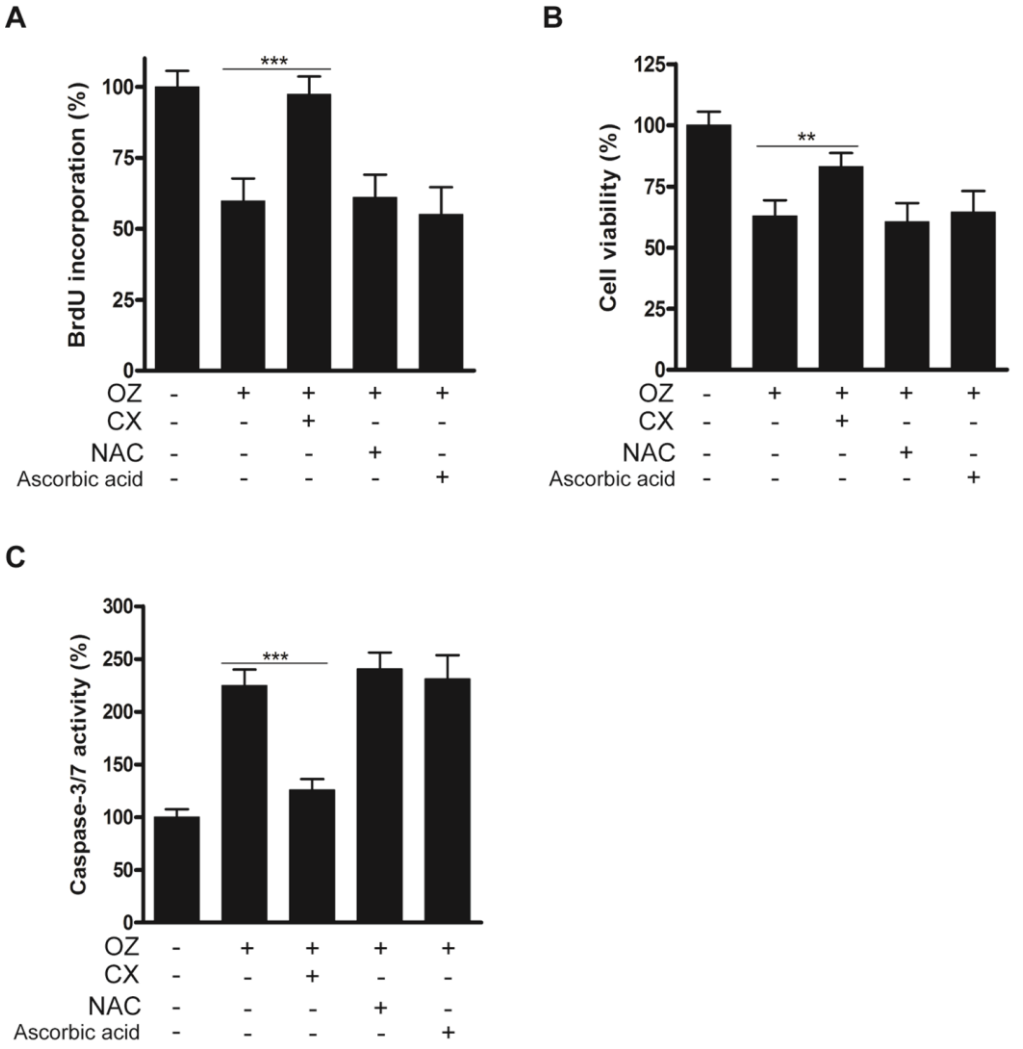

Fig. S3. Modulation of proteotoxic, not oxidative, stress affects antitumour activity of oprozomib in HepG2 cells. (A) Cell proliferation rate. (B) Cell viability. (C) Caspase-3/7 activity. Values represent the mean ± SD. *p<0.05, **p<0.01, ***p<0.001 compared to oprozomib alone. OZ: oprozomib 400 nM. CX: cycloheximide. NAC: N-acetyl-L-cysteine. Results are representative of 2 independent experiments.

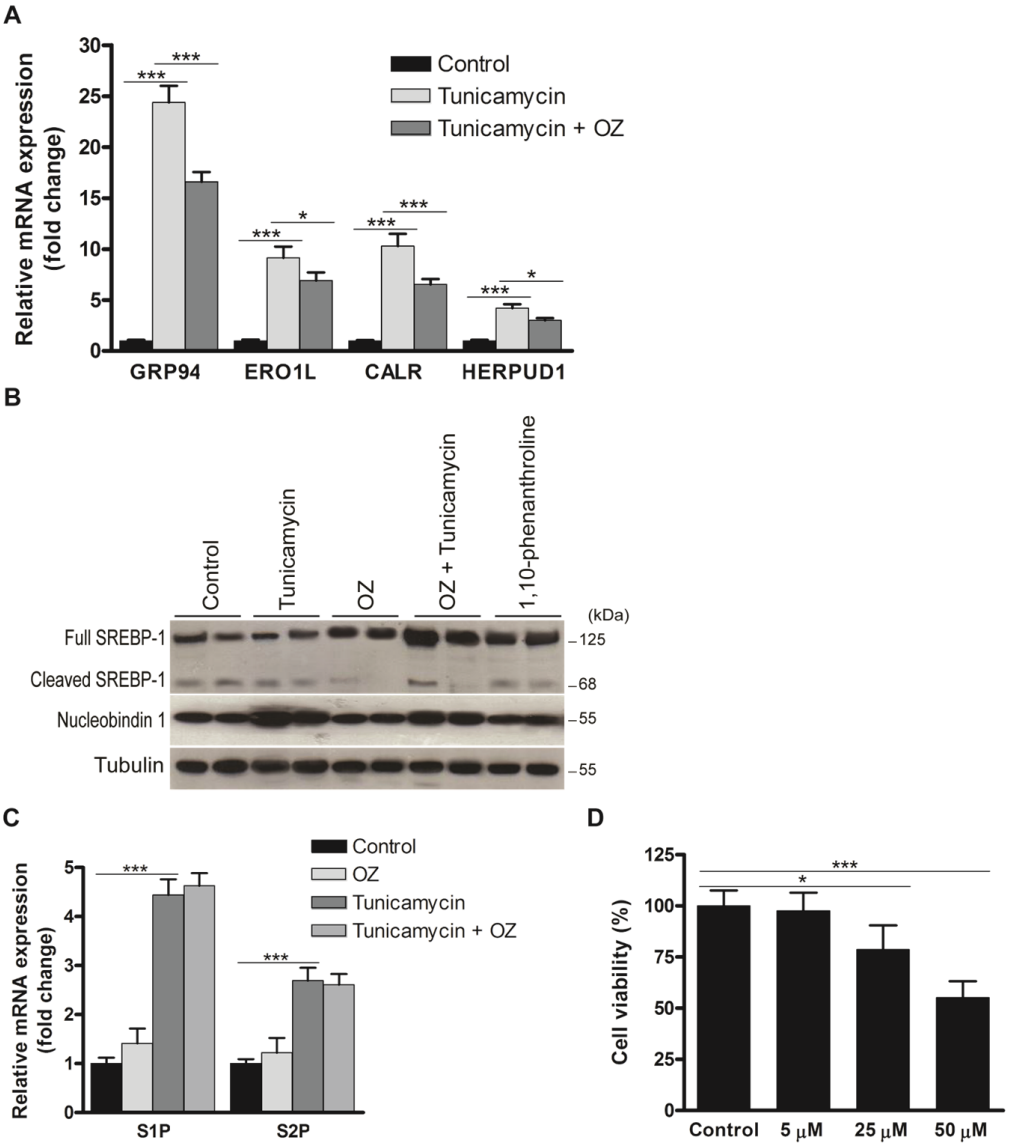

Fig. S4. OZ inhibits cytoprotective ATF6 activation in HepG2 cells. (A) Quantitative real-time PCR analysis of the ATF6 targets GRP94, ERO1L, CALR and HERPUD1. (B) Western blotting for RIP-dependent SREBP-1 cleavage and the ATF6 repressor Nucleobindin 1. RIP inhibitor 1,10-phenanthroline was applied at a dose of 25 μM. (C) Quantitative real-time PCR analysis of S1P and S2P. OZ: oprozomib 400 nM. (D) Effect of 5 to 50 μM 1,10-phenanthroline on the MTT cell viability of HepG2 cells. Results are representative of 2 independent experiments. *p<0.05, **p<0.01, ***p<0.001.

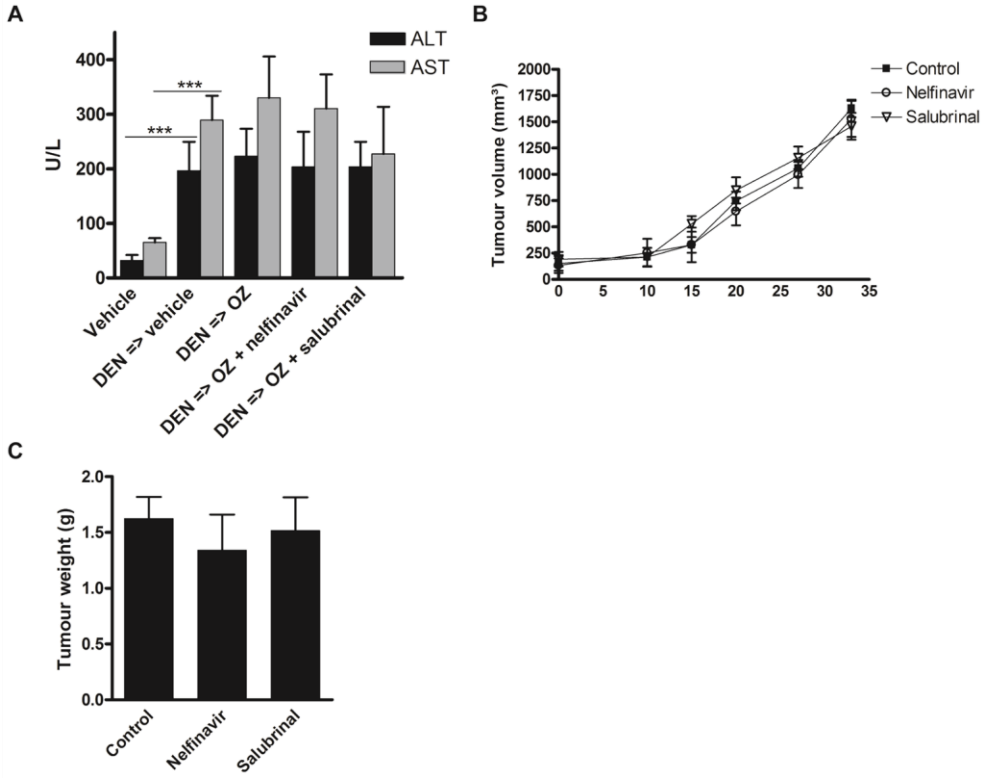

Fig. S5. Effect of nelfinavir and salubrinal on the serum levels of liver enzymes in the DEN-induced model and on HepG2 xenograft growth. (A) Liver damage was assessed by measuring ALT and AST levels in the serum of surviving mice after the indicated treatments. Values represent the mean ± SD (n=7). ***p<0.001. (B) Evolution of tumour volume in mice bearing HepG2-derived xenograft tumours. (C) Final tumour weights. Values represent the mean ± SD of the tumour volumes of each group.

Chapter 4

Conclusions and future perspectives

1. Conclusions and future perspectives

1.1. Introduction

Hepatocellular carcinoma (HCC) is a common cancer worldwide with a very poor prognosis [1]. Few therapeutic strategies have been proven efficient, particularly for those patients not indicated for curative resection or transplantation [2]. To date, sorafenib remains the only approved, targeted molecule for the treatment of advanced HCC. Although a small survival benefit was demonstrated, it remains only true in the population of patients with Child-Pugh A liver disease [3]. Moreover, sorafenib has distinct side effects that require close monitoring [2]. Recently, newer but similar tyrosine kinase inhibitors (TKIs) and angiogenesis inhibitors have been evaluated in clinical trials with disappointing results [4]. Therefore, innovative therapeutic strategies are urgently required.

Cancer cells survive the self-created hostile microenvironmental conditions, such as hypoglycaemia, hypoxia, acidosis and nutrient scarcity by activation of **adaptive processes** [5]. These processes render cancer cells resistant to stress-induced cell death allowing for continuous proliferation. However, elucidation of these adaptive processes makes it possible to exploit this characteristic feature to selectively target the cancer cells. The aim of the present thesis is to explore this hypothesis in the setting of HCC.

The **unfolded protein response** (UPR) and **autophagy** are two fundamental adaptive mechanisms [6]. As a consequence of the already engaged ER stress system, fewer contingencies may be left to accommodate additional intensities of ER stress in cancer cells. In comparison, normal cells without chronic ER stress may harbour greater reserves to withstand intervention with agents aimed at aggravating the pro-apoptotic UPR signalling. Thus, manipulation of the UPR could provide a novel strategy to treat HCC.

1.2. The unfolded protein response is dynamically fine-tuned during murine multistep hepatocarcinogenesis

Animal models can provide essential knowledge about the pathogenesis of cancer, particularly when they mimic the natural environment in which human tumours develop. Diethylnitrosamine (DEN) has been shown to induce hepatic tumours, which are similar to human HCC with poor prognosis [7]. In our study, weekly intraperitoneal injections with 35 mg/kg DEN gave rise to HCC formation in a background of inflammation and fibrosis, thus mimicking the human setting. By monitoring the UPR in this model, we provided the, to our knowledge, first evaluation of the **UPR dynamics in a long-term cancer model** [8]. Surprisingly, we observed that the UPR is not an all-or-nothing system. Activation of the UPR pathways is dynamically fine-tuned during the different phases of hepatocarcinogenesis. In fact, each phase of hepatocarcinogenesis is characterized by a specific pattern of UPR signalling. For example, a peak in Ire1 signalling was observed during tumour initiation, while the Perk pathway was activated during tumour progression. Possibly, the dynamic regulation of the UPR is mediated by variations in tissue oxygen levels, which is influenced by the interactions between the UPR and angiogenesis [9].

How the shift from pro-survival to pro-apoptotic UPR signalling is regulated remains unclear with both IRE1 and PERK signalling associated with pro-survival as well as pro-apoptotic signalling [10], [11]. A recent study indicated that the relative dynamics of IRE1/XBP1 and PERK/ATF4 signalling rather than a switch between branches determine cell survival [11]. Moreover, the exact role of **cell apoptosis** [12] and, more specifically, UPR-induced cell apoptosis in the different steps of hepatocarcinogenesis is also unclear. Counterintuitively, recent studies have demonstrated that hepatocyte apoptosis is a pathogenic event in several liver diseases [13], [14]. Chronically increased hepatocyte apoptosis in genetic mouse models is carcinogenic and leads to compensatory liver regeneration, oxidative stress and DNA hypermethylation [13], [15]. However, once tumours are established and develop resistance against cell death signaling pathways, pharmacological or genetic induction of tumour cell apoptosis slows down the tumour growth [12]. Again, the timing of the event determines its outcome.

It is important to note that the hepatic expression of major ER stress markers is **age-dependent**. For example, we observed a decrease in Grp78 mRNA levels and an increase in Chop mRNA levels in the control mice of 5 weeks of age compared to those of 35 weeks of age (fold change: 0.57 and 1.43 respectively). Apparently, there is a shift in the balance between the adaptive response of the UPR and pro-apoptotic signalling during aging; where the protective arm is reduced and the apoptotic arm is more robust [16]. Hence, we decided to use age-matched controls during the monitoring of the UPR dynamics in hepatocarcinogenesis.

Carrara et al. (2015) revealed that transient conversion from a dimeric to a previously unknown and more active **tetrameric** state of PERK is an important regulatory mechanism in PERK signalling [17]. Therefore, analysis of the state and effect of tetramerization of PERK in HCC may offer important insights in the downstream effects of this UPR pathway.

We strengthened the manuscript by performing transmission electron microscopy of the tumours in the mouse model at week 30 revealing an extensive **expanded ribosome-bound ER** in a lamellar pattern and the presence of remarkable **ER reorganization** in HCC cells [18]. Additional investigation of the temporal pattern of these changes in size, preferably measured quantitatively, and organization of the ER in experimental and human HCC is indicated.

Also, exploration of the UPR dynamics in the multistep process of **human** hepatocarcinogenesis from low-grade to high-grade dysplastic nodules, dysplastic nodules with HCC foci to HCCs and comparison to the UPR dynamics in experimental HCC is indicated.

During the progress of our work on the UPR in the DEN model, we encountered the need for functional assessment of the tumour burden in this model. Therefore, we validated innovative **small animal imaging** techniques for the functional assessment of the experimental HCC burden, including ^{18}F-Fluoro-deoxyglucose (FDG) positron emission tomography–computed tomography (PET/CT), ^{18}F-Choline PET/CT and (dynamic contrast-enhanced) magnetic resonance imaging ((DCE-)MRI), and compared these different imaging techniques evaluating the tumour burden in the DEN-induced mouse model (in collaboration with Infinity Lab, Ghent University). We concluded that **^{18}F-Choline PET/CT**, which visualizes the increased cell membrane synthesis requiring choline uptake in tumour cells, was the optimal imaging technique providing high spatial resolution and 3D image reconstructions to assess tumour burden in this model. Furthermore, we validated the quantification of this technique by using the left kidney as reference density and calculating the standardized uptake values of the voxels within the mouse liver [19]. This technique is and will be of uttermost importance in the setting of testing new pharmacological or genetic tools minimizing the number of animals needed, creating smaller standard deviations and eliminating possible confounders between animals.

1.3. Role of the unfolded protein response in the pathogenesis of hepatocellular carcinoma

1.3.1. Modulation of the unfolded protein response impedes tumour cell adaptation to proteotoxic stress: a PERK for hepatocellular carcinoma therapy

In an effort to better understand the underlying mechanisms of HCC cell survival under ER stress, we demonstrated that under ER stress, Perk inhibition and not Ire1 inhibition reduced HCC cell viability and proliferation via escalating proteotoxic stress, and that the small-molecule inhibitor of PERK leads to HCC regression in the orthotopic mouse model [8]. However, important **drawbacks to clinical application of Perk modulation** were identified and need to be discussed.

First, we observed only a modest antitumour effect *in vivo* compared to the dramatic effects on cell viability under chemically induced ER stress *in vitro*. Our preliminary validation studies of the Perk inhibitor used (GSK2656157 [20] at 100 mg/kg bid) showed that the tunicamycin-mediated activation of the Perk pathway in hepatocytes was inhibited for only 6 hours following administration (data not shown), explaining the use of twice a day dosing. Consequently, tumoural Perk signalling was probably not completely and continuously inhibited during the treatment. Development of sustained release formulations containing GSK2656157 could solve this issue.

Secondly, the Perk inhibitor-treated mice exhibited hyperglycaemia compared to the vehicle-treated mice. Induction of diabetes in cancer patients could be an important limitation of therapeutic Perk inhibition. Possibly, the development of a targeted drug delivery system could reduce the toxicity of this compound. A recent study showed that nanoparticles conjugated with an antibody against GRP78 promote drug delivery of 5-fluorouracil into human HCC cells with high expression of surface-exposed GRP78 [21]. Nanoparticles increase the stability of chemical agents by encapsulation, protecting these agents from the extracellular environment and regulating the drug release in a prolonged and controllable manner. The technical feasibility of Perk inhibitor-loaded nanoparticles conjugated with anti-Grp78 and the effect of Perk inhibition on the surface Grp78 expression of HCC cells require further investigation. Taken together, although our results are promising, pharmacological efforts to establish a drug formulation with sustained release and tumour-targeted drug delivery are required.

Recently, the small-molecule N,N'-trans-(cyclohexane-1,4-diyl)-bis-(2-(4-chlorophenoxy) acetamide (integrated stress response inhibitor, **ISRIB**), which prevents translational inhibition downstream of the Perk/phospho-eIf2α pathway, was developed [22]. Interestingly, this small-molecule partially restores global translation without adverse effects on the pancreas, such as induction of diabetes. In prion disease, restoration of global protein synthesis using the Perk inhibitor was profoundly neuroprotective [23]. However, in line with our results, this also occurred at the cost of toxicity to the pancreas. Recently, the effect of ISRIB was tested in this model and conferred similar neuroprotection in prion-diseased mice but without the pancreatic toxicity [24]. Whether the ISRIB-mediated modulation of translational control could mimic the antitumour effects of the Perk inhibitor in the DEN-induced mouse model without the observed deleterious effects is currently unknown.

1.3.2. Tauroursodeoxycholic acid dampens oncogenic apoptosis induced by endoplasmic reticulum stress during hepatocarcinogen exposure

To assess the role of ER stress in the biology of tumour initiation and progression, we applied the chemical chaperone TUDCA in preventive and therapeutic settings of experimental HCC [25], [26]. We discovered that TUDCA attenuates hepatocarcinogenesis by suppressing carcinogen-induced ER stress-mediated cell death and inflammation without stimulating tumour progression [25]. Therefore, this chemical chaperone could represent a novel chemopreventive agent. An important limitation of these interpretations is that the effect of TUDCA was assessed in a model induced by the carcinogen DEN. Although this is a commonly used and well-known carcinogen for experimental HCC, it is noteworthy that assessment of the effects of TUDCA on hepatocarcinogenesis induced by **human-relevant carcinogens**, such as chronic HCV replication or alcohol exposure, could further support the clinical application of this putative chemopreventive strategy. Regarding HCV, preliminary experiments with HCV-infected humanized livers in $Fah^{-/-}/Rag2^{-/-}/Il2rg^{-/-}$ (FRG) mice [27] and with transgenic mice expressing the full HCV protein repertoire at levels corresponding to the natural human infection [28] were initiated in collaboration with Prof. Ph. Meuleman, Ghent university, Ghent, Belgium and Prof. H. Lerat, INSERM U955, Créteil, France. Assessment of the tumour-promoting effects of chronic HCV infection and effects of targeted UPR modulation in these models is planned.

The **mechanism of action of chemical chaperones** is complex and their application is hindered by limited knowledge of their molecular activities [29]. It is thought that chemical chaperones are typically poor solvents for a protein backbone and hence facilitate native structure formation [30]. However, it is unknown whether different chemical chaperones can act differently to modulate folding energy landscapes. Recently, a classification of chemical chaperones based on their thermodynamic effect on protein folding landscapes was proposed [29]. The canonical chemical chaperones, trimethylamine-N-oxide and trehalose, accelerate refolding by decreasing the flexibility of the refolding intermediate, thereby decreasing the entropic barrier of refolding (i.e. reduced disorder of the refolding intermediate), while other small-molecules stabilize the transition state enthalpically (i.e. reduced sum of the internal energy of the refolding intermediate). Additional studies on the exact chaperone mechanism of TUDCA are required.

Next to TUDCA, assessment of the effects of other established and safe chemical chaperones, such as **4-phenylbutyric acid** (4-PBA) or the novel 4-PBA derivatives with a greater chemical chaperone activity than 4-PBA [31], on hepatocarcinogenesis, is indicated to better understand the exact role of chemically improved protein folding capacity in carcinogenesis during carcinogen exposure.

TUDCA has next to its chaperone properties other direct or indirect downstream effects [32]. For example, the reported mechanisms involved in the antiapoptotic properties of TUDCA include targeting of mitochondrial function and integrity and interactions with survival signals in the cAMP, Akt, NF-κB, mitogen-activated protein kinase and phosphatidylinositol 3-kinase signalling pathways [33]. Next to the reduced pro-apoptotic UPR signalling, these cytoprotective effects could attribute to the observed chemopreventive action of TUDCA.

The cellular and molecular pathways involved in metastasis have been studied in many models; however, the link between ER stress signaling and **invasion/metastasis** is poorly understood [34]. Because ER stress was previously linked to cell invasion [29,30], we assessed the effect of TUDCA on cell invasion in a hepatocyte growth factor-induced invasion assay in which spheroids of Hepa1-6 HCC cells embedded in collagen matrix were observed over time. Additionally, we assessed its effect in a Boyden chamber assay.

In the spheroid assay, the perimeter of the TUDCA-treated spheres increased compared to controls after 24 and 48 hours of incubation, suggesting an altered invasive phenotype. However, in the Boyden chamber assay, addition of TUDCA induced no significant alterations in the hepatocyte growth factor-stimulated invasion of these HCC cells over a 48 hour period. These differential results could possibly be explained by the different experimental set-up to assess cell invasion. In the spheroid assay, cells at the border of the spheroid directly invade the surrounding collagen without a chemoattractant force. In contrast, in the Boyden chamber assay, plated HCC cells migrate in the direction of the source of chemoattractants (i.e. added serum in the lower chamber) through the microporous filter membrane and subsequently invade into the attached basement membrane extract. Indeed, adequate *in vivo* evaluation of invasion/metastasis could solve this issue. Despite recent advances in this field [34], systematic studies on the role of the UPR in cancer invasion and metastasis and its effects on the degradation of the extracellular matrix by matrix metalloproteinases are required.

In conclusion, improved cellular coping with carcinogen-induced stress by **assisting protein folding holds great potential to prevent tumourigenesis**. However, validation in other models and identification of the best chemical chaperone in this context is required prior to clinical evaluation.

1.4. Sorafenib interacts reciprocally with the unfolded protein response in hepatocellular carcinoma

While the **multi-kinase inhibitor sorafenib** heralded a major breakthrough in HCC therapy, the clinical benefit is at best modest and transient [3]. Biomarkers determined at diagnosis to identify the patients who will have the best tumour response and/or survival benefit are currently lacking and efforts to attenuate the sorafenib resistance or toxicity were hitherto disappointing [37]. Numerous clinical trials have been conducted to evaluate a large number of molecularly targeted drugs for treating HCC, but most drugs exhibited less efficacy and/or higher toxicity compared to sorafenib. Therefore, considering that this 'specific' inhibitor could target unexpected molecules depending on the biological context [38], defining the mechanisms underlying sorafenib resistance of HCC cells is critical for treating HCC by maximizing its treatment efficacy, while minimizing adverse effects [39].

We found that sorafenib dose-dependently **activates the IRE1/XBP1/RIDD and PERK/eIF2α/ATF4/CHOP/GADD34 pathways** leading to adaptive protein refolding, but reduced the GRP78 protein expression. Since IRE1 knockdown increased induction of apoptosis by sorafenib in MHCC97-L and PLC/PRF/5 HCC cells [40], we hypothesized that IRE1 inhibition could boost the effect of sorafenib. Unexpectedly, a small-molecule inhibitor binding the IRE1 RNase domain [41] attenuated the antiproliferative effect of sorafenib in HepG2 cells. In our experiments, IRE1 is still present, upregulated and able to mediate the well-known protein-protein interactions, such as the IRE1-TRAF2 interaction [10]. In addition, the IRE1 RNase performs RIDD on specific target transcripts, a pro-apoptotic process unexpectedly but significantly activated by the multi-TKI sorafenib [42]. Mechanistically, further characterisation of the mRNA targets of sorafenib-activated RIDD in HCC cells could offer important insights into its mechanism of action.

Recently, So et al. (2015) showed that the IRE1/RIDD pathway could mediate the inhibitory effects of ER stress on global protein translation by decay of the mRNA of **CReP/Ppp1r15b**, a regulatory subunit of eIF2α phosphatase, which is similar to the PERK-mediated GADD34/Ppp1r15a. Therefore, analysis of the effects of sorafenib on this IRE1/RIDD/CReP/eIF2α/translation-axis could provide additional information on the mechanism of action of sorafenib.

Interestingly, **GRP78 protein** expression, a chaperone protein classically induced during the UPR [10], was decreased in sorafenib-treated cells, whereas no major change was observed in the protein levels of PDIA4, another chaperone protein. In view of evidence that GRP78 overexpression confers resistance to sorafenib in HCC cells [43] and that GRP78 plays a cytoprotective role in the setting of ER stress [44], these findings raise the possibility that the decrease in GRP78 levels contribute to the pro-apoptotic effects of sorafenib and that additional blockade of GRP78 induction may enhance the sorafenib-mediated lethality. To elucidate the underlying mechanism of the selective decrease in GRP78 protein expression by sorafenib, analysis of the protein half-life of GRP78 in the presence of sorafenib is indicated to differentiate between decreased production and increased degradation.

Next, we selected two **clinically applicable ER stress inducers**: the proteasome inhibitor bortezomib and the HIV protease inhibitor nelfinavir [45]. Interestingly, only nelfinavir induces an additive effect in combination with sorafenib in HCC, suggesting that the effect of UPR activation depends on the used ER stress inducer. By analysis of the effect of proteasome inhibition in HCC, we found that the proteasome inhibitor oprozomib did not activate the canonical UPR signalling pathway but rather increased the protein levels of UPR proteins by reduced proteasomal degradation. This observation could possibly explain the differential impact of the used ER stress inducers. Finally, further elucidation of clinical applicable pharmacological ER stress inducers is ongoing and a recent study confirmed that several commonly used drugs modulate the UPR pathways [46]. Evaluation of the effects of combination with these newly identified ER stress inducers is optional.

Sorafenib also promotes **autophagic flux** in HCC cells, as shown previously [47]. However, combination of sorafenib with these autophagy inhibitors again induces only additive, but no synergistic, effects in HCC cells. The role of autophagy in sorafenib resistance was previously investigated in other HCC cell lines [48], [49]. These studies indicate that the autophagic responsiveness to sorafenib is distinct between Hep3B and Huh7 cells and that resistance of Hep3B cells to sorafenib may be associated with altered autophagy signalling pathways. Accordingly, in our study we used HepG2 cells, but further research in other HCC cell lines could improve our understanding of the exact role of autophagy in sorafenib resistance.

Since sorafenib activates the UPR and thereby induces adaptive protein refolding and autophagy, we assessed whether **triple therapies** could improve the antitumour efficacy of sorafenib. It was striking that combination of sorafenib with an ER stress inducer and an inhibitor of the observed compensatory mechanisms, i.e. adaptive protein refolding or autophagy, synergistically potentiated the antitumour efficacy of sorafenib *in vitro.* Of these multiple combinations, we assessed the combination with nelfinavir and clarithromycin in different models for HCC, which showed the strongest antiproliferative effects *in vitro*. Of note, nelfinavir and clarithromycin synergized with sorafenib to reduce tumour growth *in vivo* without significant toxicity.

In the last section of our study, we assessed whether it is possible to **omit sorafenib** in this strategy. Interestingly, the threshold for ER stress-induced cell apoptosis during autophagy inhibition in HCC cells is elevated by omission of sorafenib, however, this can be counterbalanced by increasing the dose of nelfinavir without increased toxicity given its relatively high maximum tolerated dose (MTD) [50]. Further investigations need to determine whether daily or cyclic administration of this dual therapy is feasible and sufficient for sustained antitumour response, as evidenced for sorafenib [3]. In line with these results, a patent application involving the use of ER stress inducers together with autophagy inhibitors in HCC with or without sorafenib was filed (P2014/060, Ghent University, in collaboration with Bimetra). Prior to clinical evaluation of these combinations, further investigations including the determination of the optimal dose and ratio of the involved compounds and the efficacy in sorafenib-resistant HepG2 cells [51] is required.

Rudalska et al. (2014) elegantly identified by *in vivo* shRNA screening the **p38/ATF2 pathway** as a mechanism of sorafenib resistance in HCC [52]. Investigating the effect of the proposed triple therapy modulating the induced UPR/autophagy on this presumed sorafenib-resistance pathway may uncover downstream interconnections. For example, oligomerized IRE1 binds TNF receptor-associated factor 2 (TRAF2), activating apoptosis signal-regulating kinase 1 (ASK1) and downstream kinases that activate p38 [10], [53]. Therefore, we speculate that an altered IRE1 pathway activation pattern modulates the p38/ATF2 pathway and thereby sorafenib resistance.

The complex, highly heterogeneous nature of HCC makes it unlikely that targeting only one pathway will achieve optimal disease control. Moreover, the efficacy of multi-TKIs including sorafenib and the recently tested compounds, such as sunitinib, also appears to be insufficient [4] to meaningfully prolong the overall survival of the patients. However, the strategy of combining targeted disruption of the cellular protein homeostasis with inhibition of the cellular "waste disposal" via autophagy (and/or proteasomal degradation) alone or added to the multi-TKI could offer new perspectives in HCC therapy. Combined therapy with multiple drugs is a common practice in cancer therapy and can achieve better therapeutic effects than a single drug. Furthermore, the utility of combining approved drugs by rational drug repositioning may be rapidly clinically implemented in patients. Therefore, **clinical evaluation** of the investigated combinations subverting ER stress in HCC cells towards apoptosis is indicated.

1.5. Therapeutic effects of Artesunate in hepatocellular carcinoma: repurposing an ancient antimalarial agent

The antimalarial Artesunate exerts potent cytotoxic effects on HCC *in vitro* and *in vivo* without inducing body weight reduction, hepatotoxicity or increased mortality in experimental HCC [54]. Furthermore, we found that Artesunate fortified the PERK pathway but did not affect the IRE1 pathway. However, the relevance of this effect on the UPR in the cytotoxic effects of Artesunate requires further investigation.

Of note, the antitumour activity of Artesunate was increased under hypoxia and dual therapy with Artesunate and sorafenib exerted an additive effect on the microscopic tumour burden and further reduced tumour neovascularization compared to sorafenib monotherapy, the current standard-of-care [2], without cumulative toxicity. Again, whether the altered UPR signalling is involved in the efficacy of this dual therapy remains to be elucidated.

Experience in the use of both Artesunate and sorafenib in clinical practice is a considerable advantage. However, in contrast to sorafenib, the safety of Artesunate in HCC patients with mild impaired liver function is currently unknown. Therefore, we recently initiated the **DESPARTH trial** (NCT02304289; in collaboration with Prof. Dr. L. Van Bortel, clinical pharmacology, Ghent University, Belgium and the "Anticancer Fund"), a phase I dose-escalation trial, to assess the safety and determine the MTD of oral Artesunate in HCC patients with mild impaired liver function. This trial is approved and now recruiting. In parallel, the effect of DEN-induced liver dysfunction on Artesunate metabolization and pharmacokinetics following intragastric administration will be investigated (in collaboration with Prof. Dr. B. De Spiegeleer. Lab of Drug Quality & Registration, Ghent University, Belgium). We consider the present studies as an important step forward in moving our understanding of Artesunate mechanisms into the clinical stage.

1.6. PlGF inhibition modulates hypoxia and the unfolded protein response in hepatocellular carcinoma

Our group previously showed that the inhibition of PlGF exerts antitumour effects and induces vessel normalisation [55]. Our most recent study indicates that **PlGF inhibition significantly suppresses UPR activation**, potentially by tempering hypoxia in HCC and that the UPR, in turn, is able to induce PlGF, suggesting the existence of a feedback mechanism of hypoxia-mediated UPR that stimulates PlGF-mediated angiogenesis. Thus, anti-angiogenic therapies, including the blockade of the PlGF pathway that 'normalise' the abnormal blood vessels in tumours, seem to effectively temper tumour hypoxia and hypoxia-induced adaptation processes, such as the UPR, in experimental HCC. However, whether the diminished activation of these adaptation processes accounts for the observed reduction in tumour growth remains elusive.

Our present work in HCC models confirmed the excellent safety profile of monoclonal antibodies against PlGF. Because previous studies on transgenic mice have revealed that PlGF expression is mainly **restricted to pathological conditions** [56], characterisation of the role of ER stress in the selectivity of PlGF expression to pathological angiogenesis, potentially characterised by ER stress, is indicated. Finally, the role of the UPR in **vessel abnormalisation** induced by excessive production of angiogenic factors [57] remains to be elucidated. The UPR induces angiogenic factors [9], possibly resulting in an excessive production and hence vessel abnormalisation.

Because we observed that the **chemotherapeutic doxorubicin** promotes PlGF production and that PlGF inhibition leads to hypoxia-reducing vessel normalisation, potentially decreasing hypoxia-mediated chemoresistance and improving tumoural drug delivery, we questioned whether the inhibition of this angiogenic factor was able to increase the antitumour effect of doxorubicin *in vivo*. However, addition of anti-PlGF to doxorubicin did not alter the weight, survival or tumour burden compared to mice treated with doxorubicin and IgG (data not shown). Thus, we were not able to detect any improvement, suggesting the inhibition of this specific angiogenic factor was insufficient to improve the efficacy of doxorubicin. Possibly, the lack of PlGF can be bypassed by increased production of other angiogenic factors or the tumoural drug delivery may be still impaired despite the observed vessel normalisation. Further investigation is needed to support these hypotheses.

1.7. Proteasome inhibition and the unfolded protein response in hepatocellular carcinoma: an unexpected pathway dysregulation provides an opportunity to boost its efficacy

At its most simple level the **ubiquitin-proteasome system** (UPS) is composed of an E3 ligases-mediated tagging factor in the form of ubiquitin which marks unwanted or damaged proteins for degradation, and the proteasome, a large molecular shredder that degrades proteins into smaller peptides for use in other anabolic processes [58]. The multifaceted role of the UPS includes the degradation of misfolded and damaged proteins, cell cycle regulators, oncogene and tumour suppressor proteins, as well as the regulation of antigen processing and control of transcription factor activity [59].

The next-generation orally bio-available irreversible proteasome inhibitor **oprozomib** (OZ) is assumed to have less adverse events and improved antitumour activity compared to the first-in-class proteasome inhibitor bortezomib [60]. Recently, OZ was shown to exert antitumour activity on myeloma and head and neck cancer xenograft models [60]. Our study showed for the first time that OZ exerted potent anti-tumour effects *in vitro* and in different *in vivo* models for HCC, supporting the therapeutic potential of irreversibly targeting the proteasome.

Theoretically, decreased protein degradation by proteasome inhibition could lead to oxidative stress and UPR activation. However, the mechanism of action and links with the UPR pathways are not well understood. We showed that the cytotoxic effect of OZ depends on the build-up of proteotoxic stress without an important contribution of oxidative stress. Although OZ did not induce the transcriptional UPR program and even inhibited the protease-dependent activation of the cytoprotective ATF6 pathway, OZ elevated the protein levels of different UPR markers. Notably, OZ increased the protein stability of the pro-apoptotic transcription factor CHOP. Thus, **decreased proteasomal degradation of pro-apoptotic UPR proteins** leads to elevated levels of these proteins rather than a general UPR activation by increased unfolded protein load in the ER. Apparently, rapid proteasomal degradation of UPR proteins is a pivotal negative feedback mechanism following recovery of the ER protein homeostasis.

Identification of the specific components of the UPS regulating degradation of these UPR proteins is indicated. Therefore, we initiated a research project investigating the role of **deubiquitinases** (DUBs) in the regulation of the UPR and autophagic flux in HCC. DUBs are components of the UPS that catalyse the removal of ubiquitin moieties from target proteins or polyubiquitin chains, resulting in altered signalling or changes in protein stability. Analysis of the human genome shows the presence of ~80 functional DUBs [61]. A number of DUBs regulate processes associated with cell proliferation and apoptosis, and as such represent candidate targets for cancer therapeutics [62]. Interestingly, the majority of DUBs are cysteine proteases and are more "druggable" compared to the E3 ligases.

Intriguingly, addition of ER stress inducers nelfinavir or salubrinal enhanced the growth-inhibitory effects of OZ in both models without cumulative toxicity, suggesting that this rational combination could represent a safe strategy to potentiate the antitumour effect of proteasome inhibition in HCC. Finally, assessment of the role of **autophagy** in OZ effect and of the effect and toxicity of a triple strategy consisting of oprozomib, an autophagy inhibitor (i.e. clarithromycin) and an ER stress inducer (i.e. nelfinavir), a concept that may retain the unfolded proteins in the ER by blocking the major degradation pathways while inducing additional ER stress, provides great opportunities for future research.

Of note, **human HCC**, in contrast to the unaffected adjacent liver tissue, is characterized by extensive CHOP staining and, assuming the cellular threshold for CHOP-induced apoptosis is similar in hepatocytes and HCC cells, CHOP-promoting therapy could selectively drive the HCC cells toward apoptosis [63]. Because ER stress potentiates the antitumour efficacy of OZ, we assume a stronger effect on the hypoxic ER-stressed tumour cells compared to normal liver tissue. Consequently, we speculate that OZ could be more efficacious in combination with **antiangiogenic** treatments, presumably increasing tumour hypoxia-induced UPR [9], [10], [25].

In conclusion, modulation of the interplay between OZ and the UPR enhances the antitumour efficacy of OZ *in vitro* and in experimental HCC models without cumulative toxicity. Therefore, OZ monotherapy or in combination with UPR modulators may represent a novel and clinically applicable therapeutic strategy for advanced HCC.

2. General conclusions

Although extensive HCC research is in progress, to this date, the results are unsatisfactory with limited long-term survival. In the fight against this lethal disease, there is still a long way to go. New therapeutic tools need to be not only therapeutically effective but also tolerable and economically within the reach of the neediest people. The potential impact of the UPR in many human diseases makes UPR signalling a promising target for therapeutic intervention. In this thesis, the role and translational potential of the UPR in HCC biology were explored.

The UPR protects cells against defects in protein folding in the ER. Because many mechanisms come into play, the cell carefully balances various means at its disposal to protect against proteotoxicity while also providing adequate protein synthesis to sustain cellular fitness. Tumour cells continuously divide and grow under oncogenic stress caused by hypoxia, nutrient deprivation, metabolic stress and oxidative stress, leading to UPR activation as a central cellular adaptation strategy. The role of the UPR in malignancy has inspired great interest in exploring the therapeutic potential of targeting UPR components. Because most normal cells are not subjected to stress and the UPR pathways remain inactive in these cells, this difference between tumour and normal cells might offer the advantage of achieving specificity in cancer therapy by UPR targeting. If tumour cells are exposed to another form of ER stress in addition to the pre-existent ER stress, the intensity of ER stress might exceed a threshold, thereby inducing cell death specifically in tumour cells. Therefore, it is of considerable importance to understand the impact and dynamics of the UPR in HCC.

As a general conclusion, this thesis provides evidence that the UPR plays a pivotal role in the multistep process of hepatocarcinogenesis. Furthermore, this work indicates that modulation of the UPR could potentially be applied as an innovative strategy against HCC initiation and progression and as a method to enhance the efficacy of certain drugs acting on these adaptive signalling pathways. Based on the novel concepts discussed here, the future challenge is to integrate our understanding of how the UPR regulates distinct aspects of cancer biology as a global network integrating the different cellular stress responses. Although the obtained results hold great potential, several questions remain and require further fundamental and clinical research in the near future.

3. References

[1] International Agency for Research on Cancer, "GLOBOCAN 2012," *Estimated Incidence, Mortality and Prevalence Worldwide in 2012*, 2012. [Online]. Available: http://globocan.iarc.fr/Pages/fact_sheets_cancer.aspx.

[2] "EASL-EORTC clinical practice guidelines: management of hepatocellular carcinoma.," *J. Hepatol.*, vol. 56, no. 4, pp. 908–43, Apr. 2012.

[3] J. M. Llovet, S. Ricci, V. Mazzaferro, P. Hilgard, E. Gane, J.-F. Blanc, A. C. de Oliveira, A. Santoro, J.-L. Raoul, A. Forner, M. Schwartz, C. Porta, S. Zeuzem, L. Bolondi, T. F. Greten, P. R. Galle, J.-F. Seitz, I. Borbath, D. Häussinger, T. Giannaris, M. Shan, M. Moscovici, D. Voliotis, and J. Bruix, "Sorafenib in advanced hepatocellular carcinoma.," *N. Engl. J. Med.*, vol. 359, no. 4, pp. 378–90, Jul. 2008.

[4] J. M. Llovet and V. Hernandez-Gea, "Hepatocellular carcinoma: reasons for phase III failure and novel perspectives on trial design.," *Clin. Cancer Res.*, vol. 20, no. 8, pp. 2072–9, Apr. 2014.

[5] D. Ackerman and M. C. Simon, "Hypoxia, lipids, and cancer: surviving the harsh tumor microenvironment.," *Trends Cell Biol.*, vol. 24, no. 8, pp. 472–8, Aug. 2014.

[6] D. Senft and Z. A. Ronai, "UPR, autophagy, and mitochondria crosstalk underlies the ER stress response," *Trends Biochem. Sci.*, Feb. 2015.

[7] F. Heindryckx, K. Mertens, N. Charette, B. Vandeghinste, C. Casteleyn, C. Van Steenkiste, D. Slaets, L. Libbrecht, S. Staelens, P. Starkel, A. Geerts, I. Colle, and H. Van Vlierberghe, "Kinetics of angiogenic changes in a new mouse model for hepatocellular carcinoma," *Mol. Cancer*, vol. 9, no. 1, p. 219, 2010.

[8] Y.-P. Vandewynckel, D. Laukens, E. Bogaerts, A. Paridaens, A. Van den Bussche, X. Verhelst, C. Van Steenkiste, B. Descamps, C. Vanhove, L. Libbrecht, R. De Rycke, B. N. Lambrecht, A. Geerts, S. Janssens, and H. Van Vlierberghe, "Modulation of the unfolded protein response impedes tumor cell adaptation to proteotoxic stress: a PERK for hepatocellular carcinoma therapy," *Hepatol. Int.*, vol. 9, no. 1, pp. 93–104, Oct. 2015.

[9] A. Paridaens, D. Laukens, Y.-P. Vandewynckel, S. Coulon, H. Van Vlierberghe, A. Geerts, and I. Colle, "Endoplasmic reticulum stress and angiogenesis: is there an interaction between them?," *Liver Int.*, Jan. 2014.

[10] Y.-P. Vandewynckel, D. Laukens, A. Geerts, E. Bogaerts, A. Paridaens, X. Verhelst, S. Janssens, F. Heindryckx, and H. Van Vlierberghe, "The paradox of the unfolded protein response in cancer.," *Anticancer Res.*, vol. 33, no. 11, pp. 4683–94, Nov. 2013.

[11] F. Walter, J. Schmid, H. Düssmann, C. G. Concannon, and J. H. M. Prehn, "Imaging of single cell responses to ER stress indicates that the relative dynamics of IRE1/XBP1 and PERK/ATF4 signalling rather than a switch between signalling branches determine cell survival.," *Cell Death Differ.*, Jan. 2015.

[12] J. M. Schattenberg, M. Schuchmann, and P. R. Galle, "Cell death and hepatocarcinogenesis: Dysregulation of apoptosis signaling pathways.," *J. Gastroenterol. Hepatol.*, vol. 26 Suppl 1, pp. 213–9, Jan. 2011.

[13] H. Hikita, T. Kodama, S. Shimizu, W. Li, M. Shigekawa, S. Tanaka, A. Hosui, T. Miyagi, T. Tatsumi, T. Kanto, N. Hiramatsu, E. Morii, N. Hayashi, and T. Takehara, "Bak deficiency inhibits liver carcinogenesis: A causal link between apoptosis and carcinogenesis.," *J. Hepatol.*, Mar. 2012.

[14] H. Malhi and R. J. Kaufman, "Endoplasmic reticulum stress in liver disease.," *J. Hepatol.*, vol. 54, no. 4, pp. 795–809, Apr. 2011.

[15] H. Hikita, T. Tatsumi, Y. Saito, S. Tanaka, S. Shimizu, W. Li, R. Sakamori, T. Miyagi, N. Hiramatsu, and T. Takehara, "Poster 1793: Oxidative stress induced by continuous hepatocyte apoptosis drives liver carcinogenesis independently of regeneration and DNA methylation status," *Hepatology*, vol. 58, no. S1, pp. 92–207, 2013.

[16] M. K. Brown and N. Naidoo, "The endoplasmic reticulum stress response in aging and age-related diseases.," *Front. Physiol.*, vol. 3, p. 263, Jan. 2012.

[17] M. Carrara, F. Prischi, P. R. Nowak, and M. M. Ali, "Crystal structures reveal transient PERK luminal domain tetramerization in endoplasmic reticulum stress signaling," *EMBO J.*, Apr. 2015.

[18] Y.-P. Vandewynckel, D. Laukens, E. Bogaerts, A. Paridaens, A. Van den Bussche, X. Verhelst, C. Van Steenkiste, B. Descamps, C. Vanhove, L. Libbrecht, R. De Rycke, B. N. Lambrecht, A. Geerts, S. Janssens, and H. Van Vlierberghe, "Modulation of the unfolded protein response impedes tumor cell adaptation to proteotoxic stress: a PERK for hepatocellular carcinoma therapy," *Hepatol. Int.*, vol. 9, no. 1, pp. 93–104, 2015.

[19] J. A. Thie, "Understanding the standardized uptake value, its methods, and implications for usage.," *J. Nucl. Med.*, vol. 45, no. 9, pp. 1431–4, Sep. 2004.

[20] J. M. Axten, S. P. Romeril, A. Shu, J. Ralph, J. R. Medina, Y. Feng, W. H. H. Li, S. W. Grant, D. A. Heerding, E. Minthorn, T. Mencken, N. Gaul, A. Goetz, T. Stanley, A. M. Hassell, R. T. Gampe, C. Atkins, and R. Kumar, "Discovery of GSK2656157: An Optimized PERK Inhibitor Selected for Preclinical Development.," *ACS Med. Chem. Lett.*, vol. 4, no. 10, pp. 964–8, Oct. 2013.

[21] L. Zhao, H. Li, Y. Shi, G. Wang, L. Liu, C. Su, and R. Su, "Nanoparticles inhibit cancer cell invasion and enhance antitumor efficiency by targeted drug delivery via cell surface-related GRP78.," *Int. J. Nanomedicine*, vol. 10, pp. 245–56, Jan. 2015.

[22] C. Sidrauski, D. Acosta-Alvear, A. Khoutorsky, P. Vedantham, B. R. Hearn, H. Li, K. Gamache, C. M. Gallagher, K. K.-H. Ang, C. Wilson, V. Okreglak, A. Ashkenazi, B. Hann, K. Nader, M. R. Arkin, A. R. Renslo, N. Sonenberg, and P. Walter, "Pharmacological brake-release of mRNA translation enhances cognitive memory.," *Elife*, vol. 2, p. e00498, Jan. 2013.

[23] J. A. Moreno, M. Halliday, C. Molloy, H. Radford, N. Verity, J. M. Axten, C. A. Ortori, A. E. Willis, P. M. Fischer, D. A. Barrett, and G. R. Mallucci, "Oral treatment targeting the unfolded protein response prevents neurodegeneration and clinical disease in prion-infected mice.," *Sci. Transl. Med.*, vol. 5, no. 206, p. 206ra138, Oct. 2013.

[24] M. Halliday, H. Radford, Y. Sekine, J. Moreno, N. Verity, J. le Quesne, C. A. Ortori, D. A. Barrett, C. Fromont, P. M. Fischer, H. P. Harding, D. Ron, and G. R. Mallucci, "Partial restoration of protein synthesis rates by the small molecule ISRIB prevents neurodegeneration without pancreatic toxicity," *Cell Death Dis.*, vol. 6, no. 3, p. e1672, Mar. 2015.

[25] Y.-P. Vandewynckel, D. Laukens, L. Devisscher, A. Paridaens, E. Bogaerts, X. Verhelst, A. Van den Bussche, S. Raevens, C. Van Steenkiste, M. Van Troys, C. Ampe, B. Descamps, C. Vanhove, O. Govaere, A. Geerts, and H. Van Vlierberghe, "Tauroursodeoxycholic acid dampens oncogenic apoptosis induced by endoplasmic reticulum stress during hepatocarcinogen exposure," *Oncotarget*, vol. under revi, 2015.

[26] D. Laukens, L. Devisscher, L. Van den Bossche, P. Hindryckx, R. Vandenbroucke, Y.-P. Vandewynckel, C. Cuvelier, B. Brinkman, C. Libert, P. Vandenabeele, and M. De Vos, "Tauroursodeoxycholic acid inhibits experimental colitis by preventing early intestinal epithelial cell death," *Lab. Invest.*, 2014.

[27] M. Grompe and S. Strom, "Mice with human livers.," *Gastroenterology*, vol. 145, no. 6, pp. 1209–14, Dec. 2013.

[28] M. R. Higgs, H. Lerat, and J.-M. Pawlotsky, "Hepatitis C virus-induced activation of β-catenin promotes c-Myc expression and a cascade of pro-carcinogenetic events.," *Oncogene*, vol. 32, no. 39, pp. 4683–93, Sep. 2013.
[29] R. Dandage, A. Bandyopadhyay, G. G. Jayaraj, K. Saxena, V. Dalal, A. Das, and K. Chakraborty, "Classification of chemical chaperones based on their effect on protein folding landscapes.," *ACS Chem. Biol.*, Dec. 2014.
[30] H. Kraskiewicz and U. Fitzgerald, "InterfERing with endoplasmic reticulum stress.," *Trends Pharmacol. Sci.*, vol. 33, no. 2, pp. 53–63, Feb. 2012.
[31] S. Mimori, Y. Koshikawa, Y. Mashima, K. Mitsunaga, K. Kawada, M. Kaneko, Y. Okuma, Y. Nomura, Y. Murakami, T. Kanzaki, and H. Hamana, "Evaluation of synthetic naphthalene derivatives as novel chemical chaperones that mimic 4-phenylbutyric acid.," *Bioorg. Med. Chem. Lett.*, Jan. 2015.
[32] S. Vang, K. Longley, C. J. Steer, and W. C. Low, "The Unexpected Uses of Urso- and Tauroursodeoxycholic Acid in the Treatment of Non-liver Diseases.," *Glob. Adv. Health Med.*, vol. 3, no. 3, pp. 58–69, May 2014.
[33] M.-J. Perez and O. Briz, "Bile-acid-induced cell injury and protection.," *World J. Gastroenterol.*, vol. 15, no. 14, pp. 1677–89, Apr. 2009.
[34] E. Dufey, H. Urra, and C. Hetz, "ER proteostasis addiction in cancer biology: Novel concepts.," *Semin. Cancer Biol.*, Apr. 2015.
[35] Y. Li, H. Liu, Y. Y. Huang, L. J. Pu, X. D. Zhang, C. C. Jiang, and Z. W. Jiang, "Suppression of endoplasmic reticulum stress-induced invasion and migration of breast cancer cells through the downregulation of heparanase," *Int. J. Mol. Med.*, vol. 31, no. 5, pp. 1234–1242, May 2013.
[36] N. Dejeans, O. Pluquet, S. Lhomond, F. Grise, M. Bouchecareilh, A. Juin, M. Meynard-Cadars, A. Bidaud-Meynard, C. Gentil, V. Moreau, F. Saltel, and E. Chevet, "Autocrine control of glioma cells adhesion and migration through IRE1α-mediated cleavage of SPARC mRNA.," *J. Cell Sci.*, vol. 125, no. Pt 18, pp. 4278–87, Sep. 2012.
[37] G. Ferrín, P. Aguilar-Melero, M. Rodríguez-Perálvarez, J. L. Montero-Álvarez, and M. de la Mata, "Biomarkers for hepatocellular carcinoma: diagnostic and therapeutic utility.," *Hepat. Med.*, vol. 7, pp. 1–10, Jan. 2015.
[38] M. Cervello, D. Bachvarov, N. Lampiasi, A. Cusimano, A. Azzolina, J. A. McCubrey, and G. Montalto, "Molecular mechanisms of sorafenib action in liver cancer cells.," *Cell Cycle*, vol. 11, no. 15, pp. 2843–55, Aug. 2012.
[39] H. Sun, M.-S. Zhu, W.-R. Wu, X.-D. Shi, and L.-B. Xu, "Role of anti-angiogenesis therapy in the management of hepatocellular carcinoma: The jury is still out.," *World J. Hepatol.*, vol. 6, no. 12, pp. 830–5, Dec. 2014.
[40] Y.-H. Shi, Z.-B. Ding, J. Zhou, B. Hui, G.-M. Shi, A.-W. Ke, X.-Y. Wang, Z. Dai, Y.-F. Peng, C.-Y. Gu, S.-J. Qiu, and J. Fan, "Targeting autophagy enhances sorafenib lethality for hepatocellular carcinoma via ER stress-related apoptosis.," *Autophagy*, vol. 7, no. 10, pp. 1159–72, Oct. 2011.
[41] B. C. S. Cross, P. J. Bond, P. G. Sadowski, B. K. Jha, J. Zak, J. M. Goodman, R. H. Silverman, T. A. Neubert, I. R. Baxendale, D. Ron, and H. P. Harding, "The molecular basis for selective inhibition of unconventional mRNA splicing by an IRE1-binding small molecule.," *Proc. Natl. Acad. Sci. U. S. A.*, Feb. 2012.
[42] M. Maurel, E. Chevet, J. Tavernier, and S. Gerlo, "Getting RIDD of RNA: IRE1 in cell fate regulation.," *Trends Biochem. Sci.*, Mar. 2014.
[43] J.-F. Chiou, C.-J. Tai, M.-T. Huang, P.-L. Wei, Y.-H. Wang, J. An, C.-H. Wu, T.-Z. Liu, and Y.-J. Chang, "Glucose-regulated protein 78 is a novel contributor to acquisition of resistance to sorafenib in hepatocellular carcinoma.," *Ann. Surg. Oncol.*, vol. 17, no. 2, pp. 603–12, Feb. 2010.

[44] D. Dong, C. Stapleton, B. Luo, S. Xiong, W. Ye, Y. Zhang, N. Jhaveri, G. Zhu, R. Ye, Z. Liu, K. W. Bruhn, N. Craft, S. Groshen, F. M. Hofman, and A. S. Lee, "A critical role for GRP78/BiP in the tumor microenvironment for neovascularization during tumor growth and metastasis.," *Cancer Res.*, vol. 71, no. 8, pp. 2848–57, Apr. 2011.

[45] E. Mahoney, K. Maddocks, J. Flynn, J. Jones, S. L. Cole, X. Zhang, J. C. Byrd, and A. J. Johnson, "Identification of endoplasmic reticulum stress-inducing agents by antagonizing autophagy: a new potential strategy for identification of anti-cancer therapeutics in B-cell malignancies.," *Leuk. Lymphoma*, vol. 54, no. 12, pp. 2685–92, Dec. 2013.

[46] N. A. Doudican, S. Y. Wen, A. Mazumder, and S. J. Orlow, "Identification of agents that promote endoplasmic reticulum stress using an assay that monitors luciferase secretion.," *J. Biomol. Screen.*, vol. 19, no. 4, pp. 575–84, Apr. 2014.

[47] S. Shimizu, T. Takehara, H. Hikita, T. Kodama, H. Tsunematsu, T. Miyagi, A. Hosui, H. Ishida, T. Tatsumi, T. Kanto, N. Hiramatsu, N. Fujita, T. Yoshimori, and N. Hayashi, "Inhibition of autophagy potentiates the antitumor effect of the multikinase inhibitor sorafenib in hepatocellular carcinoma.," *Int. J. Cancer*, vol. 131, no. 3, pp. 548–57, Aug. 2012.

[48] T. D. Fischer, J.-H. Wang, A. Vlada, J.-S. Kim, and K. E. Behrns, "Role of autophagy in differential sensitivity of hepatocarcinoma cells to sorafenib.," *World J. Hepatol.*, vol. 6, no. 10, pp. 752–8, Oct. 2014.

[49] H. Yuan, A.-J. Li, S.-L. Ma, L.-J. Cui, B. Wu, L. Yin, and M.-C. Wu, "Inhibition of autophagy significantly enhances combination therapy with sorafenib and HDAC inhibitors for human hepatoma cells.," *World J. Gastroenterol.*, vol. 20, no. 17, pp. 4953–62, May 2014.

[50] G. M. Blumenthal, J. J. Gills, M. S. Ballas, W. B. Bernstein, T. Komiya, R. Dechowdhury, B. Morrow, H. Root, G. Chun, C. Helsabeck, S. M. Steinberg, J. LoPiccolo, S. Kawabata, E. R. Gardner, W. D. Figg, and P. A. Dennis, "A phase I trial of the HIV protease inhibitor nelfinavir in adults with solid tumors.," *Oncotarget*, vol. 5, no. 18, pp. 8161–72, Sep. 2014.

[51] H. van Malenstein, J. Dekervel, C. Verslype, E. Van Cutsem, P. Windmolders, F. Nevens, and J. van Pelt, "Long-term exposure to sorafenib of liver cancer cells induces resistance with epithelial-to-mesenchymal transition, increased invasion and risk of rebound growth.," *Cancer Lett.*, vol. 329, no. 1, pp. 74–83, Feb. 2013.

[52] R. Rudalska, D. Dauch, T. Longerich, K. McJunkin, T. Wuestefeld, T.-W. Kang, A. Hohmeyer, M. Pesic, J. Leibold, A. von Thun, P. Schirmacher, J. Zuber, K.-H. Weiss, S. Powers, N. P. Malek, M. Eilers, B. Sipos, S. W. Lowe, R. Geffers, S. Laufer, and L. Zender, "In vivo RNAi screening identifies a mechanism of sorafenib resistance in liver cancer.," *Nat. Med.*, vol. 20, no. 10, pp. 1138–46, Sep. 2014.

[53] D. Ron and P. Walter, "Signal integration in the endoplasmic reticulum unfolded protein response.," *Nat. Rev. Mol. Cell Biol.*, vol. 8, no. 7, pp. 519–29, Jul. 2007.

[54] Y.-P. Vandewynckel, D. Laukens, A. Geerts, C. Vanhove, B. Descamps, L. Devisscher, E. Bogaerts, A. Paridaens, X. Verhelst, C. Van Steenkiste, L. Libbrecht, I. Colle, B. Lambrecht, S. Janssens, and H. Van Vlierberghe, "Therapeutic Effects of Artesunate in Hepatocellular Carcinoma: Repurposing an Ancient Antimalarial Agent," *Eur. J. Gastroenterol. Hepatol.*, 2014.

[55] S. Van de Veire, I. Stalmans, F. Heindryckx, H. Oura, A. Tijeras-Raballand, T. Schmidt, S. Loges, I. Albrecht, B. Jonckx, S. Vinckier, C. Van Steenkiste, S. Tugues, C. Rolny, M. De Mol, D. Dettori, P. Hainaud, L. Coenegrachts, J.-O. Contreres, T. Van Bergen, H. Cuervo, W.-H. Xiao, C. Le Henaff, I. Buysschaert, B. Kharabi Masouleh, A. Geerts, T. Schomber, P. Bonnin, V. Lambert, J. Haustraete, S. Zacchigna, J.-M.

Rakic, W. Jiménez, A. Noël, M. Giacca, I. Colle, J.-M. Foidart, G. Tobelem, M. Morales-Ruiz, J. Vilar, P. Maxwell, S. A. Vinores, G. Carmeliet, M. Dewerchin, L. Claesson-Welsh, E. Dupuy, H. Van Vlierberghe, G. Christofori, M. Mazzone, M. Detmar, D. Collen, and P. Carmeliet, "Further pharmacological and genetic evidence for the efficacy of PlGF inhibition in cancer and eye disease.," *Cell*, vol. 141, no. 1, pp. 178–90, Apr. 2010.

[56] M. Autiero, A. Luttun, M. Tjwa, and P. Carmeliet, "Placental growth factor and its receptor, vascular endothelial growth factor receptor-1: novel targets for stimulation of ischemic tissue revascularization and inhibition of angiogenic and inflammatory disorders," *J. Thromb. Haemost.*, vol. 1, no. 7, pp. 1356–1370, Jul. 2003.

[57] K. De Bock, F. De Smet, R. Leite De Oliveira, K. Anthonis, and P. Carmeliet, "Endothelial oxygen sensors regulate tumor vessel abnormalization by instructing phalanx endothelial cells.," *J. Mol. Med. (Berl).*, vol. 87, no. 6, pp. 561–9, Jun. 2009.

[58] D. M. Benbrook and A. Long, "Integration of autophagy, proteasomal degradation, unfolded protein response and apoptosis.," *Exp. Oncol.*, vol. 34, no. 3, pp. 286–97, Oct. 2012.

[59] A. Hershko and A. Ciechanover, "The ubiquitin system.," *Annu. Rev. Biochem.*, vol. 67, pp. 425–79, Jan. 1998.

[60] M.-V. Mateos, E. M. Ocio, and J. F. San Miguel, "Novel generation of agents with proven clinical activity in multiple myeloma.," *Semin. Oncol.*, vol. 40, no. 5, pp. 618–33, Oct. 2013.

[61] D. Komander, M. J. Clague, and S. Urbé, "Breaking the chains: structure and function of the deubiquitinases.," *Nat. Rev. Mol. Cell Biol.*, vol. 10, no. 8, pp. 550–63, Aug. 2009.

[62] P. D'Arcy, X. Wang, and S. Linder, "Deubiquitinase inhibition as a cancer therapeutic strategy.," *Pharmacol. Ther.*, vol. 147, pp. 32–54, Mar. 2015.

[63] D. Dezwaan-McCabe, J. D. Riordan, A. M. Arensdorf, M. S. Icardi, A. J. Dupuy, and D. T. Rutkowski, "The Stress-Regulated Transcription Factor CHOP Promotes Hepatic Inflammatory Gene Expression, Fibrosis, and Oncogenesis.," *PLoS Genet.*, vol. 9, no. 12, p. e1003937, Dec. 2013.

Chapter 5

Curriculum Vitae

1. Curriculum Vitae

1.1.1. Personal information

- Address: Warandemolen 20, 9890 Gavere, Belgium
- Tel: +32 495/342794
- E-mail: yvespaul.vandewynckel@ugent.be
- Nationality: Belgian
- Date of birth: 06/07/1987

1.1.2. Education

- 01/09/2012: PhD student, Ghent University, Dept. of Gastroenterology; http://www.ugent.be/ge/inwgen/en/research/gastroenterology/hepatology
- 30/06/2012: Resident Internal Medicine, Ghent University Hospital
- 2008-2012: Master of Medicine, Ghent University
  Achieved with "magna cum laude"

- 2005-2008: Bachelor of Medicine, Ghent University
  Achieved with "magna cum laude"

- 1999-2005: Latin, Latin-Mathematics, Science-Mathematics, St. Aloysius College, Diksmuide, Belgium. *Graduated laureate*

1.1.3. Courses

- 24/04/2015: Abdominal **ultrasound** hands-on course: "Hepatology diagnostics by US" during ILC of EASL 2015 at Vienna, Austria
- 16-17/04/2015: Advanced **endoscopy** hands-on course in SkillsLab of Erasmus MC, Rotterdam, The Netherlands.
- 14/06/2014: Young VVGE course: "Pre-malign conditions of the GI tract", Belgium
- 06/2014:"Medical **English**" with proof of competence (UGent)
- 09/2013: Doctoral schools: **clinical trial design** course (UGent)
- 07/2013: Interuniversity Special Education **Antibiotic Policy** course (4 days) + certificate
- 06/2013: "*Advanced academic conference skills*" doctoral schools course (UGent)
- 13/06/2013: Course and certificate of **clinical trial investigator** skills (UGent)
- 16/03/13: Spring symposium 2013 **VVGE**, Groot-Bijgaarden. Travel bursary by VVGE for best abstract
- 29/09/2012: Course and certificate **Abdominal ultrasound** at "Flemish Association for Ultrasound"
- 09/2012: Doctor in "**Child and Family**" after training course
- 08/2012: Doctoral schools: "*English presentation techniques*" course (UGent)
- 06/2012: "Medical **French**" with proof of competence (UGent)
- 20/01/2012: Laboratory animal science course (FELASA approved)
- 2011-12: Introductory Statistics: principles of statistical interference, SPSS and ANOVA, Institute for Continuing Formation in Sciences (UGent)
- 2011: Radiation and radioprotection (UGent)
- 2009: Postacademic formation in electrocardiography (UGent)

1.1.4. **Teaching experience**

- Start in 03/2015: Clinical education: tutor 2nd Bachelor, Medicine: Skills Lab, UGent: "Clinical examination of the abdomen".
- 09/2014-06/2016: Thesis supervisor of M.Sc project **Astrid Vandierendonck**, Biomedical sciences, Ghent University: "*Therapeutic potential of deubiquitinase inhibition in HCC*".
- 09/2014-06/2016: Thesis supervisor of M.Sc project **Margot Vandenbossche**, Biomedical sciences, Ghent University: "*The interconnection between chaperone-mediated autophagy and endoplasmic reticulum stress in HCC*".
- 09/2014-06/2016: Thesis co-supervisor of M.Sc project **Laure De Maere**, Biomedical sciences, Ghent University: "*The role of endoplasmic reticulum stress in the neuronal cell death in a rat model for hepatic encephalopathy*".
- 09/2013-06/2015: Thesis supervisor of M.Sc project **Céline Coucke**, Biomedical sciences, Ghent University: "*Therapeutic potential of next-generation proteasome inhibitor Oprozomib in HCC*".
- 09/2012-06/2014: Thesis supervisor of M.Sc project **Ine De Saegher**, Biomedical sciences, Ghent University: "*Modulation of Sorafenib resistance in HCC*".

1.1.5. **Management skills**

- 18/08/2014: Member of the steering committee UGent for Internal Medicine lectures
- 17/06/2014: Elected president of "Young BASL" + active member of BASL as Young BASL representative
- 08/2012: Member of program committee UGent "ManaMa Specialist Medicine" as Resident representative for Internal Medicine

1.1.6. **Conference presentations**

- **Yves-Paul Vandewynckel**. Journal Watch in Internal Medicine: What's new?. *Internal Medicine lecture (Ghent University)*, 11/06/2015, Ghent, Belgium. Oral presentation

- **Yves-Paul Vandewynckel**, Debby Laukens, Lindsey Devisscher, Annelies Paridaens, Eliene Bogaerts, Xavier Verhelst, Anja Van den Bussche, Sarah Raevens, Christophe Van Steenkiste, Marleen Van Troys, Christophe Ampe, Benedicte Descamps, Chris Vanhove, Olivier Govaere, Anja Geerts, Hans Van Vlierberghe. Tauroursodeoxycholic acid dampens oncogenic apoptosis induced by endoplasmic reticulum stress during hepatocarcinogen exposure. *International Liver Congress (EASL)*, 24/04/2015, Vienna, Austria. Poster presentation. Awarded as Top 10% abstract.

- **Yves-Paul Vandewynckel**, Xavier Verhelst, Klara Rombauts, Bart De Spiegeleer, Luc Van Bortel, Anja Geerts, Hans Van Vlierberghe. Phase I dose-escalation study evaluating the safety and pharmacokinetics of oral Artesunate in patients with advanced hepatocellular carcinoma (DESPARTH trial). *International Liver Congress (EASL)*, 24/04/2015, Vienna, Austria. Poster presentation

- **Yves-Paul Vandewynckel**, Debby Laukens, Lindsey Devisscher, Annelies Paridaens, Eliene Bogaerts, Anja Van den Bussche, Sarah Raevens, Xavier Verhelst, Christophe Van Steenkiste, Bart Jonckx, Louis Libbrecht, Anja Geerts, Peter Carmeliet, Hans Van Vlierberghe. Placental growth factor inhibition modulates the interplay between hypoxia and

the unfolded protein response in hepatocellular carcinoma. *International Liver Congress (EASL)*, 24/04/2015, Vienna, Austria. Poster presentation

- **Yves-Paul Vandewynckel**, Debby Laukens, Lindsey Devisscher, Annelies Paridaens, Eliene Bogaerts, Anja Van den Bussche, Sarah Raevens, Xavier Verhelst, Christophe Van Steenkiste, Bart Jonckx, Louis Libbrecht, Anja Geerts, Peter Carmeliet, Hans Van Vlierberghe. Placental growth factor inhibition modulates the interplay between hypoxia and the unfolded protein response in hepatocellular carcinoma. *27th Belgian Week of Gastroenterology*, 25/02/2015, Brussels, Belgium. Oral presentation

- Olivier Govaere, M. Petz, Jasper Wouters, **Yves-Paul Vandewynckel**, A. Ceulemans, Baki Topal, Chris Verslype, Hans Van Vlierberghe, Frederick Nevens, W. Mikulits, Tania Roskams. PDGFRA-mediated Laminin B1 deposition induces invasion in human hepatocellular carcinoma. *27th Belgian Week of Gastroenterology*, 25/02/2015, Brussels, Belgium. Oral presentation

- **Yves-Paul Vandewynckel**, Debby Laukens, Lindsey Devisscher, Annelies Paridaens, Eliene Bogaerts, Xavier Verhelst, Anja Van den Bussche, Sarah Raevens, Christophe Van Steenkiste, Marleen Van Troys, Christophe Ampe, Benedicte Descamps, Chris Vanhove, Olivier Govaere, Anja Geerts, Hans Van Vlierberghe. Tauroursodeoxycholic acid dampens oncogenic apoptosis induced by endoplasmic reticulum stress during hepatocarcinogen exposure in mice. *27th Belgian Week of Gastroenterology*, 25/02/2015, Brussels, Belgium. Oral presentation

- **Yves-Paul Vandewynckel**. Young BASL Forum. introduction as Young BASL President. *27th Belgian Week of Gastroenterology*, 25/02/2015, Brussels, Belgium. Oral presentation

- **Yves-Paul Vandewynckel**, Debby Laukens, Lindsey Devisscher, Annelies Paridaens, Eliene Bogaerts, Xavier Verhelst, Anja Van den Bussche, Sarah Raevens, Christophe Van Steenkiste, Marleen Van Troys, Christophe Ampe, Benedicte Descamps, Chris Vanhove, Olivier Govaere, Anja Geerts, Hans Van Vlierberghe. Tauroursodeoxycholic acid dampens oncogenic apoptosis induced by endoplasmic reticulum stress during hepatocarcinogen exposure. *Oncopoint III*, 11/02/2015, Ghent, Belgium. Oral presentation

- **Yves-Paul Vandewynckel**. Introduction of the Young BASL. *BASL winter meeting*, 05/12/2014, La Hulpe, Belgium. Oral presentation

- Annelies Paridaens, **Yves-Paul Vandewynckel**, Eliene Bogaerts, Anja Van den Bussche, Hans Van Vlierberghe, Anja M. Geerts, Isabelle Colle. Endoplasmic Reticulum stress inhibitors diminish acetaminophen toxicity. *American Association for the Study of Liver Diseases (AASLD)*, 07/11/2014, Boston, USA. Poster presentation

- **Yves-Paul Vandewynckel**, Debby Laukens, Eliene Bogaerts, Annelies Paridaens, Anja Van den Bussche, Xavier Verhelst, Christophe Van Steenkiste, Benedicte Descamps, Chris Vanhove, Louis Libbrecht, Riet De Rycke, Bart N. Lambrecht, Anja Geerts, Sophie Janssens, Hans Van Vlierberghe. Temporal Dynamics and Therapeutic Potential of the Unfolded Protein Response in Hepatocellular Carcinoma. *International Liver Congress (EASL)*. 12/04/2014, London, UK. Oral presentation

- **Yves-Paul Vandewynckel**, Debby Laukens, Eliene Bogaerts, Annelies Paridaens, Anja Van den Bussche, Xavier Verhelst, Christophe Van Steenkiste, Benedicte Descamps, Chris Vanhove, Louis Libbrecht, Riet De Rycke, Bart N. Lambrecht, Anja Geerts, Sophie Janssens, Hans Van Vlierberghe. The therapeutic potential of the unfolded protein response in HCC. *International Liver Congress (EASL)*. 12/04/2014, London, UK. Poster presentation

- **Yves-Paul Vandewynckel**, Debby Laukens, Anja Geerts, Chris Vanhove, Benedicte Descamps, Isabelle Colle, Lindsey Devisscher, Eliene Bogaerts, Annelies Paridaens, Xavier Verhelst, Christophe Van Steenkiste, Louis Libbrecht, Bart Lambrecht, Sophie Janssens, Hans Van Vlierberghe. Therapeutic effects of Artesunate in Hepatocellular Carcinoma: repurposing an ancient antimalarial agent. *International Liver Congress (EASL)*. 12/04/2014, London, UK. Poster presentation. Selected laureate Best poster presentation.

- Annelies Paridaens, Eliene Bogaerts, **Yves-Paul Vandewynckel**, Hans Van Vlierberghe, Anja Geerts, Isabelle Colle. Effect of tauroursodeoxycholic acid on ER stress in cholestatic liver disease. *International Liver Congress (EASL)*. 12/04/2014, London, UK. Poster presentation

- **Yves-Paul Vandewynckel**, Debby Laukens, Anja Geerts, Isabelle Colle, Eliene Bogaerts, Annelies Paridaens, Xavier Verhelst, Lindsey Devisscher, Christophe Vansteenkiste, Benedicte Descamps, Christian Vanhove, Louis Libbrecht, Bart Lambrecht, Sophie Janssens, Hans Van Vlierberghe. Temporal dynamics and therapeutic potential of the unfolded protein response in HCC. *26th Belgian Week of Gastroenterology*, 14/02/2014, La Hulpe, Belgium. Oral presentation

- Eliene Bogaerts, Annelies Paridaens, **Yves-Paul Vandewynckel**, Anja Geerts, Femke Heindryckx, Hans Van Vlierberghe. Time-dependent effects of hypoxia on liver progenitor cell activation in HCC. *26th Belgian Week of Gastroenterology*, 14/02/2014, La Hulpe, Belgium. Oral presentation

- Annelies Paridaens, Eliene Bogaerts, **Yves-Paul Vandewynckel**, Lien Thoen, Hans Van Vlierberghe, Leo Van Grunsven, Anja Geerts, Isabelle Colle. Effect of tauroursodeoxycholic acid on endoplasmic reticulum stress in cholestatic liver disease. *26th Belgian Week of Gastroenterology*, 14/02/2014, La Hulpe, Belgium. Oral presentation

- Eliene Bogaerts, Aurelie Comhaire, Annelies Paridaens, **Yves-Paul Vandewynckel**, Peter Carmeliet, Anja Geerts, Femke Heindryckx, Hans Van Vlierberghe. The role of hypoxia on liver progenitor cell activation in HCC. *26th Belgian Week of Gastroenterology*, 14/02/2014, La Hulpe, Belgium. Oral presentation

- Eliene Bogaerts, Femke Heindryckx, Lindsey Devisscher, Annelies Paridaens, **Yves-Paul Vandewynckel**, Anja Van den Bussche, Xavier Verhelst, Louis Libbrecht, Leo A. Van Grunsven, Anja Geerts, Hans Van Vlierberghe. Role of hypoxia on liver progenitor cell activation in a mouse model for HCC. EASL HCC Summit, 13/02/2014, Geneva, Switzerland. Poster presentation

- **Yves-Paul Vandewynckel**, Debby Laukens, Eliene Bogaerts, Annelies Paridaens, Anja Van den Bussche, Xavier Verhelst, Christophe Van Steenkiste, Benedicte Descamps, Chris Vanhove, Louis Libbrecht, Riet De Rycke, Bart N. Lambrecht, Anja Geerts, Sophie

Janssens, Hans Van Vlierberghe. Temporal dynamics and therapeutic potential of the unfolded protein response in hepatocellular carcinoma. *Oncopoint II*, 06/02/14, Ghent, Belgium. Oral presentation

- **Yves-Paul Vandewynckel**, Debby Laukens, Anja Geerts, Chris Vanhove, Benedicte Descamps, Isabelle Colle, Lindsey Devisscher, Eliene Bogaerts, Annelies Paridaens, Xavier Verhelst, Christophe Van Steenkiste, Louis Libbrecht, Bart Lambrecht, Sophie Janssens, Hans Van Vlierberghe. Therapeutic Potential of Artesunate in Hepatocellular Carcinoma. *American Association for the Study of Liver Diseases (AASLD)*, 05/11/2013, Washington, DC, USA. Poster presentation

- **Yves-Paul Vandewynckel**, Debby Laukens, Eliene Bogaerts, Annelies Paridaens, Anja Van den Bussche, Xavier Verhelst, Christophe Van Steenkiste, Benedicte Descamps, Chris Vanhove, Louis Libbrecht, Riet De Rycke, Bart N. Lambrecht, Anja Geerts, Sophie Janssens, Hans Van Vlierberghe. Therapeutic potential of the unfolded protein response in hepatocellular carcinoma. *United European Gastroenterology week (UEGW)*, 14/10/2013, Berlin, Germany. Oral presentation

- **Yves-Paul Vandewynckel**, Debby Laukens, Eliene Bogaerts, Annelies Paridaens, Anja Van den Bussche, Xavier Verhelst, Christophe Van Steenkiste, Benedicte Descamps, Chris Vanhove, Louis Libbrecht, Riet De Rycke, Bart N. Lambrecht, Anja Geerts, Sophie Janssens, Hans Van Vlierberghe. Temporal dynamics of the unfolded protein response in hepatocellular carcinoma. *European CanCer Organisation (ECCO) conference*, 28/09/2013, Amsterdam, The Netherlands. Poster presentation

- **Yves-Paul Vandewynckel**, Debby Laukens, Eliene Bogaerts, Annelies Paridaens, Anja Van den Bussche, Xavier Verhelst, Christophe Van Steenkiste, Benedicte Descamps, Chris Vanhove, Louis Libbrecht, Riet De Rycke, Bart N. Lambrecht, Anja Geerts, Sophie Janssens, Hans Van Vlierberghe. The unfolded protein response in HCC: a role for PERK? *International Liver Congress of EASL*, 24/04/2013, Amsterdam, The Netherlands. Poster presentation

- **Yves-Paul Vandewynckel**, Debby Laukens, Eliene Bogaerts, Annelies Paridaens, Anja Van den Bussche, Xavier Verhelst, Christophe Van Steenkiste, Benedicte Descamps, Chris Vanhove, Louis Libbrecht, Riet De Rycke, Bart N. Lambrecht, Anja Geerts, Sophie Janssens, Hans Van Vlierberghe. The unfolded protein response in HCC. *EASL Monothematic conference: "Systems Biology of the Liver*, 21/02/2013, Luxembourg, Luxembourg. Poster presentation

- **Yves-Paul Vandewynckel**, Debby Laukens, Eliene Bogaerts, Annelies Paridaens, Anja Van den Bussche, Xavier Verhelst, Christophe Van Steenkiste, Benedicte Descamps, Chris Vanhove, Louis Libbrecht, Riet De Rycke, Bart N. Lambrecht, Anja Geerts, Sophie Janssens, Hans Van Vlierberghe. The time-dependent alterations of the unfolded protein response and multidrug resistance in HCC. *Belgian week of Gastroenterology*, 13/02/2013, Antwerp, Belgium. Oral presentation

- **Yves-Paul Vandewynckel**, Debby Laukens, Eliene Bogaerts, Annelies Paridaens, Anja Van den Bussche, Xavier Verhelst, Christophe Van Steenkiste, Benedicte Descamps, Chris Vanhove, Louis Libbrecht, Riet De Rycke, Bart N. Lambrecht, Anja Geerts, Sophie Janssens, Hans Van Vlierberghe. Impact on angiogenesis and ER stress and its effect on

chemoresistance through PlGF inhibition in a mouse model of hepatocellular carcinoma. *Interuniversity ER stress conference Ghent University/VIB*, 10/09/2012, Ghent, Belgium. Oral presentation

1.1.7. **Awards and patents**

- 22/04/2015: **EASL** Vienna, Austria: "**Top 10% abstract**" award for "TUDCA dampens oncogenic apoptosis induced by endoplasmic reticulum stress during hepatocarcinogen exposure".
- 10/03/2015: **Patent** application: invention of a novel treatment option for HCC.
- 27/02/2015: "**Belgian Week of Gastroenterology (BWGE) Research Grant"** based on evaluation by external referees of previous work, CV and research project proposal (TUDCA in HCC).
- 14/10/2013: "**National Award**" for best Belgian UEG abstract 2013 of the "United European Gastroenterology" (**UEG**) week in Berlin, Germany.
- 30/05/2005: Finalist international "Flemish **Biology** Olympiad".

1.1.8. **Research skills**

- qRT-PCR
- Western blotting, IHC and ELISA
- Cell culture techniques
- Cell viability and proliferation assays and colony formation assays
- Mouse models for HCC and cirrhosis
- Clinical trial design

1.1.9. **Reviewer for journals**

Reviewed manuscripts for the following international scientific journals:

- 20/05/2015: *Journal of Hepatology* (IF: 10.4)
- 13/04/2015: *Apoptosis* (IF: 3.6)
- 16/03/2015: *World Journal of Gastroenterology* (IF: 2.4)
- 02/05/2013: *Carcinogenesis* (IF: 5.7)
- 01/02/2014: *European Journal of Gastroenterology and Hepatology* (IF: 2.2)

1.1.10. **Participation in popular media**

- 10/11/2014: Interview regarding the foundation of Young BASL in "*Artsenkrant*"

1.1.11. **Active memberships**

- **EASL**: European association for the study of the liver
- AASLD: American association for the study of liver diseases
- ECCO: European cancer organisation
- VVGE: Vlaamse vereniging van Gastro-enterologie
- Jong-VVGE: Jong Vlaamse vereniging van Gastro-enterologie
- BASL: Belgian association for the study of liver diseases
- ***Young BASL***: Young Belgian association for the study of liver diseases (*President*: 2014-up till now)

1.1.12. **Bibliography**

[1] **Y.-P. Vandewynckel**, A. Geerts, X. Verhelst, H. Van Vlierberghe. Cerebellar stroke in a low cardiovascular risk patient associated with sorafenib treatment for fibrolamellar hepatocellular carcinoma. Clin Case Rep. 2014,2: 4–6.

=> Case report showing the increased risk of stroke by sorafenib in low cardiovascular risk patient.

[2] **Y.-P. Vandewynckel**, D. Laukens, A. Geerts, E. Bogaerts, A. Paridaens, X. Verhelst, S. Janssens, F. Heindryckx, H. Van Vlierberghe. The paradox of the unfolded protein response in cancer. Anticancer Res. 2013;33:4683-94.

=> Review of the literature concerning the unfolded protein response in cancer.

[3] **Y.-P. Vandewynckel**, D. Laukens, A. Geerts, C. Vanhove, B. Descamps, L. Devisscher, E. Bogaerts, A. Paridaens, X. Verhelst, C. Van Steenkiste, L. Libbrecht, I. Colle, B. Lambrecht, S. Janssens, and H. Van Vlierberghe. Therapeutic Effects of Artesunate in Hepatocellular Carcinoma: Repurposing an Ancient Antimalarial Agent. Eur. J. Gastroenterol. Hepatol. 2014, 26:861-70.

=> In this study, we showed the therapeutic potential of the antimalarial Artesunate in HCC. This study led to the start of a phase I trial of Artesunate in advanced HCC patients (NCT02304289).

[4] A. Paridaens, D. Laukens, **Y.-P. Vandewynckel**, S. Coulon, H. Van Vlierberghe, A. Geerts, and I. Colle. Endoplasmic reticulum stress and angiogenesis: is there an interaction between them? Liver Int. 2014.

=> Review concerning the unfolded protein response and angiogenesis.

[5] E. Bogaerts, F. Heindryckx, **Y.-P. Vandewynckel**, L. A. Van Grunsven, H. Van Vlierberghe. The roles of transforming growth factor-β, Wnt, Notch and hypoxia on liver progenitor cells in primary liver tumours (Review). Int. J. Oncol. 2014,44:1015–22.

=> Review concerning the key pathways regulating liver progenitor cells in HCC.

[6] **Y.-P. Vandewynckel**, X. Verhelst, A. Geerts, and H. Van Vlierberghe. Nieuwe therapie voor hepatitis C: 'an end of life story ?' Tijdschr. voor Geneeskunde, 2014.

=> Review concerning the new treatment options for hepatitis C in a Belgian context.

[7] **Y.-P. Vandewynckel**, R. De Rycke, E. Bogaerts, and H. Van Vlierberghe. Intestinal metaplasia in an orthotopic mouse model for hepatocellular carcinoma. Dig. Liver Dis. 2014,46:e17.

=> In this paper, we observed the presence of intestinal metaplasia following carcinogen-induced liver damage and regeneration.

[8] D. Laukens, L. Devisscher, L. Van den Bossche, P. Hindryckx, R. Vandenbroucke, **Y.-P. Vandewynckel**, C. Cuvelier, B. Brinkman, C. Libert, P. Vandenabeele, and M. De Vos. Tauroursodeoxycholic acid inhibits experimental colitis by preventing early intestinal epithelial cell death. Lab. Invest. 2014,94:1419-30.

=> Cytoprotective effect of the chemical chaperone TUDCA reduces experimental colitis.

[9] **Y.-P. Vandewynckel**, D. Laukens, E. Bogaerts, A. Paridaens, A. Van den Bussche, X. Verhelst, C. Van Steenkiste, B. Descamps, C. Vanhove, L. Libbrecht, R. De Rycke, B. N. Lambrecht, A. Geerts, S. Janssens and H. Van Vlierberghe. Modulation of the unfolded protein response impedes tumor cell adaptation to proteotoxic stress: a PERK for hepatocellular carcinoma therapy. Hepatol. Int. 2014,9:93-104.

=> In this study, we showed that UPR activation is fine-tuned during the different phases of tumorigenesis and that the PERK pathway is essential for tumour cell survival upon ER stress.

[10] E. Bogaerts, F. Heindryckx, L. Devisscher, A. Paridaens, **Y.-P. Vandewynckel**, A. Van den Bussche, X. Verhelst, L. Libbrecht, L. A. van Grunsven, A. Geerts, H. Van Vlierberghe. Time-Dependent Effect of Hypoxia on Tumor Progression and Liver Progenitor Cell Markers in Primary Liver Tumors. *PLoS One* 2015;10:e0119555.

=> In this study, we demonstrated that the effect of hypoxia depends on the phase of tumorigenesis.

[11] **Y.-P. Vandewynckel**, D. Laukens, L. Devisscher, A. Paridaens, E. Bogaerts, X. Verhelst, A. Van den Bussche, S. Raevens, C. Van Steenkiste, M. Van Troys, C. Ampe, B. Descamps, C. Vanhove, O. Govaere, A. Geerts, H. Van Vlierberghe. Tauroursodeoxycholic acid dampens oncogenic apoptosis induced by endoplasmic reticulum stress during hepatocarcinogen exposure. Oncotarget 2015,6,X.

=> In this study, we demonstrated the chemopreventive potential of TUDCA and the pivotal role of the pro-apoptotic UPR in the initiation of hepatocarcinogenesis.

Chapter 6

Acknowledgments

1. Dankwoord

Graag zou ik graag iedereen die de voorbije jaren rechtstreeks of onrechtstreeks bijgedragen heeft bij het verwezenlijken van deze doctoraatsthesis oprecht en van harte bedanken.

Als eerste, wil ik mijn diepste dankbaarheid uiten aan mijn promotor **Prof. Dr. Hans Van Vlierberghe**. Zijn enthousiasme, wetenschappelijke ervaring en kritische ingesteldheid maakten dat ik dit proefschrift tot een goed einde heb gebracht. Ondanks zijn drukke agenda, kon hij toch steeds tijd vrij maken om mij te woord te staan. Onze maandelijkse meetings vormden een belangrijke bron van inspiratie en meestal kwam ik er buiten met talrijke nieuwe ideeën en inzichten. Verder wil ik hem bedanken voor de voortdurende aanmoediging en intellectuele vrijheid. Hans, het was/is een waar genoegen met je samen te werken. Ik ben er zeker van dat dit niet het einde, maar wel het begin vormt van onze samenwerking. Natuurlijk ook een speciaal woord van dank aan mijn toegewijde co-promotor **Prof. Dr. Anja Geerts**. Je bent er altijd geweest voor alle praktische begeleiding en ondersteuning van ons labo. Steeds stond je klaar en had je een kordaat antwoord op alle kleine en grote problemen.

Verder wil ik graag **Prof. Dr. Sc. Debby Laukens** bedanken voor haar begeleiding gedurende het hele project. Ze is een briljante wetenschapper. Debby, van het moment dat ik in het labo aankwam, stond je paraat voor alles wat ik vroeg. Je leerde me pipetteren, centrifugeren en relativeren. Je prikkelde mijn enthousiasme en vormde de basis van al mijn wetenschappelijk werk. Maar bovenal, je bent een vriendin voor het leven geworden.

Ook wil ik het diensthoofd, **Prof. Dr. Martine De Vos,** bedanken voor haar ondersteuning van het labo en continue inzet voor optimaal onderwijs en onderzoek.

Dank aan **Prof. Dr. Louis Libbrecht** voor zijn deskundige evaluatie van alle histologische coupes en verhelderende discussies.

Naast het begeleidende kader, wil ik mijn collega's bedanken voor hun hulp, discussie en vriendschap. **Femke, Stephanie, Xavier, Christophe en Isabelle**, dank om me wegwijs te maken in de labo's tijdens het begin van mijn onderzoek. **Eliene** en **Annelies**, ik wil jullie van harte bedanken voor het gezelschap, de leuke babbels en vriendschap. Jullie stonden steeds klaar om me te helpen. En Eliene, nogmaals dank voor je onbeperkte hulp aan deze hulpbehoevende digibeet. Zonder jouw hulp zag deze thesis er compleet anders uit. **Lindsey**, na een prachtig doctoraat, ben je sinds kort onze nieuwe postdoc geworden. Je energie en enthousiasme zijn aanstekelijk voor elke PhD student. **Sarah** en **Sander**, ik wens jullie alle succes bij het begin van jullie doctoraat!

Naast blok B, wil ik ook alle mensen van 3K12 -**Sarah, Lien, Sophie, Evi, Elien, Hugo**- bedanken voor alle advies, de nieuwste roddels, leuke feestjes en aangename middagpauzes.
Een speciaal woord van dank voor de laboranten. **Anja**, ik heb echt enorm veel aan jou te danken. Teveel om op te sommen! Je was een ongelofelijke ondersteuning voor al mijn werk. Merci voor alles! Ik vergeet dit nooit. **Kim**, je hebt me van het prille begin veel bijgeleerd. Jammer genoeg heb je ons intussen verlaten, maar ik wens je alle succes met de brouwerij! **Petra**, **Hilde** en **Griet**, dank om bij te springen als ik weer eens net wat te veel op 1 dag gepland had.

Tom, Bart, Sam en **Diego** (1ste verdiep blok B), bedankt voor het winkeltje en de technische hulp. **Melissa Bol, Marijke de Bock** en **Sarah Cosyns**, dank voor de hulp bij immunofluorescentie, de aangename gesprekken over de middag, en uiteraard, de laatste roddels.
Het **Infinity Lab,** en meer bepaald, **Bénédicte** en **Prof. Vanhove,** voor de small animal imaging en de constructieve discussies.
Mensen van Vlaams Instituut voor Biotechnologie (VIB) Gent, **Sophie Janssens** en **Prof. Bart Lambrecht**, dank voor jullie kritische opmerkingen en opvolging. Graag had ik ook mijn dank geuit aan **Riet De Rycke** voor de vriendelijke ondersteuning bij de electronenmicroscopie.
Julien, je vrolijkte het labo op met snoep en gezang. Je hielp me met het fijnere muizenwerk.
Ik waardeerde de administratieve bijstand van **Annette** en **Maud**.

Verder wil ik ook de study nurses, **Karen Roels** en **Delphine Muylaert**, bedanken voor hun ondersteuning bij opstart van de fase I trial. **Prof. Bart De Spiegeleer** en **Prof. Luc Van Bortel,** dank voor Uw hulp bij opstellen van de fase I trial vanuit farmacologische hoek. In dit kader, wil ik ook zeker **Klara Rombauts** van het Antikankerfonds vermelden. Je was een grote hulp bij de aanvraag bij het FAGG en ethisch comité.

Collega's van de **Young BASL** steering committee, dank voor jullie engagement en bijdrage bij het oprichten van dit nieuw een veelbelovend onderzoeksplatform. Het is een grote eer om voorzitter te zijn van dit prille initiatief.

Ook wil ik alle leden van de **examencommissie**- Prof. Dr. Johan Van De Voorde, Dr. sc. Michael Drennan, Prof. Dr. Marleen Praet, Prof. Dr. Roberto Troisi, Dr. sc. Francesca Fornari, Prof. Dr. Hendrik Reynaert en Dr. sc. Olivier Govaere - bedanken voor hun kritische revisie en constructieve feedback.

Ik wil graag mijn **ouders** en **zus** bedanken voor hun onvoorwaardelijke liefde en steun. Ten slotte, wil ik mijn grootste waardering uitspreken voor mijn vriendin **Tina**, voor haar liefde, continue ondersteuning, aanmoediging en verdraagzaamheid, als ik bijv. weer eens te laat ben voor het avondeten, in de gehele duur van mijn doctoraat.

Chapter 7

Supplemental information

1. **Supplementary files**

Supplementary files can be downloaded using the following URL:

https://docs.google.com/document/d/15PN0_GCWz3y_i0Z7XMNgvrJCNgqqfFmUrw6aaLMYbV4/edit?usp=sharing

Or by scanning the following QR-code: